School of Chemistry and Physics

A phytochemical and elemental analysis of *Senecio serratuloides* DC, and its antidiabetic potential

2024

ANDILE GUMEDE

A phytochemical and elemental analysis of *Senecio serratuloides*, and its antidiabetic potential

ANDILE GUMEDE (216054407)

2024

A thesis submitted to the School of Chemistry and Physics, College of Agriculture, Engineering and Science, University of KwaZulu-Natal, Westville, for the degree of Master of Science.

This thesis has been prepared according to **Format 1** as outlined in the Information for the guidance of examiners of higher degrees, which states:

Format 1: As a single coherent book, with a single Introduction, Materials and Methods, Results, Discussion, Conclusion and References.

As the candidate's supervisors, we have approved this thesis for submission.

Professor Neil A. Koorbanally

Professor Roshila Moodley

……. ……..

Dr Bongiwe Mshengu

Date: 12 July 2024

ABSTRACT

Senecio serratuloides DC, from the Asteraceae, has been widely used in South African traditional medicine for the treatment of various conditions such as swollen gums, chest pains, sores, cuts, burns and ulcers. This study was conducted to determine a chemical profile of the plant, both in terms of the secondary metabolites and essential and toxic elements contained in the plant. The plant extracts were further tested for their antibacterial (minimal inhibitory concentrations) and antidiabetic potential (α-amylase and α-glucosidase inhibitory activity). The phytochemical analysis of the leaves and stems resulted in the isolation of the sterols, *β*-sitosterol (**S1**) from the stems, and stigmasterol (**S2**) and stigmasterol glucoside (**S3**) from the leaves. A further rare sterol, 18α-ursa-12,20(30)-dien-3*β*-ol (**S4**) was also isolated from the leaves. Three flavonoids, quercetin (**S5**), quercetin-3-*O*-glucoside (**S6**) and hesperidine (**S7**) were also isolated from the leaves, along with an aromatic acid, caffeic acid (**S8**). Extracts of the plant showed good *in vitro* antidiabetic activity, with the methanol extract from the leaves exhibiting the highest activity against *α*-glucosidase and *α*-amylase. However, the extracts did not exhibit any significant antibacterial activity in the assays carried out. The elemental analysis of the plant indicated a decreasing order of Ca > Mg > Zn > Fe > Co > Cu > Cr > Mn > Ni > As > Se. The leaves also showed good quantities of vitamin C, with an appreciable amount being extracted during the cooking phase. The results also show that moderate consumption of the leaves pose no probable threats of metal poisoning. The extracts obtained from *S. serratuloides* DC were found to have no antibacterial activity. This is surprising, since some of the isolated compounds were reported to have shown some antibacterial properties, however, these may have been too low to have any significant effect in the crude extracts.

STRUCTURES OF COMPOUNDS

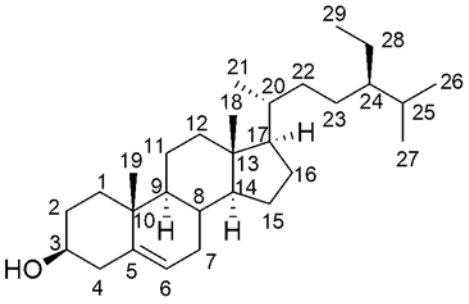

β–sitosterol

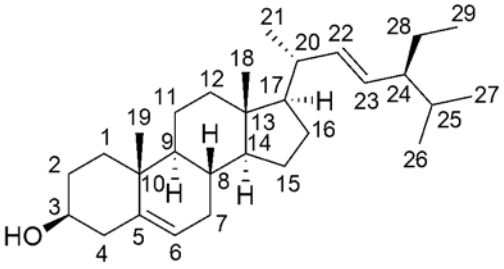

stigmasterol

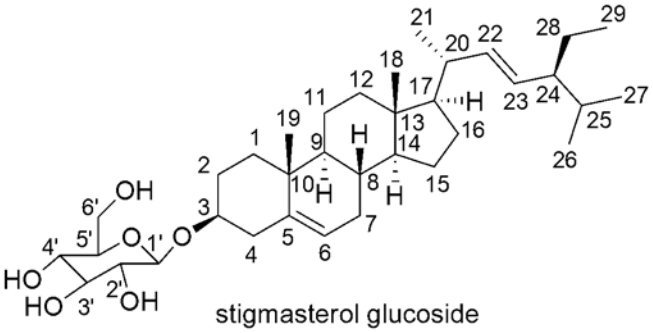

stigmasterol glucoside

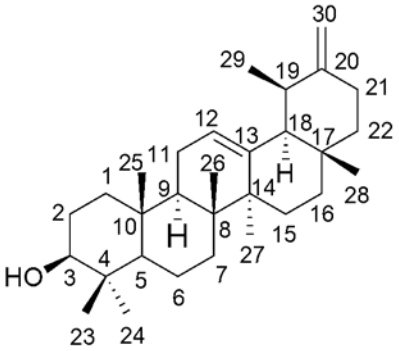

18α-ursa-12,20(30)-dien-3β-ol

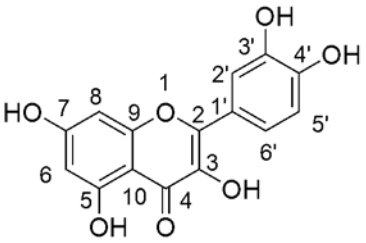

Quercetin

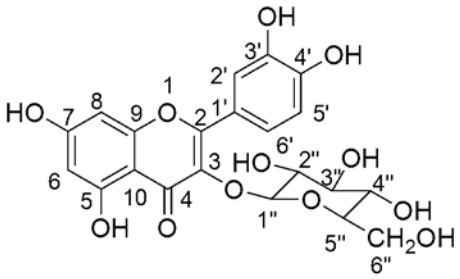

Quercetin-3-*O*-glucoside

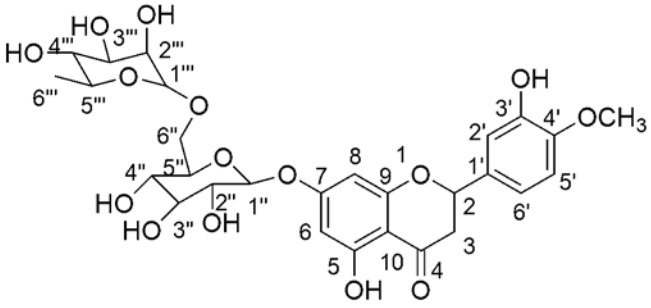

hesperidin

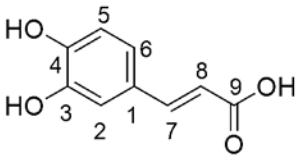

caffeic acid

ABBREVIATIONS

^{13}C NMR	C-13 nuclear magnetic resonance spectroscopy
^{1}H NMR	proton nuclear magnetic resonance spectroscopy
Ac	acetate
EtOH	ethanol
MeOH	methanol
aq	aqueous
br	broad
c	concentration
cc	column chromatography
CRM	certified reference material
CD_3OD	deuterated methanol
$CDCl_3$	deuterated chloroform
D_2O	deuterated water
COSY	correlated spectroscopy
d	doublet
dd	doublet of doublets
DEPT	distortionless enhancement by polarization transfer
HMBC	heteronuclear multiple bond coherence
HSQC	heteronuclear single quantum coherence
Hz	hertz
IR	infrared
m	multiplet
Me	methyl
MS	mass spectroscopy
NOESY	nuclear overhauser effect spectroscopy
s	singlet
t	triplet
TLC	thin layer chromatography
UV	ultraviolet

DECLARATIONS

DECLARATION 1 – PLAGIARISM

I, **Andile Gumede** declare that

1. The research reported in this thesis is my original research, except where otherwise indicated.
2. This thesis has not been submitted for any degree or examination at any other university.
3. This thesis does not contain other persons' data, pictures, graphs or other information, unless specifically acknowledged as being sourced from other persons.
4. This thesis does not contain other persons' writing, unless specifically acknowledged as being sourced from other researchers. Where other written sources have been quoted, then:
    a. Their words have been re-written but the general information attributed to them have been referenced, and
    b. Where their exact words have been used, then their writing has been placed in italics and inside quotation marks, and referenced.
5. This thesis does not contain text, graphics or tables copied and pasted from the Internet, unless specifically acknowledged, and the source being detailed in the thesis and in the References section/s.

Signed ……  ……

Andile Gumede

Preface

The experimental work described in this thesis was carried out in the School of Chemistry and Physics at the University of KwaZulu-Natal, Durban, from May 2021 to May 2023 under the supervision of Dr B. Mshengu, Prof. R. Moodley and Prof. N. Koorbanally.

These studies present original work by the author and have not otherwise been submitted in any form for any degree or diploma to any tertiary institution. Where use has been made of the work of others, it is duly acknowledged in the text.

Signed: _____ Name: _Andile Gumede_____

Date: 12 July 2024

DEDICATION

I dedicate this study to my late grandmother, **Thenjiswa Gumede**. Lala uphumule salukazi sami lapho ukhona.

ACKNOWLEDGEMENTS

Firstly, I would like to thank Shembe (uNyazilwezulu) for giving me the ability and confidence to take such a big step in my career.

I would also like to thank my family especially my mother, Elizabeth Shezi, MaJalamba, my father, Muziwakhe Themba Khuzwayo, and my sisters, Nomfundo Princess Gumede and Nonhle Ntombikayise Gumede, for their prayers, motivation and encouragement.

This study would never have been completed without support from a number of people. I am highly indebted to my supervisors, Dr. B. Mshengu, and Prof. R. Moodley for their guidance. And a special thanks to Prof. N.A. Koorbanally for his endless guidance, commitment, and constructive criticism throughout the duration of the writeup process.

I would also like to acknowledge the following individuals who encouraged me, gave me words of wisdom and helped me through my research; Amanda, and Thabile. And to the rest of the NPRG, ningamabhoza.

I would also like to thank uMakoti wakithi, Sinothile Msomi for her constant support, prayers and encouragement.

I would also like to acknowledge the following individuals and organizations:

- The technical team in the School of Chemistry and Physics at UKZN, Westville for their assistance.
- My colleagues in the Natural Products Research Group for moral support.
- I would also like to acknowledge the National Research Foundation (NRF) for financial support.

Table of Contents

LIST OF TABLES

LIST OF FIGURES

Chapter 1 Introduction

There are two main sources of drugs and treatment for diseases and ailments that plague man. These are the common pharmaceutical drugs that one buys from a pharmacy, and which is prescribed by medical practitioners, and there are treatments administered by herbalists and traditional practitioners who administer herbal remedies, extracts and concoctions derived and prepared from medicinal plants, whose secrets have been handed down through the ages (Lupton, 2012).

1.1 Traditional medicine

In order to maintain health and prevent, diagnose and treat disease, traditional medicine uses knowledge, skills, and practices based on theories, beliefs and experiences unique to certain cultures (WHO, 2019a). The terms traditional medicine and supplementary or alternative medicine are often used interchangeably (Ryan, 1996). They refer to medicine that has not gone through the rigorous trials of scientific medicine, which costs millions of rands to produce a single tablet. Between 60% to 80% of South Africans depend on traditional medicine for their primary medical needs due to the high cost of western medications and the difficulty in accessing medical facilities (Mhlongo, 2019, Prakash et al., 2021). Plants with therapeutic properties are used to treat a wide range of illnesses, from bacterial infections to heart disease, arthritis, stomach-ache, cough, diarrhea and skin problems. Examples of these medicinal plants are *Aloe ferox* Mill, *Boophone disticha* (Lf), *Datura stramonium* L, *Hypericum perforatum* L, and *Cinnamomum camphora* (L.) Presl (camphor tree) (Barnes et al., 2007, Brown et al., 2014, Mavimbela et al., 2018).

Traditional medicine is an ancient practice where plants with curative properties have been identified, and extracts used to treat patients (Brown et al., 2014, Ramawat et al., 2009). Half of medicinal drugs used currently are derived from natural compounds (McChesney et al.,

2007). An example is quinine (Figure 1-1) that originates from *Cinchona officinalis* L, used to treat malaria (Okombo et al., 2011). Paclitaxel, traded as Taxol, a remarkable drug used to treat cancer was isolated from the bark of *Taxus brevifolia* Nutt. Aspirin, a household medicinal cabinet drug used to alleviate pain, reduce fever, and treat inflammation was first isolated from the willow bark. Digoxin, isolated from *Digitalis lanata* Ehrh is used to treat heart disease. Morphine was isolated from *Papaver somniferum* L and used to reduce pain (Adeleye et al., 2019, Atanasov et al., 2015, Cragg and Newman, 2005, Newman and Cragg, 2016). Other examples of natural products which developed into drugs include the anticancer medications vinblastine, podophyllotoxin (Condylin^{TM}) and etoposide; steroidal hormones like cortisone, progesterone and norgestrel; cardiac glycosides like digitoxigenin; and antibiotics like penicillin and streptomycin (Dhyani et al., 2022).

In modern medicine, the drugs mentioned above have proven to be essential and have been used as a source for further drug development. Newman and Cragg have conducted a comprehensive review on the origin of several types of drugs authorized by regulatory bodies for use as antibacterial agents, antifungal drugs, anticancer medication and antidiabetic medication. There have also been some recent discoveries. For example, vernodalin (Figure 1-2), isolated from *Vernonia colorata* (Willd) Drake (Asteraceae), serves as an effective cure for abdominal pain, fever, diarrhea and rheumatism (Newman and Cragg, 2016). Meropenem is another natural product derivative approved by the Food and Drug Administration (FDA) as an antibacterial drug. Wighteone is another example of a plant-derived drug obtained from *Erythrina lysistemon* Hutch (Fabaceae) and commonly used to treat sprains, earache and toothache (Cragg and Newman, 2005, Newman and Cragg, 2016).

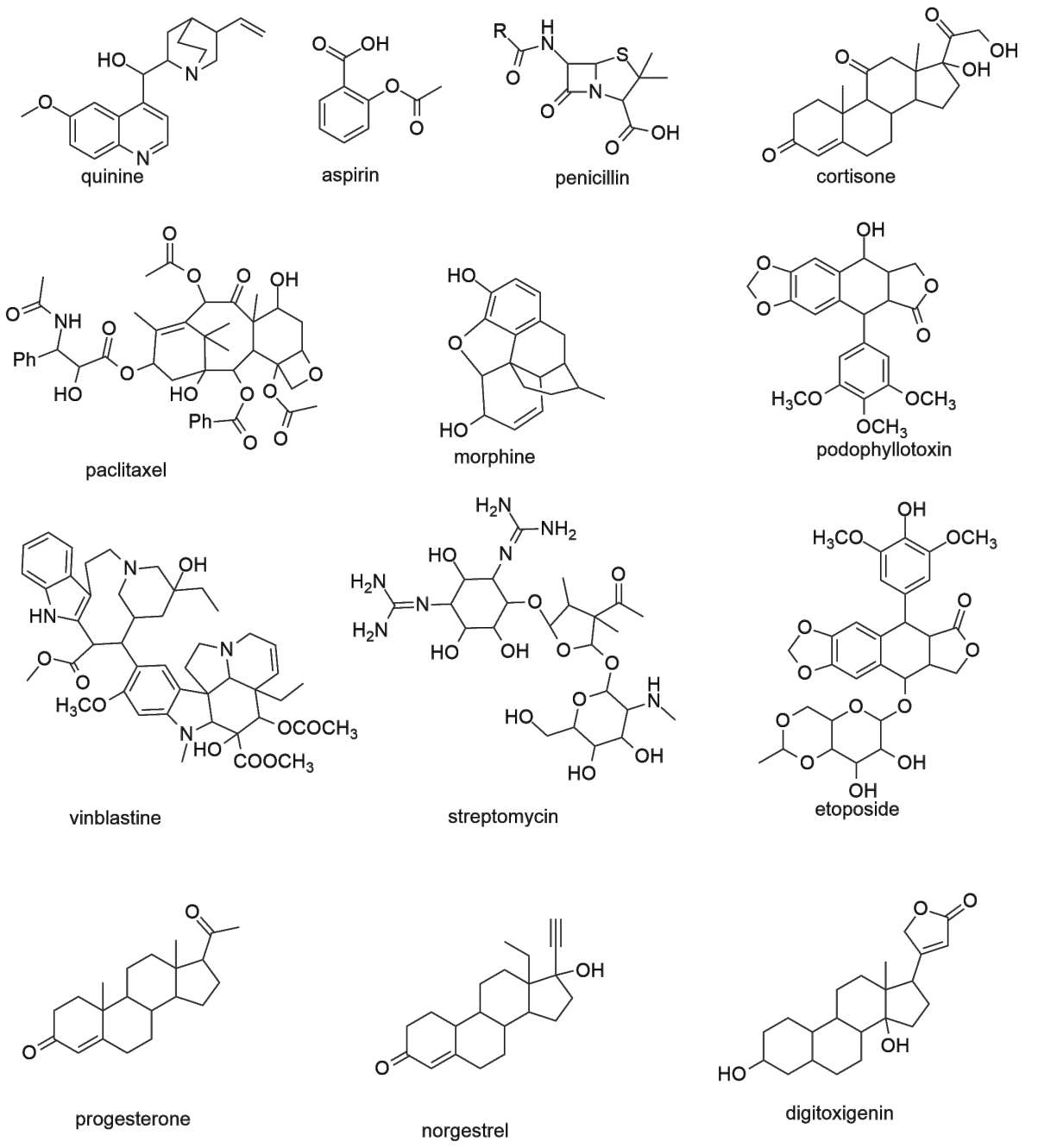

Figure 1-1 Structures of natural products used commonly in modern medicine

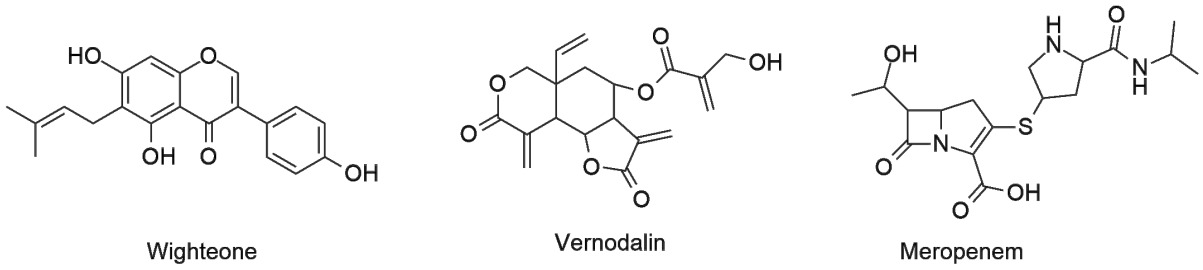

Figure 1-2 Some recent natural products used in modern medicine

Several drugs for the treatment of cancer and diabetes have been developed using the healing power of natural products. For example, midostaurin, a potent anticancer drug, was isolated from *Streptomyces staurosporeus* and approved as an anticancer drug (Zhou et al., 2019). D-pinitol, proven effective in the treatment of diabetes was isolated from the leaves of *Bougainvillea spectabilis* of the Nyctaginaceae family and approved by the FDA (Park and Lee, 2013). Another plant-derived drug used to treat type II diabetes is metformin, made possible by galegine, a naturally occurring nutrient from *Galega officinalis* (Campbell et al., 1996). Other valuable antidiabetic drugs approved by the FDA derived from natural products include voglibose, acarbose, miglitol, D-pinitol, metformin and vidostaurin (Figure 1-3) (Levis, 2017, Newman, 2019, Newman and Cragg, 2016).

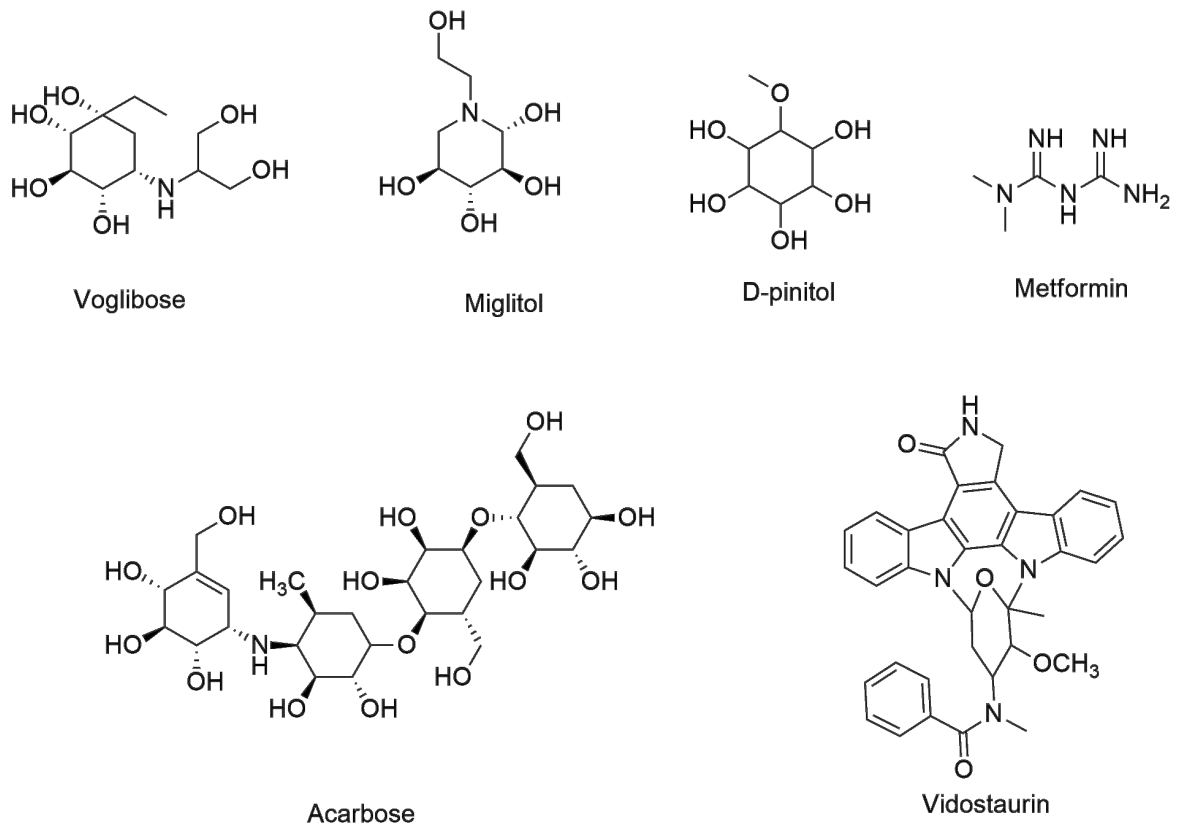

Figure 1-3 Anticancer and antidiabetic natural product derived drugs

Other examples of drugs originated from natural products include reserpine (Figure 1-4), isolated from *Rouvolfia serperntina* and used to treat high blood pressure, betulinic acid isolated from the leaves of *Syzigium claviflorum* (Myrtaceae), and known to have anti-HIV properties and homoharringtonine, an anticancer agent isolated from *Cephalotaxus hainanensis* (Cragg and Newman, 2005, Newman, 2019, Newman and Cragg, 2016).

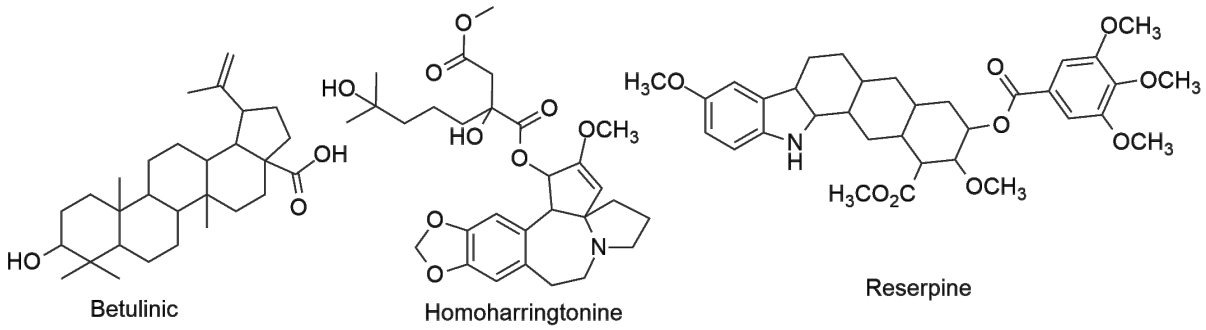

Figure 1-4 More examples of natural product derived drugs

The full potential of the biodiversity of plants has not yet been fully investigated, despite major discoveries in the past century. Approximately 6% of plants have had their biological activity documented, with 15% investigated for their phytochemistry (Vitale et al., 2022). It is important to continue research on the phytochemistry and pharmacology of medicinal plants, which could lead to major new discoveries in medicine and pharmacology.

African traditional medicine has been practiced for decades and their practices passed on from healer to healer for the diagnosis and treatment of illnesses using mainly plants (Mothibe and Sibanda, 2019). Approximately 80% of Africans rely on traditional medicine, with the global percentage being much lower at 60% (WHO, 2018a). Traditional treatments are used for a variety of medical conditions and diseases such as hypertension, pain, gynaecological problems, asthma, mental conditions and diabetes mellitus among others. People in Africa are

known to first consult traditional healers before seeing a conventional health provider such as a nurse in a clinic or medical practitioner. As such, in many developing countries, both traditional and westernized healthcare systems are recognized (Dar et al., 2017).

The African continent has a high biological diversity, resulting in a diverse array of medicinal plants. Table 1-1 lists various African medicinal plant species and their traditional uses.

Table 1-1: Some medicinal plants common in African countries

Scientific Name	**Plant part(s)**	**Traditional uses**	**Country**	**References**
Artemisia aftra L.	Leaf and stems	Coughs, fever, colds, headache, loss of appetite and intestinal worms	Kenya, South Africa, Uganda, Tanzania and Namibia	(Gerard, 2015)
Momordica balsamica L.	Leaf	Stomach and intestinal complaints, burns and haemorrhoids	Tropical Africa	(Raimundo, 2017, Tembe, 2006)
Aloe ferox L.	Leaf	Conjunctivitis, venereal sores	South Africa	(Loots du et al., 2007)
Leonotis leonurus L.	Leaf and roots	Headache, fever, asthma, coughs and dysentery	South Africa	(De Wet et al., 2013)
Brucea antidysenterica JF Mill	Leaf, root and bark	Skin diseases	Ethiopia	(Madzinga et al., 2018)
Vernonia amaygdaline Del.	Leaf	Hypertension	Nigeria	(Ifeoma and Chukwunonso, 2011)

1.2 Diabetes

One of the most prevalent metabolic illnesses in South Africa is diabetes mellitus, whose incidence and prevalence have risen alarmingly during the past 20 years. In South Africa 1 826 100 people were predicted to have diabetes up to 2017, with an additional 1 548 500

people estimated to have undiagnosed diabetes up to that year (Wild et al., 2004, IDF Diabetes Atlas, 2021). Diabetes causes damage to nerves, kidneys, heart, eyes and blood vessels. According to the International Diabetes Federation (IDF), in 2019 the total population of adults living with diabetes in the age group 20-79 stood at 463 million. This figure is estimated to increase to 578 million by 2030. It is reported that every six seconds a patient dies of diabetes mellitus, higher than malaria, tuberculosis and HIV combined. Other factors contributing to this rise in diabetes include rapid cultural and social changes, such as aging, diet, population and reduced physical activity (IDF Diabetes Atlas, 2021).

Diabetes can be categorised into two main types, type I and type II. Type I is categorised by insufficient production of insulin. People with type I diabetes need to take insulin daily to live. This type of diabetes commonly develops in children and young adults. However, when insulin secretion is sufficient, but its effects are deficient, this results in type II diabetes mellitus. Weight gain, changes in diet, urbanisation, and a sedentary lifestyle all contribute to diabetes (Hasanpour et al., 2020, IDF Diabetes Atlas, 2021, Kim et al., 2014).

1.2.1 Management of diabetes mellitus

Healthy eating, physical activity, and weight control are the centre of any therapeutic program for patients with diabetes mellitus. These lifestyle modifications not only lower blood glucose levels, but lower many risk factors for cardiovascular disease and help with weight loss. However, most patients depend on medication for treatment since most people cannot practise good lifestyles (Kavishankar et al., 2011). Treating diabetes involves maintaining blood glucose at normal levels. Both traditional and modern medicine have similar mechanisms to treat diabetes. These involve stimulating the release of more insulin, acting on hormones that

increase blood glucose levels, inhibiting hydrolysis of glycogen, and improving sensitivity of the insulin receptor sites (Kim et al., 2014, Loots et al., 2011).

The synthetic drugs currently used for diabetes include biguanides (metformin) (Figure 1-3), sulfonylureas, thiazolidinediones (glitazones), α-glucosidase inhibitors, DPP-4 inhibitors and meglitinides (glinides). The class of medication given as injections include insulin and incretin mimetics (Barnes et al., 2007, Park and Lee, 2013, Zhou et al., 2019). However, not everyone can afford these drugs. For example, the majority of South Africans, who have no access to modern healthcare and live below the poverty line, rely on traditional medicine to treat diabetes and its consequences. Therefore, when thinking about how to treat this condition in the future, the topic of traditional drugs used for diabetes control is quite relevant. There are a variety of plant species used by herbalists and traditional healers to treat diabetes mellitus (Erasto et al., 2005, Newman, 2019, Newman and Cragg, 2016).

Pharmaceutical drugs have many side effects. Metformin is a biguanide that inhibits glucose production in the liver. Its side effects are gastrointestinal problems, dyspepsia, nausea and diarrhoea. Metformin should not be prescribed to patients with compromised renal function, de-compensated heart failure, liver disease and in patients with serious medical problems (Tran et al., 2020).

Thiazolidinediones are used in the treatment of diabetes to improve sensitivity to insulin, and to decrease insulin resistance and cardiovascular problems. Weight gain and fluid retention are the most common side-effects that can lead to peripheral oedema and heart failure. They are avoided in patients with heart failure and severe liver problems. Rosiglitazone (Figure 1-5) may contribute to cardiovascular disease and a risk of a heart attack, while Pioglitazone has

been associated with an increased risk of bladder cancer (Newman, 2019, Newman and Cragg, 2016, Oyedemi et al., 2009, Park and Lee, 2013, Zhou et al., 2019).

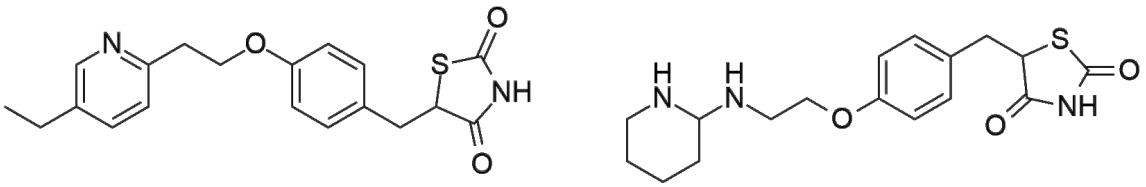

Pioglitazone Rosiglitazone

Figure 1-5 The structures of the antidiabetic drugs, rosiglitazone and pioglitazone

1.2.2 Antidiabetic activity of plants

Plants have been the source of pharmaceutics for treating and managing diseases. For diabetes, these were listed above and include acarbose, miglitol, voglibose and galegine (Figure 1-3 and Figure 1-6). *Galega officinalis* L. (Fabaceae) was the first medicinal plant to have potent antidiabetic activity, which led to the isolation of galegine, the parent compound of metformin (Figure 1-3). This plant was also found to have potent anti-obesity activity (Odeyemi and Bradley, 2018, Oyedemi et al., 2009).

In South Africa, much attention has been placed on screening plants with antidiabetic effects. Plants found to have antidiabetic activity in South Africa are presented in Table 1-2. These are only the ones that have been documented and there may be many others being used in traditional African medicine, but not reported. The presence and concentration of phytochemicals are influenced by genetics and environmental factors such as soil types, climate, vegetation kinds, and the presence of other species. The mechanism of action of these medicinal herbs used in South Africa is unknown (Deutschländer et al., 2011), however extracts from many species have undergone extensive *in vivo* physiological, pharmacological,

and biochemical testing to ascertain how they function in the treatment of diabetes mellitus (Odeyemi and Bradley, 2018).

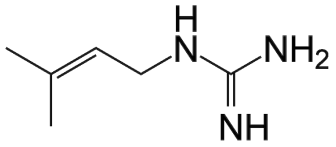

Galegine

Figure 1-6: The structure of galegine

Catharanthus roseus (L.) G. Don. showed both *in vitro* and *in vivo* anti-diabetic properties. The most potent compound in the plant was found to be the alkaloid vindolicine (Figure 1-7) (Afolayan and Sunmonu, 2010, van de Venter et al., 2008). It exhibits free radical scavenging activity and improved glucose utilisation properties. Plants such as *Senna alexandri* Mill*, Cymbopogon citrutus* DC*, Nuxia floribunda* Lam*,* and *Curcubita pepo* L have been reported to contain *α*-amylase and *α*-glucosidase inhibitors, which may help reduce post-prandial hyperglycemia. Other antidiabetic plants such as *Carica papaya* and *Heeria argentae* may also act by preserving and increasing the regeneration of pancreatic *β*-cells, hence increasing insulin release (van de Venter et al., 2008). *Vinca major* has also shown antidiabetic activity *in vitro* (Comfort et al., 2019).

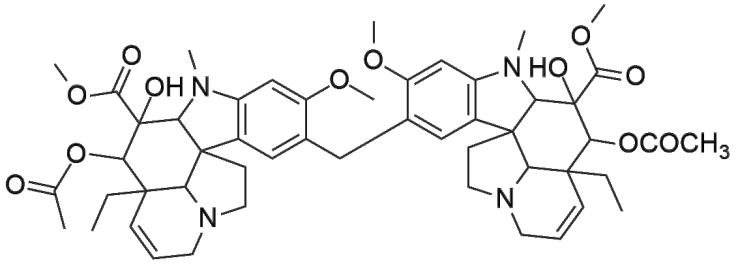

Vindolicine

Figure 1-7 The structure of vindolicine

1.2.3 Some antidiabetic compounds isolated from plants

Research on South African medicinal plants with antidiabetic activity is ongoing in an effort to identify the active components to corroborate this activity (Ríos et al., 2015). A phytochemical analysis of *Catharanthus roseus* (Apocynaceae), originally from Madagascar but widespread in South Africa and used for the management of diabetes, resulted in the presence of the alkaloids catharanthine, vindoline and leurosine (Figure 1-8), all showing antidiabetic activity (Deutschländer et al., 2009).

An *in vivo* study conducted on rats showed that *D*-pinitol (Figure 1-3), a compound isolated from Pinaceae and Leguminosae plants, and used in the management of diabetes, played a positive role in the regulation of insulin-mediated glucose utilization in the liver through translocation and activation of the PI3K/Akt signalling pathway (Gao et al., 2015).

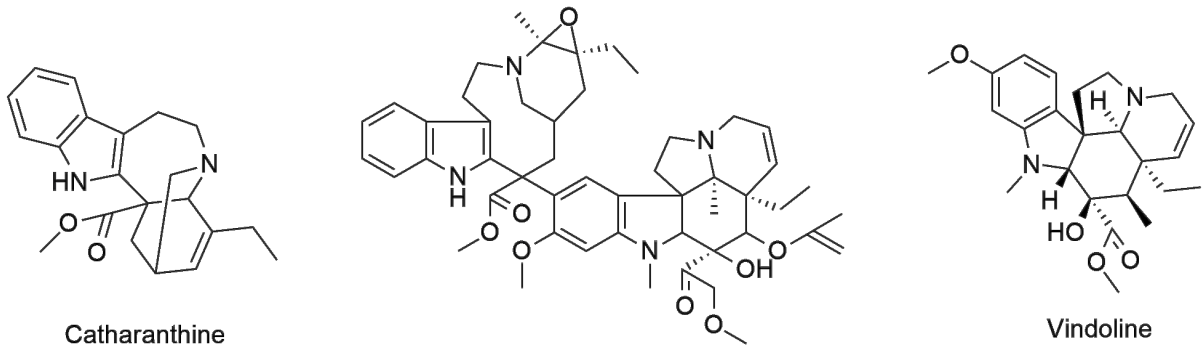

Figure 1-8: Antidiabetic compounds from *Catharanthus roseus*

Table 1-2: South African plants with antidiabetic activity

Family Name	**Scientific Name**	**Local Name and Region where used**	**Plant part used**	**Methods of Herbal Material Preparation**	**References**
Alliaceae	*Allium sativum L. fam.*	Garlic (English), Ikonofile (IsiZulu), Ivimbampunzi (IsiXhosa)	Whole plant	The plant parts are used to make an infusion that is taken orally	(Thomson et al., 2007)
Anacardiaceae	*Sclerocarya birrea (A. Rich)* Hochst. *subsp caffra*	Cider/Marula (English) Umganu (Zulu)	Bark	The bark is used to make a decoction, which is taken orally	(Ojewole et al., 2006, Thomson et al., 2007)
Anacampserotaceae	*Anacampseros ustulata E.Mey. ex Fenzl*	Igwele (IsiXhosa)	Corns	Aqueous extract which is taken orally	(Oyedemi et al., 2009)
Asphodelaceae	*Aloe ferox* Mill	Ikhala (IsiXhosa), Bitter Aloe (English), Inhlaba (IsiZulu)	Leaves	The leaves are used to make an infusion which is taken orally	(Loots et al., 2011, Sibuyi et al., 2007)
Asphodelaceae	*Bulbine frutescens (L.)* Willd.	Ibhucu (IsiXhosa)	Roots	The root is used to make a decoction which is taken orally	(Erasto et al., 2005)
Cactaceae	Opuntia *ficus-indica* Mill.	Motloro; Limpopo Province	Roots	The roots are used to make a decoction which is taken orally	(Frati et al., 1990)
Asteraceae	*Herichrysum petiolare* H & B.L.	Imphepho	Whole plant	The different parts are used to make a decoction which is taken orally	(Grauso et al., 2020)
Caryophyllaceae	*Dianthus thunbergii* S.S.Hooper forma thunbergii.	Indlela-zimhlope	Roots	The roots are used to make a decoction which is taken orally	(Erasto et al., 2005)
Cucurbitaceae	*Cucurbita pepo* L.	Intsunga (pumpkin leaves)	Upper parts (leaves and stems)	Leaves and stems are crushed and used to make a decoction which is taken orally	(Odeyemi and Bradley, 2018)

Family Name	Scientific Name	Local Name and Region where used	Plant part used	Methods of Herbal Material Preparation	References
Buddlejaceae	*Chilianthus olearaceus* Burch.	Umgeba	Leaves, and twigs	The twigs are used to make a decoction which is taken orally	(Boaduo et al., 2014)
Asteraceae	*Artemisia afra* Jacq. ex Willd.	Umhlonyane (IsiXhosa) African wormwood	Leaves, roots	The roots and leaves are used to make a decoction; which is taken orally	(Erasto et al., 2005)
Asteraceae	*Herichrysum nudifolium* L.	Ichochol	Leaves, roots	The leaves are used to make an infusion which is taken orally	(De Wet et al., 2013)
Stilbaceae	*Nuxia floribunda* Benth.	Umlulama (forest elder)	Whole plant	The different parts are used to make a decoction which is taken orally	(Erasto et al., 2005)
Poaceae	*Cymbopogon citrutus* Stapf	Isiqunga (lemon grass)	Whole plant	The different parts are used to make a decoction which is taken orally	(Boaduo et al., 2014)
Hyacinthaceae	*Hypoxis iridifolia* Baker Monna maledu	Monna maledu; Limpopo Province	Roots	The roots are used to make a decoction which is taken orally	(Boaduo et al., 2014, Ojewole, 2006)
Hyacinthaceae	*Hypoxis hemerocallidea* Fisch. & C. A	African potato Inongwe	Corms	The plant crushed and used to make a decoction that is taken orally	(Semenya et al., 2012)
Fabaceae	*Lessertia microphylla* (Burch. Ex DC.) Goldblatt & J.C. Manning	Mosapelo; Limpopo Province	Roots	The roots are used to make a decoction which is taken orally	(Semenya et al., 2012)
Cucurbitaceae	*Momordica balsamina* L.	Mothwatwa; Limpopo Province	Roots	The roots are used to make a decoction which is taken orally	(Boaduo et al., 2014)

Psidium guajava L. (Myrtaceae) commonly known as guava is known to possess hypoglycaemic activity. This was attributed to the flavonoids guiajaverin and quercetin as well as ellagic acid present in the plant (Figure 1-9) (Blancas-Benitez et al., 2017, Mensah et al., 2019). The indigenous plant *Leonotis leonurus* (L.) R.Br. (Lamiaceae), also known as wild dagga, is used by the Zulu, Xhosa, and Sotho for the treatment of several diseases and ailments, including diabetes mellitus. The plant has been found to contain the diterpenoid lactones premarrubiin and marrubiin (Figure 1-9). Marrubiin is known to enhance insulin secretion, according to an *in vivo* study conducted on rats (Newman and Cragg, 2016).

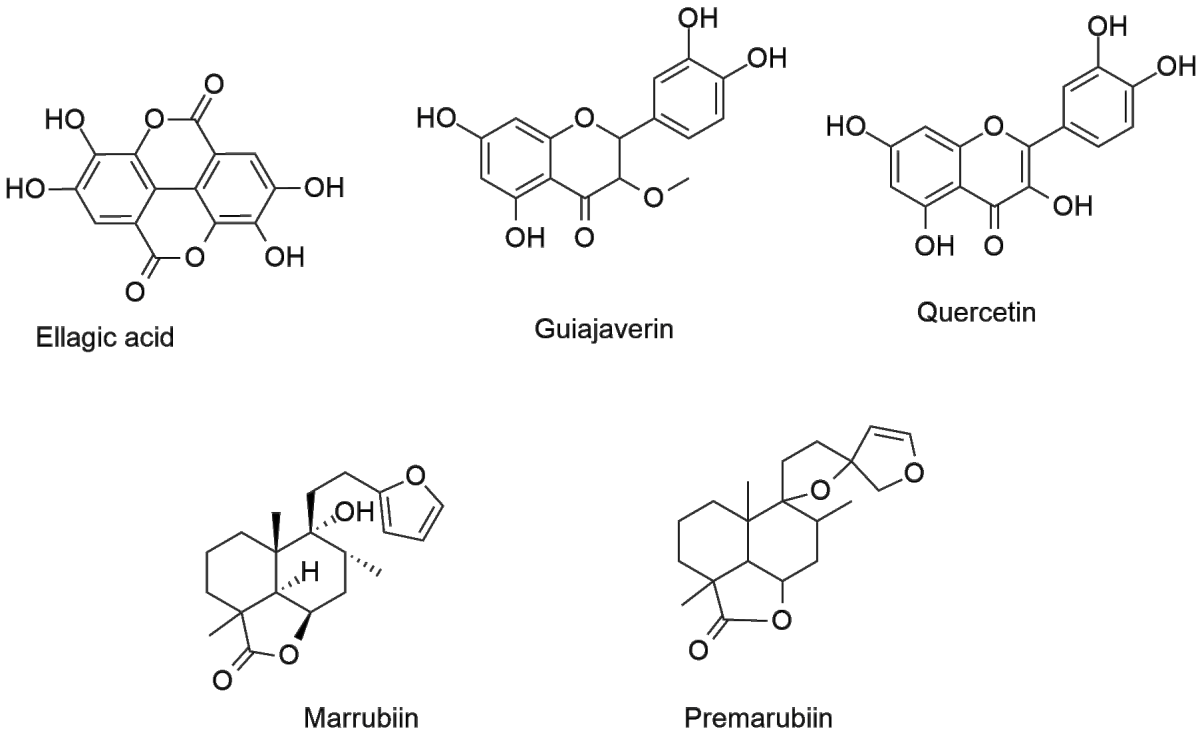

Figure 1-9: Antidiabetic compounds from *Psidium guajava* and *Leonotis leonurus*

1.2.4 Antidiabetic activity assays

Humans, plants, bacteria, fungi, and animals all produce the hydrolytic enzyme *α*-amylase that catalyse the hydrolysis of starch. Its activity is affected by the presence of a metal co-factor (calcium). Amylases are found in the salivary glands, which secrete the enzyme into the mouth, and the pancreas, which in turn secretes the enzyme into the small intestine in humans.

Amylases are endo-acting enzymes since they attack the inside of starch chains. Starch, the most common storage polysaccharide in plants, is a macromolecule composed of two types of polysaccharides, amylose and amylopectin. Amylases, in particular, hydrolyze the α-(1→4)-glycosidic linkages in starch molecules, resulting in the production of maltose, maltotriose, maltotetraose, maltodextrins, fructose and glucose (Kim et al., 2014, Oyedemi et al., 2009).

Glycosidase is another carbohydrate hydrolytic enzyme present in microorganisms, plants, animals and humans. It is found on the luminal surface of enterocytes and secreted into the small intestine. *α*-Glucosidase is a key enzyme that catalyzes the hydrolysis of disaccharides (maltose and sucrose) into monosaccharides (glucose and fructose). As a result, inhibition of α-glucosidase can delay blood sugar elevation and reduce postprandial hyperglycemia (Kim et al., 2014).

1.3 Antibiotic resistance

Antibiotic resistance is currently one of the most significant global public health concerns. It occurs when bacteria acquire the ability to withstand antibiotics that were previously effective against them. According to the World Health Organization, it is projected that by 2050, approximately 4.1 million people in Africa may lose their lives as a result of infections resistant to antibiotics (WHO, 2018b). Antibiotic resistance is an innate characteristic in specific bacterial strains. It can also be acquired through genetic alterations, or transferred between bacteria. The result is mutated variants with a better chance of survival against currently used antibiotics. Being resistant to antibiotics, they can rapidly spread through entire populations, and with globalisation being so rife in the 21st century can lead to epidemics and pandemics, similar to the recent COVID-19 pandemic experienced in 2020-2022. Contagious diseases are

normally transmitted through physical contact, coughing, sneezing, and bodily fluids (Adedeji, 2016).

Antibacterial agents are drugs capable of inhibiting bacterial growth and at the same time not harmful to the host. These compounds act as chemo-therapeutic agents for the treatment or prevention of bacterial infections. An antibacterial agent is considered as bactericidal if it kills bacteria or as bacteriostatic if it inhibits their growth. Methods such as agar well diffusion, broth dilution and disk diffusion have been adopted for the assessment and investigation of antibacterial activity *in vitro* (Van Vuuren, 2008).

Medicinal plants may have different mechanisms and modes of action to treat antimicrobial resistance compared to currently used antibiotics (Motyl et al., 2005)**.** This is due to the synergistic effects of antibacterial compounds that may be present in the plant extracts which show antibacterial activity. Extracts from medicinal plants have better therapeutic potential than synthetic drugs due to having fewer side effects and lower chances of the microorganisms developing resistance to them (Silva and Fernandes Júnior, 2010). The effectiveness of medicinal plant extracts to inhibit bacterial growth is related to the synergistic effect between active compounds in the extracts (Sofowora et al., 2013, Street and Prinsloo, 2013).

1.3.1 Medicinal plants with good antibacterial activity

In response to the shortage of novel antibiotics and the increase in antibiotic resistance, plants may offer a promising solution. They possess a range of efficient defence mechanisms, including the production of secondary metabolites to fend off pests and pathogens before they can cause significant harm to the plant. In a study of more than 80 Fabaceae plant species, the most active antibacterial plants were *Dichrostachys cinerea* (L.) Wight & Arn*., Albizia*

myriophylla Benth*, Glycyrrhiza triphylla* Fisch. and *Copaifera publifora* Benth (Chassagne et al., 2021).

Dichrostachys cinerea is a shrub found mostly in Africa, whose leaves and fruits are used for the treatment of diarrhea, fever and headache (Shandukani et al., 2018). The methanol and dichloromethane extracts of the plant showed an MIC of 0.19 µg mL^{-1} against *Staphylococcus epidermidis* (Nciki et al., 2016).

Psidium guajava commonly known as guava, has been traditionally used to help with diarrhea. It is also used for various other health issues such as treating bacterial infections, coughs, diabetes, stomach problems, fevers, and more (Hirudkar et al., 2020). The methanol and acetone extracts from guava leaves can inhibit the growth of certain bacteria. Methanol leaf extracts showed MICs ranging from 31 to 128 µg mL^{-1} against *Staphylococcus aureus, Pseudomonas aeruginosa,* and *Enterobacter aerogenes.* The acetone extract of the leaf demonstrated a MIC of 78 µg mL^{-1} against *Salmonella typhi, Enterococcus faecalis* and *Shigella flexneri* (Dzotam and Kuete, 2017). The reason behind this antibacterial effect is likely a combination of various natural compounds present in guava leaves, including quercetin, quercetin derivatives, kaempferol, avicularin, guiajaverin, and morin glycosides (Figure 1-9 and Figure 1-10) (Sanches et al., 2005).

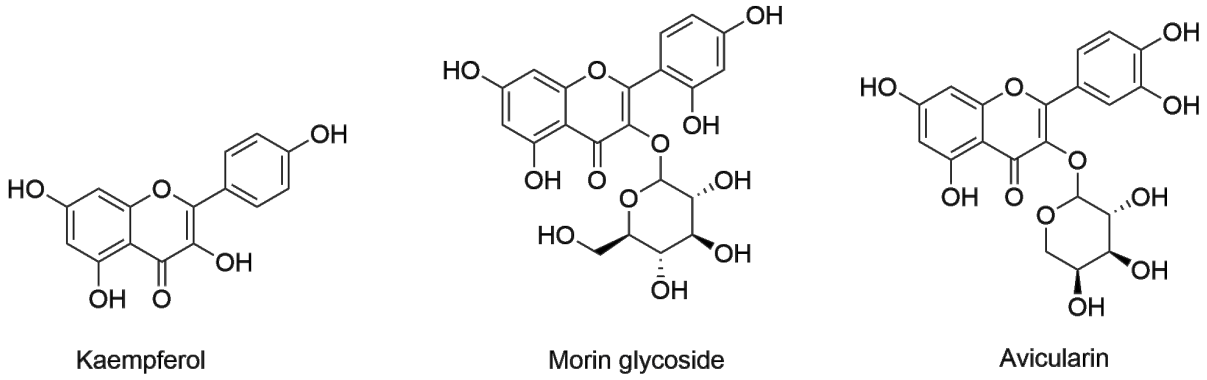

Figure 1-10: Structures of kaempferol, avicularin and morin glycoside

The *Acacia karroo* tree is found in various parts of southern Africa. Its gum is used to treat conditions like abscesses, oral problems, and osteomyelitis, while the bark is used to treat colds, diarrhea, dysentery, influenza, haemorrhage, ringworm, and stomach-ache. Additionally, the tree's root is employed in managing genitourinary disorders such as gonorrhoea, syphilis, urinary schistosomiasis, and venereal diseases (Maroyi, 2017). The methanol extract from the tree's aerial parts were shown to inhibit the growth of *S. aureus, Micrococcus luteus*, and *Pseudomonas aeruginosa*, with MICs ranging from 7.5 to 125 μg mL^{-1}. Furthermore, the methanol extract from the tree's stems have MICs of 78 to 156 μg mL^{-1} against bacteria such as ampicillin-resistant *Klebsiella pneumoniae*, MRSA, and *β*-lactamase producing *E. coli*. This biological activity has been attributed to compounds such as *β*-sitosterol and epigallocatechin (Figure 1-11) (Nyila et al., 2012).

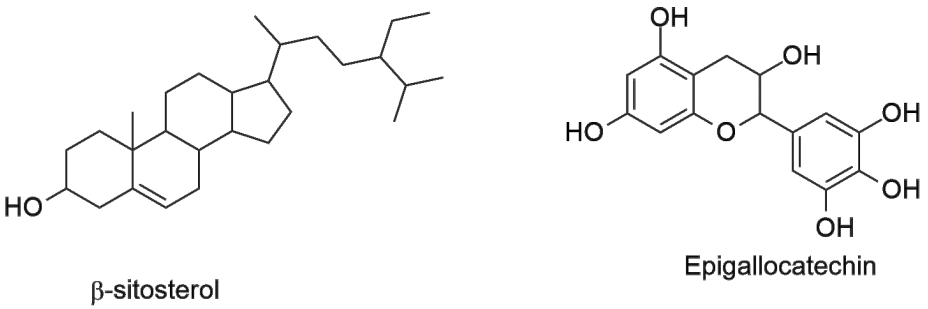

Figure 1-11 The structures of sitosterol and epigallocatechin

1.3.2 Plant derived compounds with good antibacterial activity

Licochalcone A, obtained from the roots of *Glycyrrhiza inflata* Batalin (Fabaceae) and *Glycyrrhiza glabra* L, exhibited potent inhibition in the growth of *S. aureus* (Simmler et al., 2017). In a study by Zuo et al. (2016), coumarins isolated from *Zanthoxylum nitidum (Roxb.)* DC. (Rutaceae) roots were investigated for their activity against *S. aureus* strains. Among the isolated coumarins, artanin and 5-geranyloxy-7-methoxycoumarin demonstrated the highest activity. Notably, 5-geranyloxy-7-methoxycoumarin and artanin (Figure 1-12) were

particularly effective against both *S. aureus* and MRSA, with both having minimum inhibitory concentrations of 8 μg mL^{-1}. In the same study, phellopterin exhibited strong activity against a susceptible *S. aureus* strain and moderate activity against MRSA with minimum inhibitory concentrations of 8 and 16 μg mL^{-1} respectively.

Dzotam and Kuete (2017) explored the growth inhibitory properties of two flavones, 3′,4′,7-trihydroxyflavone and 6-prenylpinocembrin (Figure 1-12), isolated from *Myristica fragrans* Houtt. (Myristicaceae). The flavone 3′,4′,7-trihydroxyflavone showed good activity against *Providencia stuartii* and *E. coli*, with minimum inhibitory concentrations of 4 and 8 μg mL^{-1} respectively and moderate activity against *K. pneumoniae* with an activity of 32 μg mL^{-1}. Additionally, 6-prenylpinocembrin displayed strong activity against *E. coli, K. pneumoniae,* and *S. aureus*, with moderate activity against *E. faecalis* and *P. aeruginosa* with MICs of 16 and 32 μg mL^{-1} respectively.

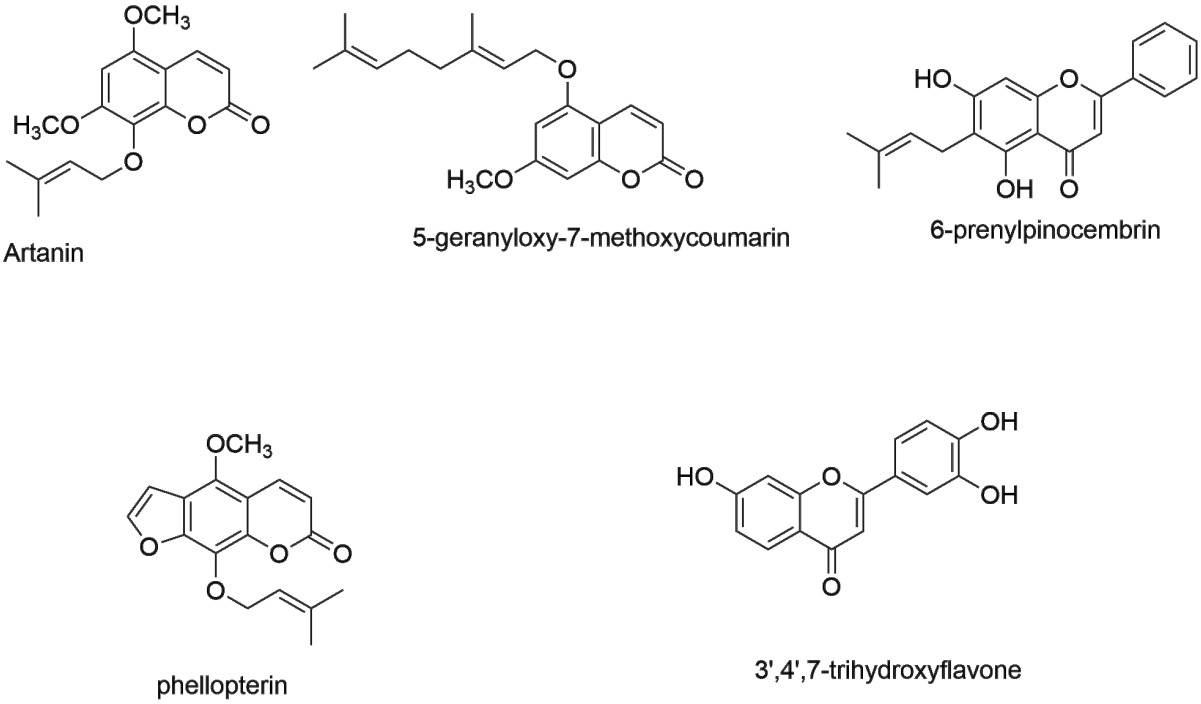

Figure 1-12: Coumarins and flavonoids with antibacterial activity from *Zanthoxylum nitidium* and *Myristica fragrans*

Two glycosides, 3-*O*-*β*-D-glucopyranosyloxy-4-methyl-2(5*H*)-furanone and pinnatoside A (Figure 1-13) isolated from the stems of *Paullinia pinnata* (Sapindaceae) had a moderate effect on *Salmonella enterica* but a high efficacy against *E. aerogenes*, *P. aeruginosa*, and *Klebsiella pneumoniae* with MIC of 1.562 μg mL^{-1} (Tamokou et al., 2012). Only pinnatoside A was active against *E. coli*. The plant has traditionally been used to treat malaria, erectile dysfunction, and a variety of bacterial diseases.

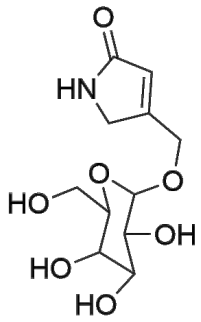

Pinnatoside A

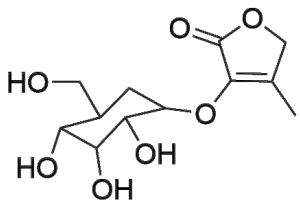

3-O-β-D-glucopyranosyloxy-4-methyl-2(5*H*)-furanone

Figure 1-13 Antibacterial compounds from *Paullinia pinnata*

The fatty acid, 3-(dodecanoyloxy)-2-(isobutyryloxy)-4-methylpentanoic acid, isolated from *Sigesbeckia glabrescens* (Makino) (Asteraceae) aerial portions showed moderate to high activity in *S. aureus, B. subtilis, S. pyogenes* and *E. faecalis,* with minimum inhibitory concentrations of 3.12, 6.25, 6.25 and 25.0 μg mL^{-1} respectively. Three fatty acids, dodec-9,11-diynoic acid, (12*E*)-heptadec-12-en-8,10-diynoic acid, and exocarpic acid (Figure 1-14) were extracted from *Thesium chinense* Turcz. (Santalaceae). Exocarpic acid showed moderate antibacterial activity with minimum inhibitory concentrations of 13.7 μg mL^{-1} against *Streptococcus mutans* and strong activity against *Fusobacterium nucleatum* and

Porphyromonas gingivalis with minimum inhibitory concentrations of 3.4 and 0.86 μg mL^{-1} respectively (Lee et al., 2013).

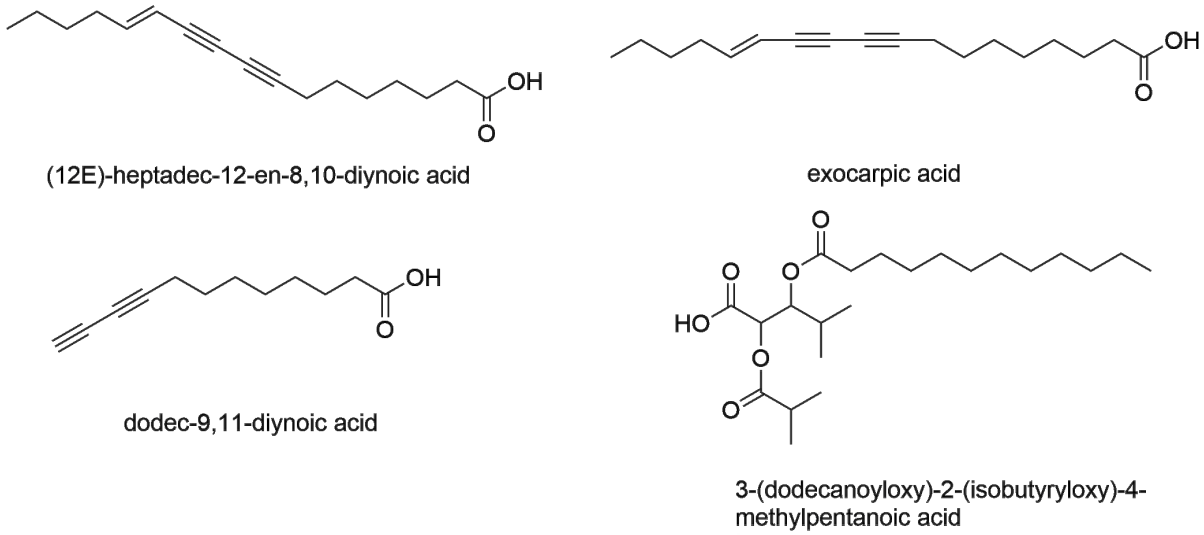

Figure 1-14: Fatty acids with good antibacterial activity

1.4 Nutrients and anti-nutrients in plants

The WHO and Food and Agriculture Organisation (FAO) review the major nutrient requirements and recommended dietary intake for all age groups each decade. They then update parameters such as trace elements, fats, oils, carbohydrates, vitamins and minerals for human nutrition (WHO, 2019b). These trace elements and biomolecules are essential for a number of metabolic activities, including formation of seeds, fruit, roots, flowers, hormones, cell and plant tissues, and physiological processes such as fertilization and protein synthesis. They are also involved in the synthesis and transport of carbohydrates and calcium, and play a role in the structural and physiological stability of an organism. They are categorised as either macronutrients or micronutrients (Soetan et al., 2010).

Macronutrients include carbohydrates, lipids and proteins, and are usually required in large amounts. Carbohydrates supply energy for metabolic functioning, and is essential for the optimal functioning of brain cells, the nervous system and blood. Carbohydrates are made up

of simple and complex sugars obtained from one's diet. Proteins are a source of amino acids, used as building blocks for proteins and enzymes. They help maintain tissues, regulate water and in supplying energy to an organism. Lipids are a source of energy as well as being insulation for organs and responsible for absorption of fat-soluble vitamins (DalCorso et al., 2014).

Calcium is primarily responsible for strong and healthy bones and teeth, but is also an essential element in blood clotting, stabilizing blood pressure, and assisting with brain function. Excess Ca levels leads to fatigue, muscle and joint pain, vomiting, constipation, abdominal pain, extreme urination and thirst (Mehri, 2020). Magnesium is important for strong and healthy bones. It helps with functioning of muscles as well as the nervous and immune systems; it assists in regulating blood sugar levels and blood pressure, and has a role in protein synthesis. High Mg levels can lead to lowered blood pressure, cardiac problems, reduced kidney function, weakening of muscles, respiratory complications and diarrhoea (Jahnen-Dechent and Ketteler, 2012).

Chromium acts together with insulin to regulate blood sugar levels, has a role in building muscle mass, lowering cholesterol and helps to regulate blood pressure, however excess chromium causes nostril and skin irritation, can lead to stomach ulcers, respiratory problems and male reproductive defects. Chromium is normally expelled before becoming lethal and generally does not cause poisoning. Copper is important for the functioning of melanin, maintaining the sheath that covers the nerves, assists with phospholipid and haemoglobin biosynthesis, and responsible for healthy hair. It also plays a role in the biosynthesis of enzymes needed for oxidation of fatty acids, however excess concentrations can also cause cancers and renal failure (Laudermilk et al., 2012, Mehri, 2020).

Cobalt is found in vitamins B12 and C. It assists in absorbing Fe and with functioning of the heart. Excess Co can cause liver damage, neurological problems, impaired senses, seizures and headaches, as well as cancer, tissue death and hip problems (Lange et al., 2017). Manganese is important in tissue and bone formation, preventing osteoporosis and for controlling blood sugar levels, brain and nerve function and preventing arthritis, diabetes, and epilepsy. Excessive amounts of Mn can affect the nervous system and brain, cause behavioural changes, reproductive effects, and lung irritation. Iron is an important component of haemoglobin and the production of red blood cells, as well as the transport of oxygen, but can also cause liver damage, heart disease and cancer at increased concentrations (DalCorso et al., 2014).

At low concentrations, nickel is used to build strong bones, absorb Fe and has a role in breaking down glucose and the formation of enzymes. At higher concentrations, it can cause eczema, cancer, nasal problems, sinusitis, bronchitis, asthma, kidney toxicity and shortness of breath, (Hassan et al., 2019). In low concentrations, Selenium contributes to protein synthesis, prevention of cell damage, and prevention of cancer and heart disease. It can also assist with the recovery from metal toxicity. Increased amounts of selenium causes hair loss, irritability, fatigue, nerve damage, gastrointestinal pains, kidney and liver problems and blood clotting (Mehdi et al., 2013). Zinc has a role in DNA synthesis, ensures a healthy immune system and helps heal wounds. An excess of Zn can cause vomiting, diarrhoea, increased urine output, gastrointestinal pains, low blood pressure and convulsions (Shahzad et al., 2018).

Toxic elements are those elements which affect the health of individuals, even at low concentrations, and can lead to poisoning and death. This is dependent on the speciation of the element. These elements should therefore not be ingested or inhaled, and if they are, should be expelled by the body as quick as possible. Cadmium, is a highly toxic element, causing damage

to lungs, liver and kidneys, and can lead to vomiting, diarrhoea, weak bones, anaemia and brain damage. It is also linked to mental illness, and can cause cardiovascular and skin problems. When accumulated in the kidneys, it leads to hypertension. It can displace Zn, leading to a loss of function of certain organs and enzymes (Jaishankar et al., 2014).

Both arsenic and lead are not essential elements and toxic at very low concentrations. In trace amounts, arsenic can help produce red and white blood cells and the growth of hair, nails, skin, bones and teeth. Slightly higher concentrations will lead to vomiting, bloody diarrhea, and stomach pain. It also leads to thickening and blotching of the skin, cancer, diabetes and reproductive problems. It can cause seizures, nervous systems disorders, and even death. In trace amounts, lead has been known to help with bone, muscle and brain function. However, slightly higher concentrations can cause anaemia, irritability, seizures, comas, heart attacks and kidney failure (Moodley et al., 2013, Suriyagoda et al., 2018).

In summary, Ca, Mg, Fe, Mn, Zn, Ni, Cu, Se, Cr and Co are essential for the body's functioning as long as they are not present in amounts in excess of what is needed. Cd, As and Pb however are non-essential elements, toxic even at low concentrations.

1.5 Dietary reference intakes (DRIs)

Dietary reference intake (DRI) is a term used to describe the amounts of nutrients one needs to consume, and provides information on several reference values: estimated average requirements (EAR); recommended dietary allowances (RDA); adequate intake (AI); tolerable upper intake limits (UL); and acceptable macronutrient distribution ranges (AMDR). Age, gender, growth, pregnancy and lactation plays a role in these values.

The one most commonly used and referred to is the recommended dietary allowances (RDAs), and describes the amount of nutrients needed to adequately meet the needs of a person (Table

1-3). Tolerable upper intake levels (ULs) is another important reference value, and is the highest level of daily nutrient intake regarded as safe with no risk of illness or death (Table 1-4).

Table 1-3: Recommended Dietary Allowances (RDAs) of essential elements for individuals

Life Stage (yr)	Ca	Mg	Fe	Mn	Zn	Cu	Se	Cr
	(mg d^{-1})					(µg d^{-1})		
Children (1-3)	700	80	7	1.2	3	340	20	11
Children (4-8)	1000	130	10	1.5	5	440	30	15
Adults (9-18)	1300	240-410	8-11	1.9-2.2	8-11	700-890	40-55	25-35
Adults (19-70)	1000	400-420	8	2.3	11	900	55	35
Adults (>70)	1200	420	8	2.3	11	900	55	30

* Neither Recommended Dietary Allowances nor Adequate Intakes have been established for nickel.

Table 1-4: Tolerable Upper Intake Levels (ULs) of essential elements for individuals

Life Stage (yr)	Ca	Mg	Fe	Mn	Zn	Ni	Cu	Se	Cr
	(mg d^{-1})						(µg d^{-1})		
Children (1-3)	2500	80	40	2	7	0.2	1000	90	ND
Children (4-8)	2500	130	40	3	12	0.3	3000	150	ND
Adults (9-18)	3000	385	40-45	6-9	23-34	0.6-1	8000	400	ND
Adults (19-70)	2500	420	45	11	40	1	10000	400	ND
Adults (>70)	2000	420	45	11	40	1	10000	400	ND

1.6 Phytochemical and analytical techniques

The following phytochemical and analytical techniques have been used to achieve the objectives of the study which included extraction, isolation and characterisation of phytocompounds from *S. serratuloides.*

1.6.1 Extraction

Solvent extraction is a method commonly used to remove compounds from within a plant into a solvent. It involves adding solvent to a mass of dried plant sample and allowing it to shake on an orbital shaker (Figure 1-15), typically between 1-3 days. Another typical method is Soxhlet extraction, however this method can lead to artefacts and involves hot solvent extraction. The solvent is filtered and evaporated in order to obtain the crude extract after which another solvent of a higher polarity is then added to the same plant material to remove compounds of a higher polarity. The crude extract is then the mass that remains after solvent evaporation (Patil et al., 2012).

Figure 1-15: Image of an orbital shaker used for extraction.

1.6.2 Column chromatography

Column chromatography is used to separate components in crude extracts and to purify them, resulting in pure compounds that could be subject to biological testing. This technique uses a glass column (Figure 1-16) filled with a stationary phase (commonly silica gel) and a mobile phase which is generally organic solvents alone or in combination that runs through the column, either being forced through the column by pressure or allowed to pass through by gravity. Eluted fractions are collected from the column into a receiving beaker and monitored by thin-layer chromatography (TLC) (Coskun, 2016).

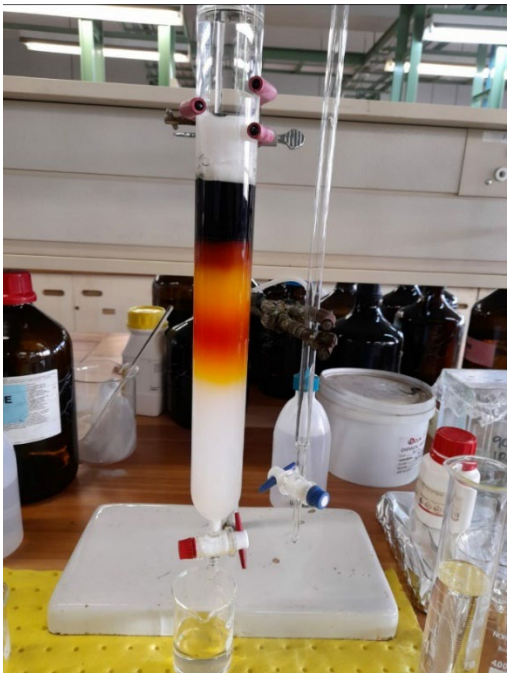

Figure 1-16: Separation of a crude extract in a typical glass column.

1.6.3 Thin-layer chromatography (TLC)

Thin-layer chromatography (TLC) is a solid-liquid adsorption chromatography, which is one of the most inexpensive and simple techniques used to separate organic substances. The stationary phase is a solid adsorbent material such as silica gel supported on a glass or aluminium plate. This technique is used to monitor the progress of a chemical reaction and determine the purity of isolated compounds during the separation and purification process. The

plate with a small aliquot of sample spotted at the bottom (Figure 1-17) is placed in a tank containing a mobile phase, which is either a single solvent or combination of organic solvents. The components travel up the plate through capillary action, the non-polar compounds travelling further up the plate than the more polar ones. Retention factor (Rf) values (ratio of the distance that the molecule travelled to the distance that the solvent travelled) are determined, and these values are specific for a certain organic compound. Compounds with similar Rf values are deemed to be similar in polarity, and together with the colour from suitable stains are normally combined, purified and subject to further analytical techniques such as NMR to determine their purity and structure (Ciura et al., 2017).

$$Rf = distance\ of\ molecule\ travelled\ /\ distance\ solvent\ travelled$$

Figure 1-17: Image of a thin layer chromatographic plate

1.7 Spectroscopic techniques

The following spectroscopic techniques have been used to characterise the isolated phytocompounds. These methods are based on the interaction of radiation and matter. The amount of radiation produced or absorbed by molecular or atomic species is measured using suitable instruments. These measurements are based on electromagnetic radiation.

1.7.1 Nuclear magnetic resonance (NMR) spectroscopy

Nuclear magnetic resonance (NMR) spectroscopy works on the property and principle of magnetic field effects. It is used to determine the chemical structure of a compound by the environment the atoms find themselves in a molecule and the interaction between NMR active nuclei. When molecules are placed in a strong magnetic field the magnetic moment of nuclei aligns with the magnetic field. This equilibrium can be disturbed by applying radio frequency (RF) radiation, which brings the nuclei into an excited state. When nuclei return to equilibrium by emitting RF radiation, this change in radiation is detected and plotted against the intensity, resulting in an NMR spectrum (Hofmann, 2010).

Slight increases and decreases in this radiation brought about by neighbouring NMR active nuclei, depending on whether they are aligned with or against the applied magnetic field, results in splitting of the resonance and splitting patterns (doublets, triplets, quartets, quintets etc.) that are most useful in structural determination. The exact frequency of the radiation is depended upon the chemical environment. Figure 1-18 shows a picture of the NMR spectrometers housed in the School of Chemistry and Physics at the University of KwaZulu-Natal, Durban, South Africa.

A number of experiments can be carried out using NMR. These experiments include proton (^{1}H) and carbon (^{13}C) NMR, both 1D experiments, and are the most commonly acquired spectra. They show the chemical shifts of proton resonances, together with their chemical shifts. These days, proton and carbon NMR spectra are standardly used to prove the structures of molecules either synthesised or found in plants and microbes. 1D DEPT (distortionless enhancement by polarization transfer) is used to differentiate between CH, CH_2 and CH_3 carbon resonances. Among the 2D spectra, a COSY (homonuclear correlation spectroscopy)

spectrum is used to determine resonances coupled to each other in a vicinal environment, while a NOESY (nuclear Overhauser effect spectroscopy) spectrum allows one to see which proton resonances are close to each other through space interactions. HSQC (heteronuclear single quantum correlation), is a 2D experiment that correlates proton resonances to carbon resonances to which they are directly attached. HMBC (heteronuclear multiple-bond correlation), is quite a useful 2D experiment that correlates carbon and proton resonances normally 2 and 3 bonds away (neighbours) from each other. At times, 4 bond correlations can also be seen in the HMBC spectrum.

Figure 1-18: Bruker Avance III NMR instrument, a) 400 MHz and b) 600 MHz

1.7.2 Fourier-transform infrared spectroscopy (FTIR)

Fourier-transform infrared spectroscopy (FTIR) makes use of the vibration of bonds and produces a spectrum that can be used to identify functional groups for the identification of pure organic and inorganic compounds. Each IR spectrum has a unique pattern that can be used to

identify a compound if a spectrum of the compound is known. This technique is quick and inexpensive and often used in forensics. For structural elucidation of organic compounds in natural products chemistry, it is used to identify functional groups in the molecule, particularly hydroxy and carbonyl functional groups. The technique has been proven to possess high sensitivity, resolution and great speed (Hofmann, 2010).

1.7.3 Gas chromatography-mass spectrometry

In gas chromatography-mass spectrometry (GC-MS), the gas chromatograph operates by heating a sample, converting it to the gaseous phase to separate its volatile components. These gaseous substances are then carried through a column using an inert gas such as helium. Compounds are separated based on their chemistry and affinity to the column packing. As they exit the column, they enter the mass spectrometer (MS) where they undergo fragmentation. The mass spectrometer measures the mass-to-charge ratio (*m/z*) of ions generated from the sample (Sparkman et al., 2011). Most of these ions have a single positive charge (z = 1).

There are various sources for ionization in MS, with one of the most commonly used being electron impact. In this method, molecules are bombarded with high-energy electrons, ejecting electrons from the sample and breaking weak bonds leading to the fragmentation of the molecule, resulting in the production of positive ions, negative ions, and neutral species. These fragments are valuable in identifying the specific molecular species that enter the spectrometer.

1.8 Problem statement

Diseases such as diabetes mellitus is one of the recent concerns in healthcare around the world. It is a widespread metabolic health issue with significant impact on healthcare (Odeyemi and Bradley, 2018), and particularly alarming in South Africa, where the healthcare system is

already overburdened by the rising prevalence of tuberculosis (TB) and the human immunodeficiency virus (HIV). A better alternative to the currently used drugs for diabetes with fewer side-effects would be highly desirable.

Effective treatment of infectious diseases is threatened globally by antimicrobial resistance (AMR). Inappropriate prescription of antimicrobial drugs and their application in agriculture, contribute to AMR. Concomitantly, there has been a reduction in the number of new antibiotics (WHO, 2018b). The global annual mortality caused by AMR is on an upward trajectory, currently standing at approximately 750 000 deaths, with estimates suggesting it could surge to as much as 10 million by 2050 (O'Neill, 2016).

The consumption of medicinal plants for their organic components does not preclude intake of the inorganic constituents, which could lead to poisoning. Heavy metals from the environment can easily be absorbed and stored by medicinal plants. Consumption of these "contaminated plants", can lead to serious illness brought about by metal toxicities. Both essential and toxic metals are detrimental to human health in high concentrations.

1.9 Aims and objectives

S. serratuloides is a plant that belongs to the Asteraceae family and widely used by traditional healers to treat a variety of health conditions, including the treatment of wounds, burns, sores, and ulcers (Suntar, 2014, Tata et al., 2020). In rural areas the plant is also used to treat stomach ulcers (personal communication). However, despite its prominent role in South African traditional medicine, no detailed phytochemical studies on *S. serratuloides* have been reported.

Aims

The aim of the study is to carry out a phytochemical analysis of *Senecio serratuloides* DC, isolating and identifying the secondary metabolites and analytically investigating the plant for both essential and toxic metals, providing a chemical profile of the plant, essential for its use as a herbal remedy. Subjecting the plant extracts to bioassays to assess their antibacterial and antidiabetic activity would provide scientific credence to using the plants for medicinal purposes, while publishing the data on essential and toxic metals would provide guidance on the dosage of the extracts to be used.

Objectives

- To extract and isolate the secondary metabolites from different parts of the plant using various organic solvents.
- To identify and characterize the phytocompounds using spectroscopic techniques, mainly Nuclear Magnetic Resonance (NMR) and Mass spectrometry (MS).
- To determine the elemental concentration in *S. serratuloides* collected from 10 different sites in KwaZulu-Natal using ICP-OES, and compare them to acceptable metal concentrations.
- To test the crude plant extracts for antidiabetic and antibacterial activities.

Chapter 2 A review of *Senecio* species

The genus *Senecio* is within the Asteraceae family, and comprises 1100 species, often used in Asia, South America and Africa as a food source and in traditional medicine as 'bush teas', anti-emetics and anti-inflammatories. Other traditional uses include the treatment of amenorrhoea, menopausal neurosis, leucorrhoea, influenza, diarrhoea, eczema, asthma, bronchitis, blood purification for skin eruptions, stomach-ache and burns (Barnes et al., 2007). This genus is known to produce secondary metabolites including alkaloids, saponins, sesquiterpenoids, phenols, flavonoids and semiquinones, and is particularly known for its pyrrolizidine alkaloids. Thus, it is an interesting subject for phytochemical analysis and leads for future drug development (Ali et al., 2018, Kumar and Mathela, 2018).

2.1 Asteraceae

Asteraceae is among the plant families containing the highest number of plant species, reaching into the thousands. The family contains widely distributed shrubs, herbaceous plants, and trees, constituting approximately 24 000 recognised species worldwide with approximately 1600 to 1700 genera. Plants belonging to Asteraceae are recognized due to their aggregate flower heads and fruits that are one-sided achenes. Numerous illnesses are treated with plants belonging to the Asteraceae (Michel et al., 2020, Moreira-Muñoz and Muñoz-Schick, 2007).

Flavonoids, phenolic acids, alkaloids, steroids, terpenoids, lignans, benzofuranones, lactones, jacaranones, saponins, and tannins have all been found in plants of Asteraceae. Various studies have shown that species belonging to the Asteraceae have attributes to combat bacterial and fungal infections, reduce inflammation, and impede the progress of tumorous growths (Rolnik and Olas, 2021).

Many traditionally used medicinal plants in this family have been well documented. The *Acmella oleracear* Murr species, belonging to the Asteraceae has been used since ancient times for its anti-inflammatory, antiseptic, and anaesthetic properties. Traditionally, the plant has been used to treat toothaches, throat infections, and to paralyze the tongue (Spinozzi et al., 2022). Another promising species in the Asteraceae is *Biden Pilosa* L. It has known therapeutic properties, such as its ability to stabilize blood sugar, safeguard the liver, mitigate inflammation, and lower blood pressure (Moreira-Muñoz and Muñoz-Schick, 2007). To combat serious illnesses, such as bronchitis, malaria, anaemia, and tuberculosis, traditional healers have used flowering branches of *Inula crithmoides* L. and *Parthenium hysterophorus* L., which are found worldwide and used in ethnomedicine for the treatment of various infections and degenerative diseases (Rolnik and Olas, 2021). Table 2-1 below summarises some of the common plant species found in this family.

Table 2-1: Medicinal plants found in the Asteraceae family

Scientific Name	**Plant part (s)**	**Ailment**	**Reference**
Vernonia natalensis Sch.	Leaf and roots	Used to treat malaria and kidney pain	(Semenya and Maroyi, 2019)
Calendula officinalis L.	Leaf	Used to treat fever and menstrual pains. Also used to heal skin wounds	(Verma et al., 2018)
Dicoma anomala Sond.	Roots	Roots are used to treat intestinal worms, diarrhoea, sores and wounds	(Balogun and Ashafa, 2017)
Eriocephalus africanus L.	Leaf	Used for coughs swelling, and delayed menstruation	(Magura et al., 2021)
Helichrysum odoratissimum L.	Leaf and stems	Commonly used for coughs, colds and insomnia	(Afuape et al., 2022)
Senecio serratuloides DC.	Leaf	Widely used to treat burns, internal and external sores	(Tata et al., 2020)
Osmitopsis asteriscoides L.	Leaf and stems	Used to treat colds, fever, cuts, and swelling	(Sello, 2020)
Eriocephalus punctulatus L.	Leaf	Used for treating urinary infections and for stomach diseases	(Lall and Kishore, 2014)

2.2 *Senecio serratuloides* DC

Senecio serratuloides (Figure 2-1) is commonly known as the "two-day-cure" or uNsukumbili in IsiZulu. It is a small woody herb growing up to a meter high with leaves containing serrated edges up to 60 mm long. The plant is widespread throughout South Africa and prevalent in KwaZulu-Natal and Eastern Cape (Gould et al., 2015). *S. serratuloides* is used widely in South Africa in traditional medicine and is one of the most commonly used plants to control hypertension, both alone and in combination with several other medicinal plants. The crushed and powdered leaves are used to treat swollen gums, chest pain, heal sores, cuts and burns (Kuete and Efferth, 2015). It is also used in Northern Maputuland together with heated leaves of *Ranunculus multifidus* to cleanse the blood during pregnancy, and ease labour pains (De Wet and Ngubane, 2014).

Figure 2-1: *Senecio serratuloides* DC in habitat (picture taken by Andile Gumede)

Pharmacologically, *S. serratuloides* has been reported to have antioxidant, antifungal and anti-inflammatory activities (De Wet et al., 2013, Tata et al., 2019, Van Vuuren and Holl, 2017). There is little information regarding its efficacy, however, it is known to contain hepatotoxic

pyrrolizidine alkaloids, which are toxic and can lead to cell damage, and liver and lung cancer (Mariri, 2017).

In South Africa, the herb *S. serratuloides* is recognized for its reported ability to accelerate the healing of cuts, sores, and burns. Whether in fresh, dried, or charred form, the leaves of this herb are directly applied to the wounds (Mariri, 2017, Tata et al., 2020). Studies have demonstrated the efficacy of *S. serratuloides* treatment in improving the healing process of deep partial thickness wounds in a pig model (Gould et al., 2015). In other studies, the hydro-ethanol extract derived from *S. serratuloides* demonstrated significant antihypertensive, antihyperlipidemic, and cardioprotective effects in rats and these findings affirm the plant's efficacy in traditional treatments for hypertension and suggest its potential as a candidate for the development of antihypertensive drugs (Tata et al., 2019, Tata et al., 2020).

2.3 Secondary metabolites from *Senecio* species

Secondary metabolites in *Senecio* species include jacaranones, alkaloids, flavones and terpenes (Kumar and Mathela, 2018, Saxena et al., 2013). In the Himalayan region, numerous *Senecio* species have been reported to have constituents such as eudesmolides, germacrene D, *β*-pinene, *β*-caryophyllene, *β*-longipinene, cuprenene, zingiberene, curcumene and carotol (Figure 2-2) (Kumar and Mathela, 2018).

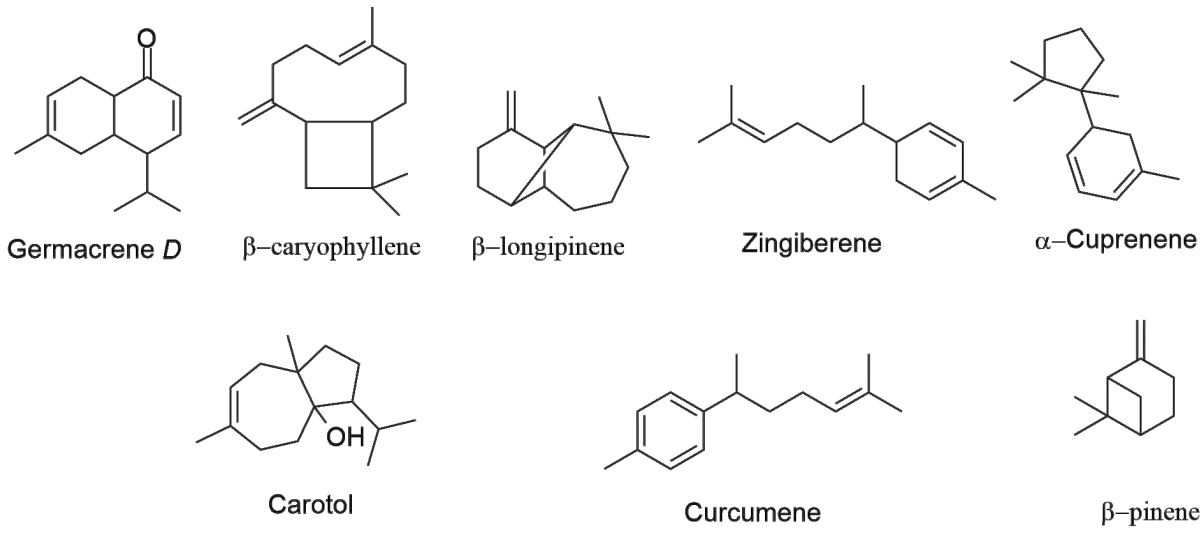

Figure 2-2 Compounds isolated from *Senecio* species in the Himalayan region

2.3.1 Alkaloids

Alkaloids are nitrogen containing compounds, usually heterocyclic, and are compounds of low molecular weight that form approximately 20% of all plant based secondary metabolites. They are usually colourless with a bitter taste. There are many classes of alkaloids that include isoquinoline, quinoline, pyridine-piperidine and pyrrolidine-pyridine. They were first isolated from medicinal plants in the nineteenth century (Saxena et al., 2013). Many of these compounds together with their synthetic derivatives are used as basic medicinal agents for bactericidal, antispasmodic and analgesic effects. Many species in the genus *Senecio* are rich in pyrrolizidine alkaloids that exhibit carcinogenic, hepatotoxic, antitumor and mutagenic activities. Pyrrolizidine alkaloids are classified based on their structure and include those with a saturated nucleus (non-toxic) and those with an unsaturated nucleus (toxic) (Barnes et al., 2007, Kaur and Arora, 2015).

Senecio species have been reported to contain pyrrolizidine alkaloids, tropane alkaloids, and indole alkaloids, some of which are poisonous to both humans and animals when consumed

(Alvarado-Avila et al., 2022, Bhambhani et al., 2021, Cortinovis and Caloni, 2015). Woolly groundsel, or *S. longilobus*, is a plant commonly known for its pyrrolizidine alkaloids, integerrimene and seneciphylline, which are reported to be toxic to sheep, cattle, and horses (Kalač and Kaltner, 2021). *Senecio nemerensis* L. is a medicinal plant frequently used to treat diabetes, and taken in the form of a herbal tea. The plant is a member of the *Senecio* tribe, known to contain pyrrolizidine alkaloids. The plant contains retroisosenine, senecionine, and seneciphylline (Figure 2-3) (Lu et al., 2021).

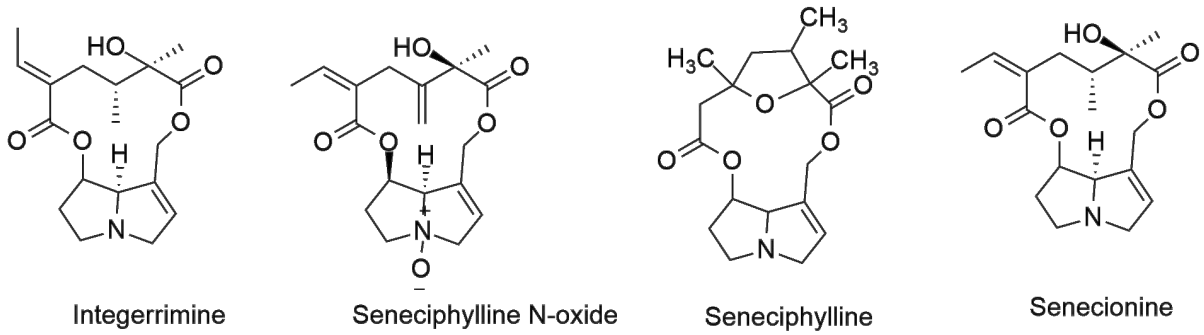

Figure 2-3: Pyrolizidine alkaloids from *Senecio longilobus* and *Senecio nemerensis*

Senecio vulgaris contains poisonous pyrrolizidine alkaloids, which makes it an especially destructive weed in horticultural and agricultural crops. Some pyrrolizidine alkaloids isolated from the plant include senkirkine, senecivernine, and retrorsine-*N*-oxide (Flade et al., 2019). *Senecio cannabifolius*, another plant that contains alkaloids, has been used to treat viral influenza and enteritis. Jaconine, retronecine-9-(3-acetoxy-2-hydroxy-2-methylbutanoate), 7-senecioate *N*-oxide, and seneciphyllinine are among the chemicals identified from this plant (Figure 2-4) (Niu et al., 2013).

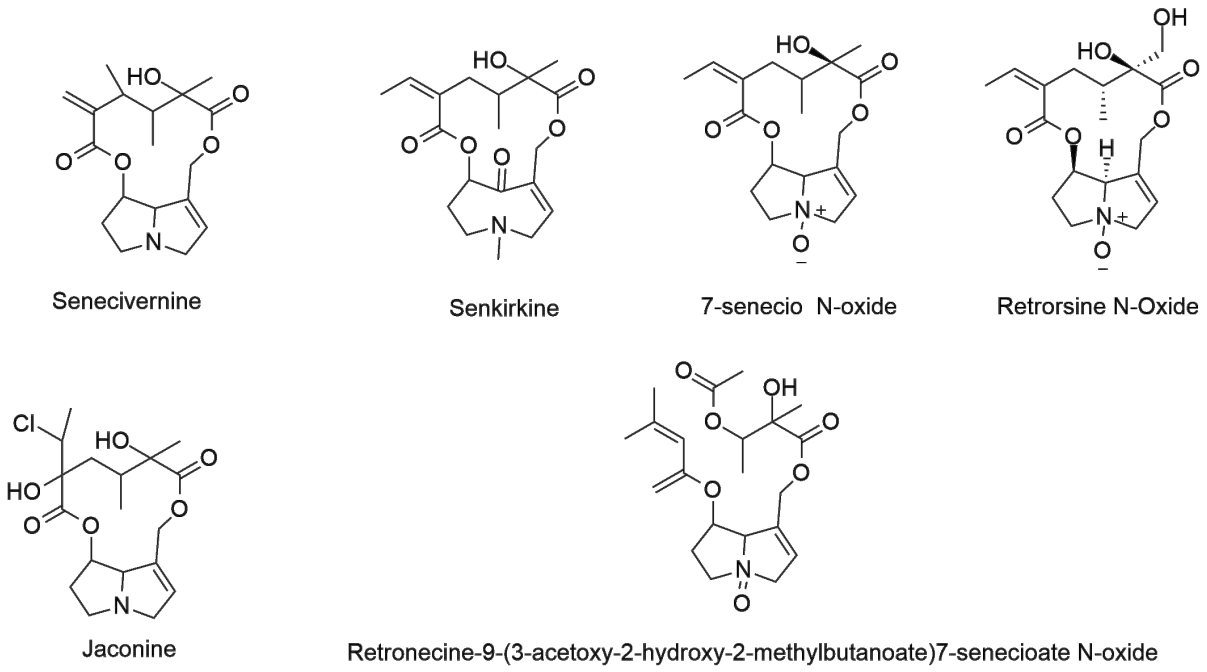

Figure 2-4 Pyrolizidine alkaloids from *Senecio vulgaris* and *Senecio cannabifolius*

Senecio jacobae and *Senecio scandenes* have yielded compounds such as planchonelline, jacidine, jacozine, sarracine, seneciphylline, and doronenine (Figure 2-5) (Lu et al., 2021).

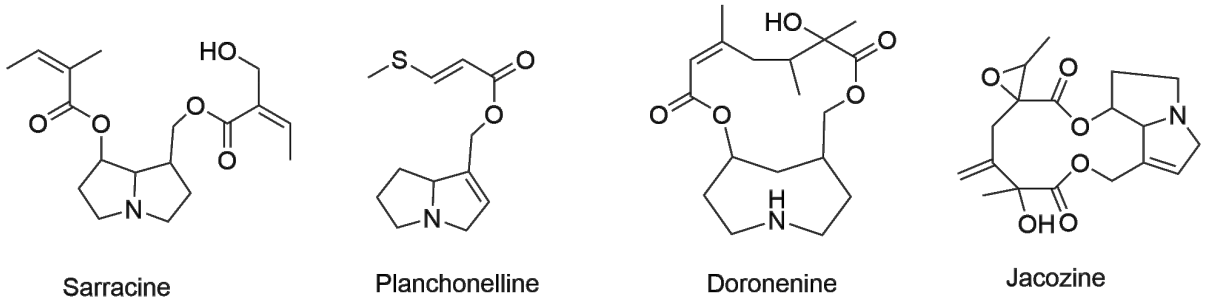

Figure 2-5 Pyrolizidine alkaloids from *Senecio jacobae* and *Senecio scandenes*

Two unsaturated pyrrolizidine alkaloids were extracted from *Senecio fistulosus*, identified as rosmarinine and 9-*O*-angeloylpetasinecine. Meanwhile, in *Senecio vernalis, S. nemerensis* and *S. adenotrichius*, senkirkine, senecionine, and seneciphylline (Figure 2-3 and Figure 2-4) emerged as the most prevalent pyrrolizidine alkaloids. Additionally, *Senecio aquaticus* was

found to contain erucifoline, erucifoline *N*-oxide, otosenine, ridelliine, lycopsamine, symphytine and lithosenine among its constituents (Figure 2-6).

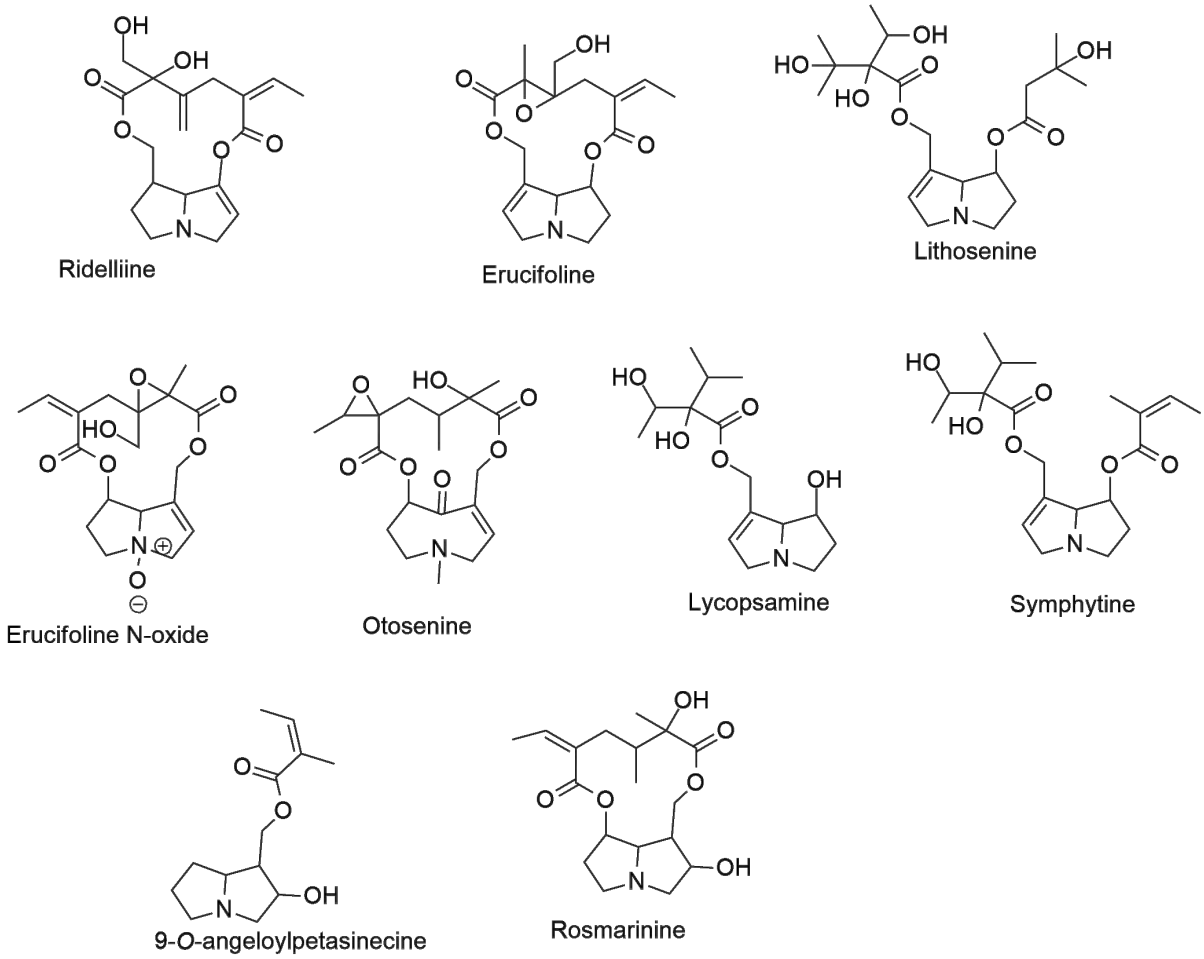

Figure 2-6: Pyrolizidine alkaloids from *Senecio fistulosus* and *Senecio aquaticus*

Senecio coronatus, S. brasiliensis, S. vernonioides, S. conyzaefolius, S. coronatus, S. grisebachii, S. angustifolius, S. platyphyllus, and *S. polypodioides* were discovered to have mainly flavonoids in their composition. However, they did contain pyrrolizidine alkaloids such as neosarracine *N*-oxide, sarracine, 7*β*-angeloyloxy-1-methylene-8*α*-pyrrolizidine, senecionine, retrorsine, and senecivernine (Figure 2-3, Figure 2-4, Figure 2-5 and Figure 2-7).

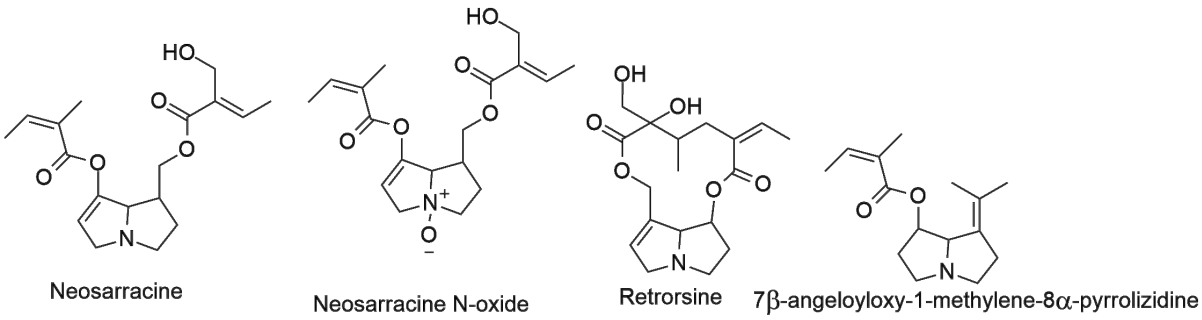

Figure 2-7 Other pyrrolizidine alkaloids from *Senecio* species

2.3.2 Flavonoids

Flavonoids are polyphenolic compounds with 15 carbon atoms (two benzene rings joined by a three-carbon moiety). They are widely found in flowering plants, often being responsible for the colour of the flowers, however their occurrence is not restricted to the flowers and they are found in other parts of the plant as well (Sultan et al., 2022, Yang et al., 2011). Flavonoids possess a basic flavan moiety with two aromatic rings (A and B) interconnected by a heterocyclic ring (C). The most widespread flavonoids contain a double bond between C-2 and C-3 and a keto function at C-4 of the C-ring as shown in Figure 2-8.

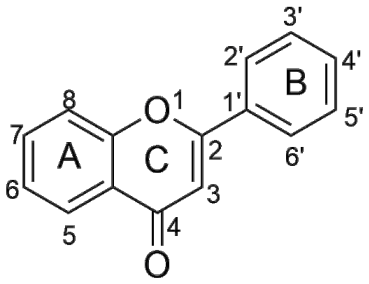

Figure 2-8: Basic structure of flavonoids

Flavonoids are known antioxidants and found in fruits and vegetables. It is advised that humans should consume at least 100 mg of flavonoids per day (Sultan et al., 2022). They are classified according to the substitution in ring C yielding major groups such as flavones, flavonols,

flavanones, anthocyanins and isoflavonoids (Figure 2-9). Chalcones, the precursor to flavonoids is also regarded as a class of flavonoids.

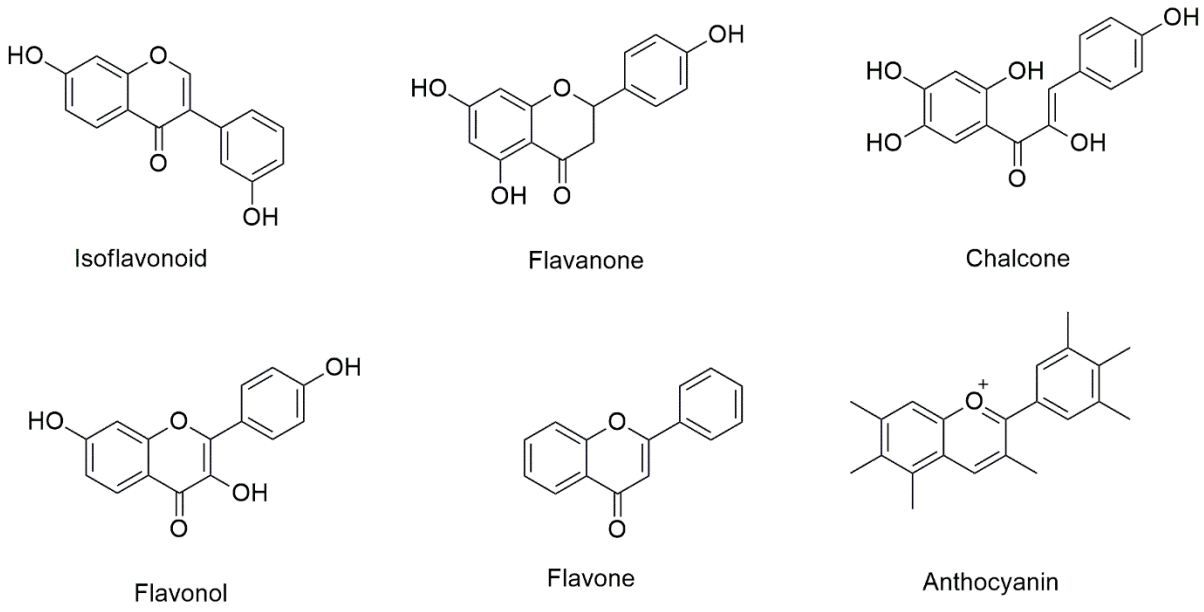

Figure 2-9: Examples of flavonoid structures

Senecio kingii contained several flavonoids, such as kaempferol-3-methyl ether, kaempferol, humatakenin, 3,7,4'-trimethylquercetin, and dihydroxy-3,7,4'-trimethoxyflavone (Figure 2-10) (Ruiz-Vásquez et al., 2015). In a study conducted by Niu et al. (2013), nine previously unidentified flavonoids emerged from the 70% ethanol extract of *Senecio cannabifolius*. Among these were quercetin-7-*O*-*β*-D-glucopyranoside, quercetin-3-*O*-*β*-D-glucopyranoside, kaempferol-3-*O*-*β*-D-galactopyranoside, isorhamnetin, isorhamnetin-5-*O*-*β*-D-glucopyranoside, kaempferol-5-*O*-*β*-D-glucopyranoside, and kaempferol-3-*O*-*β*-D-glucopyranoside (Figure 2-10).

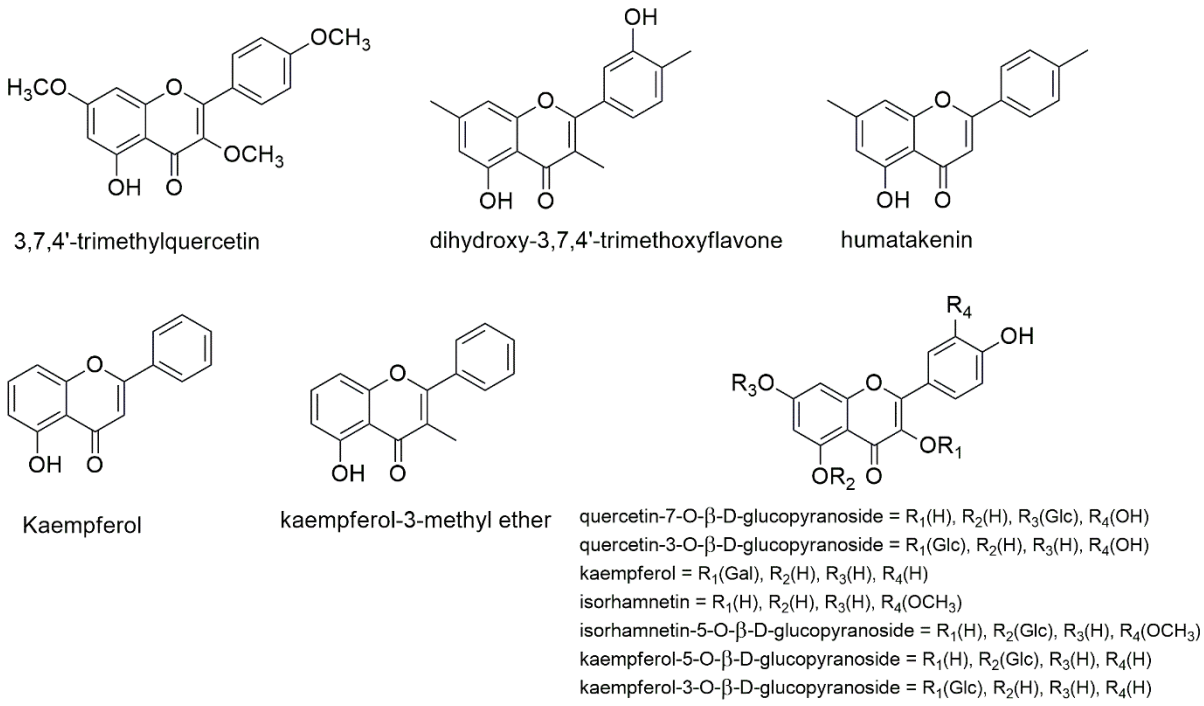

Figure 2-10: Various flavonoids isolated from *Senecio* species

High levels of quercetin and kaempferol were found in *Senecio chrysanthemoides, S. densiflorus, S. diversifolius, S. scandens, S. cineraria,* and *S. vagans* (Joshi et al., 2013). Rutin and quercetin-3-*O*-glucoside was isolated from *Senecio clivicolus* (Faraone et al., 2018), while cyanidin-3,5-diglucoside was isolated from *S. cineraria* (Tundis et al., 2007). *S. gossypinus*, often used for treating eczema and wounds, was found to contain kaempferol-3-*O*-*α*-L-arabinopyranoside (Randriamampionona et al., 2020). Phytochemical studies of *S. angulatus* led to the identification of various flavonoids such as morin, hyperoside, naringenin, naringin, hesperidin, apigetrin, fisetin and tamarixetin (Figure 2-11) (Bousetla et al., 2023).

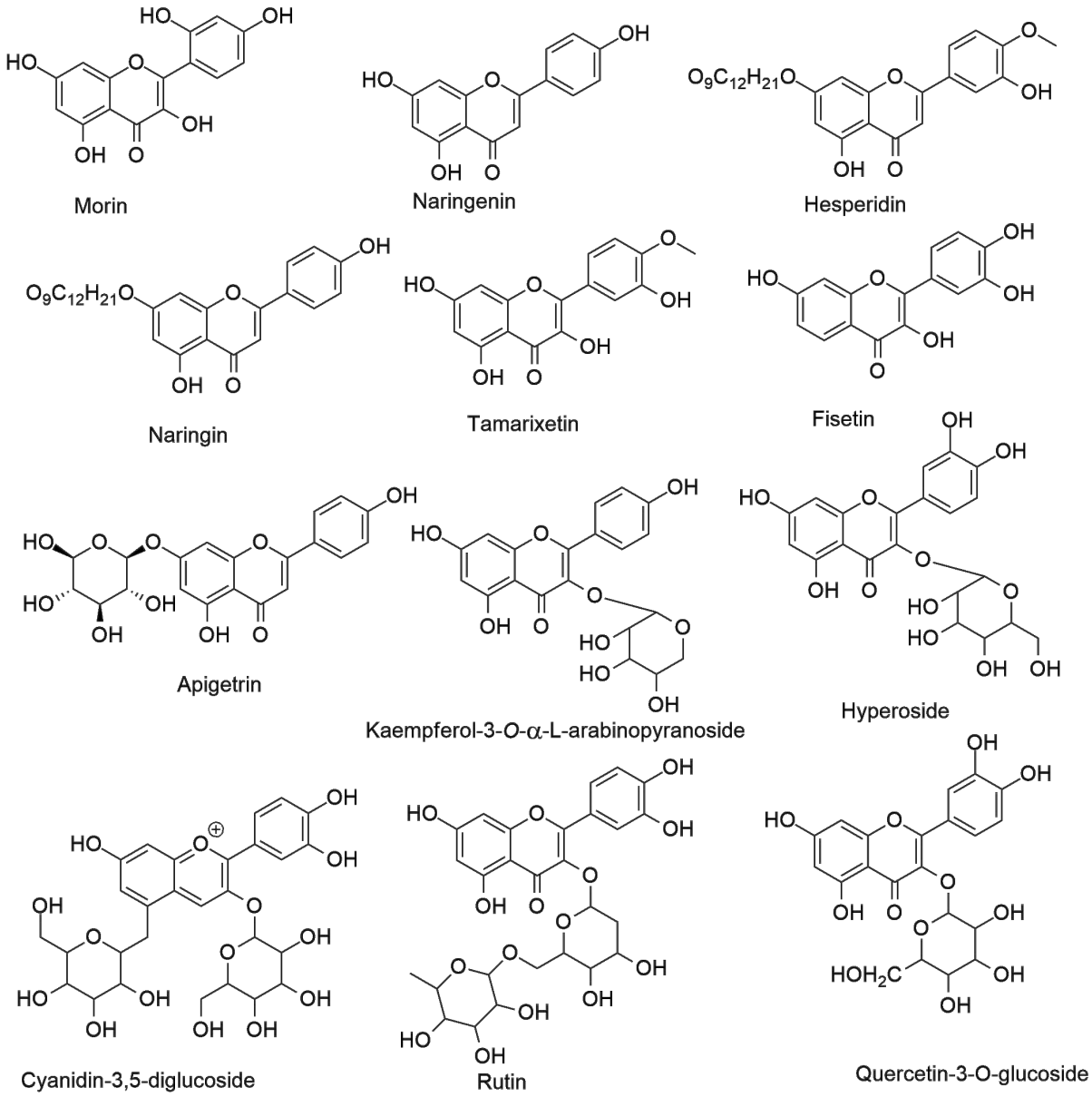

Figure 2-11: More flavonoids isolated from *Senecio* species

Senecio asperulus was found to contain 8-methoxy-5,6,4'-trihydroxyisoflvavone-7-*O*-*β*-D-glucopyranoside (Figure 2-12) (Polo-Ma-Abiele et al., 2023). The flavonoids isoquercetin, quercetin, isorhamnetin-3-*O*-*β*-glucopyranoside, quercetin-3-*O*-*β*-glucoside, and quercetin-7-*O*-*β*-glucoside (Figure 1-9, Figure 2-10 and Figure 2-12) were found to be the most prevalent flavonoids in *Senecio glaucus, S. aegyptius, S. belbeysius, S. hoggariensis, S. leucanthemifolius* and *S. acaulis* (Sultan et al., 2022).

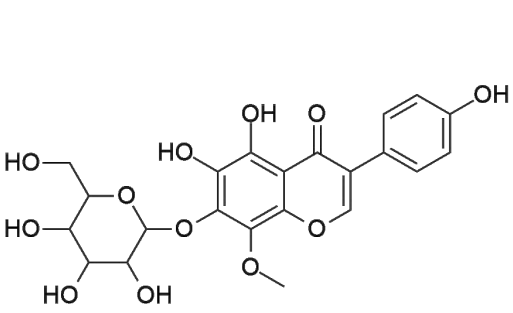

8-methoxy-5,6,4-trihydroxyisoflvavone-7-*O*-β–D-glucopyranoside

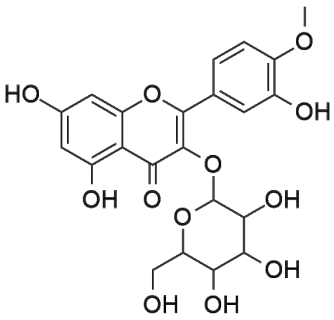

Isorhamnetin-3-*O*-β-glucopyranoside

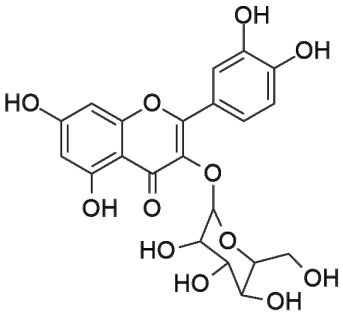

isoquercetin

Figure 2-12: Additional flavonoids from *Senecio* species

Quercetin (Figure 1-9), known for its antibacterial properties, has been isolated from many *Senecio* species including *S. hoggariensis* and *S. asperulus* (Polo-Ma-Abiele et al., 2023). It exhibits high *in vitro* activity against *Streptococcus pyogenes* (200 µg mL^{-1}) and moderate activity against various bacteria, such as *S. aureus* (20 µg mL-1), *Mycobacterium tuberculosis* (50 µg mL^{-1}), *P. aeruginosa* (20 µg mL^{-1}), *Aggregatibacter actinomycetemcomitans* (8 mg mL^{-1}) and *K. pneumoniae* (4 µg mL^{-1}) (Polo-Ma-Abiele et al., 2023).

Quercetin has also been identified as an inhibitor of diverse bacterial virulence factors (Siriwong et al., 2016). This includes its ability to interfere with quorum sensing in *Chromobacterium violaceum* and impede biofilm formation and exopolysaccharide (EPS) production in *K. pneumoniae, P. aeruginosa* and *Yersinia enterocolitica* (Gopu et al., 2015). Ashour et al. (2018) observed significant efficacy of isoquercetin (Figure 2-12) isolated from *S. acaulis,* against *E. coli* (4 µg mL^{-1}). Isoquercetin also showed notable activity against *P.*

aeruginosa (2 μg mL^{-1}) and moderate activity against *S. aureus* (197.98 μg mL^{-1}) (Ashour et al., 2018).

2.3.3 Jacaranones

Jacaranones are derivatives of benzoquinone with a hydroxyl group and methyl ester. There are two forms of benzoquinones, *p*-benzoquinone with the two carbonyl groups *para* to each other and *o*-benzoquinone with the carbonyl groups adjacent to each other. It is easily identified with bright yellow crystals. These compounds are known to exhibit pharmacological and biological activities. The methanolic extracts from *Jacaranda caucana* (Bignoniaceae) were found to have activity against P-388 lymphocytic leukemia ranging from 1 to 8 μg mL^{-1} and found to be due to the benzoquinone jacaranone (Figure 2-13) (Wang et al., 2013). Since then, this compound was isolated from numerous species within the Asteraceae.

Tetrahydrojacaranone, 2,3-dihydro-3-hydroxyjacaranone ethyl ester, jacaranone ethyl ester 4-*O*-glucoside, 2-jacaranone amide-D-pyranoid glucose ester, 2,6-dijacaranone acyl-D-glucosyl esters, and 1,6-dijacaranone acyl-D-glucosyl ester were all isolated from *Senecio scandens* (Figure 2-13) (Tian et al., 2009). *Senecio inaequidens* contained 2,3-dihydro-2-methoxy-jacaranone (Loizzo et al., 2004).

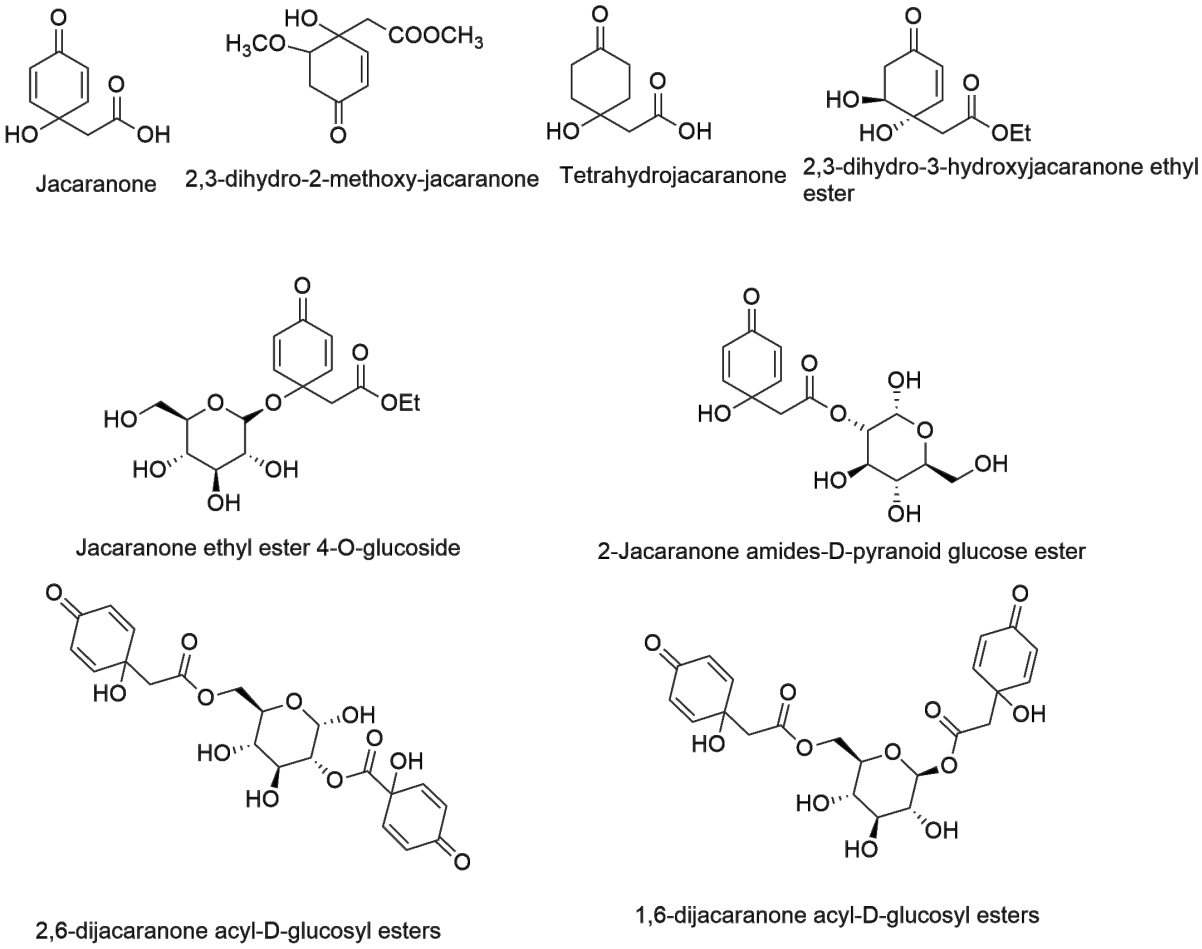

Figure 2-13: The structure of jacaranone and jacaranones isolated from *Senecio scandens* and *Senecio inaequidens*

2.3.4 Terpenoids

Terpenoids are ubiquitous in higher plants; they are used for perfumery, cooking, fuel and medicine. Terpenoids are compounds consisting of isoprene (5 carbon) units. Most terpenes are hydrocarbons having a molecular formula $(C_5H_8)_n$ in a cyclic or acyclic, saturated or unsaturated structure. The classes of terpenoids are hemiterpenes (5C), monoterpenes (10C), sesquiterpenes (15C), diterpenes (20C), triterpenes (30C), and tetraterpenes (40C) as shown in Figure 2-14.

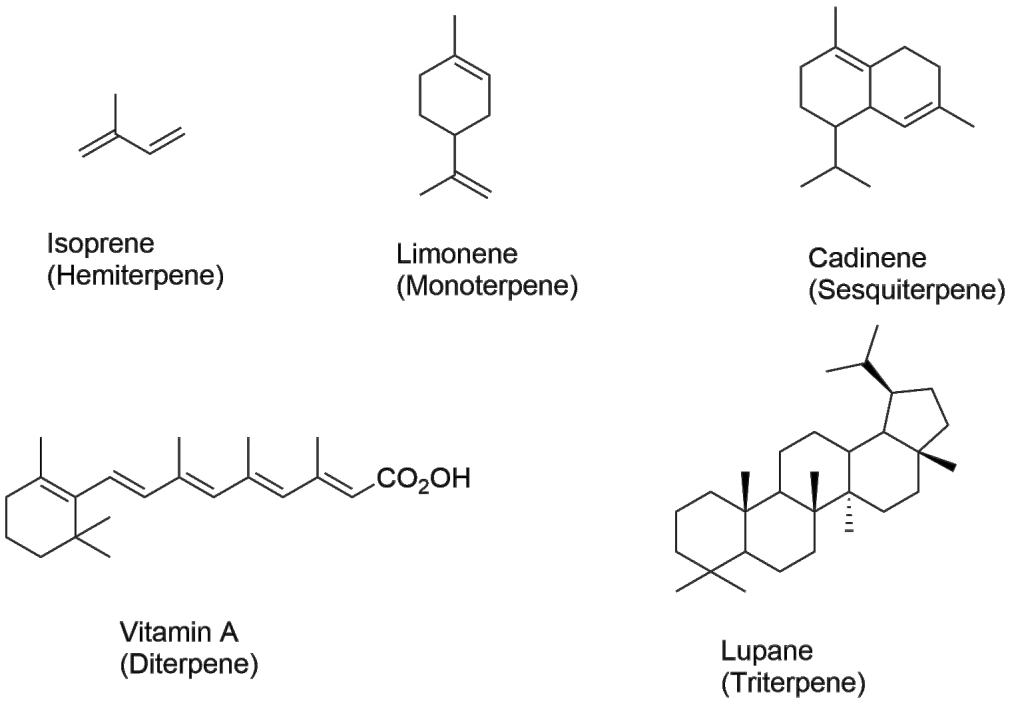

Figure 2-14: Examples of basic terpenoids

Carvacrol (Figure 2-15) is a safe monoterpene isolated from *Senecio bombayensis*. It is considered safe for ingestion and frequently used in a variety of prepared dishes as a flavoring agent. Carvacrol causes *L. monocytogenes* cell death by increasing membrane permeability and inducing membrane depolarization (Suntres et al., 2015). Linalool (Figure 2-15), another monoterpenoid with a tertiary alcohol group, was isolated from *Senecio stabianus* Lacaita (Asteraceae) (Tundis et al., 2009). Linalool was shown to have antibacterial activity against *Salmonella enteritidis* (31 μg mL^{-1}), *B. cereus* (19 μg mL^{-1}), *B. subtilis* (23 μg mL^{-1}) and *E. coli* (11 μg mL^{-1}), *P. aeruginosa* and *S. sonnei* (56 μg mL^{-1}) (Miladi et al., 2016).

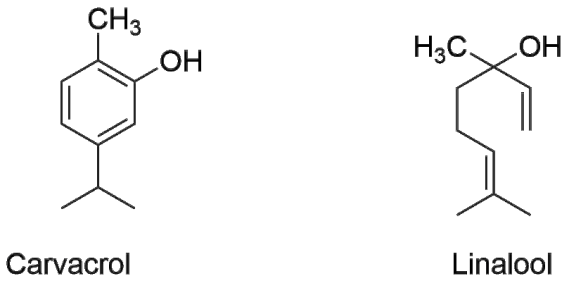

Figure 2-15 Monoterpenoids from *Senecio bombayensis* and *Senecio stabianus*

A dehydroabietic acid (diterpenoid) (Figure 2-16) was isolated from *Senecio jacobaea*, which showed strong antibacterial activity against *P. gingivalis* (14 mm zone of inhibition) and intermediate activity against *Actinomyces naeslundii*, *C. acnes, S. mitis*, *Bacteroides fragilis* and *P. intermedia* with activities of 8, 11, 6, 4.4 and 9 mm zones of inhibition respectively (Brockbals et al., 2018). Oleanolic acid, which is frequently found in conjunction with its isomer ursolic acid (Figure 2-16) was isolated from *Senecio chionophilus* (Gu et al., 2004). Significant growth inhibitory action against *E. faecalis, L. monocytogenes, B. cereus,* and *M. tuberculosis* was shown by oleanolic acid, with activities of 25, 21, 12.5 and 13 mm zones of inhibition respectively (Zhou and Xing, 2015).

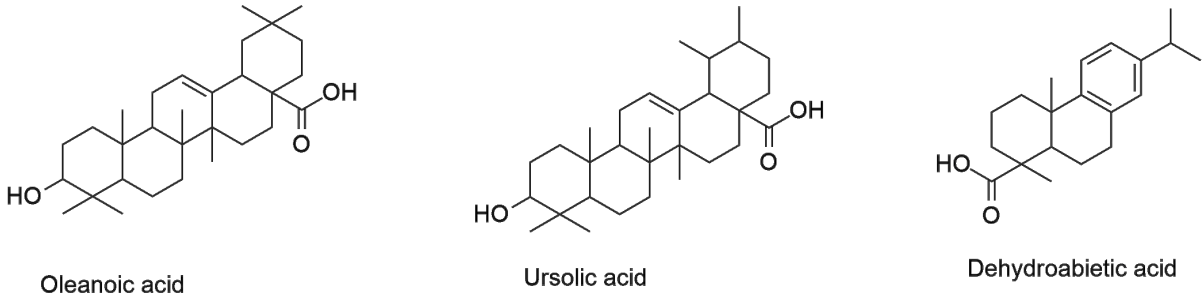

Figure 2-16 Terpenoids isolated from *Senecio jacobaea* and *Senecio chionophilus*

An investigation of *Senecio densiserratus* resulted in the isolation of the sesquiterpenoids tinocordifolioside, teuclatriol, homalomenol, dehydrocostuslactone, 10-epit-euclatriol, 4*β*,5*α*-epoxygermacr-1(10)-*E*-en-2*β*, 6*β*-diol (Figure 2-17) (Ruiz-Vásquez et al., 2015). In another study, *Senecio graciliflorus* yielded the compounds, α-lylangene, α-pinene, α-thujene, cubenol, verbenone and limonene (Figure 2-17) and *Senecio acaulis* yielded sabinene, P-cymene, *α*-copaene, cryptone, camphor, *α*-terpineol, and terpin-1-ol (Figure 2-18) (Li et al., 2020).

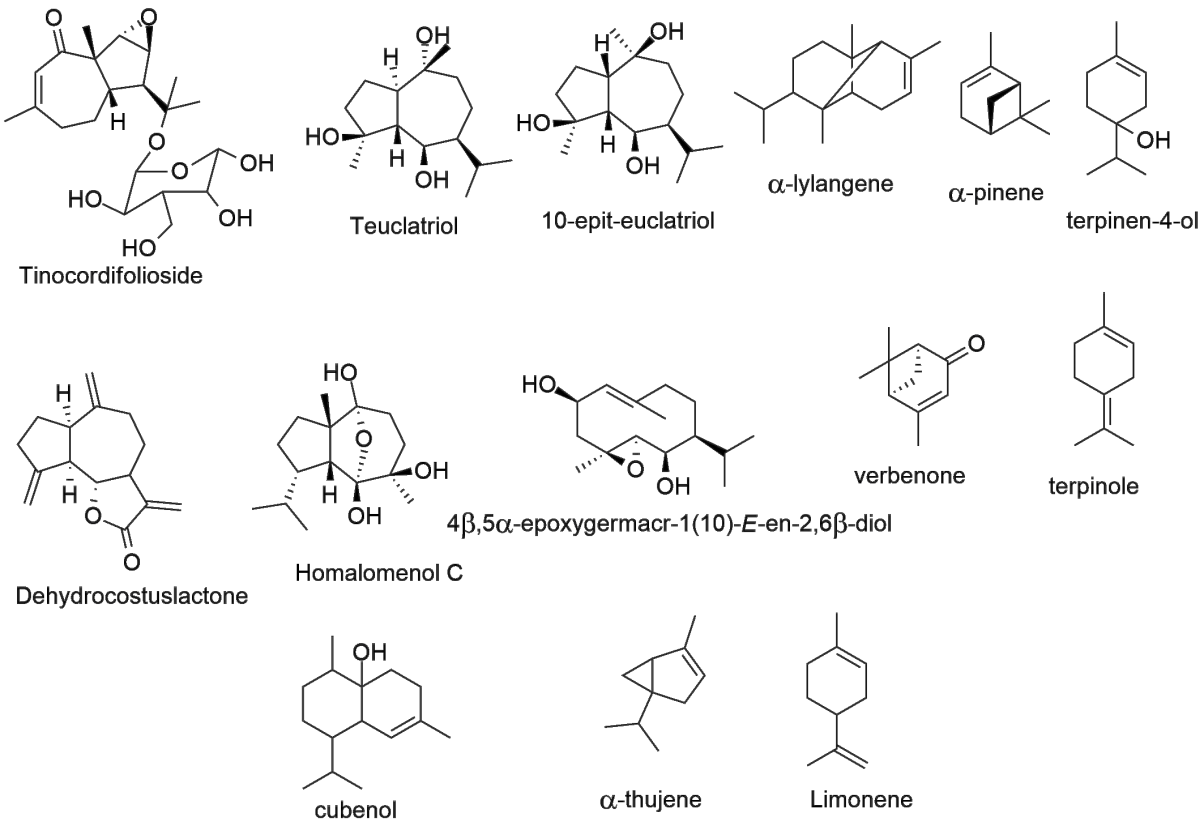

Figure 2-17: Terpernoids isolated from *Senecio densiserratus* and *Senecio graciliflorus*

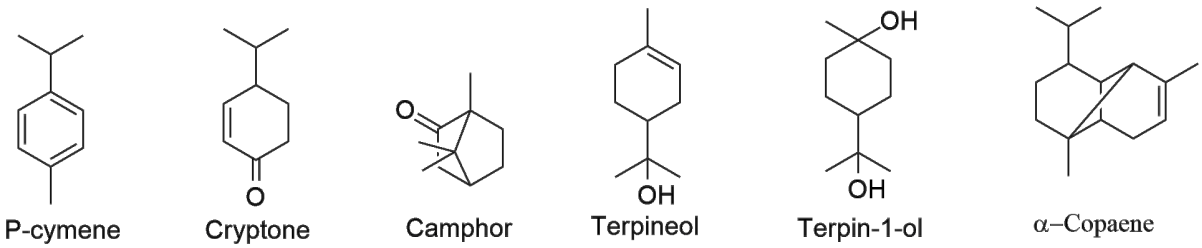

Figure 2-18 Terpenoids from *Senecio acaulis*

The terpenoids 1,10*β*-epoxyfuranoeremophilan and 1,10*β*-epoxy-6-oxo-furanoeremophilan were both isolated from *Senecio royleanus,* with 1,10*β*-epoxy 6-oxo-furanoeremophilan showing antibacterial activity against *Agrobacterium tumefaciens* (13 mm), *Bacillus subtilis* (12 mm) and *Fusarium oxysporum* (15mm) in a disc diffusion assay (Ashour et al., 2018). *Senecio smithiodes* yielded the terpenoids 9-oxoeuryopsin and epoxydecompostin, while

Senecio subcandidus, Senecio klugii and *Senecio ayapatensis* resulted in the isolation of two diterpenoids kaurenoic acid and kaurenol (Figure 2-19) (Singh Bisht et al., 2019).

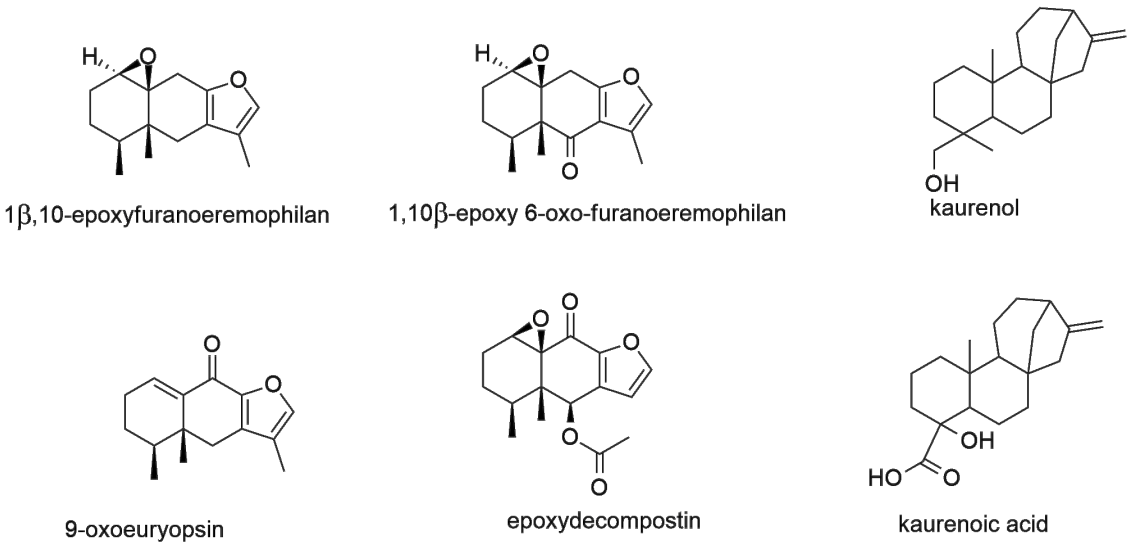

Figure 2-19 Terpenoids from *Senecio* species

Senecio cruentus contained the terpenoids, phytol, hexadecanoic acid, *cis*-vaccenic acid, nonacosane, dotriacontane, glycidyl oleate, methyl stearate and 1-heptatriacotanol (Figure 2-20) (Malak et al., 2023).

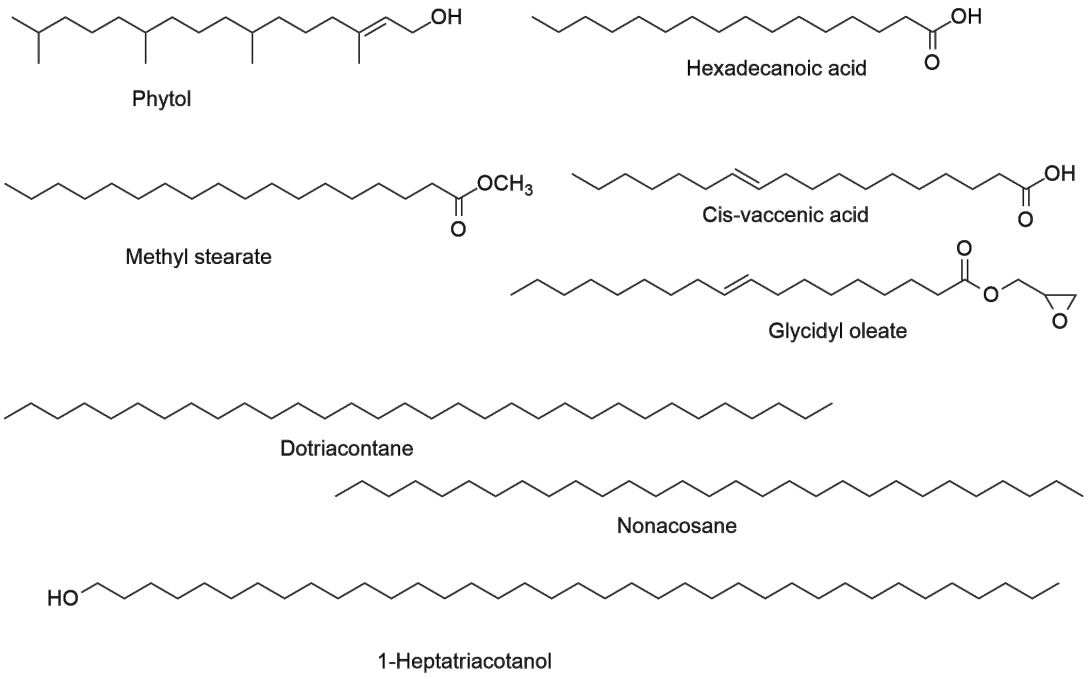

Figure 2-20 Terpenoids from *Senecio cruentus*

2.4 Antidiabetic activity of *Senecio* species

Senecio abyssinicus leaf extracts were investigated for their antidiabetic effects using an *in vitro* α-glucosidase (AGI) assay, where the n-hexane extract exhibited the highest inhibition at 76.55%, followed closely by the methanol extract at 75.13%, while the ethyl acetate extract showed the lowest activity at 54.23%. Although activity was not as high as the standard, Acarbose (92.95%), activity of extracts are always desirable since in general, they have fewer side-effects compared to synthesised drugs (Egharevba et al., 2023).

The petroleum ether extract from *Senecio biafrae* exhibited notable antidiabetic effects when orally administered to diabetic rats induced by streptozotocin that were comparable to the effects of the standard drug, glibenclamide (Okoro et al., 2014). *Senecio biafrae* contains a range of secondary metabolites, including dihydroisocoumarins, terpenoids, sesquiterpenes, and amino acids (Adelakun et al., 2018, Hossain et al., 2017).

The methanol extract of *Senecio stabianus* showed good inhibition of α-amylase with an IC_{50} of 0.29 mg mL^{-1} (Tundis et al., 2012). The methanol extracts of both *Senecio inaequidens* and *S. vulgaris* exhibited substantial α-amylase inhibitory activity, reaching 93% and 82% at a concentration of 1 mg mL^{-1} (Hamid and Kadhim, 2016). The methanolic extract of *Senecio leucanthemifolius* had a substantial inhibition of α-amylase (78%) at a concentration of 1 mg mL^{-1}, with the dichloromethane extract reaching 56.6% at 0.05 mg mL^{-1} and the n-butanol extract having an inhibition of 89.2% at a concentration of 0.1 mg mL^{-1} (Tundis et al., 2010).

2.5 Antimicrobial activity of *Senecio* species

Crude extracts from *Senecio* are recognized for their diverse range of biological properties. These include antimicrobial effects, encompassing antibacterial, antifungal, and antitubercular activities (Marete, 2013). The ethanol extract of *Senecio scandens* showed broad-spectrum

antibacterial activity against *S. aureus*, *Streptococcus pneumonie*, *Haemophilus influenzae* and *β*-hemolytic *Streptococcus* (Newman and Cragg, 2016, Rios and Recio, 2005, Van Vuuren, 2008, York et al., 2012). The essential oils extracted from *Senecio graciliflorus* demonstrating significant antibacterial efficacy against several bacterial strains including *B. cereus, B. subtilis, E. coli,* and *P. aeruginosa* with inhibition zones ranging from 3.3 to 8.6 mm (Joshi et al., 2019). The highest activity was seen against *S. aureus* (with an inhibition zone of 8.6 mm), while it also effectively inhibited *E. coli* (with an inhibition zone of 6.0 mm).

β-sitosterol was identified as an active compound in the methanol extract of *Senecio lyratus*, which possesses both antifungal and antibacterial properties (Kiprono et al., 2000). The methanol extract from *Senecio vulgaris* had a MIC of 0.5 mg mL^{-1} for the Gram-positive *B. subtilis* and 0.125 mg mL^{-1} for *S. aureus*. *Senecio inaequidens* however, showed no antimicrobial activity against these bacterial strains at concentration of 1 mg mL^{-1} and lower (Loizzo et al., 2004). The study also showed that the Gram-negative bacteria, *E. coli* and *P. aeruginosa*, were not affected by the methanol extracts of both *S. inaequidens* and *S. vulgaris*. Additionally, *Senecio samnitum* methanol extract exhibited an MIC of 500 µg mL^{-1} against *S. aureus*.

Chapter 3 Experimental

3.1 Collection and preparation of samples

Leaves and stems of *Senecio serratuloides* DC were gathered from ten different locations in KwaZulu-Natal (KZN), South Africa, including Mandeni (S1), Stanger (S2), Reservoir Hills (S3), Palmiet (S4), Richards Bay (S5), Shongweni (S6), Eshowe (S7), Uthongathi (S8), Vryheid (S9) and Ndwedwe (S10). The sample chosen for phytochemical isolation was obtained from Stanger (S2) (Figure 3-1). The dried leaves weighing 946 g, were subjected to consecutive extraction with dichloromethane (DCM) and methanol (MeOH) for 48 hours each, using a Reflecta orbital shaker (100- 500 rpm). The resulting extracts were then filtered using a filter paper (Whatman qualitative filter paper, grade 1), and the solvent concentrated by evaporation under reduced pressure using a Buchi R210 rotary evaporator at 50 °C, yielding the crude extracts of hexane (36.145 g), dichloromethane (22.943 g) and methanol (15.746 g). These crude extracts were subsequently stored in the refrigerator until further usage.

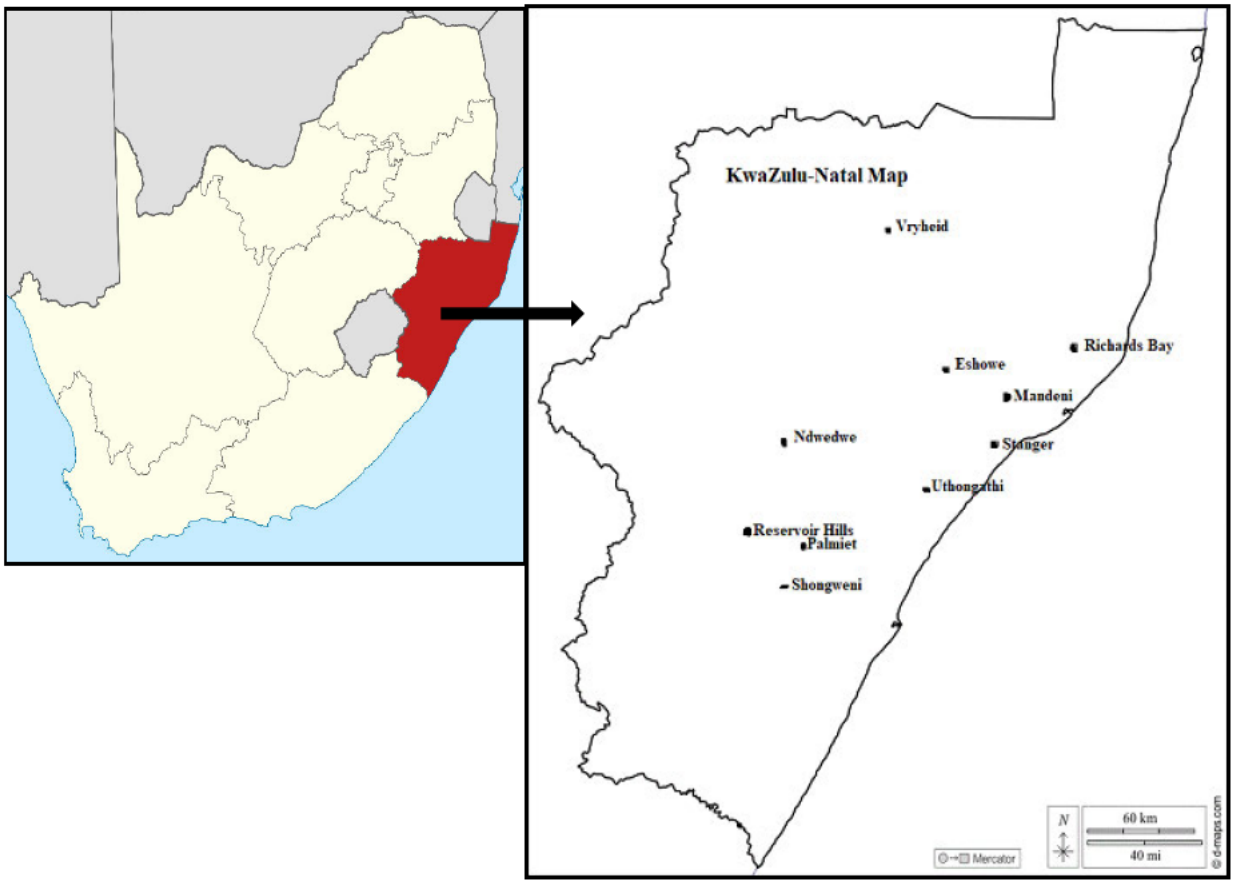

Figure 3-1 Map of sampling sites in KwaZulu-Natal, South Africa

Sampling was done in April when temperatures were typically 25 °C. Plant samples were washed with double distilled water, oven dried at 50 ºC to obtain a constant mass, and crushed into fine powder using a mortar and pestle. Each sample was divided into two portions, where portion (A) was stored in polyethylene bags and refrigerated until elemental analysis was carried out, while portion B was cooked using double distilled water at 70 °C on a hot plate for 15 min. Portion B was cooled, sieved, dried again, and stored in polyethylene bags.

3.2 Reagents and chemicals

Analytical grade reagents and chemicals were all acquired from Sigma-Aldrich in Germany. Double distilled water was used for dilutions, and all plastic and glassware were thoroughly cleaned by soaking in diluted nitric acid and rinsed with double distilled water prior to use. Elemental standards were prepared using 1000 mg L^{-1} stock solutions provided by Fluka Analytical, Sigma, Switzerland.

3.3 Isolation of compounds from *Senecio serratuloides*

The initial DCM extract from the leaves weighing 8.97 g was applied to a column filled with a silica gel slurry and separated using a gradient solvent system of hexane and ethyl acetate (beginning with 100% hexane and incrementally increasing this by 10% to reach 100% EtOAc) as illustrated in Figure 3-2. TLC was employed to monitor the fractions being eluted, and those with similar profiles were combined and concentrated using a rotary evaporator.

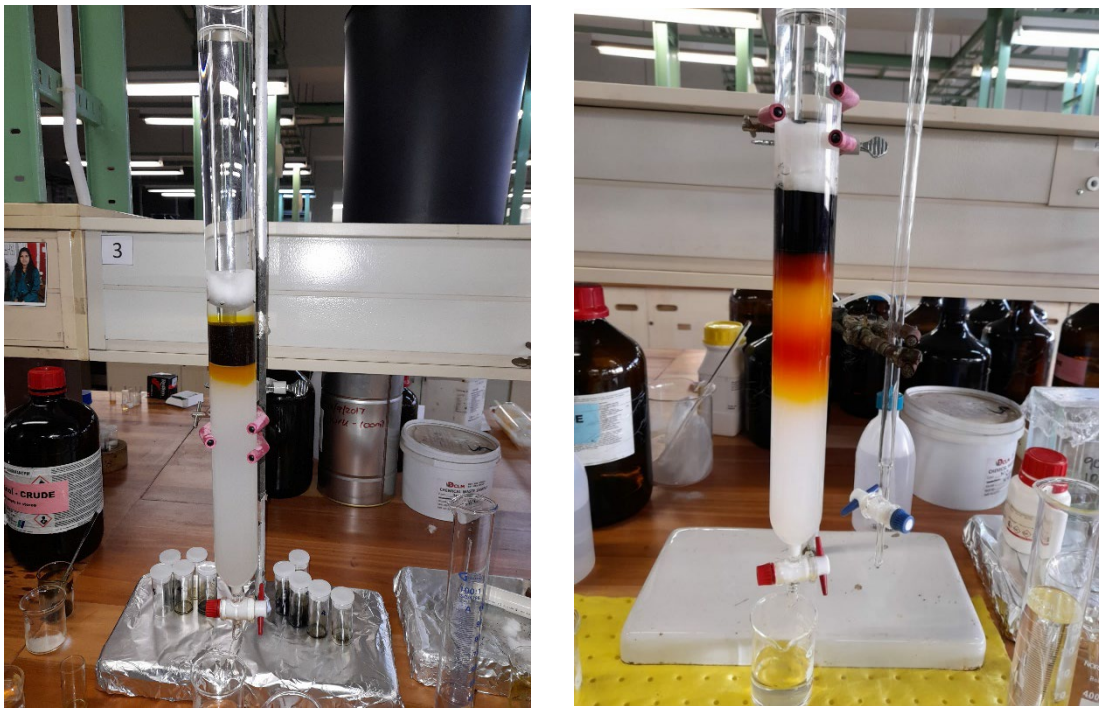

Figure 3-2: Column showing fractionation of the crude extract of hexane (left) and DCM (right)

The methanol extract from the leaves was re-dissolved in 100 mL methanol and partitioned using water (100 mL) and DCM (200 mL). The bottom DCM layer was concentrated on the rotary evaporator, and weighed to give a mass of 0.177 g. The aqueous-MeOH layer was further partitioned with EtOAc, and the EtOAc layer evaporated and weighed to give a mass of 0.154 g. The DCM and EtOAc fractions were subjected to column chromatography using a gradient solvent system starting with 100% hexane that was stepped up by 10% to 100% EtOAc, and finally with 5% to 20% MeOH.

The DCM crude extract of the leaves (6.31 g) and stems (4.73 g) of *S. serratuloides* were separated by column chromatography using a gradient elution system of n-hexane: ethyl acetate, starting from 100% n-hexane and stepped up by 10% to 100% EtOAc. The column was then washed with 100% MeOH. Fractions of 60 mL were collected for each eluent step and analysed on TLC, where similar compounds were combined.

Compounds **S2** (125 mg) and S**3** (150 mg) were obtained from fraction 5 from the leaves and were purified using 10% ethyl acetate in hexane. Fractions 9 and 10 from the stems yielded compound **S1** (70 mg) and purified again with 10% ethyl acetate in hexane. The EtOAc fraction from the MeOH extract from the leaves (0.154 g) was subjected to column chromatography using a gradient elution starting from 100% n-hexane that was stepped up by 10% to 100% EtOAc. Fraction 2 yielded compound **S4** (37 mg) and **S5** (30 mg), and was purified using 10% ethyl acetate in hexane and 90% ethyl acetate in hexane respectively. Fractions 11 and 12 yielded compounds **S6** (21 mg) and **S7** (18 mg) and were both purified using 90% ethyl acetate in hexane, while fraction 15 yielded compound **S8** (26 mg) and was purified using water: methanol: ethyl acetate in a 5:15:80 ratio.

3.4 Characterization methods and spectroscopic data

Various spectroscopic techniques were employed to characterise the compounds. Nuclear Magnetic Resonance (NMR) spectra (both 1D and 2D) were recorded at room temperature in deuterated chloroform ($CDCl_3$) using Bruker AVANCE III 400 MHz and 600 MHz spectrometers, with tetramethylsilane (TMS) as the internal standard. Infrared (IR) spectra were obtained using a Perkin Elmer Universal ATR Spectrometer. Mass spectra were recorded using a Waters Micro-mass LCT Premier TOF-MS. Column chromatography was carried out using silica gel (Merck Kieselgel 60, 0.063-0.200 mm, 70-230 mesh ASTM). TLC was used to monitor the fractions collected from columns, using Merck silica gel 60, 20 × 20 cm F_{254} aluminium sheets. TLC plates were observed under an ultraviolet lamp (254 nm) and developed using 10% H_2SO_4 in MeOH.

β-sitosterol (S1): white crystalline; IR (KBr) V_{max} cm^{-1} 3313 (O-H), 2925 (C-H); ^{1}H-NMR ($CDCl_3$, 400MHz): δ_H 5.32 (1H, d, J = 5.1 Hz, H-6); 3.46-3.52 (1H, m, H-3), 0.98 (3H, s, CH_3-19), 0.90 (3H, d, J = 6.6 Hz, CH_3-21), 0.84 (3H, t, J = 6.5 Hz, CH_3-29), 0.80 (3H, d, J = 6.6

Hz, CH_3-26), 0.82 (3H, d, *J* = 6.6 Hz, H-27), 0.65 (3H, *s*, CH_3-18); ^{13}C-NMR ($CDCl_3$, 100 MHz) δ_C 140.5 (C-5), 121.5 (C-6), 71.6 (C-3), 56.6 (C-14), 55.8 (C-17), 49.9 (C-9), 45.6 (C-24), 42.10 (C-13), 42.08 (C-4), 39.6 (C-12), 37.0 (C-1), 36.3 (C-10), 35.9 (C-20), 33.7 (C-22), 31.7 (C-8), 31.4 (C-7), 28.9 (C-2), 28.1 (C-25), 28.0 (C-16), 25.9 (C-23), 24.1 (C-15), 22.8 (C-28), 20.9 (C-11), 19.6 (C-26), 19.2 (C-19), 18.8 (C-27), 18.6 (C-21), 11.8 (C-29), 11.6 (C-18).

Stigmasterol (S2): white needles; IR (KBr) V_{max} cm^{-1} 3419 (O-H), 2926 (C-H), 2850 (C-H), 1707 (C=C); ^{1}H-NMR (400 MHz, $CDCl_3$) δ_H 5.34 (1H, m, H-6), 5.14 (1H, dd, *J* = 15.4, 8.0 Hz, H-22), 5.02 (1H, dd, *J* = 15.4, 8.0 Hz, H-23), 3.48-3.56 (1H, m, H-3), 1.00 (3H, s, CH_3-19), 0.86 (3H, t, *J* = 7.2 Hz, CH_3-29), 0.82 (6H, d, *J* = 6.5 Hz, CH_3-26/27), 0.80 (3H, s, CH_3-18), 0.68 (3H, d, *J* = 7.2 Hz, CH_3-21); ^{13}C-NMR (100 MHz, $CDCl_3$) δ_C 140.9 (C-5), 138.4 (C-22), 129.4 (C-23), 121.8 (C-6), 71.9 (C-3), 57.0 (C-14), 56.9 (C-17), 51.4 (C-24), 50.3 (C-9), 42.4 (C-13), 42.3 (C-4), 40.6 (C-20), 39.8 (C-12), 37.4 (C-1), 36.6 (C-10), 34.0 (C-25), 32.0 (C-7), 31.8 (C-8), 29.8 (C-2), 28.4 (C-16), 25.5 (C-28), 24.4 (C-15), 21.3 (C-27), 21.2 (C-11), 19.9 (C-21), 19.2 (C-19), 18.9 (C-26), 12.1 (C-29), 12.0 (C-18).

The NMR and mass spectral data for **S3** (stigmasterol glucoside), **S4** (18α-ursa-12,20(30)-dien-3*β*-ol), **S5** (quercetin), **S6** (quercetin-3-*O*-glucoside), **S7** (hesperidine) and **S8** (caffeic acid) are contained in tables in the next chapter.

3.5 Nutritional value

3.5.1 Moisture content

The moisture content was determined following methodology reported by Sigel and Sigel (1983). Briefly, *S. serratuloides* fresh leaf samples were dried at room temperature. The dried leaf samples weighing 2 g were placed in crucibles and oven dried at 105 °C, to constant mass, M2. Thereafter, the crucibles containing the dried samples were removed from the oven,

cooled in a desiccator. and weighed to a constant mass, (M3) (Sigel and Sigel, 1983). The percentage moisture was calculated using the following equation:

$$\%Moisture\ content\ =\ M2-M3/M3-M1\ x\ 100$$

Where M1 is the mass of the crucible, M2 is the mass of the crucible with the fresh sample and M3 is the mass of the crucible with the dried sample.

3.5.2 Ash content

The ash content was established by drying a porcelain crucible at 105 ℃ for 30 min and weighed to a mass of M1. Dried leaf samples were placed in the crucibles, after which it was weighed again to mass M2. The samples were then incinerating in a muffle furnace at 600 ℃ for 6 h, cooled in a desiccator, and weighed to a mass (M3) (Sigel and Sigel, 1983). The percentage ash in the sample is given by the following equation:

$$\%Ash\ =\ M2-M3/M3-M1\ x\ 100$$

3.5.3 Fat content

The total fat content was obtained by extracting 2.50 g of dried leaf samples in 50 mL diethyl ether and shaking the mixture for 24 h using an orbital shaker. The extracts were collected in previously weighed beakers (M1). The resulting residuals were collected using the same weighed beakers after they were equilibrated with 50 mL diethyl ether and then shaken again for 24 h (M1). The ether residuals were dried in the oven at 50 ℃ after being concentrated to dryness using a steam bath, and the beakers were weighed again (M2). The fat content was calculated using the following equation (Adamu et al., 2013):

$$\%Fat\ content\ =\ M2\ -\ M1\ /\ E\ x\ 100$$

Where M1 is the mass of the empty beaker, M2 is the mass of the beaker with concentrated extract, and E is the mass of the original sample, 2.50 g.

3.5.4 Crude Fiber

Dried leaf samples (2 g) were soaked in 50 mL of 1.25% H_2SO_4 for 30 min, filtered, and the resulting residuals washed with hot water. This process was repeated on the residuals using 50 mL of 1.25% NaOH solution. The resulting filtrates were dried at 100℃ and weighed (M2), followed by incinerating in a muffle furnace at 500 ℃ for 6 hours and then reweighed (M1) (Sigel and Sigel, 1983). The crude fiber content was established using the following equation:

$$\%Crude\ fiber\ =\ M2\ -\ M1/\ Mass\ of\ original\ sample\ x\ 100$$

3.6 Phytochemical screening

3.6.1 Saponins

A 2.50 g sample of finely ground leaves was combined with 25 mL of 20% ethanol, and subjected to extraction on an orbital shaker for 30 min. The mixture was then heated on a water bath at 60 ℃ for 3 h. After filtration, the resulting residue was re-extracted with 50 mL ethanol. The ethanol extract was reduced to 20 mL through evaporation using a water bath set at 100 ℃. The concentrated solution was transferred to a separating funnel and extracted with 20 mL diethyl ether. The ether layer was discarded and the aqueous layer was retained in a beaker. The aqueous layer was further extracted with 25 mL n-butanol. The butanol layer was retained and subjected to two washes with 5% sodium chloride. The resulting solution was collected and evaporated in a water bath, followed by drying to a constant mass at 40 ℃ in an oven (Sigel and Sigel, 1983).

$$\%Saponin\ =\ (Weight\ of\ residue/Weight\ of\ original\ sample)\ x\ 100$$

3.6.2 Alkaloids

A 2.50 g dried leaf sample, was combined with 25 mL of 10% acetic acid in ethanol, and allowed to sit covered for 4 h. The mixture was then filtered and concentrated to a quarter of its original volume using a water bath. Concentrated NH_4OH was introduced to the extract until

precipitation was achieved. The solution was subsequently washed with dilute NH_4OH and then filtered. The resulting residue was dried, weighed, and the alkaloid content calculated using the formula below (Sigel and Sigel, 1983).

$$\%Alkaloid = Weight\ of\ precipitate/Weight\ of\ original\ sample\ x\ 100$$

3.6.3 Flavonoids

A 5.0 g sample of plant leaf powder underwent extraction with 50 mL of 80% aqueous methanol for a duration of 3 days. After extraction, the solution was filtered, and the filtrate carefully transferred into a crucible. Subsequently, the solution was evaporated to dryness using a water bath, and weighed to a constant mass. The weight obtained gave the estimation of the flavonoid content in the plant leaf sample (Grauso et al., 2020).

$$\%Flavonoid = Weight\ of\ dried\ sample/Weight\ of\ original\ sample\ x\ 100$$

3.7 Elemental analysis

Samples of *S. serratuloides* leaves (0.25 g) and a certified reference material (0.25 g) underwent digestion using the CEM MARS microwave reaction system (CEM Corporation, Matthews, North Carolina, USA). Ground leaf samples were precisely placed in liners, and 10 mL 70% HNO_3 added. For digestion, the power was set at 100% at 1600 W and the temperature ramped to 180 ºC for 15 min, where it was held for a further 15 min. Once cooled, the samples were filtered using a 0.45 µL syringe filter into a 25 mL volumetric flask, which was topped up to the mark with double distilled water and stored in ICP vials for analysis. Samples were analysed for the following elements As, Ca, Cd, Co, Cr, Cu, Fe, Mg, Mn, Ni, Pb, Se and Zn. Elemental analysis was carried out using inductively coupled plasma-optical emission spectrometry (ICP-OES). The accuracy of the elemental composition was measured by the use of CRM, LGC7162- Strawberry Leaves. All samples were analysed in triplicate.

3.8 Antidiabetic activity

3.8.1 α-Amylase and α-glucosidase inhibition assay

The α-amylase and α-glucosidase inhibitory activity was performed using a previously established procedure (Chandran et al., 2016). Acarbose was used as a positive control and a mixture containing all reagents except test sample was used as a control. All experiments were done in triplicate. The absorbance was measured using a UV spectrophotometer (Biochrom Libra S11, wavelength range; 325-999 nm, Cambridge, England) at 540 nm for α-amylase inhibition and 405 nm for α-glucosidase inhibition. Percentage inhibition was calculated as follows:

$$\%\ inhibition\ =\ [Ac - As/Ac]\ x\ 100$$

Where A_C is the absorbance of the control and A_S is the absorbance of the sample.

3.9 Antibacterial activity

3.9.1 Culture media and microbial strains

The microorganisms under investigation were grown on Mueller-Hinton Agar for a full day before conducting the tests. A group of 10 indicator microbes, consisting of both susceptible and multidrug resistant Gram-negative strains (*Acinetobacter baumannii* ATCC 19606; *Escherichia coli* ATCC 25922, *E. coli* ATCC 35218, *Klebsiella pneumoniae* ATCC 700603, and *Pseudomonas aeruginosa* ATCC 27853) and Gram-positive strains (*Staphylococcus aureus* ATCC 29213; methicillin- resistant *S. aureus* ATCC 43300; *Staphylococcus epidermidis* ATCC 12228; *Enterococcus faecalis* ATCC 29212; and vancomycin-resistant *E. faecalis* ATCC 51299) were used in the assay (Motyl et al., 2005).

3.9.2 Determination of bacterial susceptibility

The broth microdilution assay was performed to assess the minimal inhibitory concentrations (MICs) of seven *Senecio serratuloides* extracts (HEX-leaves, HEX-stems, DCM-leaves and

fruit, DCM-stems, EA stems and leaves, MeOH-leaves and MeOH-stem) against the group of 10 bacteria using the procedures outlined by Motyl et al. (2005) and Eloff (1998) with modifications.

In a 96-well microtiter plate, 100 µL of room temperature cation-adjusted Mueller-Hinton (MH) broth was placed in each well. The initial well in each row received 100 µL of the specific extract or compound solution (prepared in DMSO/MH broth). A two-fold serial dilution was carried out across the plate's rows up to column 11, with the last 100 µL discarded. This resulted in extract concentrations ranging from 1025 µg mL^{-1} in the first well to 1 µg mL^{-1} in the 11th well. Column 12 wells were growth controls containing no drug. A volume of 100 µL of bacterial inocula in MH broth equivalent to a 0.5 McFarland standard were added to drug-containing wells. After 24 h at 37 °C, wells with bacterial growth were compared visually to a no-drug control (well 12). The lowest sample concentration inhibiting colour change post addition of INT indicated the minimum inhibitory concentration (MIC), with values >1 mg mL^{-1} considered inactive (CLSI, 2018) (Eloff, 1998).

Chapter 4 Results and discussion

The extracts of *Senecio serratuloides* was subject to phytochemical analysis, nutritional and elemental analysis, and antibacterial and antidiabetic assays to provide a rationale for using the plant in ethnomedicine, as well as to determine their nutritional value and potential toxicity, and their potential to be used as an antidiabetic or antibacterial herbal remedy.

4.1 Phytochemical analysis

The phytochemical investigation of the stems and leaves of *Senecio serratuloides* DC plant extracts resulted in the isolation of the sterols, β-sitosterol (**S1**) from the stems, and stigmasterol (**S2**) and stigmasterol glucoside (**S3**) from the leaves. A further rare sterol, 18α-ursa-12,20(30)-dien-3β-ol (**S4**) was also isolated from the leaves. Three flavonoids, quercetin (**S5**), quercetin-3-*O*-glucoside (**S6**) and hesperidine (**S7**) were also isolated from the leaves, along with an aromatic acid, caffeic acid (**S8**) (Figure 4-1).

Compound **S1** was obtained as white needles and identified as the common β-sitosterol (Figure 4-2). The IR spectrum showed absorption frequencies of the O-H stretch at 3313 cm^{-1}, as well as C-H stretching bands at 2925 cm^{-1}. The ^{1}H NMR spectrum showed the characteristic multiplet of H-3 at δ_H 3.50 and olefinic proton resonance of H-6 at δ_H 5.31 (H-6), as well as six methyl proton resonances, a singlet at δ_H 0.98 (CH_3-19), a doublet for CH_3-21 at δ_H 0.90 (J = 6.6 Hz), a triplet at δ_H 0.84 for the CH_3-29 resonance with J = 6.5 Hz, two doublets at δ_H 0.80 (CH_3-26) and δ_H 0.82 (CH_3-27) and a singlet at δ_H 0.69 for CH_3-18. Evident in the ^{13}C NMR spectrum were the twenty-nine carbon resonances of sitosterol, including the two olefinic proton resonances of C-5 and C-6 at δ_C 140.5 and δ_C 121.5 respectively, and the oxygenated methine carbon resonance at δ_C 71.6. The ^{13}C NMR data compare well with that in the literature (Kamal et al., 2016).

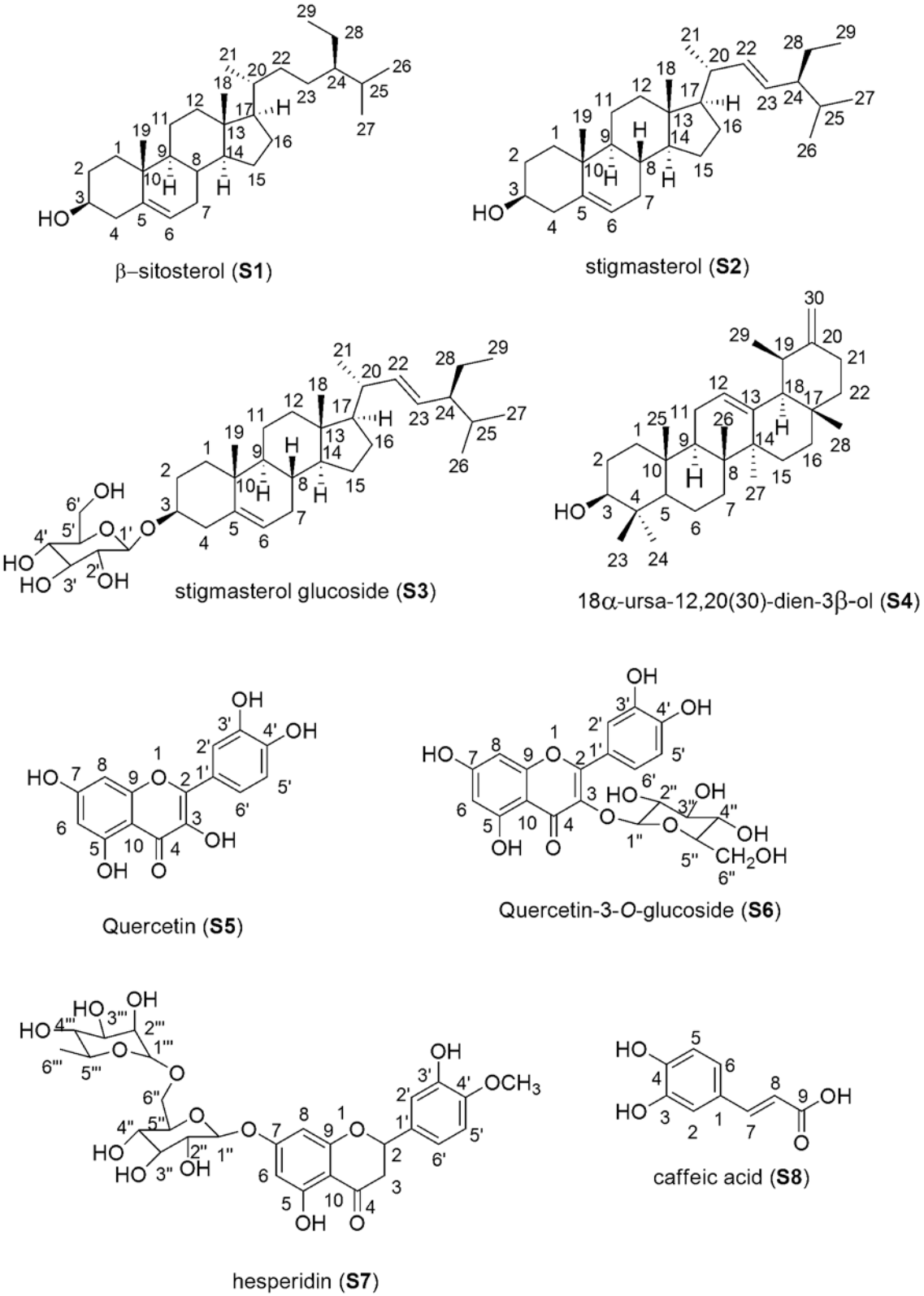

Figure 4-1 Structures of the compounds isolated from the stems and leaves of *Senecio serratuloides* DC

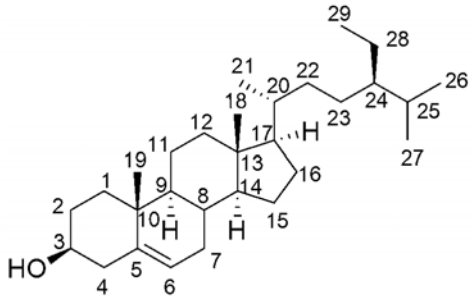

Figure 4-2 Chemical structure of *β*-sitosterol (**S1**)

This compound finds application in various cosmetic products. It is also frequently employed for reducing high levels of cholesterol, ameliorating symptoms associated with an enlarged prostate, and alleviating the symptoms accompanied with heart problems (Ambavade et al., 2014, Khan et al., 2022, Luhata and Usuki, 2021). In another study, sitosterol proved to be successful in combating *Salmonella typhi* and *E. coli*, showing inhibition zones of 20 and 35 mm, respectively. The minimum inhibitory concentration against *S. typhi* and *E. coli* was 6.25 and 12.5 μg mL^{-1}, respectively, demonstrating good antibacterial activity against these strains (Nweze et al., 2019). Moreover, sitosterol showed significant antioxidant activity in a DPPH test at 10 μg mL^{-1} (Bhat et al., 2019).

Compound **S2** was obtained as white needles and showed the characteristic ^{1}H NMR spectrum of the ubiquitous stigmasterol (Figure 4-3). This was indicated by the characteristic multiplet proton resonance at δ_H 3.54 (H-3), and olefinic proton resonances, at δ_H 5.34 (H-6), a doublet with J = 4.7 Hz, and two double doublets at δ_H 5.14 (H-22), and 5.02 (H-23), each with J values of 15.2 and 8.5 Hz. Five methyl resonances could also be seen in the upfield region of the NMR spectrum, which indicated six methyl resonances, since one of them integrated to six protons. These were the singlet resonance at δ_H 1.00 assigned to CH_3-19, the three-proton triplet at δ_H 0.86 (CH_3-29), the six-proton doublet resonance attributed to CH_3-26 and CH_3-27, the singlet resonance of CH_3-18 at δ_H 0.80 and the doublet resonance of CH_3-21 at δ_H 0.68. The ^{13}C NMR

spectrum showed the C-3 resonance at δ_C 71.9 (C-3). The olefinic carbon resonances of C-5 and C-6 were present at δ_C 140.9 and 121.8, and that of C-22 and C-23 were present at δ_C 138.4 and 129.4 respectively. The NMR data compare well with that in the literature (Kamal et al., 2016). The IR spectrum showed an OH peak at 3419 cm^{-1} as well as C-H stretching bands at 2926 cm^{-1} and 2850 cm^{-1}.

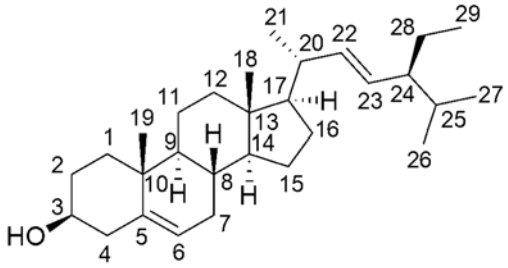

Figure 4-3 Chemical structure of stigmasterol (**S2**)

Stigmasterol shows promising anti-cancer effects on several types of cancer cells, including those in the liver, endometrium, gallbladder, skin, stomach, cervix, breast, prostate, and ovaries, suggesting that stigmasterol could be a potential avenue for the development of new cancer treatments (Bakrim et al., 2022). It has also been shown to trigger signals from pro-apoptotic proteins and promote the cleavage of specific proteins like caspase-3, caspase-9, cytochrome c, BAK, and BAX in ES2 and OV90 cells in a dose-dependent manner, leading to inhibition of cell clumping, proving to be a promising compound for preventing ovarian cancer (Bae et al., 2020). Stigmasterol administered in oral doses of 200 and 400 mg kg^{-1} three times a week for 16 weeks significantly decreased the size of tumours, lowered the overall number of papillomas, and extended the average time before tumours appeared to 13.10 weeks (Ali et al., 2015).

Numerous studies suggest that stigmasterol could serve as a potent antibacterial agent, targeting a wide range of harmful bacteria, both Gram-positive and Gram-negative (Alawode et al., 2021, Ibrahim and Yaacob, 2017). It has been shown to successfully inhibit the growth of bacteria

such as *S. aureus*, *E. coli, P. aeruginosa,* and *S. typhimurium*, with inhibition zones ranging from 11 to 18 mm (Mailafiya et al., 2018). Another study assessed its antibacterial effectiveness against *S. aureus, E. faecalis,* and *S. typhi*, revealing that stigmasterol was effective against all tested strains with MIC values ranging from 6.25 to 1000 μg mL^{-1} (Tamokou et al., 2011).

Stigmasterol was demonstrated to have antidiabetic potential by notably enhancing the translocation of GLUT4 and the uptake of glucose in L6 cells (Wang et al., 2017). Diabetic KK-Ay mice given 50 and 100 mg kg^{-1} of stigmasterol for 4 weeks, showed significant improvement in their hyperglycaemic condition (Wang et al., 2017). Diabetic rats, supplemented with 0.25 and 0.50 mg kg^{-1} of stigmasterol for 21 days, experienced a significant reduction in fasting blood glucose levels along with an increase in serum insulin (Nualkaew et al., 2015).

Compound **S3** was identified as stigmasterol glucoside from its ^{1}H and ^{13}C NMR spectrum. The ^{1}H NMR spectrum was very similar to stigmasterol, with the H-6 broad singlet at δ_H 5.32 and the H-22 and H-23 pair of doublets of doublets at δ_H 5.15 and 5.03 with coupling constants of 15.1 and 8.9 Hz for H-22 and 15.1 and 8.3 Hz for H-23. The methyl groups were also in similar positions at δ_H 0.66, the doublet of CH_3-21, and singlet resonances for CH_3-18 and CH_3-19 at δ_H 0.80 and 0.96 respectively. The glucoside moiety was indicated by the additional resonances at δ_H 4.82, a broad singlet attributed to the hydroxy groups of 2'-OH, 3'-OH and 4'-OH, δ_H 4.40, another broad singlet assigned to the 6'-OH resonance, and the proton resonances of the glucose moiety at δ_H 4.23 for the anomeric proton, a doublet with J = 7.8 Hz, and then multiplet resonances at δ_H 2.91 (H-2'), 3.13 (H-3'), 3.07 (H-4'), 3.03 (H-5'), and 3.64 and 3.50 for CH_2-6'.

The ^{13}C NMR spectrum was also similar to stigmasterol, with the C-5 and C-6 resonances at δ_C 141.0 and 121.6 respectively, and the C-22 and C-23 resonances at δ_C 138.5 and 129.3 respectively, as well as the characteristic upfield methyl resonances of C-29 and C-18 at δ_C 12.1 and 12.3 respectively. The glucose moiety was indicated by the additional resonances at δ_C 101.3 (C-1'), the anomeric carbon resonance, and 70.6 (C-2'), 77.3 (C-3'), 74.0 (C-4'), 77.2 (C-5') and 61.6 (C-6'). Compound **S3** was thus identified as stigmasterol glucoside (Figure 4-4), a common natural product. The NMR data compared favourably with that published in (Ridhay et al., 2012) (Table 4-1).

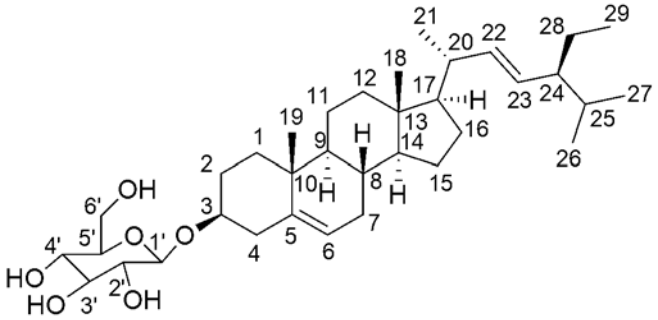

Figure 4-4 Chemical structure of stigmasterol glucoside (**S3**)

Table 4-1 ^{1}H and ^{13}C NMR data of stigmasterol glucoside (DMSO-d_6, 600 MHz)

Pos	**Stigmasterol glucoside (^{1}H)**	**Lit. (Ridhay et al., 2012)**	**Stigmasterol glucoside (^{13}C)**	**Lit. (Ridhay et al., 2012)**
1	2.36 (dd, 9.0, 1.8), 2.13 (m)	2.36 (m) & 2.13 (m)	38.8	38.28
2		1.30 (m)	33.8	33.33
3	3.40 (m)	3.42 (m)	77.4	76.95
4	1.80 (m), 1.16 (m)	180 (br d, 10.2) & 1.16 (br d 6.6)	36.7	36.76
5	-	-	141.0	140.43
6	5.32 (br s)	5.32 (br d, 4.5)	121.6	121.04
7	1.40 (m)	1.46 (m)	31.8	31.30
8	1.50 (m)	1.51 (br s)	31.9	31.38
9	0.99 (s)	0.99 (br s)	50.1	49.57

10	-	-	35.9	36.15
11	1.16 (m)	1.17 (m)	23.1	22.59
12	1.92 (m), 1.15 (m)	1.94 (m) & 1.13 (m)	45.6	41.69
13	-	-	42.3	41.80
14	1.08 (m)	1.08 (m)	56.6	56.20
15	1.15 (m)	1.12 (m)	25.8	24.72
16	1.90 (m), 1.80 (m)	1.91 (br s) & 1.77 (br s)	29.2	29.20
17	1.00 (m)	1.01 (m)	56.7	56.11
18	0.80 (s)	0.65 (s)	12.3	11.76
19	0.96 (s)	0.99 (s)	19.4	18.99
20	1.40 (m)	1.34 (m)	37.3	35.37
21	0.66 (d, 6.6)	0.91 (d, 6.3)	20.1	18.76
22	5.15 (dd, 15.1, 8.9)	5.18 (dd, 15.0, 8.4)	138.5	137.85
23	5.03 (dd, 15.1, 8.3)	5.04 (dd, 8.4, 8.1)	129.3	128.79
24	0.99 (m)	0.99 (br s)	31.7	31.20
25	1.62 (m)	1.63 (m)	29.7	31.20
26	0.82 (d, 7.0)	0.84 (d, 6.3)	19.3	19.28
27	0.80 (d, 7.0)	0.80 (d, 6.9)	19.0	18.89
28	1.01 (m)	1.01 (br s)	25.3	23.76
29	0.86 (t, 7.0)	0.79 (d, 8.1)	12.1	11.58
1’	4.23 (d, 7.8)	4.23 (d, 7.8)	101.3	100.77
2’	2.91 (m)	2.91 (m)	70.6	70.14
3’	3.13 (m)	3.15 (m)	77.3	76.75
4’	3.07 (m)	3.08 (m)	74.0	73.43
5’	3.03 (m)	3.04 (m)	77.2	76.63
6’	3.64 (d, 7.5), 3.50 (m)	3.66 (m) & 3.50 (m)	61.6	61.10
2’-OH	4.82 (br s)	4.73 (br s)		
3’-OH	4.82 (br s)	4.75 (br s)		
4’-OH	4.82 (br s)	4.71 (br s)		
6’-OH	4.40 (br s)	4.30 (t, 6.0)		

The double bond in the aliphatic chain was shown to be important for antibacterial activity, since stigmasterol glucoside demonstrated better antibacterial activity than daucosterol (without the double bond in the aliphatic chain) against *Mycobacterium smegmatis*, *Klebsiella*

oxytoca, *K. pneumonia* and *Proteus mirabilis* (Kamdem et al., 2022). Stigmasterol glucoside also exhibited better antioxidant activity (14.541 ± 0.22 %) compared to luteolin (12.725 ± 0.326 %) (Amina et al., 2018).

Compound **S4** was obtained as white needles. The IR spectrum contained O-H (3311 cm^{-1}), and C-H (2919 and 2849 cm^{-1}) stretching bands. Its ^{1}H NMR spectrum showed characteristic resonances for the H-12 olefinic resonance at δ_H 5.10, a triplet with J = 6.9 Hz, and the H-30 methylene olefinic resonances at δ_H 4.70 (H-30a) and 4.67 (H-30b), each two small doublets with J = 1.0 Hz for the geminal coupling. The H-3 proton was also characteristic at δ_H 3.17, which appeared as a doublet of doublets with coupling constants of 11.2 and 5.2 Hz. This was indicative of both axial-axial and axial-equatorial interactions, which meant that the H-3 proton was in the axial position or alpha oriented with the hydroxy group at C-3 at the beta position or equatorially oriented. Six methyl resonances could be seen in the spectrum, indicating seven methyl groups, since there were two overlapping resonances in one of them. These occurred as singlets at δ_H 1.66 (CH_3-27), 1.58 (CH_3-26), 1.22 (CH_3-25), 0.94 (6H, CH_3-23 and CH_3-28), and 0.74 (CH_3-24), and a doublet at δ_H 0.83 (J = 7.7 Hz) assigned to CH_3-29.

The ^{13}C NMR spectrum showed four characteristic resonances for the two olefinic bonds at δ_C 152.9 and δ_C 107.6 for the C-20 and C-30 carbon resonances respectively, and δ_C 124.6 and δ_C 131.6 for C-12 and C-13 respectively. The oxygenated C-3 resonance appeared at δ_C 79.1. The ^{1}H and ^{13}C NMR resonances were similar to taraxast-12,20(30)-dien-3α-ol with the configuration of the hydroxy at C-3 and the methyl at C-19 in the α position (Table 4-2), however, the slight changes in the H-3 resonance and methyl proton resonances of CH_3-26, CH_3-27 and CH_3-29, as well as changes to the carbon resonances of C-3, C-19 and C-29 led to

the configuration of the hydroxy group at C-3 and the methyl group at C-19 being placed in a β position. Compound **S4** was thus identified as 18α-ursa-12,20(30)-dien-3β-ol (Figure 4-5).

Table 4-2 ^{1}H and ^{13}C NMR data for 18α-ursa-12,20(30)-dien-3β-ol (**S4**) and taraxast-12,20(30)-dien-3α-ol (400 MHz, $CDCl_3$)

^{1}H	**18α-ursa-12,20(30)-dien-3β-ol (^{1}H)**	**Lit* (Gutiérrez et al., 2007)**	**^{13}C**	**18α-ursa-12,20(30)-dien-3β-ol (^{13}C)**	**Lit* (Gutiérrez et al., 2007)**
H-3	3.17 (dd, 11.2, 5.16 Hz)	3.49 (ddd, 12.0, 9.2, 4.1 Hz)	C-1	45.4	42.55
H-12	5.10 (t, 6.9 Hz)	5.15 (t, 3.5 Hz)	C-2	25.1	27.44
H-30	4.70 (d, 1.0 Hz, H-30a) 4.67 (d, 1.0 Hz, H-30b)	4.64 (m)	C-3	79.1	72.01
CH_3-23	0.94 (s)	0.99 (s)	C-4	29.8	38.51
CH_3-24	0.74 (s)	0.78 (s)	C-5	51.1	56.16
CH_3-25	1.22 (s)	1.20 (s)	C-6	16.0	18.46
CH_3-26	1.58 (s)	1.19 (s)	C-7	34.2	34.12
CH_3-27	1.66 (s)	1.14 (s)	C-8	40.6	42.48
CH_3-28	0.94 (s)	1.01 (s)	C-9	49.6	50.30
CH_3-29	0.83 (d, 7.7 Hz)	0.99 (d, 6.1 Hz)	C-10	29.0	37.44
			C-11	25.8	23.24
			C-12	124.6	121.94
			C-13	131.6	140.97
			C-14	39.3	42.55
			C-15	28.1	28.43
			C-16	35.6	35.96
			C-17	48.0	46.01
			C-18	56.0	56.16
			C-19	27.5	37.44
			C-20	152.9	157.11
			C-21	31.5	32.09
			C-22	37.3	39.96
			C-23	27.2	28.47
			C-24	21.5	21.28
			C-25	16.4	16.31

			C-26	17.9	16.79
			C-27	15.8	23.25
			C-28	18.4	18.91
			C-29	15.5	19.61
			C-30	107.6	106.13

* taraxast-12,20(30)-dien-3α-ol

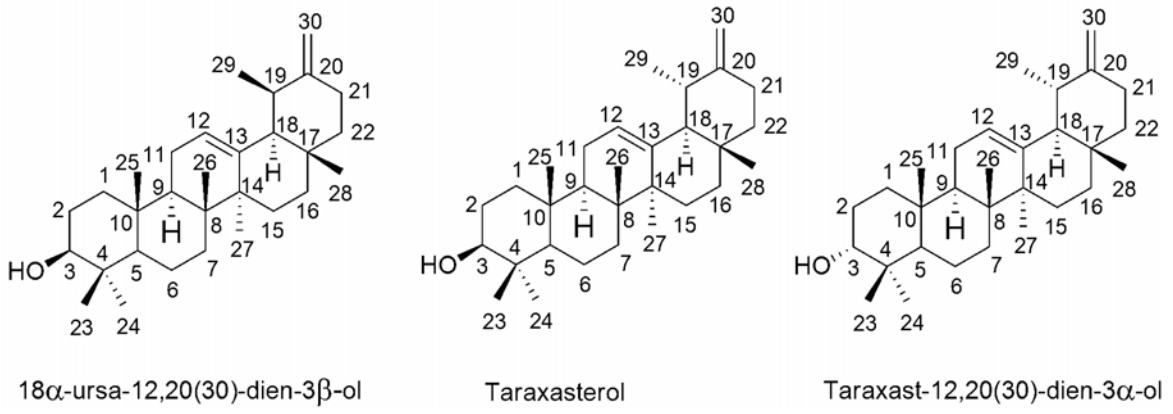

Figure 4-5 Chemical structure of 18α-ursa-12,20(30)-dien-3β-ol (**S4**), with taraxasterol and taraxast-12,20(30)-dien-3α-ol

Compound **S4** is quite a rare compound, and similar compounds have only been reported a few times previously. The 3β-acetate was reported from the roots of *Calotropis gigantea* (Ali and Gupta, 1999). Taraxasterol with the hydroxy group at C-3 in the β position and methyl at C-19 in the α position was isolated from the aerial parts of *Taraxacum mongolicum* (Li et al., 2017). Taraxast-12,20(30)-dien-3α-ol with 3α-hydroxy and 19α-methyl groups was isolated from the leaves of *Hylocereus undatus*, where it was shown to have protective microvascular activity in rabbits (Gutiérrez et al., 2007).

Compound **S5** was obtained as a yellow powder. The IR spectrum showed O-H, C=C, and C=O stretching bands at 3244 cm^{-1}, 1602 cm^{-1} and 1660 cm^{-1} respectively. The UV spectrum showed two absorption bands with a maximum peak at 370 nm. The ^{1}H NMR spectrum showed

the presence of two *ortho* coupled protons at δ_H 6.88, a doublet with J = 8.5 Hz and a doublet of doublets at δ_H 7.54 (J = 8.5, 2.1 Hz), assigned to H-5' and H-6' respectively. The H-6' resonance was in turn *meta* coupled to H-2' at δ_H 7.68, a doublet with J = 2.1 Hz. The H-6 and H-8 resonances appeared as a pair of doublets at δ_H 6.18 and 6.40 respectively with J values of 2.0 Hz. The 5-hydroxy group, hydrogen bonded to the carbonyl group at C-4 appeared as a sharp singlet resonance at δ_H 12.50. The COSY spectrum verified the coupling of H-2' with H-6' and H-6' with H-5', as well as H-6 with H-8.

The ^{13}C NMR spectrum showed the presence of 15 carbon resonances, in keeping with that of the flavonoid skeleton. The protonated carbon resonances of C-6', C-5', C-2', C-6 and C-8 at δ_C 120.4, 116.0, 115.5, 98.6 and 93.8 were all identified using the HSQC spectrum by correlating them to their respective proton resonances. The H-6 and H-8 resonances showed HMBC correlations to C-10 at δ_C 103.5, the H-2' resonance showed a correlation to C-6' and the H-5' resonance showed a correlation to C-1' at δ_C 122.4. The carbonyl group resonance was present at δ_C 176.3, which showed long range HMBC correlations to H-8. The seven oxygenated aromatic carbon resonances could be identified by HMBC correlations, H-6 and H-8 with C-7 at δ_C 164.4, H-6 with C-5 at δ_C 161.2, H-8 with C-9 at δ_C 156.6, H-2' and H-5' with C-3' at δ_C 145.5, and H-2', H-6' and H-5' with C-4' at δ_C 148.2. The C-2 and C-3 resonances remained, and were assigned to δ_C 147.3 and 136.2 respectively. Compound S5 was thus identified as quercetin (Figure 4-6). The NMR data compared well with that present in the literature and is shown in Table 4-3. The structure was confirmed by the HRMS spectrum which showed a molecular ion peak in the negative mode for $[M-H]^+$ at 301.0342 (calculated for $C_{15}H_9O_7$, 301.0348).

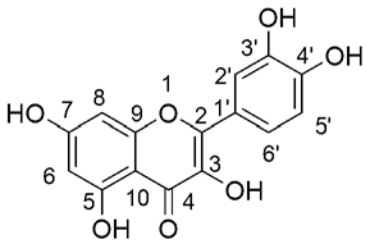

Figure 4-6 Chemical structure of quercetin (**S5**)

Quercetin has been shown to have anticancer activity against a MCF-7 cell line (Sinha et al., 2012). It is also one of the 10 standard markers in *Ginkgo biloba* herbal preparations, one of the popular herbal preparations sold internationally (Napolitano et al., 2012). Research indicates that quercetin acts as a gastroprotective agent by inhibiting gastric acid secretion and preventing lipid peroxidation in gastric cells (Lakhanpal and Rai, 2007). Quercetin was tested at doses of 50 and 100 mg kg^{-1} against ethanol-induced gastric mucosal injury in rats, and shown to possess favourable anti-ulcer properties, possibly attributed to its ability to scavenge free radicals or enhance gastric mucus production (de la Lastra et al., 1994, Suzuki et al., 1998).

Another study investigated the impact of a daily quercetin dose of 162 mg on individuals who were overweight to obese and had prehypertension or Stage I hypertension. The study found that quercetin supplementation effectively reduced ambulatory blood pressure in patients with hypertension (Brüll et al., 2015). It was also shown that taking 500 mg of quercetin daily, resulted in a decrease in systolic blood pressure among women with Type 2 diabetes (Zahedi et al., 2013).

Table 4-3 ^{1}H and ^{13}C NMR data of quercetin (600 MHz, CD_3OD)

H	**Quercetin (^{1}H)**	**Lit. (Napolitano et al., 2012)**	**C**	**Quercetin (^{13}C)**	**Lit. (Sinha et al., 2012)**
H-6	6.18 (d, J = 2.0 Hz)	6.18, d	C-2	147.3	147.4
H-8	6.40 (d, J = 2.0 Hz)	6.40, d	C-3	136.2	136.2
H-5’	6.88 (d, J = 8.5 Hz)	6.88, d	C-4	176.3	176.4
H-6’	7.54 (dd, J = 8.5, 2.1 Hz)	7.54, dd	C-5	161.2	161.2
H-2’’	7.68 (d, J = 2.1 Hz)	7.68, d	C-6	98.6	98.7
5-OH	12.50 (s)	12.49, s	C-7	164.4	164.4
			C-8	93.8	93.8
			C-9	156.6	157.0
			C-10	103.5	98.7
			C-1’	122.4	122.5
			C-2’	115.5	115.6
			C-3’	145.5	145.5
			C-4’	148.2	148.2
			C-5’	116.1	116.1
			C-6’	120.4	115.7

Compound **S6** was isolated as yellow needles. The ^{1}H NMR spectrum was similar to quercetin, but with two notable differences, the addition of the resonances between δ_H 3.00 and 4.00 attributed to that of the methine and methylene groups of the glucose moiety, the addition of broad singlet peaks between δ_H 4.00 and 5.50, and the coalescing of the H-2’ and H-6’ resonances. The H-6 and H-8 pair of doublets occurred at δ_H 6.26 and 6.46 with coupling constants of 2.1 Hz. The H-5’ resonance still appeared as a doublet with J = 9.1 Hz, and the H-1’’ anomeric proton appeared at δ_H 5.53 with J = 7.3 Hz. Expansion of the coalescing resonances of H-2’ and H-6’ revealed a doublet of doublets, which was attributed to H-6’ and the more upfield doublet also overlapped with H-2’ (Figure 4-7). Thus H-2’ occurred at δ_H 7.63 as a doublet with J = 2.1 Hz and H-6’ occurred as a doublet of doublets with J = 9.1 and 2.1 Hz.

The 5-hydroxy proton resonances could still be seen as a singlet as for quercetin at δ_H 12.71, again, due to hydrogen bonding with the carbonyl oxygen. Five other broad singlets at δ_H 5.38, 5.16, 5.04, 4.50 and 4.35 were attributed to hydroxy protons in the molecule. Deuterium exchange with the solvent caused these to be broadened singlets. The methine and methylene resonances of the glucose moiety appeared at δ_H 5.53 (H-1'', J = 7.3 Hz), attributed to the anomeric proton, and 3.34 (H-2''), 3.42 (H-3''), 3.41 (H-4''), 3.29 (H-5'') and 3.38 (H-6''). These resonances all overlapped with the broadened water peak at δ_H 3.50 and determining their coupling constants was not possible.

The ^{13}C NMR data was similar to quercetin where the carbonyl resonance could be seen at δ_C 177.9, followed by the seven oxygenated resonances at δ_C 164.6 (C-7), 161.7 (C-5), 156.8 (C-9), 156.6 (C-2), 148.9 (C-4'), 145.3 (C-3') and 133.8 (C-3). The singlet carbon resonance C-1' then appeared at δ_C 122.0, followed by the three protonated carbon resonances, C-6' at δ_C 121.6, C-5' at δ_C 116.6 and C-2' at δ_C 115.7. Further upfield, the C-10 resonance was present at δ_C 104.4, followed by the anomeric carbon resonance at δ_C 101.3 and the two protonated resonances of C-6 and C-8 at δ_C 99.1 and 94.0 respectively. The last five carbon resonances were that of the glucose moiety at δ_C 78.0 (C-3''), 77.0 (C-5''), 74.6 (C-2''), 70.4 (C-4''), and 61.4 (C-6''). The NMR data compare very well with that in the literature (Table 4-4) and was identified as quercetin-3-*O*-glucoside (Figure 4-8) (Panda and Kar, 2007). This was confirmed by HRMS analysis which showed an $[M-H]^+$ peak in the negative mode at *m/z* 463.0866, corresponding to $C_{21}H_{19}O_{12}$ (calculated 463.0877).

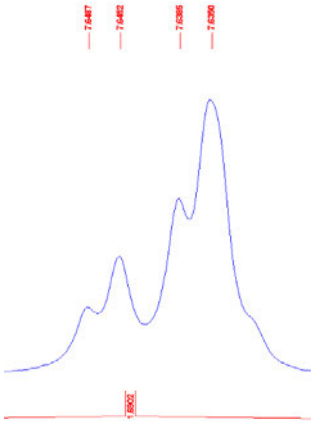

Figure 4-7 Expansion of the H-2' and H-6' overlapping resonances at δ_H 7.64

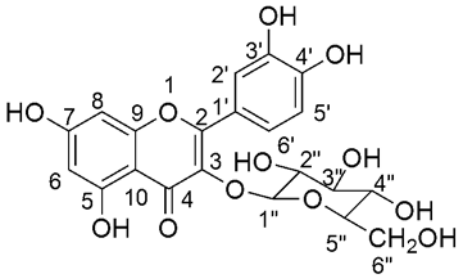

Figure 4-8 Chemical structure of quercetin-3-*O*-glucoside (**S6**)

Table 4-4 ^{1}H and ^{13}C NMR data (600 MHz, DMSO-d_6) of quercetin-3-*O*-glucoside (**S6**)

H	**Quercetin-3-*O*-glucoside (^{1}H)**	**(Panda and Kar, 2007)**	**C**	**Quercetin-3-*O*-glucoside (^{13}C)**	**(Panda and Kar, 2007)**
H-6	6.26 (d, 2.1)	6.28 (d, 2.1)	C-2	156.6	156.7
H-8	6.46 (d, 2.1)	6.31 (d, 2.1)	C-3	133.8	135.8
H-5'	6.90 (d, 9.1)	6.89 (d, 8.0)	C-4	177.9	176.5
H-6'	7.64 (dd, 9.1, 2.1)	7.57 (dd, 8.1, 2.1)	C-5	161.7	161.2
H-2'	7.63 (d, 2.1)	7.63 (d, 2.0)	C-6	99.1	99.6
5-OH	12.71 (s)		C-7	164.6	162.1
1''	5.53 (d, 7.3)	5.65 (d, 7.3)	C-8	94.0	94.2
2''	3.34 (d)	3.35 (dd)	C-9	156.8	156.6
3''	3.42 (m)	3.45 (d)	C-10	104.4	107.2
4''	3.41 (t)	3.41 (t)	C-1'	122.1	122.4

5''	3.29 (m)	3.30 (m)	C-2'	115.7	115.6
6''	3.38 (bd)	3.38 (dd)	C-3'	145.3	145.6
OH	5.38 (bs)		C-4'	148.9	148.2
OH	5.16 (bs)		C-5'	116.6	115.7
OH	5.04 (bs)		C-6'	121.6	122.1
OH	4.50 (bs)		C-1''	101.3	100.1
OH	4.35 (bs)		C-2''	74.6	74.1
			C-3''	78.0	77.5
			C-4''	70.4	70.1
			C-5''	77.0	76.3
			C-6''	61.4	61.4

Quercetin-3-*O*-glucoside has shown both antioxidant and anticancer activity. It has been reported to have powerful antioxidant effects at a concentration of 22 μg mL^{-1} (Razavi et al., 2009). In a further study, it was shown to have the ability to neutralize radicals, with percentages of 90.75% (DPPH), 88.22% (FRAP), 82.76% (ABTS), and 75.29% (ORAC) inhibition (Nile et al., 2021). When combined with apple extract, quercetin-3-*O*-glucoside was shown to effectively inhibit the growth of MCF-7 human breast cancer cells (Yang and Liu, 2009).

Compound **S7** was isolated as C-2 isomers of hesperidin (Figure 4-8). Isomers were indicated by multiplets appearing in the NMR spectrum and the doubling up of certain resonances in the ^{13}C NMR spectrum. The ^{1}H NMR spectrum showed the presence of the H-2', H-6 and H-8 resonances all coalescing between δ_H 6.90 and 6.96. The H-5' and H-6' resonances also appeared as multiplets at δ_H 6.14 and 6.13 respectively. The flavanone skeleton was indicated by the multiplets at δ_H 5.50 (H-2), 3.25 (H-3a) and δ_H 2.76 (H-3b) respectively. The anomeric proton resonances at δ_H 4.99, a triplet, and 4.52, a broadened singlet, suggested the presence of two sugar moieties in the molecule. The splitting patterns of these resonances also suggested

that isomers were present. If one isomer was present, a doublet would appear for each of these resonances. The methoxy resonance at C-4' was present as a singlet at δ_H 3.78.

The proton resonances of the sugar moieties appeared between δ_H 3.00 and 3.82, and the methyl resonance on the second sugar moiety was present as a multiplet at δ_H 1.09. Seven of the eight hydroxy proton resonances could be accounted for. The other was in the region between 3.00 to 3.80, overlapping with the proton resonances of the sugar moieties. The hydroxy proton resonance at δ_H 12.02, a broad singlet, was attributed to the 5-OH proton, which was involved in hydrogen bonding with the C-4 carbonyl group. Another broad singlet at δ_H 9.11 was also a hydroxy proton resonance, as were the doublets at δ_H 5.41, 5.20 and 5.19 with coupling constants of 5.3 Hz, and the triplet at δ_H 4.70 with a coupling constant of 6.5 Hz, and finally, a doublet of doublets at δ_H 4.62 with *J* values of 10.5 and 4.1 Hz. This splitting was due to coupling with the protons on the sugar moiety.

The ^{13}C NMR NMR spectrum showed the C-4 carbonyl resonance at δ_C 197.47, and the oxygenated aromatic carbon resonances of ring A at δ_C 165.61 (C-7), 163.50 (C-5) and 163.00 (C-9), and of ring B at δ_C 148.43 (C-4') and 146.94 (C-3'). The other four carbon resonances of ring B were present at δ_C 131, 118, 114 and 112 for C-1', C-6', C-2' and C-5', each appearing as two resonances, one for each isomer. The C-10, C-6 and C-8 resonances on ring A were present at δ_C 103.79, 96.85 and 96.07 respectively, with the anomeric protons, C-1'' and C-1''' being present at δ_C 101.07 and 99.94 respectively. The oxygenated C-2 resonance and the aliphatic C-3 resonance could be seen at δ_C 78.83 and 40.55 respectively, while the methoxy carbon resonance occurred at δ_C 56.17. The nine sugar carbon resonances of the two sugar moieties all appeared between δ_C 66.50 to 76.75, and the methyl resonance on the second sugar moiety appeared at δ_C 18.23. The ^{1}H and ^{13}C NMR data compare very well that reported for

hesperidin in the literature (Table 4-5) (Jadeja et al., 2016). The high resolution mass spectrum obtained showed a molecular ion peak in the negative mode for $[M-H]^+$ at 609.1813 corresponding to $C_{28}H_{33}O_{15}$ (calculated 609.1819).

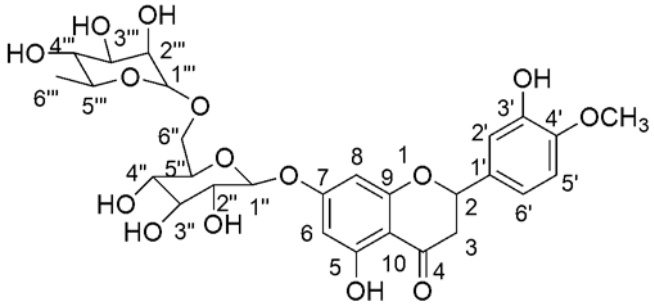

Figure 4-9 The chemical structure of hesperidin **(S7)** (a mixture of isomers with opposite configuration at C-2 were isolated)

Table 4-5 ^{1}H and ^{13}C NMR data for hesperidin (600 MHz, DMSO-d_6)

Pos	^{1}H	Lit. (Jadeja et al., 2016)	^{13}C**	Lit. (Jadeja et al., 2016)*
2	5.50, m	5.54, dd	78.83	78.34
3	3.25, m; 2.76, m	3.24, dd; 2.79, dd	40.55	41.98
4			197.47	196.98
5			163.50	163.00
6	6.90-6.96, m	6.95, s	96.85	99.38
7			165.61	165.08
8	6.90-6.96, m	6.93, s	96.07	96.34
9			163.00; 162.96	162.44
10			103.79	103.27
1’			131.45; 131.39	130.81
2’	6.90-6.96, m	6.89, s	114.62; 114.55	114.09
3’			146.94	146.38
4’			148.43; 148.39	147.97
5’	6.14, m	6.16, d	112.61; 112.54	111.92

6’	6.13, m	6.13, d	118.40; 118.23	117.93
OCH_3	3.77, s	3.77, s	56.16	55.61
1’’	4.99, t (8.4)	4.99, d	101.07	100.55
2’’	3.54, m	3.57, t	76.00	75.47
3’’	3.28, m	3.32, t	73.46	72.93
4’’	3.42, m	3.43, t	71.18	70.23
5’’	3.65, m	3.65, dd	76.74	76.68
6’’	3.44, m; 3.82, m	3.44, dd; 3.82, dd	68.79	65.97
1’’’	4.52, bs	4.54, dd	99.94; 99.89	101.96
2’’’	3.40, m	3.39, q	66.50	69.24
3’’’	3.20, m	3.19, t	70.74	70.66
4’’’	3.25, m	3.25, t	70.07	76.22
5’’’	3.18, m	3.17, t	72.54	72.03
6’’’	1.10, d (7.0)	1.10, d	18.29	17.79
OH	5.41, d (5.3)			
OH	5.20, d (5.3)			
OH	5.19, d (5.3)			
OH	4.70, t (6.5)			
OH	4.62, dd (10.5, 4.1)			
OH	9.11, bs			
5-OH	12.02, bs			

* The numbering system for ring B has been corrected. This was incorrect in Jadeja et al. (2016). The hydroxy groups were now placed at C-3’ and C-4’ instead of C-4’ and C-5’.
**Two decimal places are used for the ^{13}C NMR resonances to distinguish between resonances which are close to each other, due to the isomers being present.

Hesperidin is recognized for its ability to serve as an antioxidant, reduce inflammation, and for its antibacterial properties (Yamamoto et al., 2013). Hesperidin notably reduced cell viability in a well diffusion assay against Glioblastoma multiforme cells, with the most significant decrease occurring at concentrations of 150 and 200 μM for 48 and 72 hours, respectively (Ongun et al., 2021). Hesperidin was also found to act better against Gram-positive bacteria,

and showed an MIC of 100 μg mL^{-1} against *S. aureus*, 250 μg mL^{-1} against *B. cereus*, and 500 μg mL^{-1} against *E. coli* and *P. aeruginosa* (Iranshahi et al., 2015).

Compound **S8** was identified as caffeic acid from its ^{1}H and ^{13}C NMR spectra. This compound was isolated as light-yellow crystals. The ^{1}H NMR spectrum showed a typical ABX coupled system for the three protons on the aromatic ring at δ_H 7.06, 6.95, and 6.79 for H-2, H-6 and H-5 respectively with *ortho* coupling of 8.2 Hz and *meta* coupling of 1.9 Hz. *Trans* diaxial olefinic protons were also present at δ_H 7.54 and 6.23 for H-7 and H-8 respectively.

The ^{13}C NMR spectrum showed a carbonyl resonance of the acid at δ_C 171.6 (C-9), two oxygenated aromatic carbon resonances at δ_C 147.3 and 149.9 for C-3 and C-4 respectively, two olefinic carbon resonances at δ_C 147.5 and 116.1 (C-7 and C-8 respectively), the singlet carbon resonance at δ_C 128.3 (C-1), and the three protonated carbon resonances for C-2, C-5 and C-6 at δ_C 115.6, 117.0 and 123.3 respectively. The high resolution mass spectrum showed a molecular ion peak of $[M-H]^+$ at 179.0339 for $C_9H_7O_4$ (calculated 179.0344).

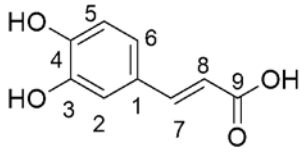

Figure 4-10 Chemical structure of caffeic acid (**S8**)

Caffeic acid is said to offer various health advantages, such as combating cancer, and having antiviral properties. Additionally, it acts as an antioxidant, reducing oxidative stress by scavenging free radicals produced in the body (Birková et al., 2020). At concentrations of 10 and 20 g mL^{-1}, the total antioxidant inhibition rates were measured as 68.2% and 75.8% respectively, comparable to those of butylated hydroxyanisole (BHA) (74.4%) and butylated

hydroxytoluene (BHT) (71.2%), but notably higher than those of α-tocopherol (54.7%) and trolox (20.1%) at 20 g mL^{-1} (Gülçin, 2006).

Table 4-6 ^{1}H and ^{13}C NMR data for caffeic acid (600 MHz, CD_3OD)

Pos.	Caffeic acid	Lit. Jeong et al., 2011	Caffeic acid	Lit. Jeong et al., 2011
1			128.3	128.3
2	7.06 (d, 1.9)	7.07 (d, 2.0)	115.6	115.7
3			147.3	147.2
4			149.9	149.8
5	6.79 (d, 8.2)	6.81 (d, 8.2)	117.0	117.0
6	6.95 (dd, 8.2, 1.9)	6.95 (dd, 8.2, 2.0)	123.3	123.4
7	7.54 (d, 15.9)	7.55 (d, 15.9)	147.5	147.6
8	6.23 (d, 15.9)	6.24 (d, 15.9)	116.1	116.0
9			171.6	171.6

Caffeic acid had significant activity against breast cancer cells. When MDA-MB-231 cells were treated with caffeic acid, the cell viability dropped from to 93.1% with a dose of 10 μM, to 66.4% with a dose of 100 μM after 24 hours (Rosendahl et al., 2015). The most noticeable effect was observed in MCF-7 cells, known to be responsive to estrogen, where it effectively halted the growth of breast cancer cells (Kabała-Dzik et al., 2017). The mechanism of action was thought to occur by interfering with certain processes and the cycle of cell division.

It was also found that caffeic acid could stop the hepatitis C virus (HCV) from multiplying by triggering a process involving Heme oxygenase 1 (HO-1) through a specific pathway in the body. This increase in HO-1 then kicked off the body's natural antiviral response, which helped stop HCV replication (Shen et al., 2018).

4.2 Nutritional analysis

Moisture content of raw *Senecio serratuloides* leaves was measured to be 58.64%, compared to 57.43% in cooked leaves. Additional nutritional analyses for *Senecio serratuloides* was determined and the results contained in Table 4-7. The leaves had a significant amount of ash, suggesting that its mineral content was high. However, ash content was found to decrease by 2.1% in cooked samples compared to the raw sample, possibly resulting from minerals leaching into boiling water during the cooking process. The level of crude fat in the leaves also dropped from 1.68% to 1.65% upon cooking.

Table 4-7: Proximate chemical composition of ash, crude fat, fibre, protein, carbohydrate (Carbo), and vitamin C of *Senecio serratuloides* DC leaves, based on dry mass

	Ash (%)	**Fat (%)**	**Fibre (%)**	**Crude protein (%)**	**Carbo (%)**	**Vit. C (%)**
Raw	19.4 (0.6)	1.68 (0.39)*	0.43 (0.22)	5.15 (0.96)	52.5 (8.1)	22.9 (4.7)
Cooked	17.3 (0.3)	1.65 (0.41)	0.59 (0.19)	6.16 (0.99)	51.9 (8.4)	16.14 (2.6)

*Values represented as mean (S.D.) n=5

Vitamin C, a vital water-soluble vitamin that aids in strengthening the immune system and having roles in the biosynthesis of collagen, decreases when the leaves are cooked. In its raw form, the leaf samples contain a rather substantial amount of this essential vitamin. Several studies point to the effectiveness of raw leaves compared to cooked leaves due to the reduction of vitamin C in the heating process. The results showed that the vitamin C level decreased by 6.8% when raw *Senecio serratuloides* leaves were cooked. The reduction in vitamin C was also seen in several vegetables, and was attributed to its high solubility in water, and subsequent degradation with elevated temperatures (Igwemmar et al., 2013).

Furthermore, with the application of heat to the leaves, there was a modest augmentation in the amount of crude fibre and protein present. Upon analysis, it was discovered that the crude protein content in the uncooked leaves increased by 1.01% after being subjected to the heating process, while there was 0.16% elevation in crude fibre. The increase in crude protein content was attributed to the denaturation of protein triggered by cooking, resulting in interior fragments gathering, and ultimately broken-down protein accumulation. Studies indicate that in cooked foods (including vegetables), the indigestible cellulose, complex starch, and stubborn fibres are broken down, leading to a greater presence of crude fibre and carbohydrates in the cooked product (Igwemmar et al., 2013, Raimundo, 2017).

Table 4-8 presents the anti-nutrient composition report on *Senecio serratuloides* leaves. These results were determined based on both raw and cooked samples of the leaves. Cooking resulted in a slight reduction of 0.40 mg per 100 g in the saponin content. Similarly, the alkaloid composition reduced by 0.01 mg per 100 g, but the flavonoid content increased by 0.03 mg per 100 g. Notably, the anti-nutrient capacity of S*enecio serratuloides* leaves decreased as a result of cooking due to the dissolution of soluble anti-nutrients in the water during the cooking process.

Table 4-8: Anti-nutrient composition of *Senecio serratuloides* DC leaves

	Alkaloids (mg 100 g^{-1})	**Flavonoids (mg 100 g^{-1})**	**Saponins (mg 100 g^{-1})**
Raw	0.16(0.1)	0.53(0.14)	15.9(2.2)
Cooked	0.15(0.1)	0.56(0.12)	15.5(1.5)

4.3 Elemental analysis

The elemental composition of the certified reference material, CRM (LGC7162- Strawberry Leaves) was used to ensure accuracy of the method of determination. The results are reported in Table 4-9. The measured values compared well with CRM values, validating the method.

In order to maintain a healthy structure, growth, and metabolism, medicinal plants require the macronutrients (Ca, Cl, N, K, Mg, etc.), and trace elements (Fe, Zn, Cu, Mn, etc.) to be the same as other plants. Since the organism is unable to synthesize these substances on its own, their uptake from the environment is essential. Table 4-10 provides a summary of the elemental concentrations for 13 selected elements in the leaves of *Senecio serratuloides* gathered from ten different sites. The plant was found to be a good source of Ca, Mg and Zn. Ca was detected in the highest quantity, followed by Mg and Zn. The concentrations of elements in the leaves were found to be in the decreasing order of Ca > Mg > Zn > Fe > Co > Cu > Cr > Mn > Ni > As > Se.

Table 4-9 Comparison of measured values of certain elements to certified values. The mean (S.D) in mg kg^{-1}, dry mass (n=3) for the certified reference material, White clover, BCR 402.

Element	***Wavelength/nm***	***Measured value/mg kg^{-1}***	***Certified value mg kg^{-1}***
As	193.96	-	-
Ca	315.88	15373.31 (119.4)	15300 (700)
Co	228.80	-	-
Cr	228.61	2.10 (0.08)	2.15 (0.340
Cu	267.71	9.57 (0.21)	10
Fe	324.75	795.13 (9.45)	818 (48)
Mg	238.20	3678.10 (9.23)	3770 (170)
Mn	279.07	187.21 (1.11)	171 (10)
Ni	257.61	2.82 (0.14)	2.61 (0.70)
Zn	213.85	26.12 (0.68)	24 (5.10)

Table 4-10 Concentration (µg g^{-1}, mean (S.D), n=3) of essential and toxic elements in *S. serratuloides* leaves (raw) from ten different sites in KwaZulu-Natal

Element	Site*	Concentration
As	S1	ND
	S2	ND
	S3	ND
	S4	1.12 (0.13)
	S5	0.92 (0.08)
	S6	1.93 (1.01)
	S7	ND
	S8	1.11 (0.12)
	S9	ND
	S10	ND
Ca	S1	52.07 (1.1)
	S2	53.80 (0.47)
	S3	27.56 (0.40)
	S4	27.52 (0.18)
	S5	27.95 (0.42)
	S6	28.83 (0.45)
	S7	27.45 (0.41)
	S8	27.24 (0.21)
	S9	26.94 (0.32)
	S10	28.98 (0.73)
Co	S1	ND
	S2	1.19 (0.13)
	S3	2.19 (1.10)
	S4	0.98 (0.21)
	S5	ND
	S6	3.87 (0.21)
	S7	ND
	S8	0.022 (0.02)
	S9	ND
	S10	ND
Cr	S1	ND
	S2	0.12 (0.001)
	S3	ND
	S4	ND
	S5	1.98 (0.03)
	S6	1.25 (0.10)
	S7	ND
	S8	0.025 (0.020)
	S9	ND

	S10	0.01 (0.001)
Cu	S1	ND
	S2	0.085 (0.03)
	S3	0.10 (0.001)
	S4	0.091 (0.01)
	S5	ND
	S6	0.36 (0.01)
	S7	0.09 (0.01)
	S8	0.097 (0.01)
	S9	0.092 (0.02)
	S10	ND
Fe	S1	1.36 (0.10)
	S2	1.37 (0.10)
	S3	1.83 (0.01)
	S4	1.87 (0.10)
	S5	1.87 (0.20)
	S6	2.06 (0.02)
	S7	1.89 (0.04)
	S8	1.96 (0.40)
	S9	1.82 (0.01)
	S10	1.59 (0.01)
Mg	S1	50.91 (0.63)
	S2	49.78 (1.1)
	S3	21.88 (0.11)
	S4	22.18 (0.18)
	S5	21.50 (0.15)
	S6	22.96 (0.26)
	S7	24.33 (0.26)
	S8	22.77 (0.22)
	S9	21.60 (0.15)
	S10	21.95 (0.17)
Mn	S1	0.20 (0.001)
	S2	0.19 (0.005)
	S3	0.54 (0.01)
	S4	1.67 (0.01)
	S5	0.54 (0.01)
	S6	2.52 (0.01)
	S7	0.56 (0.01)
	S8	0.52 (0.01)
	S9	0.54 (0.02)
	S10	0.50 (0,01)
Ni	S1	ND
	S2	0.28 (0.03)

	S3	0.53 (0.01)
	S4	0.08 (0.02)
	S5	ND
	S6	1.93 (0.13)
	S7	0.46 (0.01)
	S8	0.46 (0.3)
	S9	ND
	S10	ND
Se	S1	0.057 (0.02)
	S2	ND
	S3	0.23 (0.01)
	S4	0.05 (0.01)
	S5	ND
	S6	3.54 (0.11)
	S7	0.27 (0.02)
	S8	0.019 (0.01)
	S9	ND
	S10	ND
Zn	S1	10.11 (1.11)
	S2	19.21 (2.21)
	S3	11.32 (1.21)
	S4	1.54 (0.01)
	S5	1.39 (0.13)
	S6	ND
	S7	6.31 (1.01)
	S8	15.43 (2.13)
	S9	17.11 (1.22)
	S10	ND

*****Sites: S1-Mandeni, S2-Stanger, S3-Reservoir Hills, S4-Palmiet, S5-Richards Bay, S6-Shongweni, S7-Eshowe, S8-Thongathi, S9-Vryheid, S10-Ndwedwe. All sites are in KwaZulu-Natal, South Africa; ND: Not determinable.

The level of calcium present in all locations was observed to be high. Sites 1 and 2, Mandeni and Stanger respectively, was the highest with 52.07 and 53.80 µg g^{-1}, while the rest of the sites had concentrations between 27.24 to 28.98 µg g^{-1}. This crucial element plays a significant role in building and sustaining bones within our bodies. Without it, our nerves and muscles cannot operate accurately.

Magnesium followed the same pattern, being the highest in the first two sites, Mandeni and Stanger at 50.91 and 49.78 µg g^{-1} with the other sites ranging from 21.50 to 24.33 µg g^{-1}. Magnesium is important in activating enzymes, hence, its deficiency can cause a number of diseases such as diabetes mellitus type II, cardiovascular diseases, and metabolic syndrome (Jahnen-Dechent and Ketteler, 2012). The significant amounts of calcium and magnesium detected in *S. serratuloides* is consistent with plants storing elevated concentrations of these metals above others to satisfy their necessary physiological levels. Nevertheless, the levels of these elements remained lower compared to the amounts recorded previously. According to a recent study, the level of magnesium found in *Senecio Vernalis* Wadst was found to be 5600 µg g^{-1} (Demir et al., 2022). The magnesium content in *Senecio biafrae* and *Senecio nutans,* was found to be 392 and 290 µg g^{-1} respectively, while calcium was found to be 242 and 1390 µg g^{-1} respectively (Parra et al., 2018).

It is important that an excessive accumulation of zinc in the body is prevented. An overabundance of zinc leads to a shortage of copper, as well as cell death (Lange et al., 2017). Furthermore, a depletion of zinc leads to a diminished immune system. The recorded range of zinc levels found in *S. serratuloides* was found to be between 1.39 and 19.21 µg g^{-1}.

Iron, essential for producing red blood cells and transferring oxygen to cells, was found to be between 1.36 to 2.06 µg g^{-1}. A sufficient amount of iron is needed to prevent illnesses such as anaemia, however, excessive amounts can be harmful and potentially cause harm to cells. Copper is a useful trace element as it is a main component of the respirational enzyme system (Kaska et al., 2019). Copper was found to have concentrations of between 0.09 and 0.36 µg g^{-1}. A minimal quantity of copper is required for proper tissue functioning, but is lethal and toxic when consumed in excessive amounts. Manganese is necessary for the normal functioning of reproduction and the central nervous system. Insufficient amounts of manganese results in

heart problems and bone issues in children. Manganese was found to be present between 0.19 to 2.52 µg g^{-1}.

If there was any trace of the poisonous metals Cd and Pb, they were below the limit of detection by the measuring instrument (0.0027 mg L^{-1} and 0.042 mg L^{-1} respectively). Arsenic, however, was found in concentrations ranging from 0.92 and 1.93 µg g^{-1}. Arsenic content in terrestrial plants under typical conditions are reported to be <10 µg g^{-1} (Patel et al., 2023). The average concentration of arsenic reported in crop plants such as rice, maize, wheat, and tomato is 40 µg g^{-1} (Sandil et al., 2021).

4.4 Antidiabetic activity

Alpha amylase and alpha glucosidase are enzymes responsible for breaking down dietary carbohydrates in humans. Inhibiting these enzymes, decreases the rate of carbohydrate digestion and glucose absorption, ultimately lowering blood glucose levels. The current study evaluated six crude extracts from *Senecio serratuloides* for their ability to inhibit both α-amylase and α-glucosidase enzymes.

The methanol extract from the leaves was the most active with inhibitory activity against α-amylase and α-glucosidase at 74.86±5.54% and 75.14±9.65% respectively. The methanol extract from stems and ethyl acetate extract of the stems and leaves combined also showed significant activity against α-amylase, with activity of 65.93±6.83% and 71.66±8.74% respectively (Figure 4-11). The DCM and Ethyl acetate (EA) extracts also demonstrated good inhibitory activity against α-glucosidase at 67.34±1.41% and 72.12±16.92%, respectively (Figure 4-12). This was consistent with a previous study, where the methanol extract of *S. serratuloides* was effective in controlling high blood sugar, but with a lesser extent at 22.95±1.50% (Tata et al., 2019).

Extracts were tested by aligning the preparation techniques with those of ethnomedicine. Medicinal plants used for the treatment of diabetes is often infused or boiled in water to prepare decoctions in traditional practices. This results in the extraction of more polar compounds from the plants. Since medicinal plants contain many and varied secondary metabolites, their efficacy may be derived from individual compounds or synergistic effects of a group of compounds.

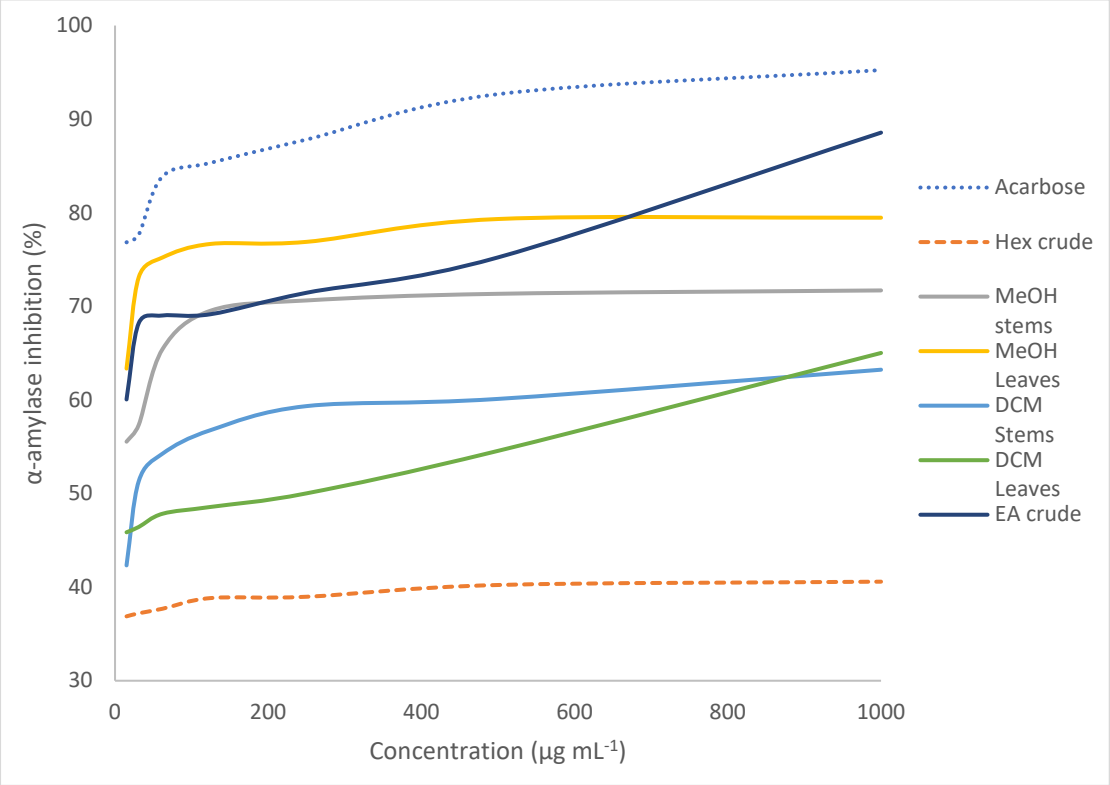

Figure 4-11: α-Amylase inhibitory activity of *S. serratuloides* (where the plant part is not indicated, this refers to the leaves and stems combined)

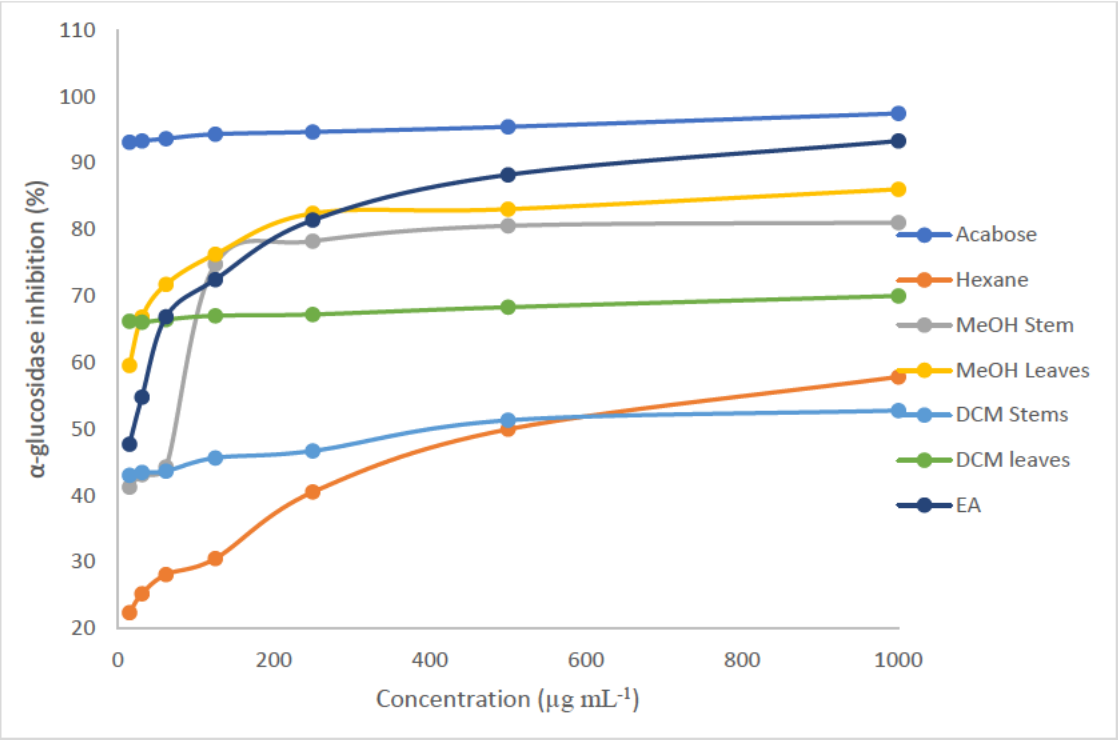

Figure 4-12: α-Glucosidase inhibitory activity of *S. serratuloides* (where the plant part is not specified, this refers to the leaves and stems combined)

4.5 Antibacterial activity

Eight extracts were tested for their antibacterial activity against 10 bacterial strains. The extracts tested were, (1) hexane extract of the leaves, (2) hexane extract of the stems, (3) dichloromethane extracts of the leaves and fruit combined, (4) dichloromethane extract of the stems, (5) ethyl acetate extract of the stems and leaves combined, (6) methanol extract from the leaves, (7) methanol extract of the stems. The ethyl acetate extracts of the stems and leaves were combined, since they showed a similar TLC profile. The 10 bacterial strains consisted of five Gram positive strains, *Enterococcus faecalis* ATCC 27853, *Enterococcus faecalis* ATCC 51299, *Staphylococcus aureus* ATCC 29213, *Staphylococcus aureus* ATCC 43300, *Staphylococcus epidermidis* ATCC 14990, and five Gram negative strains, *Acinetobacter baumannii* ATCC 19606, *Escherichia coli* ATCC 25922, *Escherichia coli* ATCC 35218, *Klebsiella pneumonia* ATCC 700603, and *Pseudomonas aeruginosa* ATCC 27853.

Unfortunately, no significant antimicrobial activity was observed with all the extracts against the bacterial strains tested against. They all showed MICs > 1025 µg mL^{-1}.

The lack of antimicrobial activity observed in this study has also been reported previously. No antibacterial activity was associated with *S. serratuloides* leaf, stem, and root extracts when tested against *Bacillus subtilis*, *E. coli*, *Micrococcus luteus*, *P. aeruginosa*, *S. aureus* and *S. epidermidis* at a range of 8.0 to 0.25 mg mL^{-1} (Kelmanson et al., 2000).

In traditional medicine practise, tea is made from *S. serratuloides* leaves and used during infections, while leaves are applied directly to purulent sores. The leaf decoction is utilised as a blood purifier for skin eruptions, while powdered leaves or roots are applied to burns and sores. *S. aureus* and *S. epidermidis* are typically associated with skin infections, however, the MICs obtained for susceptible and methicillin-resistant *S. aureus* and *S. epidermidis* were > 1025 µg mL^{-1}. According to Eloff (2019), only plant extracts with MICs lower than 0.1 mg mL^{-1} are valuable in the search for potential new antibiotics. Extracts with MICs greater than 0.5 – 1 mg mL^{-1} are not considered good candidates (Eloff, 2019). Thus, the traditional use of *S. serratuloides* extracts for treating infections, treating burns and sores and for blood purifying must occur through some other mechanism.

A review of the literature indicates that the high MICs obtained are similar to those reported for other *Senecio* species. The methanol extract of *S. vulgaris* showed poor antimicrobial activity against Gram-positive bacteria with high MIC values of 0.5 mg mL^{-1} for *Bacillus subtilis* and 0.125 mg mL^{-1} for *S. aureus* while the hexane extract of *S. inaequidens* showed similar activity against *B. subtilis* (MIC 0.5 mg mL^{-1}) and *S. aureus* (0.25 mg mL^{-1}) (Loizzo et al., 2004). All remaining extracts for *S. vulgaris* and *S. inaequidens* resulted in MICs > 1mg

mL^{-1} for *S. aureus*, *B. subtilis*, *E. coli* and *P. aeruginosa* (Loizzo et al., 2004). This reported poor antibacterial activity of *Senecio* species is consistent with the present study.

The antimicrobial activity of the methanolic extracts of nine *Senecio* species growing in Turkey were tested against eight Gram -ve and five Gram +ve bacteria where *S. olympicus* and *S. viscosus* extracts showed activity of 6.25 mg mL^{-1} against *P. aeruginosa*, while six *Senecio s*pecies extracts had MICs of 6.25 – 12.5 mg mL^{-1} against *K. pneumoniae*. No antimicrobial activity was observed against *E. coli* and *S. aureus* (Albayrak et al., 2014). The MICs obtained for Gram +ve *Bacillus cereus* and Gram -ve *Shigella flexneri* with a 50% MeOH extract of the stem and leaves of *Senecio longiflorus* (DC) extract was 6.25 and 0.1 mg mL^{-1} respectively (Asong et al., 2019).

Chapter 5 Conclusions

The present study undertook to provide a rationale for the use of *S. serratuloides* DC as a medicinal plant, as well as assess the plant's safety for use as herbal medication. This plant is used for treating various conditions such as swollen gums, chest pains, sores, cuts, burns and ulcers (Van Wyk, 2011). In particular, we were interested in the antibacterial activity of the plant, since their use in treating sores, cuts and burns suggest possible antibacterial activity. We were also interested in screening the plant for antidiabetic activity, since many South African medicinal plants were shown to have good antidiabetic activity (Table 1-2).

The phytochemical analysis was undertaken to identify the secondary metabolites present in the extract to determine information on the compounds present in the extract, with regard to their bioactivity and toxicity. Similarly, the elemental analysis of the plant was carried out to determine the concentration of both essential and toxic elements present in the plant. These studies were undertaken to provide a chemical profile of the plant, which is essential if the plant is to be used as herbal remedy, and as a guide for the dosage of the extracts to be used in ethnomedicine or herbal treatment.

5.1 Phytochemical analysis

The phytochemical analysis of the plant resulted in the isolation and identification of the sterols and triterpenoids, β-sitosterol, stigmasterol, stigmasterol glucosidase, and 18α-ursa-12,20(30)-dien-3*β*-ol, the flavonoids, quercetin, quercetin-3-*O*-glucoside and hesperidin, and an aromatic acid, caffeic acid.

Sterols and sterolins have been shown to be an effective immune booster, sitosterol being the principal component in Moducare® (Pegel, 2002), and in the prevention and treatment of several diseases and ailment such as HIV, rheumatoid arthritis and allergic rhinitis (Bouic,

2002). In addition, sitosterol has been associated with lowering cholesterol, treating enlarged prostrate and in the treatment of cardiac problems (Ambavade et al., 2014, Khan et al., 2022, Luhata and Usuki, 2021). The implication of sitosterol in treating cardiac problems may be linked to the use of the plant to treat chest pains. Sitosterol was also shown to have antibacterial and antioxidant activity (Bhat et al., 2019, Nweze et al., 2019).

Stigmasterol and stigmasterol glucoside has shown significant anticancer, antibacterial, antidiabetic and antioxidant activity (Alawode et al., 2021, Ali et al., 2015, Amina et al., 2018, Bae et al., 2020, Bakrim et al., 2022, Ibrahim and Yaacob, 2017, Kamdem et al., 2022, Mailafiya et al., 2018, Nualkaew et al., 2015, Tamokou et al., 2011, Wang et al., 2017). Since 18α-ursa-12,20(30)-dien-3*β*-ol is a rare compound, its bioactivity is not well reported.

The suite of sterols and triterpenoids found in this study, therefore provide a good rationale for the use of the plant in ethnomedicine, as these individual components may act alone or synergistically in treating the wide range of medical conditions and diseases described above. Furthermore, the immune boosting properties of these compounds, may be of importance in rural parts of South Africa, where much of the population cannot afford commercially available immune boosters such as Moducare®.

The isolation of the flavonoids, quercetin, quercetin-3-*O*-glucoside and hesperidin, is interesting, as flavonoids are known antioxidants. Quercetin and quercetin-3-*O*-glusoide was shown to be powerful antioxidants (Nile et al., 2021, Razavi et al., 2009), and hesperidin also showed good antioxidant activity (Yamamoto et al., 2013). Furthermore, these three flavonoids have been shown to have anticancer activity, possibly linked to its antioxidant potential (Ongun et al., 2021, Sinha et al., 2012, Yang and Liu, 2009). This suggests that the plant may have potential anticancer activity, and for future work, it would be worthwhile testing the extracts of the plant for their anticancer activity.

Quercetin was also found to treat hypertension (Brüll et al., 2015, Zahedi et al., 2013), and future work would also be to test the extracts for their ability to reduce hypertension. Moreover, quercetin was shown to be a gastroprotective agent (de la Lastra et al., 1994, Lakhanpal and Rai, 2007, Suzuki et al., 1998), providing a rationale for the use of the plant to treat ulcers.

Although hesperidin was shown to have some antibacterial activity (Iranshahi et al., 2015), this activity was very low, in keeping with the extracts of the plant not showing any antibacterial activity in the assays carried out in this study. It is likely that the use of the plant to treat sores, cuts and burns is not due to the antibacterial activity of the plant, but some other mode of action.

The isolation of caffeic acid was an interesting discovery, as this small molecule was seen to have anticancer, antioxidant and antiviral properties (Birková et al., 2020, Gülçin, 2006, Rosendahl et al., 2015, Shen et al., 2018). It is highly likely that this compound acts synergistically with the flavonoids in the plant extract, and future work on the antioxidant and anticancer potential of the plant extract would definitely be an interesting study.

5.2 Nutritional and elemental analysis

The leaves were shown to have a high concentration of vitamin C, 22.9% in the raw leaves, while in the cooked leaves, 16.14% of vitamin C remained. This indicated that 6.8% was extracted into the concoction during the cooking phase. Combined with the presence of sitosterol and stigmasterol in the plant, this could make the herbal or ethnomedicinal extracts quite powerful antioxidant and immune boosters.

The plant was also found to be a good source of calcium, magnesium and zinc, with concentrations as high as 52.07, 50.91 and 19.21 $\mu g\ g^{-1}$. A good amount of iron was also found in the plant, with the highest concentration at 2.06 $\mu g\ g^{-1}$. These essential elements are

important in maintaining strong and healthy bones, and for preventing anaemia (in the case of iron).

5.3 Antidiabetic and antibacterial activity

The extracts obtained from *Senecio serratuloides* DC were found to have no antibacterial activity. This is surprising, since some of the isolated compounds were reported to have shown some antibacterial properties, however, these may have been too low to have any significant effect in the crude extracts.

It was shown that the methanol extract of the leaves was the most active in the α amylase and α-glucosidase assays with activity at 74.86±5.54% and 75.14±9.65% respectively. The methanol extract from the stems and other solvent extracts were lower. This indicates the potential of herbal concoctions and remedies made in polar solvents, such as methanol and water to have possible antidiabetic activity. Thus, *Senecio serratuloides* can be added to the many known South African medicinal plants with antidiabetic activity.

5.4 Future work

From the study carried out, it emerged that the compounds isolated were good antioxidant compounds, which have also shown good anticancer activity. This indicates the need to test the extracts of the plant for their anticancer activity to determine whether or not they can be used either to supplement existing drugs or to treat the different cancers on their own. Since some of the compounds isolated have also shown cardiac, gastroprotective and antihypertensive activity, providing a rationale for their ethnomedicinal use, the information missing on the plant is now the activity of the extracts in these assays, which could provide further credence and validation to their use in ethnomedicine.

Finally, since the elemental and nutritional value of the plant is now known, a further study can also determine the dosages at which the different extracts of the plant have the greatest efficacy, and to determine the safety and cytotoxicity profile of the plant extracts.

SUPPORTING INFORMATION

Supporting information including all NMR spectra and selected IR and UV data are included in an attached file.

References

ADAMU, H. M. A., USHIE, O., GWANGWALA, A. H., YADAV, R. P., SINGH, A. V., BHARDWAJ, A. K., LONE, P. A., DAR, M. M., PARRAY, J. A., SHAH, K. W., KUMAR, B. S. A., SETTY, S. G., HARSHADA, R., ARCHANA, P. G., BEGUM, A. T. & ANBAZHAKAN, S. 2013. Estimation of total flavonoids and tannins in the stem bark and leaves of *Anogeisus leiocarpus* plant. *International Journal of Traditional and Natural Medicines,* 2**,** 141-148.

ADEDEJI, W. A. 2016. Editorial: The treasure called antibiotics. *Annals of Ibadan Postgraduate Medicine,* 14**,** 56-57.

ADELAKUN, S., OMOTOSO, O., ANIAH, J. & OYEWO, O. 2018. *Senecio biafrae* defeated tetracycline-induced testicular toxicity in adult male Sprague Dawley rats. *JBRA Assisted Reproduction,* 22**,** 314-322.

ADELEYE, O., OLAYODE, J., AJAMU, M., ODETOLA, A., OYEWO, O., ADEYINKA, O. & AYANLADE, J. 2019. Effect of simultaneous administration of alabukun and ethanol on hematological parameters and Liver of adult wistar rats (*Rattus norvegicus*). *International Journal of Recent Innovations in Academic Research,* 3**,** 199-208.

AFOLAYAN, A. J. & SUNMONU, T. O. 2010. In vivo studies on antidiabetic plants used in South African herbal medicine. *Journal of Clinical Biochemistry and Nutrition,* 47**,** 98-106.

AFUAPE, A. O., AFOLAYAN, A. J. & BUWA-KOMORENG, L. V. 2022. Proximate, vitamins, minerals and anti-nutritive constituents of the leaf and stem of *Helichrysum odoratissimum* (L.) Sweet: A folk medicinal plant in South Africa. *International Journal of Plant Biology,* 13**,** 463-472.

ALAWODE, T. T., LAJIDE, L., OLALEYE, M. & OWOLABI, B. 2021. Stigmasterol and β-sitosterol: Antimicrobial compounds in the leaves of *Icacina trichantha* identified by GC–MS. *Beni-Suef University Journal of Basic and Applied Sciences,* 10**,** 80.

ALBAYRAK, S., AKSOY, A., YURTSEVEN, L. & YAŞAR, A. 2014. A comparative study on phenolic components and biological activity of some *Senecio* species in Turkey. *Journal of Pharmacy and Pharmacology,* 66**,** 1631-1640.

ALI, H., DIXIT, S., ALI, D., ALQAHTANI, S. M., ALKAHTANI, S. & ALARIFI, S. 2015. Isolation and evaluation of anticancer efficacy of stigmasterol in a mouse model of DMBA-induced skin carcinoma. *Drug Design, Development and Therapy,* 9**,** 2793-800.

ALI, M. & GUPTA, J. 1999. New pentacyclic triterpenic esters from the roots of *Calotropis gigantea*. *Indian Journal of Chemistry, Section B,* 38**,** 877-881.

ALI, S., GOPALAKRISHNAN, B. & VENKATESALU, V. 2018. Evaluation of larvicidal activity of Senecio laetus Edgew. against the malarial vector, Anopheles stephensi, dengue vector, Aedes aegypti and Bancroftian filariasis vector, Culex quinquefasciatus. *South African Journal of Botany,* 114**,** 117-125.

ALVARADO-AVILA, L. Y., MOGUEL-ORDÓÑEZ, Y. B., GARCÍA-FIGUEROA, C., RAMÍREZ-RAMÍREZ, F. J. & ARECHAVALETA-VELASCO, M. E. 2022. Review: Presence of pyrrolizidine alkaloids in honey and the effects of their consumption on humans and honeybees. *Revista Mexicana de Ciencias Pecuarias,* 13**,** 787-802.

AMBAVADE, S. D., MISAR, A. V. & AMBAVADE, P. D. J. 2014. Pharmacological, nutritional, and analytical aspects of β-sitosterol: a review. *Oriental Pharmacy and Experimental Medicine,* 14**,** 193-211.

AMINA, M., ALARFAJ, N. A., EL-TOHAMY, M. F., AL MUSAYEIB, N. M. & ORABY, H. F. 2018. Sequential injection-chemiluminescence evaluation of stigmasterol glucoside and luteolin via green synthesis of silver nanoparticles using biomass of *Plectranthus asirensis*. *Green Chemistry Letters and Reviews,* 11**,** 523-533.

ASHOUR, R. M., EL SAYED, A. M., ELYAMANY, M. F. & ABOU-HUSSEIN, D. R. 2018. Chemical profile and biological activities of the aerial parts of *Senecio acaulis* (Lf) Sch. Bip. *Pharmacognosy Research,* 10**,** 136-144.

ASONG, J. A., AMOO, S. O., MCGAW, L. J., NKADIMENG, S. M., AREMU, A. O. & OTANG-MBENG, W. 2019. Antimicrobial activity, antioxidant potential, cytotoxicity and phytochemical profiling of four plants locally used against skin diseases. *Plants,* 8**,** 350.

ATANASOV, A. G., WALTENBERGER, B., PFERSCHY-WENZIG, E.-M., LINDER, T., WAWROSCH, C., UHRIN, P., TEMML, V., WANG, L., SCHWAIGER, S. & HEISS, E. H. 2015. Discovery and resupply of pharmacologically active plant-derived natural products: A review. *Biotechnology Advances,* 33**,** 1582-1614.

BAE, H., SONG, G. & LIM, W. 2020. Stigmasterol causes ovarian cancer cell apoptosis by inducing endoplasmic reticulum and mitochondrial dysfunction. *Pharmaceutics,* 12**,** 488-504.

BAKRIM, S., BENKHAIRA, N., BOURAIS, I., BENALI, T., LEE, L.-H., EL OMARI, N., SHEIKH, R. A., GOH, K. W., MING, L. C. & BOUYAHYA, A. 2022. Health benefits and pharmacological properties of stigmasterol. *Antioxidants,* 11**,** 1912-1944.

BALOGUN, F. & ASHAFA, A. 2017. Aqueous root extracts of Dicoma anomala (Sond.) extenuates postprandial hyperglycaemia in vitro and its modulation on the activities of carbohydrate-metabolizing enzymes in streptozotocin-induced diabetic Wistar rats. *South African journal of botany,* 112**,** 102-111.

BARNES, J., ANDERSON, L. A. & PHILLIPSON, J. D. 2007. *Herbal medicines*, pharmaceutical press.

BHAMBHANI, S., KONDHARE, K. R. & GIRI, A. P. 2021. Diversity in chemical structures and biological properties of plant alkaloids. *Molecules,* 26**,** 3374-3403.

BHAT, A. H., ALIA, A., RATHER, G. M. & KUMAR, B. 2019. Isolation & characterisation of beta-sitosterol from the rhizomes of *Arisaema utile* and its evaluation for antioxidant activity. *International Journal of Scientific Research in Biological Sciences,* 6**,** 111-118.

BIRKOVÁ, A., HUBKOVÁ, B., BOLERÁZSKA, B., MAREKOVÁ, M. & ČIŽMÁROVÁ, B. 2020. Caffeic acid: A brief overview of its presence, metabolism, and bioactivity. *Bioactive Compounds in Health Disease,* 3**,** 74-81.

BLANCAS-BENITEZ, F. J., GONZÁLEZ-AGUILAR, G. A. & SÁYAGO-AYERDI, S. G. 2017. Guava (*Psidium guajava*). *In:* YAHIA, E. M. (ed.) *Fruit and Vegetable Phytochemicals: Chemistry and Human Health, 2nd Ed.*

BOADUO, N. K. K., KATERERE, D., ELOFF, J. N. & NAIDOO, V. 2014. Evaluation of six plant species used traditionally in the treatment and control of diabetes mellitus in South Africa using in vitro methods. *Pharmaceutical biology,* 52**,** 756-761.

BOUIC, P. J. 2002. Sterols and sterolins: new drugs for the immune system? *Drug Discovery Today,* 7**,** 775-778.

BOUSETLA, A., KESKINKAYA, H. B., BENSOUICI, C., LEFAHAL, M., ATALAR, M. N. & AKKAL, S. 2023. LC-ESI/MS-phytochemical profiling with antioxidant and antiacetylcholinesterase activities of Algerian *Senecio angulatus* Lf extracts. *Natural Product Research,* 37**,** 123-129.

BROCKBALS, L., HABICHT, M., HAJDAS, I., GALASSI, F. M., RÜHLI, F. J. & KRAEMER, T. 2018. Untargeted metabolomics-like screening approach for chemical characterization and differentiation of canopic jar and mummy samples from Ancient Egypt using GC-high resolution MS. *Analyst,* 143**,** 4503-4512.

BROWN, D. G., LISTER, T. & MAY-DRACKA, T. L. 2014. New natural products as new leads for antibacterial drug discovery. *Bioorganic & Medicinal Chemistry Letters,* 24**,** 413-418.

BRÜLL, V., BURAK, C., STOFFEL-WAGNER, B., WOLFFRAM, S., NICKENIG, G., MÜLLER, C., LANGGUTH, P., ALTEHELD, B., FIMMERS, R. & NAAF, S. 2015. Effects of a quercetin-rich onion skin extract on 24 h ambulatory blood pressure and endothelial function in overweight-to-obese patients with (pre-) hypertension: a randomised double-blinded placebo-controlled cross-over trial. *British Journal of Nutrition,* 114**,** 1263-1277.

CAMPBELL, R. K., WHITE JR, J. R. & SAULIE, B. A. 1996. Metformin: a new oral biguanide. *Clinical Therapeutics,* 18**,** 360-371.

CHANDRAN, R., PARIMELAZHAGAN, T., SHANMUGAM, S. & THANKARAJAN, S. 2016. Antidiabetic activity of *Syzygium calophyllifolium* in Streptozotocin-Nicotinamide induced Type-2 diabetic rats. *Biomedicine & Pharmacotherapy,* 82**,** 547-554.

CHASSAGNE, F., SAMARAKOON, T., PORRAS, G., LYLES, J. T., DETTWEILER, M., MARQUEZ, L., SALAM, A. M., SHABIH, S., FARROKHI, D. R. & QUAVE, C. L. 2021. A systematic review of plants with antibacterial activities: A taxonomic and phylogenetic perspective. *Frontiers in pharmacology,* 11**,** 586548.

CIURA, K., DZIOMBA, S., NOWAKOWSKA, J. & MARKUSZEWSKI, M. J. 2017. Thin layer chromatography in drug discovery process. *Journal of Chromatography A,* 1520**,** 9-22.

COMFORT, M.-I., MAJESTY, D., EZE, A., KELECHI, N., AHAMEFULA, E., IJEOMA, N., PRINCE, O., CHIMARAOKE, O., ISHADE, O. & PETER, B. E. 2019. Effect of ethanolic leaf extract of *Vinca major* L. on biochemical parameters and glucose level of alloxan induced diabetic rats. *African Journal of Biotechnology,* 18**,** 1054-1068.

CORTINOVIS, C. & CALONI, F. 2015. Alkaloid-containing plants poisonous to cattle and horses in Europe. *Toxins,* 7**,** 5301-5307.

COSKUN, O. 2016. Separation techniques: Chromatography. *North Clin Istanb,* 3**,** 156-160.

CRAGG, G. M. & NEWMAN, D. J. 2005. Plants as a source of anti-cancer agents. *Journal of Ethnopharmacology,* 100**,** 72-79.

DALCORSO, G., MANARA, A., PIASENTIN, S. & FURINI, A. 2014. Nutrient metal elements in plants. *Metallomics,* 6**,** 1770-1788.

DAR, R. A., SHAHNAWAZ, M. & QAZI, P. H. 2017. General overview of medicinal plants: A review. *The journal of phytopharmacology,* 6**,** 349-351.
DE LA LASTRA, A., MARTIN, M. J. & MOTILVA, V. 1994. Antiulcer and gastroprotective effects of quercetin: a gross and histologic study. *Pharmacology,* 48**,** 56-62.
DE WET, H., NCIKI, S. & VAN VUUREN, S. F. 2013. Medicinal plants used for the treatment of various skin disorders by a rural community in northern Maputaland, South Africa. *Journal of Ethnobiology Ethnomedicine,* 9**,** 51.
DE WET, H. & NGUBANE, S. 2014. Traditional herbal remedies used by women in a rural community in northern Maputaland (South Africa) for the treatment of gynaecology and obstetric complaints. *South African Journal Botany,* 94**,** 129-139.
DEMIR, A., ESKIN, B. & RASHIDI, A. 2022. Investigation of mineral nutrient and heavy metal accumulation status of *Senecio vernalis* Waldst. & Kit. collected from different habitats of Aksaray/Turkey. *Journal of Natural Fibers,* 19**,** 1962-1973.
DEUTSCHLÄNDER, M., LALL, N. & VAN DE VENTER, M. 2009. Plant species used in the treatment of diabetes by South African traditional healers: An inventory. *Pharmaceutical Biology,* 47**,** 348-365.
DEUTSCHLÄNDER, M., LALL, N., VAN DE VENTER, M. & HUSSEIN, A. A. 2011. Hypoglycemic evaluation of a new triterpene and other compounds isolated from *Euclea undulata* Thunb. var. myrtina (Ebenaceae) root bark. *Journal of Ethnopharmacology,* 133**,** 1091-1095.
DHYANI, P., QUISPE, C., SHARMA, E., BAHUKHANDI, A., SATI, P., ATTRI, D. C., SZOPA, A., SHARIFI-RAD, J., DOCEA, A. O. & MARDARE, I. 2022. Anticancer potential of alkaloids: a key emphasis to colchicine, vinblastine, vincristine, vindesine, vinorelbine and vincamine. *Cancer Cell International,* 22**,** 206-226.
DZOTAM, J. K. & KUETE, V. 2017. Antibacterial and antibiotic-modifying activity of methanol extracts from six Cameroonian food plants against multidrug-resistant enteric bacteria. *BioMed Research International,* 2017**,** 1-20.
EGHAREVBA, G., DOSUMU, O., EVBUOMWAN, I., NJINGA, N., OLUYORI, A., HAMID, A. & AFOLABI, Y. 2023. In vitro antimicrobial, antioxidant, and antidiabetic activities of extracts of *Senecio abyssinicus* leaves. *Journal of Applied Sciences and Environmental Management,* 27**,** 939-948.
ELOFF, J. N. 1998. A sensitive and quick microplate method to determine the minimal inhibitory concentration of plant extracts for bacteria. *Planta Medica,* 64**,** 711-713.
ELOFF, J. N. 2019. Avoiding pitfalls in determining antimicrobial activity of plant extracts and publishing the results. *BMC Complementary and Alternative Medicine,* 19**,** 1-8.
ERASTO, P., ADEBOLA, P., GRIERSON, D. & AFOLAYAN, A. 2005. An ethnobotanical study of plants used for the treatment of diabetes in the Eastern Cape province, South Africa. *African Journal of Biotechnology* 4**,** 1458-1460.
FARAONE, I., RAI, D. K., CHIUMMIENTO, L., FERNANDEZ, E., CHOUDHARY, A., PRINZO, F. & MILELLA, L. 2018. Antioxidant activity and phytochemical characterization of *Senecio clivicolus* wedd. *Molecules,* 23**,** 1-17.
FLADE, J., BESCHOW, H., WENSCH-DORENDORF, M., PLESCHER, A. & WÄTJEN, W. 2019. Occurrence of nine pyrrolizidine alkaloids in *Senecio vulgaris* L. depending on developmental stage and season. *Plants,* 8**,** 54.
FRATI, A. C., JIMÉNEZ, E. & ARIZA, C. R. 1990. Hypoglycemic effect of *Opuntia ficus-indica* in non insulin-dependent diabetes mellitus patients. *Phytotherapy Research,* 4**,** 195-197.
GAO, Y., ZHANG, M., WU, T., XU, M., CAI, H. & ZHANG, Z. 2015. Effects of D-pinitol on insulin resistance through the PI3K/Akt signaling pathway in type 2 diabetes mellitus rats. *Journal of agricultural and food chemistry,* 63**,** 6019-6026.

GERARD, J. 2015. *The herbal or general history of plants: the complete 1633 edition as revised and enlarged by Thomas Johnson*, Courier Dover Publications.
GOPU, V., MEENA, C. K. & SHETTY, P. H. 2015. Quercetin influences quorum sensing in food borne bacteria: in-vitro and in-silico evidence. *PLoS ONE,* 10**,** e0134684.
GOULD, A., PENNY, C., PATEL, C. & CANDY, G. 2015. Enhanced cutaneous wound healing by *Senecio serratuloides* (Asteraceae/Compositae) in a pig model. *South Africa Journal Botany,* 100**,** 63-68.
GRAUSO, L., DE FALCO, B., LANZOTTI, V. & MOTTI, R. 2020. Stinging nettle, *Urtica dioica* L.: botanical, phytochemical and pharmacological overview. *Phytochemistry Reviews,* 19**,** 1341-1377.
GU, J.-Q., WANG, Y., FRANZBLAU, S. G., MONTENEGRO, G. & TIMMERMANN, B. N. 2004. Constituents of *Senecio chionophilus* with potential antitubercular activity. *Journal of Natural Products,* 67**,** 1483-1487.
GÜLÇIN, I. 2006. Antioxidant activity of caffeic acid (3,4-dihydroxycinnamic acid). *Toxicology,* 217**,** 213-20.
GUTIÉRREZ, R. M. P., SOLÍS, R. V., BAEZ, E. G. & FLORES, J. M. M. 2007. Microvascular protective activity in rabbits of triterpenes from *Hylocereus undatus*. *Journal of Natural Medicines,* 61**,** 296-301.
HAMID, H. K. & KADHIM, E. J. 2016. Extraction, isolation and characterization of Pyrrolizidine Alkaloids present in *Senecio vulgaris* Linn grown in Iraq. *Journal of Pharmacognosy and Phytochemistry,* 5**,** 28-37.
HASANPOUR, M., IRANSHAHY, M. & IRANSHAHI, M. 2020. The application of metabolomics in investigating anti-diabetic activity of medicinal plants. *Biomedicine & Pharmacotherapy,* 128**,** 1-20.
HASSAN, M. U., CHATTHA, M. U., KHAN, I., CHATTHA, M. B., AAMER, M., NAWAZ, M., ALI, A., KHAN, M. A. U. & KHAN, T. A. 2019. Nickel toxicity in plants: reasons, toxic effects, tolerance mechanisms, and remediation possibilities—a review. *Environmental Science and Pollution Research,* 26**,** 12673-12688.
HIRUDKAR, J. R., PARMAR, K. M., PRASAD, R. S., SINHA, S. K., LOMTE, A. D., ITANKAR, P. R. & PRASAD, S. K. 2020. The antidiarrhoeal evaluation of *Psidium guajava* L. against enteropathogenic Escherichia coli induced infectious diarrhoea. *Journal of ethnopharmacology,* 251**,** 112561.
HOFMANN, A. 2010. 12 Spectroscopic techniques: I Spectrophotometric techniques. Citeseer.
HOSSAIN, A., KHATUN, M. A., ISLAM, M. & HUQUE, R. 2017. Enhancement of antioxidant quality of green leafy vegetables upon different cooking method. *Preventive Nutrition and Food Science,* 22**,** 216.
IBRAHIM, N. & YAACOB, W. A. 2017. Transcriptome analysis of methicillin-resistant *Staphylococcus aureus* in response to stigmasterol and lupeol. *Journal of Global Antimicrobial Resistance,* 8**,** 48-54.
IDF DIABETES ATLAS 2021. *IDF Diabetes Atlas*.
IFEOMA, I. I. & CHUKWUNONSO, E. E. 2011. Current perspectives on the medicinal potentials of *Vernonia amygdalina* Del. *Journal of Medicinal Plants Research,* 5**,** 1051-1061.
IGWEMMAR, N. C., KOLAWOLE, S. A. & IMRAN, I. 2013. Effect of heating on vitamin C content of some selected vegetables. *International Journal of Scientific and Technology Research* 2**,** 209-212.
IRANSHAHI, M., REZAEE, R., PARHIZ, H., ROOHBAKHSH, A. & SOLTANI, F. 2015. Protective effects of flavonoids against microbes and toxins: The cases of hesperidin and hesperetin. *Life Sciences,* 137**,** 125-132.

JADEJA, R. N., UPADHYAY, K. K., DEVKAR, R. V. & KHURANA, S. 2016. Naturally occurring Nrf2 activators: potential in treatment of liver injury. *Oxidative Medicine and Cellular Longevity,* 2016**,** 1-13.

JAHNEN-DECHENT, W. & KETTELER, M. 2012. Magnesium basics. *Clinical Kidney Journal,* 5**,** 1-14.

JAISHANKAR, M., TSETEN, T., ANBALAGAN, N., MATHEW, B. B. & BEEREGOWDA, K. N. 2014. Toxicity, mechanism and health effects of some heavy metals. *Interdiscip Toxicol,* 7**,** 60-72.

JOSHI, B., KUMAR, V., CHANDRA, B. & KANDPAL, N. 2019. Chemical composition and antibacterial activity of essential oil of *Senecio graciliflorus*. *Journal of Drug Delivery and Therapeutics,* 9**,** 98-100.

JOSHI, S., SHRESTHA, K. & BAJRACHARYA, D. M. 2013. Secondary metabolite variation in some species of *Senecio* L. from Nepal Himalaya. *The Pharma Innovation,* 2**,** 70-76.

KABAŁA-DZIK, A., RZEPECKA-STOJKO, A., KUBINA, R., JASTRZĘBSKA-STOJKO, Ż., STOJKO, R., WOJTYCZKA, R. D. & STOJKO, J. 2017. Migration Rate Inhibition of Breast Cancer Cells Treated by Caffeic Acid and Caffeic Acid Phenethyl Ester: An In Vitro Comparison Study. *Nutrients,* 9**,** 1-19.

KALAČ, P. & KALTNER, F. 2021. Review: Pyrrolizidine alkaloids of European *Senecio/Jacobaea* species in forage and their carry-over to milk. *Animal Feed Science and Technology,* 280**,** 1-11.

KAMAL, N., CLEMENTS, C., GRAY, A. I. & EDRADA-EBEL, R. 2016. Anti-infective activities of secondary metabolites from *Vitex pinnata*. *Journal of Applied Pharmaceutical Science,* 6**,** 102-106.

KAMDEM, M. H. K., MELACHEU, G. L. F., SILIHE, K. K., MORE, G. K., MPHAHLELE, M. P., MOSWETSA, T. A., TATA, C. M., TONGA, J. L., OJO, O. & FONKUI, T. Y. 2022. Cytotoxic and antibacterial activities of compounds isolated from the fruits and stem-bark of *Tetrapleura tetraptera* (Schumach. & Thonn.) Taub.(Fabaceae). *Medicinal Chemistry,* 31**,** 1948-1958.

KASKA, A., ÇIÇEK, M. & MAMMADOV, R. 2019. Biological activities, phenolic constituents and mineral element analysis of two endemic medicinal plants from Turkey: *Nepeta italica* subsp. cadmea and *Teucrium sandrasicum*. *South African Journal of Botany,* 124**,** 63-70.

KAUR, R. & ARORA, S. 2015. Alkaloids-important therapeutic secondary metabolites of plant origin. *Journal of Critical Reviews,* 2**,** 1-8.

KAVISHANKAR, G., LAKSHMIDEVI, N., MURTHY, S. M., PRAKASH, H. & NIRANJANA, S. 2011. A review: Diabetes and medicinal plants. *International Journal of Pharmaceutical Biomedical Science,* 2**,** 65-80.

KELMANSON, J. E., JÄGER, A. K. & VAN STADEN, J. 2000. Zulu medicinal plants with antibacterial activity. *Journal of Ethnopharmacology,* 69**,** 241-246.

KHAN, Z., NATH, N., RAUF, A., EMRAN, T. B., MITRA, S., ISLAM, F., CHANDRAN, D., BARUA, J., KHANDAKER, M. U., IDRIS, A. M., WILAIRATANA, P. & THIRUVENGADAM, M. 2022. Multifunctional roles and pharmacological potential of β-sitosterol: Emerging evidence toward clinical applications. *Chemico-Biological Interactions,* 365**,** 1-16.

KIM, K.-T., RIOUX, L.-E. & TURGEON, S. L. 2014. Alpha-amylase and alpha-glucosidase inhibition is differentially modulated by fucoidan obtained from *Fucus vesiculosus* and *Ascophyllum nodosum*. *Phytochemicals,* 98**,** 27-33.

KIPRONO, P. C., KABERIA, F., KERIKO, J. M. & KARANJA, J. N. 2000. The in vitro anti-fungal and anti-bacterial activities of β-sitosterol from *Senecio lyratus* (Asteraceae). *Zeitschrift für Naturforschung C,* 55**,** 485-488.

KUETE, V. & EFFERTH, T. 2015. African flora has the potential to fight multidrug resistance of cancer. *BioMed Research International,* 2015**,** 1-24.
KUMAR, V. & MATHELA, C. 2018. Chemical constituents of essential oils of Himalayan *Nepeta ciliaris* Benth. and *Senecio nudicaulis* Buch-Ham. Ex D. Don. *Journal of Essential Oil Research,* 30**,** 207-213.
LAKHANPAL, P. & RAI, D. K. 2007. Quercetin: a versatile flavonoid. *Journal of Medical Internet Research,* 2**,** 22-37.
LALL, N. & KISHORE, N. 2014. Are plants used for skin care in South Africa fully explored? *Journal of Ethnopharmacology,* 153**,** 61-84.
LANGE, B., VAN DER ENT, A., BAKER, A. J. M., ECHEVARRIA, G., MAHY, G., MALAISSE, F., MEERTS, P., POURRET, O., VERBRUGGEN, N. & FAUCON, M. P. 2017. Copper and cobalt accumulation in plants: a critical assessment of the current state of knowledge. *New Phytologist,* 213**,** 537-551.
LAUDERMILK, M. J., MANORE, M. M., THOMSON, C. A., HOUTKOOPER, L. B., FARR, J. N. & GOING, S. B. 2012. Vitamin C and zinc intakes are related to bone macroarchitectural structure and strength in prepubescent girls. *Calcified Tissue International,* 91**,** 430-439.
LEE, K., JUNG, J., YANG, G., HAM, I., BU, Y., KIM, H. & CHOI, H. Y. 2013. Endothelium-independent vasorelaxation effects of *Sigesbeckia glabrescens* (makino) makino on isolated rat thoracic aorta. *Phytotherapy Research,* 27**,** 1308-1312.
LEVIS, M. 2017. Midostaurin approved for FLT3-mutated AML. *Blood, The Journal of the American Society of Hematology,* 129**,** 3403-3406.
LI, W., LEE, C., KIM, Y. H., MA, J. Y. & SHIM, S. H. 2017. Chemical constituents of the aerial part of *Taraxacum mongolicum* and their chemotaxonomic significance. *Natural Product Research,* 31**,** 2303-2307.
LI, Y. Y., TAN, X. M., WANG, Y. D., YANG, J., ZHANG, Y. G., SUN, B. D., GONG, T., GUO, L. P. & DING, G. 2020. Bioactive seco-sativene sesquiterpenoids from an *Artemisia desertorum* endophytic fungus, *Cochliobolus sativus*. *Journal of Natural Products,* 83**,** 1488-1494.
LOIZZO, M. R., STATTI, G. A., TUNDIS, R., CONFORTI, F., BONESI, M., AUTELITANO, G., HOUGHTON, P. J., MILJKOVIC-BRAKE, A. & MENICHINI, F. 2004. Antibacterial and antifungal activity of *Senecio inaequidens* DC. and *Senecio vulgaris* L. *Phytotherapy Research,* 18**,** 777-779.
LOOTS, D. T., PIETERS, M., ISLAM, M. S. & BOTES, L. 2011. Antidiabetic effects of *Aloe ferox* and *Aloe greatheadii* var. davyana leaf gel extracts in a low-dose streptozotocin diabetes rat model. *South African Journal of Science,* 107**,** 1-6.
LOOTS DU, T., VAN DER WESTHUIZEN, F. H. & BOTES, L. 2007. *Aloe ferox* leaf gel phytochemical content, antioxidant capacity, and possible health benefits. *Journal of Agricultural and Food Chemistry,* 55**,** 6891-6896.
LU, A.-J., LU, Y.-L., TAN, D.-P., QIN, L., LING, H., WANG, C.-H. & HE, Y.-Q. 2021. Identification of pyrrolizidine alkaloids in *Senecio* plants by liquid chromatography-mass spectrometry. *Journal of Analytical Methods in Chemistry,* 2021**,** 1-13.
LUHATA, L. P. & USUKI, T. 2021. Antibacterial activity of β-sitosterol isolated from the leaves of *Odontonema strictum* (Acanthaceae). *Bioorganic & Medicinal Chemistry Letters* 48**,** 1-5.
LUPTON, D. 2012. Medicine as culture: illness, disease and the body.
MADZINGA, M., KRITZINGER, Q. & LALL, N. 2018. Medicinal plants used in the treatment of superficial skin infections: from traditional medicine to herbal soap formulations. *Medicinal plants for holistic health and well-being.* Elsevier.

MAGURA, J., MOODLEY, R., MADURAY, K. & MACKRAJ, I. 2021. Phytochemical constituents and in vitro anticancer screening of isolated compounds from *Eriocephalus africanus*. *Natural Products Research,* 35**,** 4173-4176.

MAILAFIYA, M. M., YUSUF, A. J., ABDULLAHI, M. I., ALEKU, G. A., IBRAHIM, I. A., YAHAYA, M., ABUBAKAR, H., SANUSI, A., ADAMU, H. W. & ALEBIOSU, C. O. 2018. Antimicrobial activity of stigmasterol from the stem bark of *Neocarya macrophylla*. *Journal of Medicinal Plants for Economic Development,* 2**,** 1-5.

MALAK, Y., M. MOHAMED, K., M. A. ABD EL-MAWLA, A. & M. ZAHER, A. 2023. Cytotoxic and antimicrobial effects of selected Egyptian Asteraceae species as well as GC-MS metabolite profiling of *Senecio cruentus* lipophilic fraction *Bulletin of Pharmaceutical Sciences,* 46**,** 39-49.

MARETE, E. N. 2013. *Phytochemical and anti-microbial studies of isolates from Senecio lyratipatitus (Asteraceae).* MSc Thesis, Jomo Kenyatta University of Agriculture and Technology.

MARIRI, N. G. 2017. *In vitro evaluation of the bioactivity of Gnidia polycephala and Senecio serratuloides.* Doctoral Thesis, Central University of Technology, Free State.

MAROYI, A. 2017. Diversity of use and local knowledge of wild and cultivated plants in the Eastern Cape province, South Africa. *Journal of Ethnobiology and Ethnomedicine,* 13**,** 1-16.

MAVIMBELA, T., VERMAAK, I., CHEN, W. & VILJOEN, A. 2018. Rapid quality control of *Sutherlandia frutescens* leaf material through the quantification of SU1 using vibrational spectroscopy in conjunction with chemometric data analysis. *Phytochemistry Letters,* 25**,** 184-190.

MCCHESNEY, J. D., VENKATARAMAN, S. K. & HENRI, J. T. 2007. Plant natural products: back to the future or into extinction? *Phytochemistry,* 68**,** 2015-2022.

MEHDI, Y., HORNICK, J.-L., ISTASSE, L. & DUFRASNE, I. 2013. Selenium in the environment, metabolism and involvement in body functions. *Molecules,* 18**,** 3292-3311.

MEHRI, A. 2020. Trace elements in human nutrition (II) - an update. *International Journal of Preventive Medicine,* 11**,** 1-17.

MENSAH, M., KOMLAGA, G., FORKUO, A. D., FIREMPONG, C., ANNING, A. K. & DICKSON, R. A. 2019. Toxicity and safety implications of herbal medicines used in Africa. *Herbal Medicine,* 63**,** 1992-0849.

MHLONGO, L. S. 2019. *The Medicinal Ethnobotany of the Amandawe Area in KwaCele, KwaZulu-Natal, South Africa.* PhD thesis, University of Johannesburg (South Africa).

MICHEL, J., ABD RANI, N. Z. & HUSAIN, K. 2020. A review on the potential use of medicinal plants from Asteraceae and Lamiaceae plant family in cardiovascular diseases. *Frontiers in Pharmacology,* 11**,** 852-875.

MILADI, H., MILI, D., SLAMA, R. B., ZOUARI, S., AMMAR, E. & BAKHROUF, A. 2016. Antibiofilm formation and anti-adhesive property of three Mediterranean essential oils against a foodborne pathogen *Salmonella* strain. *Microbial Pathogenesis,* 93**,** 22-31.

MOODLEY, R., KOORBANALLY, N. & JONNALAGADDA, S. B. 2013. Elemental composition and nutritional value of the edible fruits of *Harpephyllum caffrum* and impact of soil quality on their chemical characteristics. *Journal of Environmental Science Health* 48**,** 539-547.

MOREIRA-MUÑOZ, A. & MUÑOZ-SCHICK, M. 2007. Classification, diversity, and distribution of Chilean Asteraceae: implications for biogeography and conservation. *Diversity and Distributions,* 13**,** 818-828.

MOTHIBE, M. E. & SIBANDA, M. 2019. African traditional medicine: South African perspective. *Journal of Traditional Complemental Medicine,* 3**,** 1-27.

MOTYL, M., DORSO, K., BARRETT, J. & GIACOBBE, R. 2005. Basic microbiological techniques used in antibacterial drug discovery. *Current Protocols in Pharmacology,* 31**,** 1-13.

NAPOLITANO, J. G., GÖDECKE, T., RODRÍGUEZ-BRASCO, M. F., JAKI, B. U., CHEN, S.-N., LANKIN, D. C. & PAULI, G. F. 2012. The tandem of full spin analysis and qHNMR for the quality control of botanicals exemplified with *Ginkgo biloba*. *Journal of Natural Products,* 75**,** 238-248.

NCIKI, S., VUUREN, S., VAN EYK, A. & DE WET, H. 2016. Plants used to treat skin diseases in northern Maputaland, South Africa: antimicrobial activity and in vitro permeability studies. *Pharmaceutical Biology,* 54**,** 2420-2436.

NEWMAN, D. J. 2019. From natural products to drugs. *Physical Sciences Reviews,* 4**,** 1-43.

NEWMAN, D. J. & CRAGG, G. M. 2016. Natural products as sources of new drugs from 1981 to 2014. *Journal of Natural Products,* 79**,** 629-661.

NILE, A., NILE, S. H., SHIN, J., PARK, G. & OH, J.-W. 2021. Quercetin-3-glucoside extracted from apple pomace induces cell cycle arrest and apoptosis by increasing intracellular ROS levels. *International Journal of Molecular Sciences,* 22**,** 1-11.

NIU, T.-Z., ZHANG, Y.-W., BAO, Y.-L., WU, Y., YU, C.-L., SUN, L.-G., YI, J.-W., HUANG, Y.-X. & LI, Y.-X. 2013. A validated high-performance liquid chromatography method with diode array detection for simultaneous determination of nine flavonoids in *Senecio cannabifolius* Less. *Journal of Pharmaceutical and Biomedical Analysis,* 76**,** 44-48.

NUALKAEW, S., PADEE, P. & TALUBMOOK, C. 2015. Hypoglycemic activity in diabetic rats of stigmasterol and sitosterol-3-O-b-D-glucopyranoside isolated from *Pseuderanthemum palatiferum* (Nees) Radlk. leaf extract. *Journal of Medicinal Plants Research,* 9**,** 629-635.

NWEZE, C., IBRAHIM, H. & NDUKWE, G. 2019. Beta-sitosterol with antimicrobial property from the stem bark of pomegranate (*Punica granatum* Linn). *Journal of Applied Sciences and Environmental Management* 23**,** 1045-1049.

NYILA, M. A., LEONARD, C., HUSSEIN, A. A. & LALL, N. 2012. Activity of South African medicinal plants against *Listeria monocytogenes* biofilms, and isolation of active compounds from *Acacia karroo*. *South African Journal of Botany,* 78**,** 220-227.

O'NEILL, J. 2016. Tackling drug-resistant infections globally: final report and recommendations.

ODEYEMI, S. & BRADLEY, G. 2018. Medicinal plants used for the traditional management of diabetes in the Eastern Cape, South Africa: Pharmacology and toxicology. *Molecules,* 23**,** 2759-2768.

OJEWOLE, J. 2006. Antinociceptive, anti-inflammatory and antidiabetic properties of *Hypoxis hemerocallidea* Fisch. & CA Mey.(Hypoxidaceae) corm [‘African Potato’] aqueous extract in mice and rats. *Journal of Ethnopharmacology,* 103**,** 126-134.

OJEWOLE, J. A., ADEWOLE, S. O. & OLAYIWOLA, G. 2006. Hypoglycaemic and hypotensive effects of *Momordica charantia* Linn (Cucurbitaceae) whole-plant aqueous extract in rats: Cardiovascular topics. *Cardiovascular Journal of South Africa,* 17**,** 227-232.

OKOMBO, J., OHUMA, E., PICOT, S. & NZILA, A. 2011. Update on genetic markers of quinine resistance in *Plasmodium falciparum*. *Molecular and Biochemical Parasitology,* 177**,** 77-82.

OKORO, I., UMAR, I., ATAWODI, S. & ANIGO, K. 2014. Antidiabetic effect of *Cleome rutidosperma* DC and *Senecio biafrae* (Oliv. & Hiern) extracts in streptozotocin-induced diabetic rats. *International Journal of Pharmaceutical Sciences and Research,* 5**,** 2480-2497.

ONGUN, B. C., ALTUNDAG, E. M., ALTINOGLU, G., GURAN, M., SANLITURK, G., AFSHANI, M. & BALCI, D. 2021. In vitro anticancer, antibacterial and antifungal activity analysis of natural flavonoid hesperidin. *Progress in Nutrition,* 23**,** 1-18.

OYEDEMI, S., BRADLEY, G. & AFOLAYAN, A. 2009. Ethnobotanical survey of medicinal plants used for the management of diabetes mellitus in the Nkonkobe municipality of South Africa. *Journal of Medicinal Plants Research,* 3**,** 1040-1044.

PANDA, S. & KAR, A. 2007. Antidiabetic and antioxidative effects of *Annona squamosa* leaves are possibly mediated through quercetin-3-*O*-glucoside. *Biofactors,* 31**,** 201-210.

PARK, C. & LEE, J.-S. 2013. Mini Review: Natural ingredients for diabetes which are approved by Korean FDA. *Biomedical Research* 24**,** 164-173.

PARRA, C., SOTO, E., LEÓN, G., SALAS, C. O., HEINRICH, M. & ECHIBURÚ-CHAU, C. 2018. Nutritional composition, antioxidant activity and isolation of scopoletin from *Senecio nutans*: support of ancestral and new uses. *Natural Product Research,* 32**,** 719-722.

PATEL, K. S., PANDEY, P. K., MARTÍN-RAMOS, P., CORNS, W. T., VAROL, S., BHATTACHARYA, P. & ZHU, Y. 2023. A review on arsenic in the environment: bio-accumulation, remediation, and disposal. *RSC Advances,* 13**,** 14914-14929.

PATIL, A., KOLI, S., PATIL, D. & PHATAK, A. 2012. Evaluation of extraction techniques with various solvents to determine extraction efficiency of selected medicinal plants. *International Journal of Pharmaceutical Sciences and Research,* 3**,** 2607.

PEGEL, K. H. 2002. MODUCARE®– a brief history and mode of action. 1-5.

POLO-MA-ABIELE, H. M., MANDUNA, I. T. I. T. & MASHELE, S. S. 2023. Characterisation and identification of phenolic compounds from *Asparagus laricinus* and *Senecio asperulus*. *Indian Journal of Natural Products and Resources,* 14**,** 482-489.

PRAKASH, P., RADHA, KUMAR, M., PUNDIR, A., PURI, S., PRAKASH, S., KUMARI, N., THAKUR, M., RATHOUR, S., JAMWAL, R., JANJUA, S., ALI, M., BANGAR, S. P., SINGH, C., CHANDRAN, D., RAJALINGAM, S., SENAPATHY, M., DHUMAL, S., SINGH, S., SAMOTA, M. K., DAMALE, R. D., CHANGAN, S., NATTA, S., ALBLIHED, M., EL-KOTT, A. F. & ABDEL-DAIM, M. M. 2021. Documentation of Commonly Used Ethnoveterinary Medicines from Wild Plants of the High Mountains in Shimla District, Himachal Pradesh, India. *Horticulturae,* 7**,** 1-38.

RAIMUNDO, I. M. 2017. Food insecurity in the context of climate change in Maputo city, Mozambique: challenges and coping strategies. *In:* THOMAS-HOPE, E. (ed.) *Climate Change and Food Security: Africa and the Caribbean.* Taylor and Francis.

RAMAWAT, K., DASS, S. & MATHUR, M. 2009. The chemical diversity of bioactive molecules and therapeutic potential of medicinal plants. *Herbal Drugs: Ethnomedicine to Modern Medicine,* 3**,** 7-32.

RANDRIAMAMPIONONA, H. R., RASOLOHERY, C. A., RASAMISON, V. E., BODO, B., RAFANOMEZANTSOA, R. M. & RAKOTOVAO, M. 2020. Flavonoid and triterpenes from the leaves of *Senecio gossypinus* Baker from Madagascar. *Journal of Pharmacognosy and Phytochemistry,* 9**,** 1279-1282.

RAZAVI, S. M., ZAHRI, S., ZARRINI, G., NAZEMIYEH, H. & MOHAMMADI, S. 2009. Biological activity of quercetin-3-O-glucoside, a known plant flavonoid. *Russian Journal of Bioorganic Chemistry,* 35**,** 376-378.

RIDHAY, A., NOOR, A., SOEKAMTO, N. H., HARLIM, T. & VAN ALTENA, I. 2012. A stigmasterol glycoside from the root wood of *Melochia umbellata* (Houtt) Stapf var. degrabrata K. *Indonesian Journal of Chemistry,* 12**,** 100-103.

RIOS, J.-L. & RECIO, M. C. 2005. Medicinal plants and antimicrobial activity. *Journal of Ethnopharmacology,* 100**,** 80-84.

RÍOS, J. L., FRANCINI, F. & SCHINELLA, G. R. 2015. Natural products for the treatment of type 2 diabetes mellitus. *Planta Medica,* 81**,** 975-994.

ROLNIK, A. & OLAS, B. 2021. The plants of the Asteraceae family as agents in the protection of human health. *International Journal of Molecular Sciences,* 22**,** 1-10.

ROSENDAHL, A. H., PERKS, C. M., ZENG, L., MARKKULA, A., SIMONSSON, M., ROSE, C., INGVAR, C., HOLLY, J. M. & JERNSTRÖM, H. 2015. Caffeine and caffeic acid inhibit growth and modify estrogen receptor and insulin-like growth factor receptor levels in human breast cancer. *Clinical Cancer Research,* 21**,** 1877-87.

RUIZ-VÁSQUEZ, L., REINA, M., LÓPEZ-RODRÍGUEZ, M., GIMÉNEZ, C., CABRERA, R., CUADRA, P., FAJARDO, V. & GONZÁLEZ-COLOMA, A. 2015. Sesquiterpenes, flavonoids, shikimic acid derivatives and pyrrolizidine alkaloids from *Senecio kingii* Hook. *Phytochemistry,* 117**,** 245-253.

RYAN, T. J. 1996. Fundamentals of Complementary and Alternative Medicine-E-book. Elsevier Health Sciences.

SANCHES, N. R., GARCIA CORTEZ, D. A., SCHIAVINI, M. S., NAKAMURA, C. V. & DIAS FILHO, B. P. 2005. An evaluation of antibacterial activities of *Psidium guajava* (L.). *Brazilian Archives of Biology and Technology,* 48**,** 429-436.

SANDIL, S., ÓVÁRI, M., DOBOSY, P., VETÉSI, V., ENDRÉDI, A., TAKÁCS, A., FÜZY, A. & ZÁRAY, G. 2021. Effect of arsenic-contaminated irrigation water on growth and elemental composition of tomato and cabbage cultivated in three different soils, and related health risk assessment. *Environmental Research,* 197**,** 1-15.

SAXENA, M., SAXENA, J., NEMA, R., SINGH, D. & GUPTA, A. 2013. Phytochemistry of medicinal plants. *Journal of Pharmacognosy Phytochemistry,* 1**,** 168-162.

SELLO, L. 2020. *Cracking Down on Counterfeits: Creating a DNA Barcode Reference Library of Native Plants Used in Commercial Herbal Products in South Africa.* MSc Thesis, University of Johannesburg.

SEMENYA, S. & MAROYI, A. 2019. Ethnobotanical survey of plants used by Bapedi traditional healers to treat tuberculosis and its opportunistic infections in the Limpopo Province, South Africa. *South African Journal of Botany,* 122**,** 401-421.

SEMENYA, S., POTGIETER, M. & ERASMUS, L. 2012. Ethnobotanical survey of medicinal plants used by Bapedi healers to treat diabetes mellitus in the Limpopo Province, South Africa. *Journal of Ethnopharmacology,* 141**,** 440-445.

SHAHZAD, B., TANVEER, M., REHMAN, A., CHEEMA, S. A., FAHAD, S., REHMAN, S. & SHARMA, A. 2018. Nickel; whether toxic or essential for plants and environment-A review. *Plant Biochemistry and Physiology,* 132**,** 641-651.

SHANDUKANI, P. D., TSHIDINO, S. C., MASOKO, P. & MOGANEDI, K. M. 2018. Antibacterial activity and in situ efficacy of *Bidens pilosa* Linn and *Dichrostachys cinerea* Wight et Arn extracts against common diarrhoea-causing waterborne bacteria. *BMC Complementary and Alternative Medicine,* 18**,** 1-10.

SHEN, J., WANG, G. & ZUO, J. 2018. Caffeic acid inhibits HCV replication via induction of IFNα antiviral response through p62-mediated Keap1/Nrf2 signaling pathway. *Antiviral Research,* 154**,** 166-173.

SIBUYI, N. R. S., KATERERE, D. R., BOBOYI, T. & MADIEHE, A. M. 2007. Dietary supplementation with *Aloe ferox* extracts reverses obesity in rats. *South African Journal of Botany,* 73**,** 336-342.

SIGEL, H. & SIGEL, A. 1983. *Metal Ions in Biological Systems*, CRC Press, Taylor and Francis Group.

SILVA, N. & FERNANDES JÚNIOR, A. 2010. Biological properties of medicinal plants: a review of their antimicrobial activity. *Journal of Venomous Animals and Toxins including Tropical Diseases,* 16**,** 402-413.

SIMMLER, C., LANKIN, D. C., NIKOLIĆ, D., VAN BREEMEN, R. B. & PAULI, G. F. 2017. Isolation and structural characterization of dihydrobenzofuran congeners of licochalcone A. *Fitoterapia,* 121**,** 6-15.

SINGH BISHT, C. M., IQUBAL, S. S., KHAN, A. A. & ASGHAR, B. H. 2019. Natural products in drug discovery: Antibacterial and antifungal activity of essential oil of compound isolated from *Senecio royleanus*. *Journal of Pure & Applied Microbiology,* 13**,** 1-7.

SINHA, R., GADHWAL, M., JOSHI, U., SRIVASTAVA, S. & GOVIL, G. 2012. Modifying effect of quercetin on model bio-membranes: studied by molecular dynamic simulation, DSC and NMR. *International Journal of Current Pharmaceutical Research,* 4**,** 70-79.

SIRIWONG, S., TEETHAISONG, Y., THUMANU, K., DUNKHUNTHOD, B. & EUMKEB, G. 2016. The synergy and mode of action of quercetin plus amoxicillin against amoxicillin-resistant *Staphylococcus epidermidis*. *BMC Pharmacology and Toxicology,* 17**,** 1-14.

SOETAN, K., OLAIYA, C. & OYEWOLE, O. 2010. The importance of mineral elements for humans, domestic animals and plants: A review. *African journal of food science,* 4**,** 200-222.

SOFOWORA, A., OGUNBODEDE, E. & ONAYADE, A. 2013. The role and place of medicinal plants in the strategies for disease prevention. *African Journal of Traditional, Complementary and Alternative Medicines,* 10**,** 210-229.

SPARKMAN, O. D., PENTON, Z. & KITSON, F. G. 2011. *Gas chromatography and mass spectrometry: a practical guide*, Academic press.

SPINOZZI, E., FERRATI, M., BALDASSARRI, C., CAPPELLACCI, L., MARMUGI, M., CASELLI, A., BENELLI, G., MAGGI, F. & PETRELLI, R. 2022. A review of the chemistry and biological activities of Acmella oleracea ("jambù", Asteraceae), with a view to the development of bioinsecticides and acaricides. *Plants,* 11**,** 2721.

STREET, R. & PRINSLOO, G. 2013. Commercially important medicinal plants of South Africa: a review. *Journal of Chemistry,* 2013**,** 1-17.

SULTAN, M. S., ELSAYED, A. & EL-AMIR, Y. A. 2022. In vitro effect of plant parts extract of *Senecio glaucus* L. On pathogenic bacteria. *Biointerface Research in Applied Chemistry,* 12**,** 3800-3810.

SUNTAR, I. 2014. The medicinal value of Asteraceae family plants in terms of wound healing activity. *FABAD Journal of Pharmaceutical Sciences,* 39**,** 21-31.

SUNTRES, Z. E., COCCIMIGLIO, J. & ALIPOUR, M. 2015. The bioactivity and toxicological actions of carvacrol. *Critical Reviews in Food Science and Nutrition,* 55**,** 304-318.

SURIYAGODA, L. D. B., DITTERT, K. & LAMBERS, H. 2018. Mechanism of arsenic uptake, translocation and plant resistance to accumulate arsenic in rice grains. *Agriculture, Ecosystems & Environment,* 253**,** 23-37.

SUZUKI, Y., ISHIHARA, M., SEGAMI, T. & ITO, M. 1998. Anti-ulcer effects of antioxidants, quercetin, α-tocopherol, nifedipine and tetracycline in rats. *Japanese Journal of Pharmacology,* 78**,** 435-441.

TAMOKOU, J. D. D., KUIATE, J. R., TENE, M., NWEMEGUELA, T. J. K. & TANE, P. 2011. The antimicrobial activities of extract and compounds isolated from *Brillantaisia lamium*. *Iranian Journal of Medical Sciences,* 36**,** 1-24.

TAMOKOU, J. D. D., SIMO MPETGA, D. J., KEILAH LUNGA, P., TENE, M., TANE, P. & KUIATE, J. R. 2012. Antioxidant and antimicrobial activities of ethyl acetate extract, fractions and compounds from stem bark of *Albizia adianthifolia* (Mimosoideae). *BMC Complementary and Alternative Medicine,* 12**,** 1-10.

TATA, C. M., SEWANI-RUSIKE, C. R., OYEDEJI, O. O., GWEBU, E. T., MAHLAKATA, F. & NKEH-CHUNGAG, B. N. 2019. Antihypertensive effects of the hydro-ethanol extract of Senecio serratuloides DC in rats. *BMC complementary and alternative medicine,* 19**,** 1-10.

TATA, C. M., SEWANI-RUSIKE, C. R., OYEDEJI, O. O., MAHLAKATA, F., SHAULI, M. & NKEH-CHUNGAG, B. N. 2020. *Senecio serratuloides* extract prevents the development of hypertension, oxidative stress and dyslipidemia in nitric oxide-deficient rats. *Journal of Complementary and Integrative Medicine,* 17**,** 1-8.

TEMBE, J. M. Indigenous vegetables and legumes: importance, utilization and marketing in Gaza Province, Mozambique. Conference Proceeding: International conference on indigenous vegetables and legumes. prospectus for fighting poverty, hunger and malnutrition 2006. 363-366.

THOMSON, M., AL-AMIN, Z. M., AL-QATTAN, K. K., SHABAN, L. H. & ALI, M. 2007. Anti-diabetic and hypolipidaemic properties of garlic (*Allium sativum*) in streptozotocin-induced diabetic rats. *International Journal of Diabetes and Metabolism,* 15**,** 108-115.

TIAN, X.-Y., WANG, Y.-H., YANG, Q.-Y., YU, S.-S. & FANG, W.-S. 2009. Jacaranone analogs from *Senecio scandens*. *Journal of Asian Natural Products Research,* 11**,** 63-68.

TRAN, N., PHAM, B. & LE, L. 2020. Bioactive compounds in anti-diabetic plants: From herbal medicine to modern drug discovery. *Biology,* 9**,** 252.

TUNDIS, R., LOIZZO, M. R., BONESI, M., MENICHINI, F., DODARO, D., PASSALACQUA, N. G., STATTI, G. & MENICHINI, F. 2009. In vitro cytotoxic effects of *Senecio stabianus* Lacaita (Asteraceae) on human cancer cell lines. *Natural Products Research,* 23**,** 1707-1718.

TUNDIS, R., LOIZZO, M. R. & MENICHINI, F. 2010. Natural products as α-amylase and α-glucosidase inhibitors and their hypoglycaemic potential in the treatment of diabetes: an update. *Mini Reviews in Medicinal Chemistry,* 10**,** 315-331.

TUNDIS, R., LOIZZO, M. R., STATTI, G. A., PASSALACQUA, N. G., PERUZZI, L. & MENICHINI, F. 2007. Pyrrolizidine alkaloid profiles of the *Senecio cineraria* group (Asteraceae). *Zeitschrift für Naturforschung C,* 62**,** 467-472.

TUNDIS, R., MENICHINI, F., LOIZZO, M. R., BONESI, M., SOLIMENE, U. & MENICHINI, F. 2012. Studies on the potential antioxidant properties of *Senecio stabianus* Lacaita (Asteraceae) and its inhibitory activity against carbohydrate-hydrolysing enzymes. *Natural Product Research,* 26**,** 393-404.

VAN DE VENTER, M., ROUX, S., BUNGU, L. C., LOUW, J., CROUCH, N. R., GRACE, O. M., MAHARAJ, V., PILLAY, P., SEWNARIAN, P. & BHAGWANDIN, N. 2008. Antidiabetic screening and scoring of 11 plants traditionally used in South Africa. *Journal of Ethnopharmacology,* 119**,** 81-86.

VAN VUUREN, S. 2008. Antimicrobial activity of South African medicinal plants. *Journal of Ethnopharmacology,* 119**,** 462-472.

VAN VUUREN, S. & HOLL, D. 2017. Antimicrobial natural product research: A review from a South African perspective for the years 2009–2016. *Journal of Ethnopharmacology,* 208**,** 236-252.

VAN WYK, B. E. 2011. The potential of South African plants in the development of new medicinal products. *South African Journal of Botany,* 77**,** 812-829.

VERMA, P. K., RAINA, R., AGARWAL, S. & KAUR, H. 2018. Phytochemical ingredients and Pharmacological potential of *Calendula officinalis* Linn. *Pharmaceutical and Biomedical Research,* 4**,** 1-17.

VITALE, S., COLANERO, S., PLACIDI, M., DI EMIDIO, G., TATONE, C., AMICARELLI, F. & D'ALESSANDRO, A. M. 2022. Phytochemistry and biological activity of medicinal plants in wound healing: an overview of current research. *Molecules,* 27**,** 3566.

WANG, D., HUANG, L. & CHEN, S. 2013. *Senecio scandens* Buch.-Ham.: A review on its ethnopharmacology, phytochemistry, pharmacology, and toxicity. *Journal of Ethnopharmacology,* 149**,** 1-23.

WANG, J., HUANG, M., YANG, J., MA, X., ZHENG, S., DENG, S., HUANG, Y., YANG, X. & ZHAO, P. 2017. Anti-diabetic activity of stigmasterol from soybean oil by targeting the GLUT4 glucose transporter. *Food Nutrition Research,* 61**,** 1-12.

WHO 2018a. Global report on diabetes. 2016.

WHO 2018b. WHO report on surveillance of antibiotic consumption: 2016-2018 early implementation. World Health Organisation.

WHO 2019a. WHO global report on traditional and complementary medicine 2019. World Health Organization.

WHO 2019b. *Strengthening nutrition action: A resource guide for countries based on the policy recommendations of the Second International Conference on Nutrition*, Food & Agriculture Org.

WILD, S., ROGLIC, G., GREEN, A., SICREE, R. & KING, H. 2004. Global prevalence of diabetes: estimates for the year 2000 and projections for 2030. *Diabetes care,* 27**,** 1047-1053.

YAMAMOTO, M., JOKURA, H., HASHIZUME, K., OMINAMI, H., SHIBUYA, Y., SUZUKI, A., HASE, T. & SHIMOTOYODOME, A. 2013. Hesperidin metabolite hesperetin-7-O-glucuronide, but not hesperetin-3′-O-glucuronide, exerts hypotensive, vasodilatory, and anti-inflammatory activities. *Food Functions,* 4**,** 1346-1351.

YANG, J. & LIU, R. H. 2009. Synergistic effect of apple extracts and quercetin 3-O-β-D-glucoside combination on antiproliferative activity in MCF-7 human breast cancer cells in vitro. *Journal of Agricultural and Food Chemistry,* 57**,** 8581-8586.

YANG, X., YANG, L., XIONG, A., LI, D. & WANG, Z. 2011. Authentication of *Senecio scandens* and *S. vulgaris* based on the comprehensive secondary metabolic patterns gained by UPLC–DAD/ESI-MS. *Journal of Pharmaceutical and Biomedical Analysis,* 56**,** 165-172.

YORK, T., VAN VUUREN, S. & DE WET, H. 2012. An antimicrobial evaluation of plants used for the treatment of respiratory infections in rural Maputaland, KwaZulu-Natal, South Africa. *Journal of Ethnopharmacology,* 144**,** 118-127.

ZAHEDI, M., GHIASVAND, R., FEIZI, A., ASGARI, G. & DARVISH, L. 2013. Does quercetin improve cardiovascular risk factors and inflammatory biomarkers in women with type 2 diabetes: a double-blind randomized controlled clinical trial. *International Journal of Preventive Medicine,* 4**,** 777-783.

ZHOU, B., HU, Z.-J., ZHANG, H.-J., LI, J.-Q., DING, W.-J. & MA, Z.-J. 2019. Bioactive staurosporine derivatives from the *Streptomyces sp*. NB-A13. *Bioorganic Chemistry,* 82**,** 33-40.

ZHOU, B. & XING, C. 2015. Diverse molecular targets for chalcones with varied bioactivities. *Medicinal Chemistry,* 5**,** 388-404.

ZUO, G.-Y., WANG, C.-J., HAN, J., LI, Y.-Q. & WANG, G.-C. 2016. Synergism of coumarins from the Chinese drug zanthoxylum nitidum with antibacterial agents against methicillin-resistant *Staphylococcus aureu*s (MRSA). *Phytomedicine,* 23**,** 1814-1820.

APPENDIX

A phytochemical and elemental analysis of *Senecio serratuloides*, and its antidiabetic potential

MSc Thesis

2024

ANDILE GUMEDE

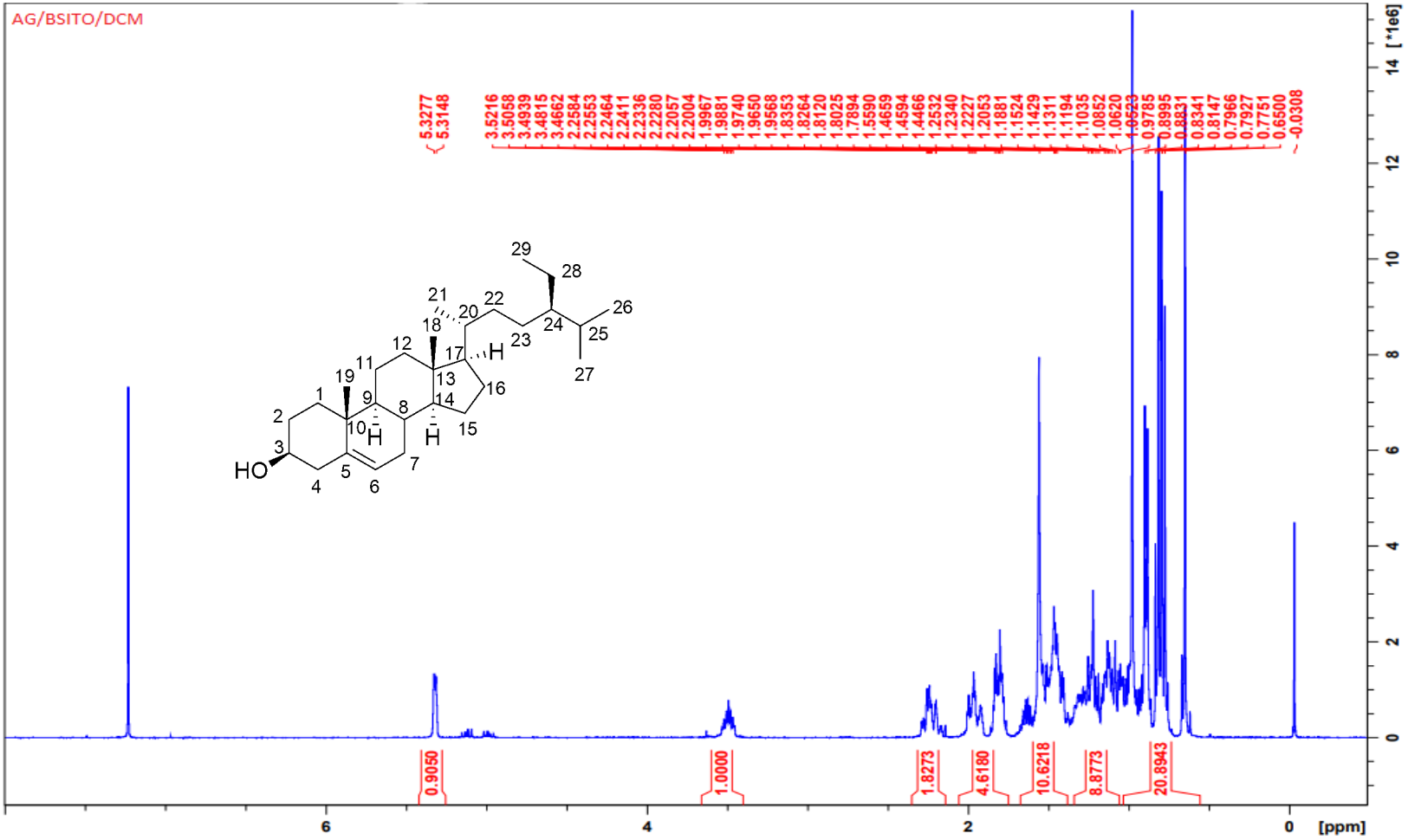

Figure S1: ^{1}H NMR spectrum of β-sitosterol (**S1**)

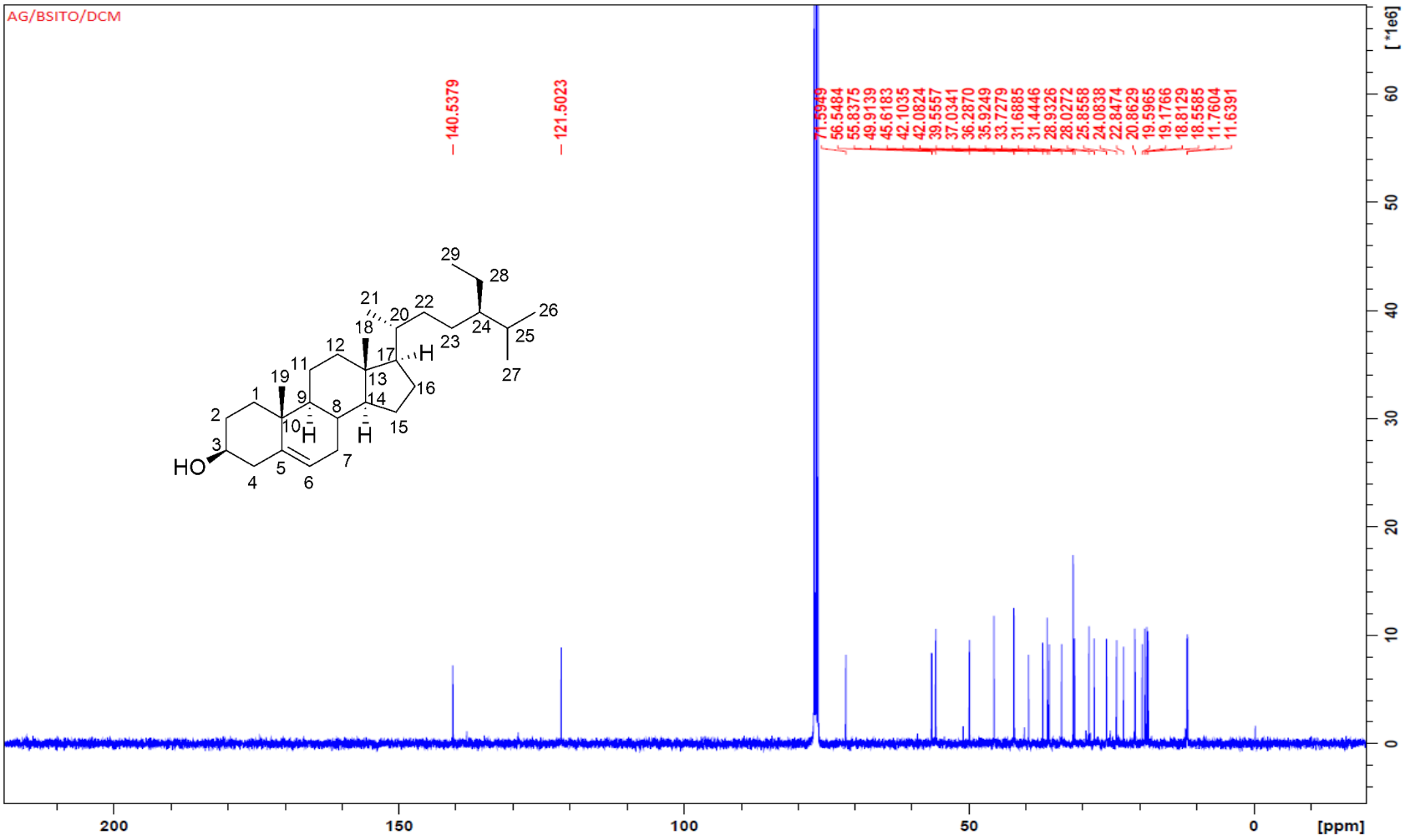

Figure S2: ^{13}C NMR spectrum of β-sitosterol (**S1**)

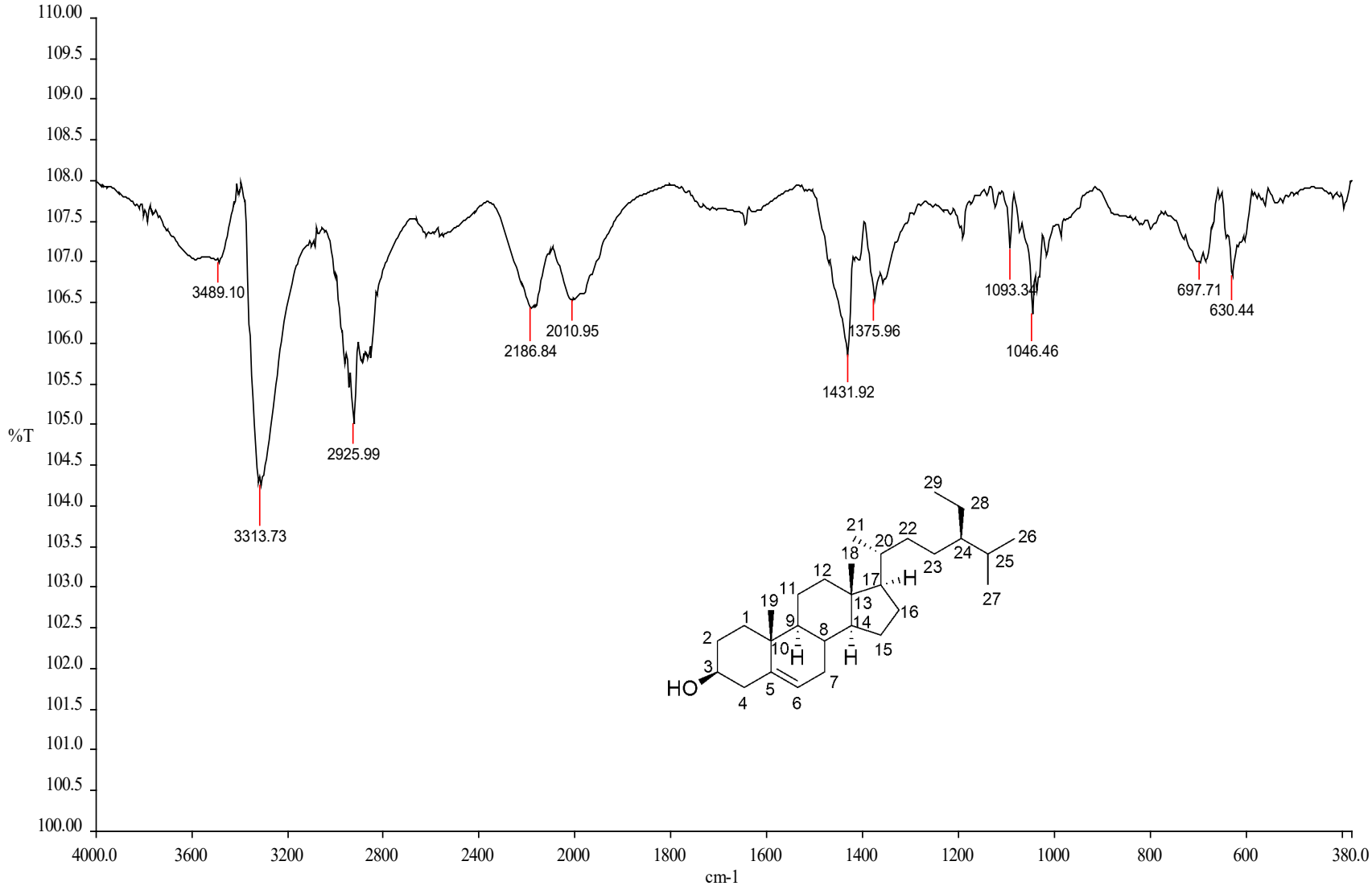

Figure S3: IR spectrum of β-sitosterol (**S1**)

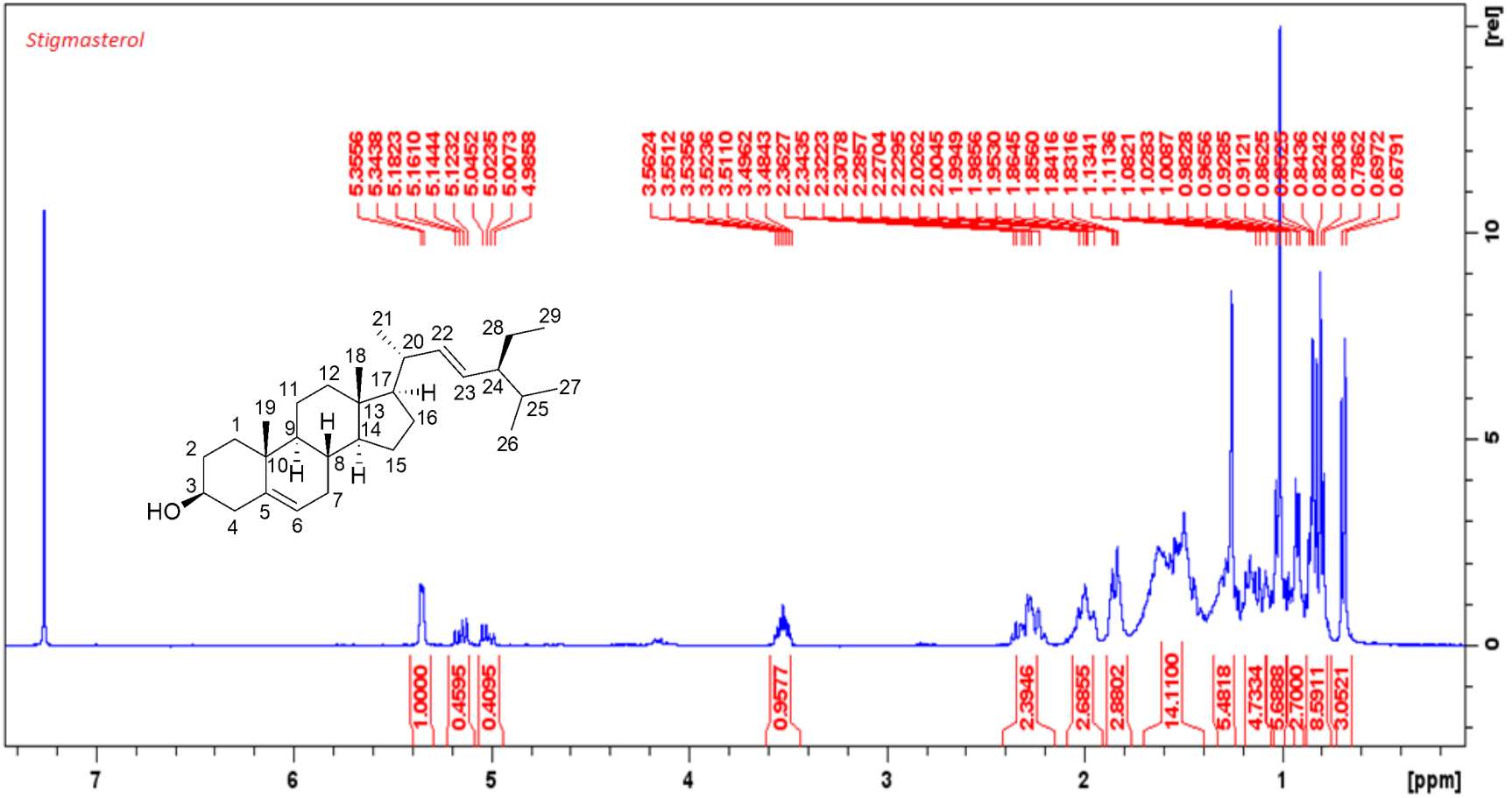

Figure S4: ^{1}H NMR spectrum of stigmasterol (**S2**)

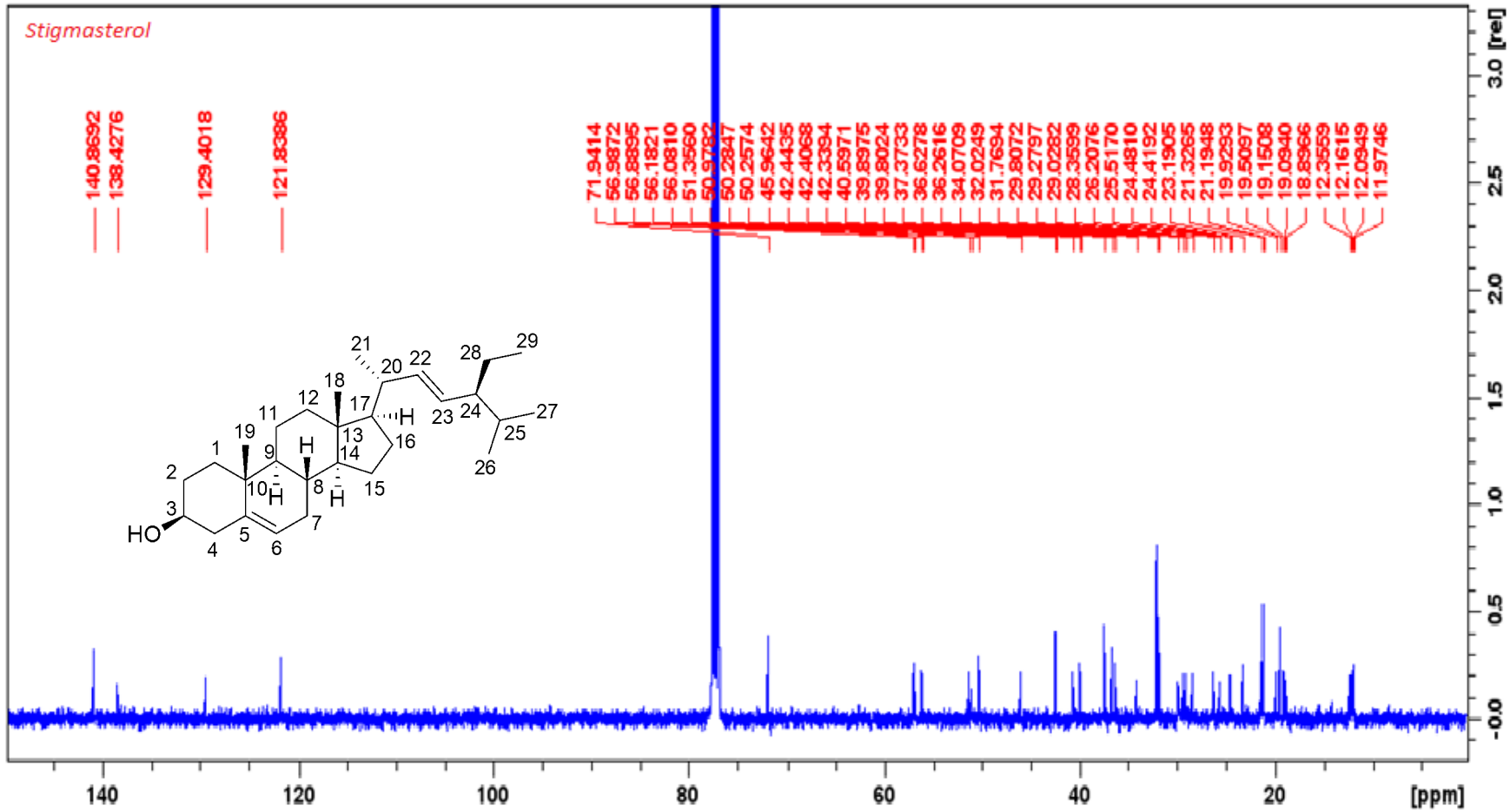

Figure S5: ^{13}C NMR spectrum of stigmasterol (**S2**)

.

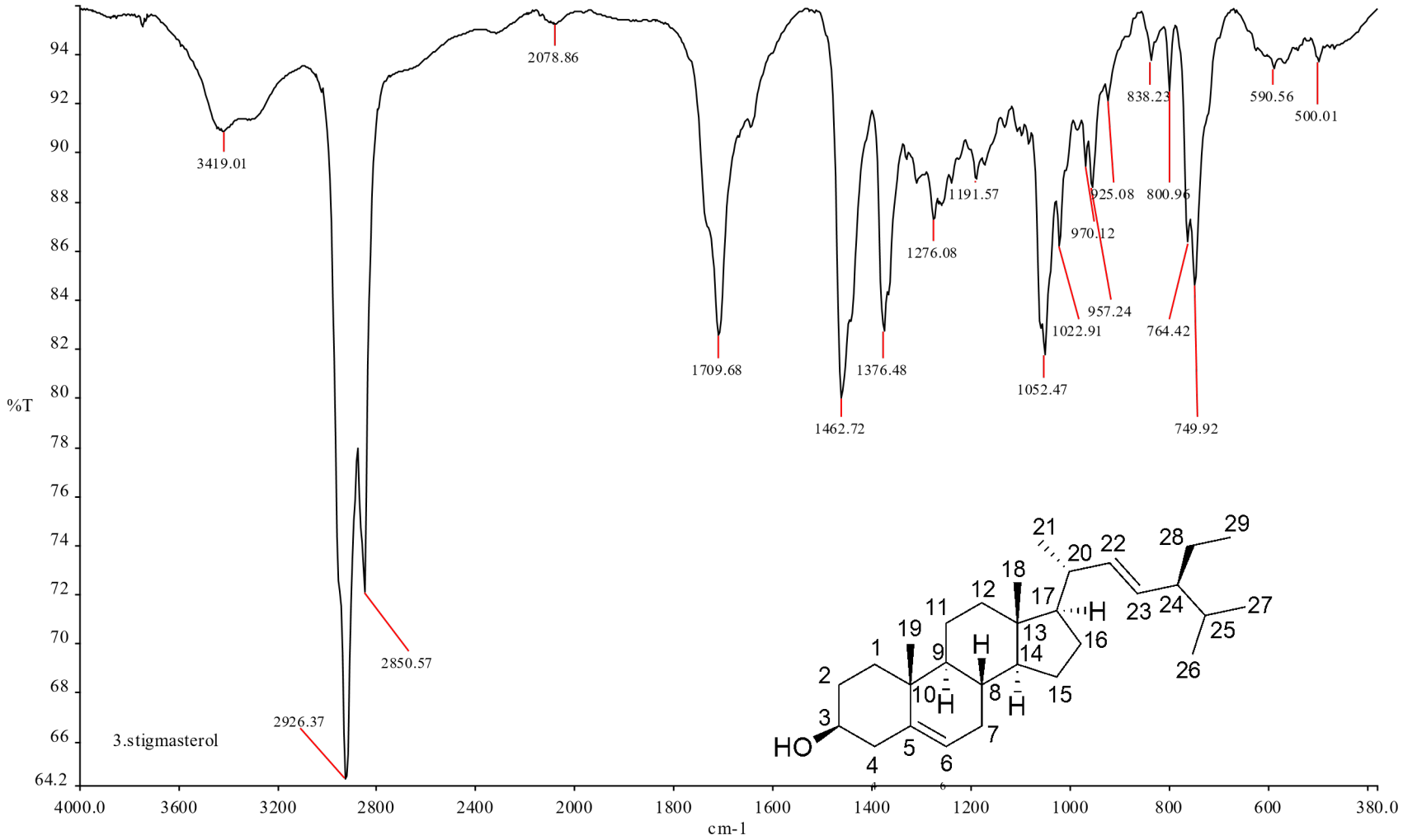

Figure S6: IR spectrum of stigmasterol (**S2**)

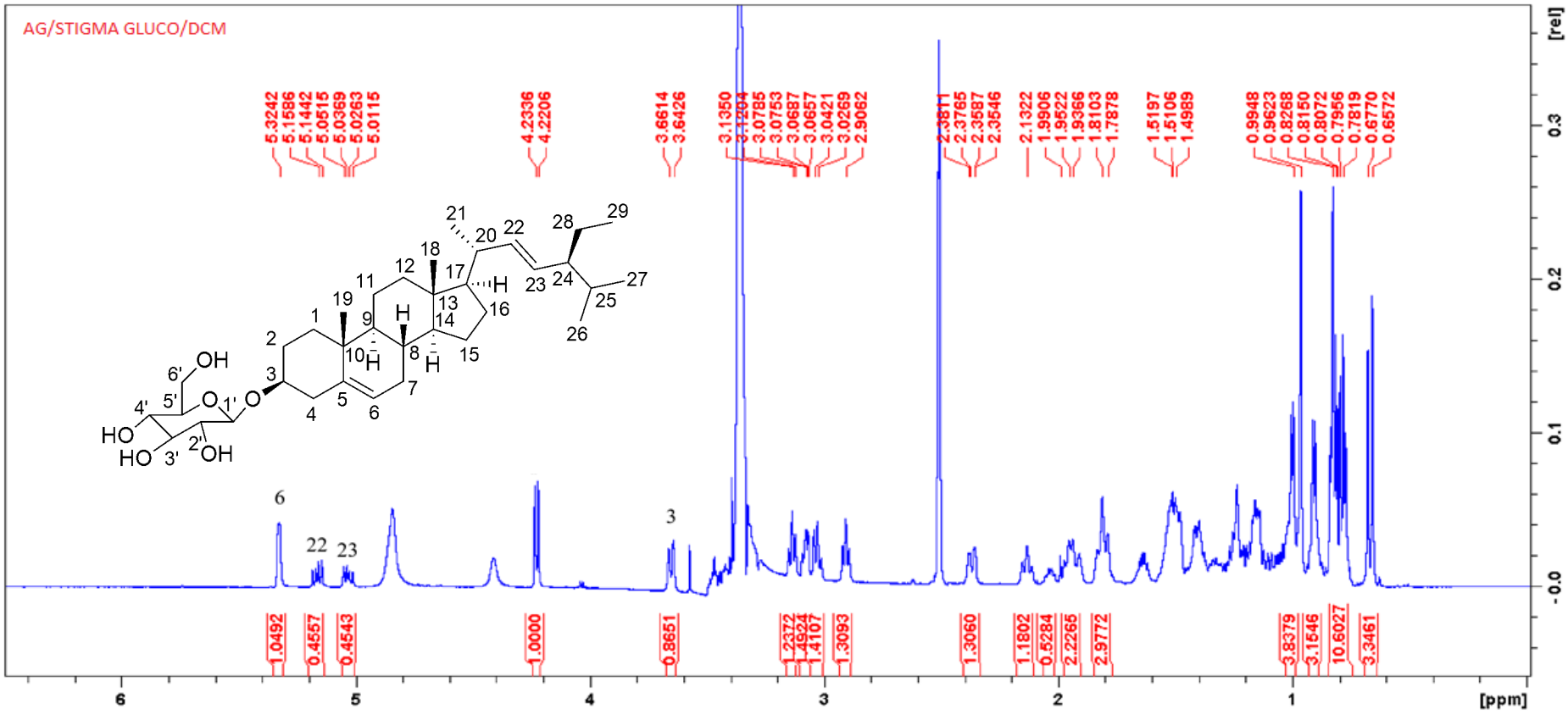

Figure S7: ^{1}H NMR spectrum of stigmasterol glucoside (**S3**)

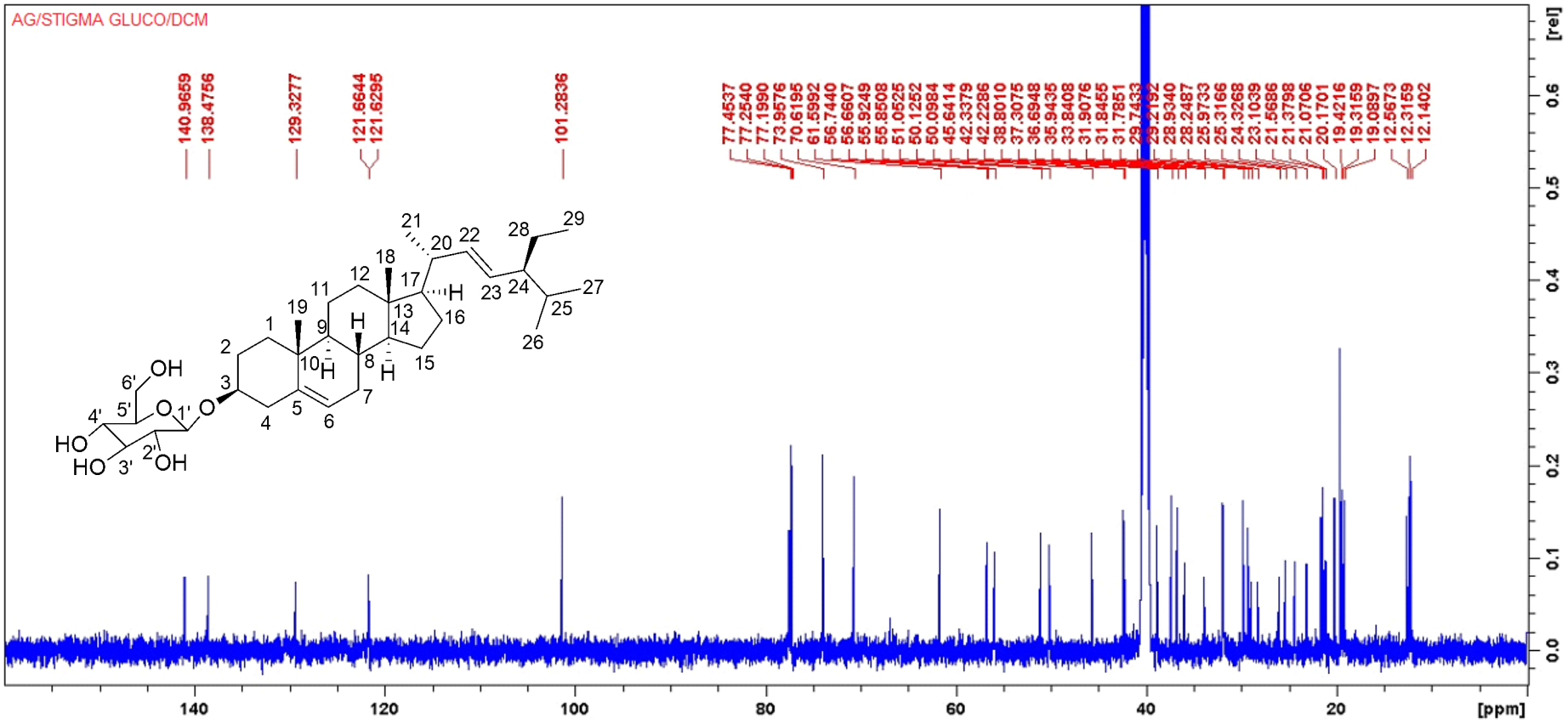

Figure S8: ^{13}C NMR spectrum of stigmasterol glucoside (**S3**)

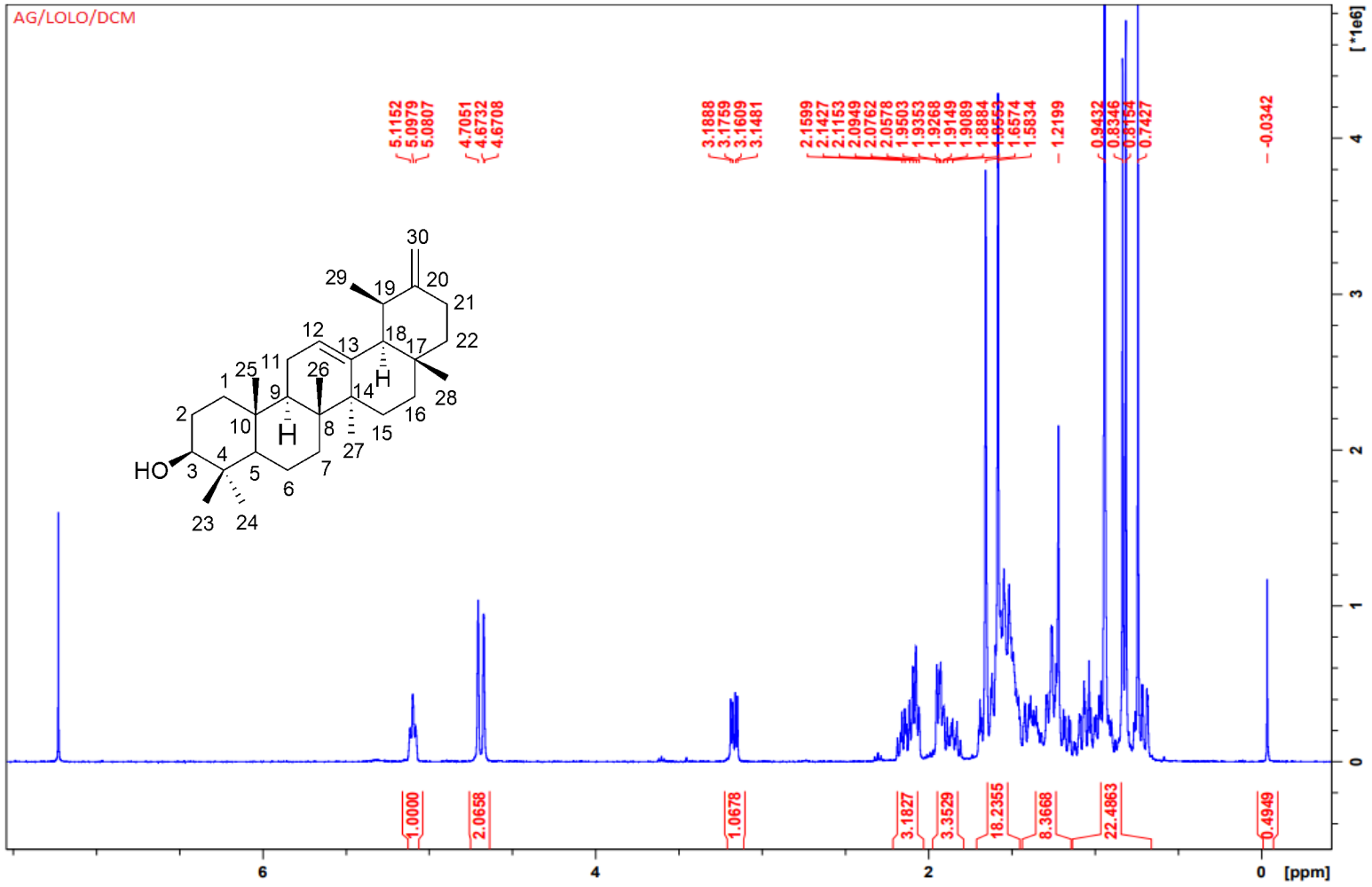

Figure S9: ^{1}H NMR spectrum of 18α-ursa-12,20(30)-dien-3β-ol (**S4**)

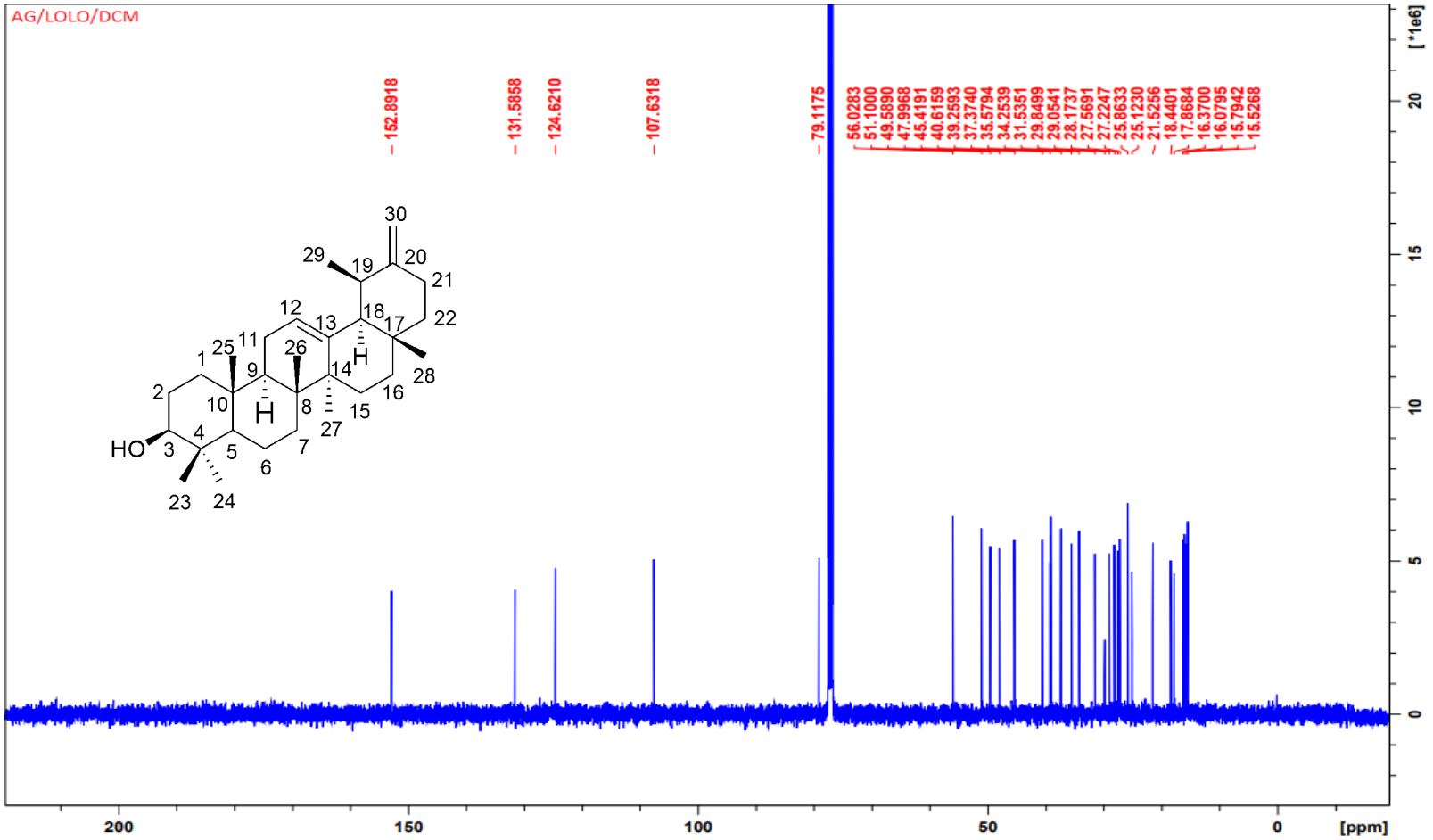

Figure S10: ^{13}C NMR spectrum of 18α-ursa-12,20(30)-dien-3β-ol (**S4**)

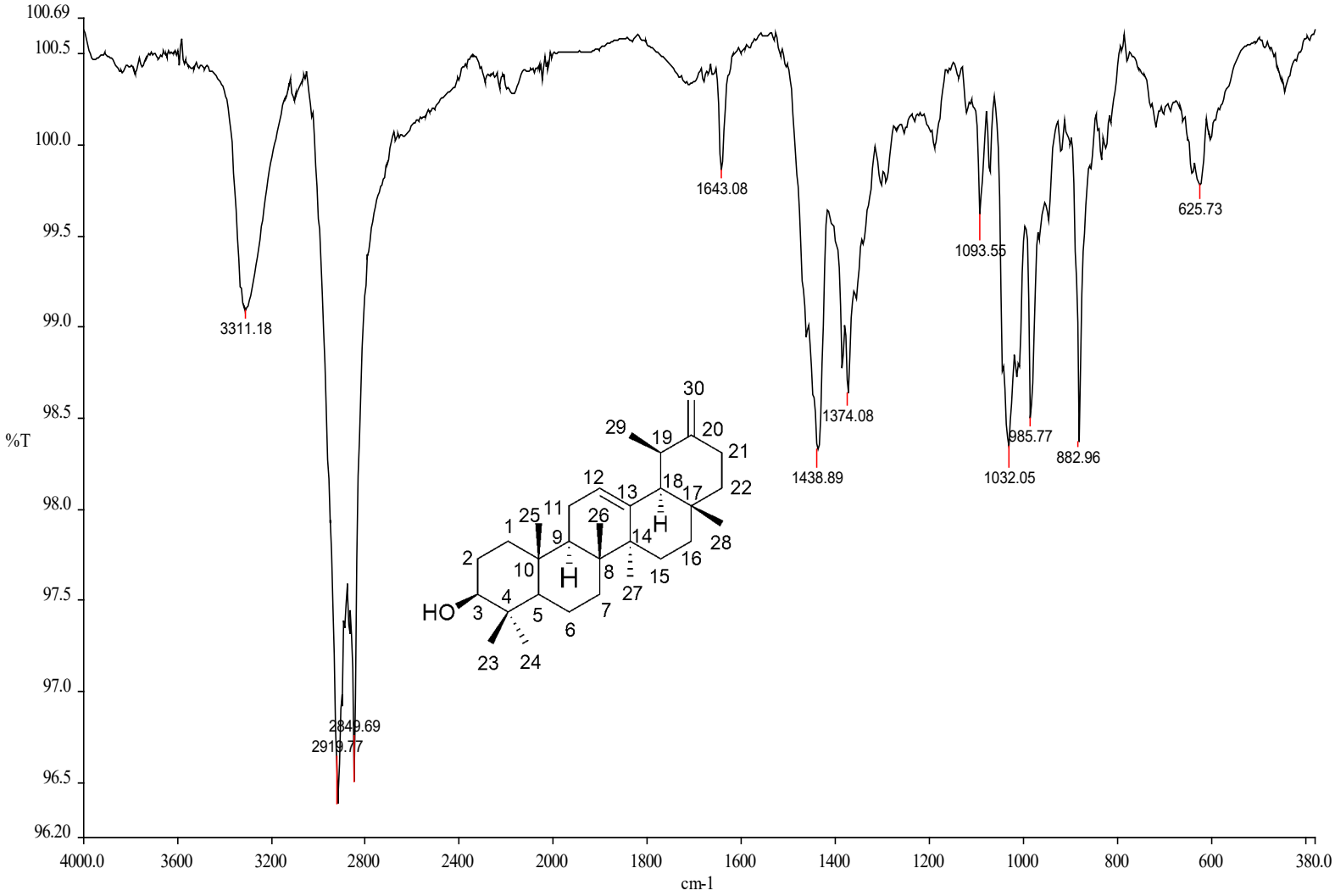

Figure S11: IR spectrum of 18α-ursa-12,20(30)-dien-3β-ol (**S4**)

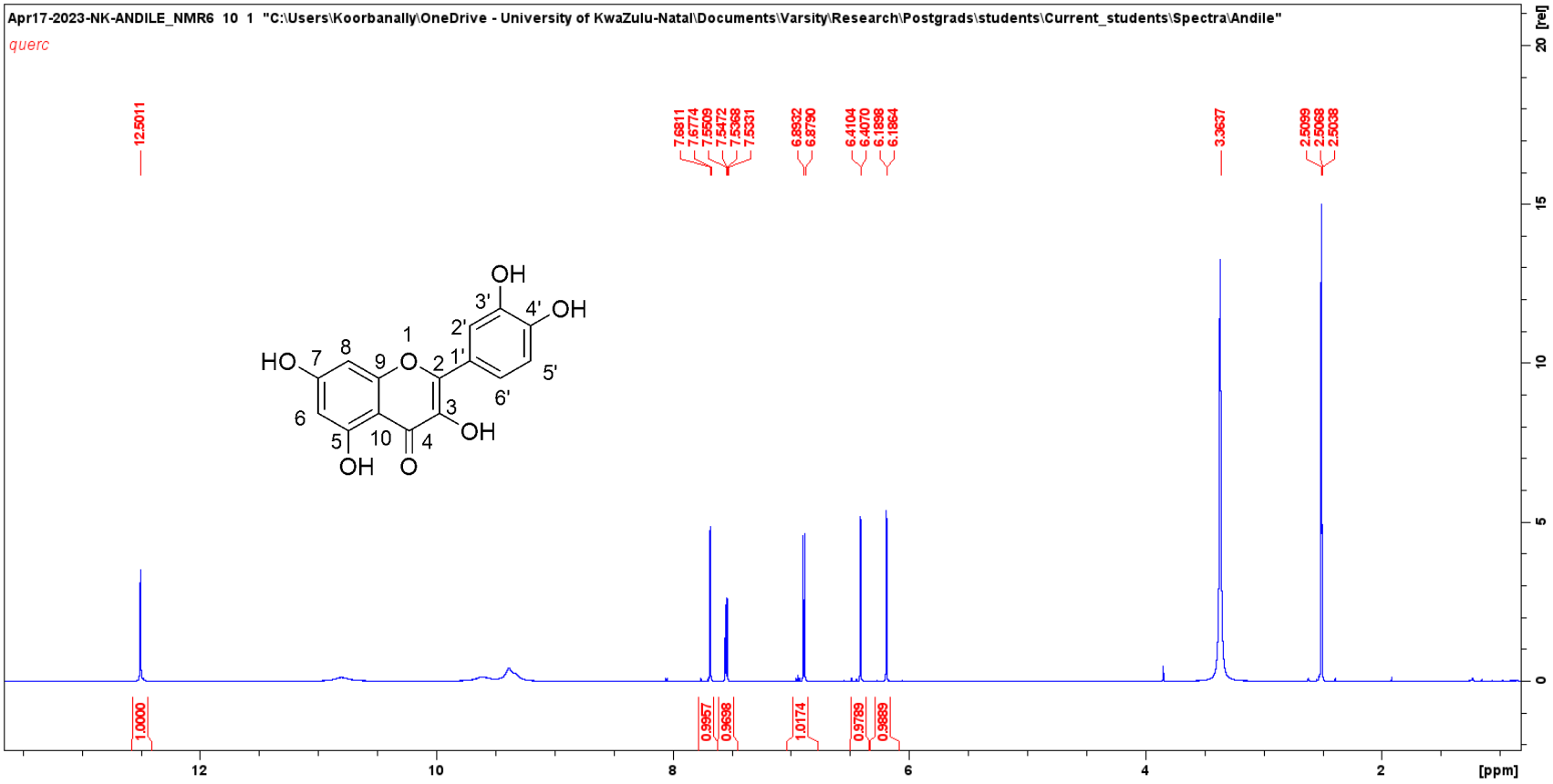

Figure S12: ^{1}H NMR spectrum of quercetin (**S5**)

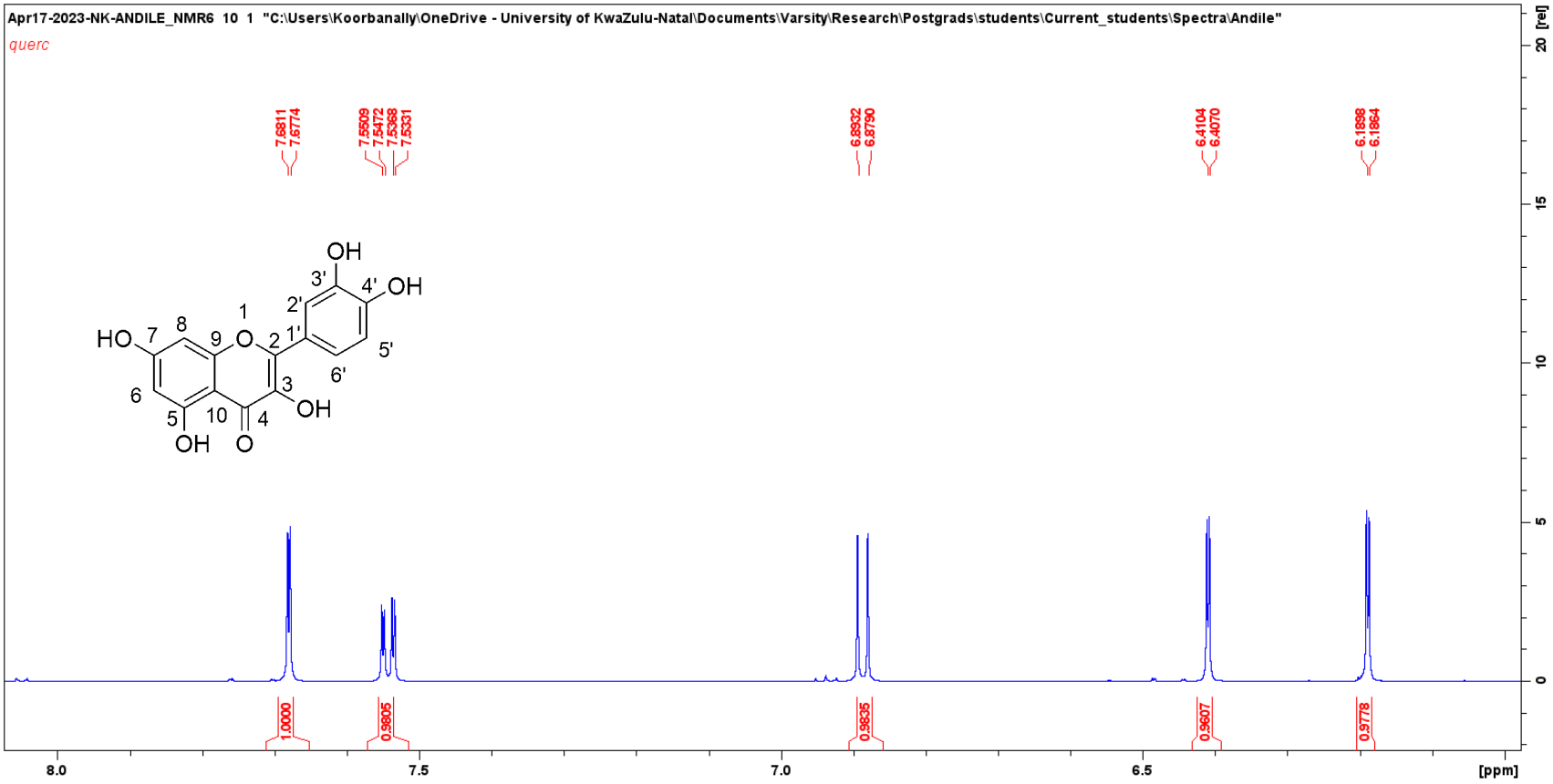

Figure S13: Expanded ^{1}H NMR spectrum of quercetin (**S5**)

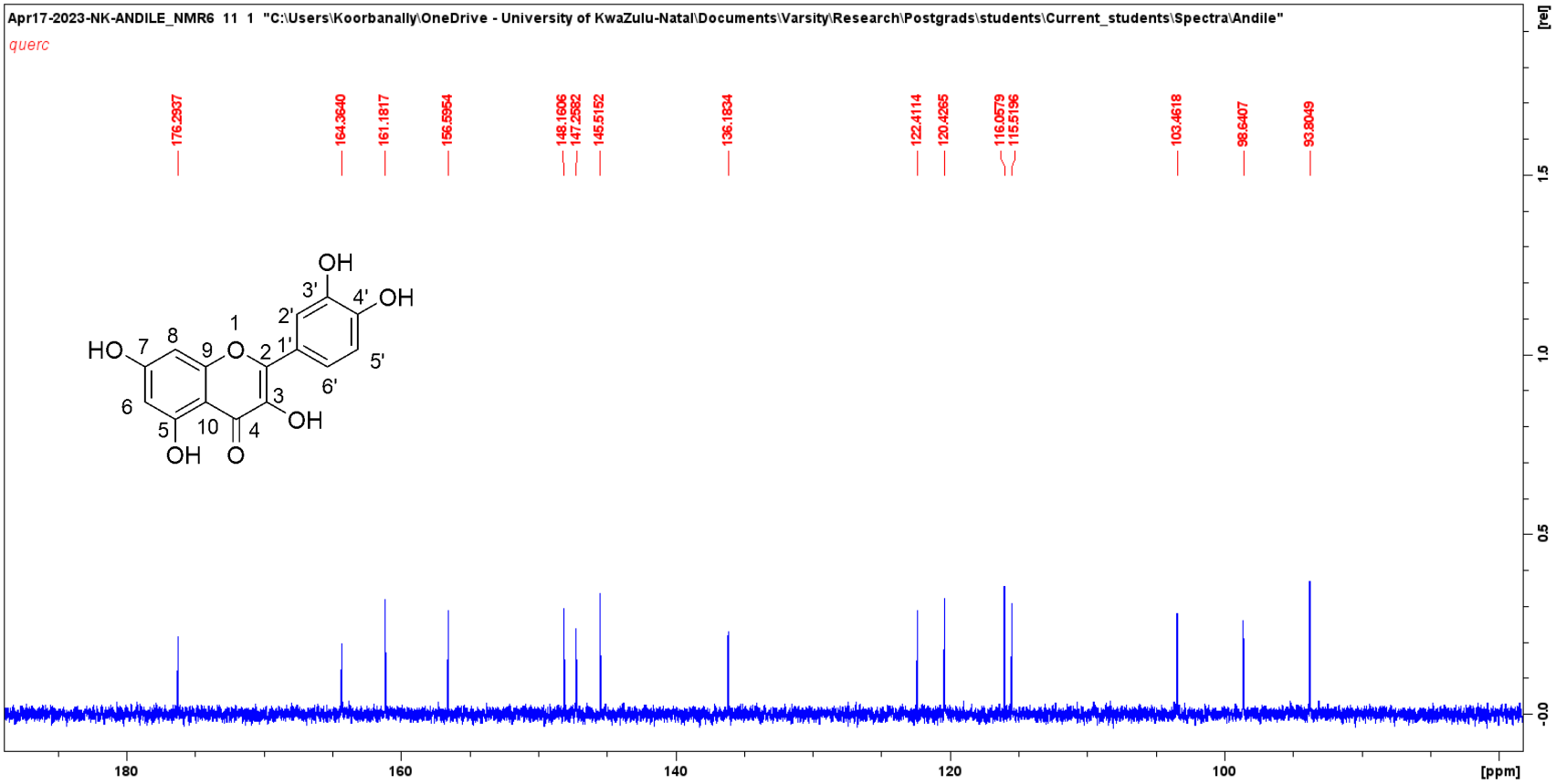

Figure S14: ^{13}C NMR spectrum of quercetin (**S5**)

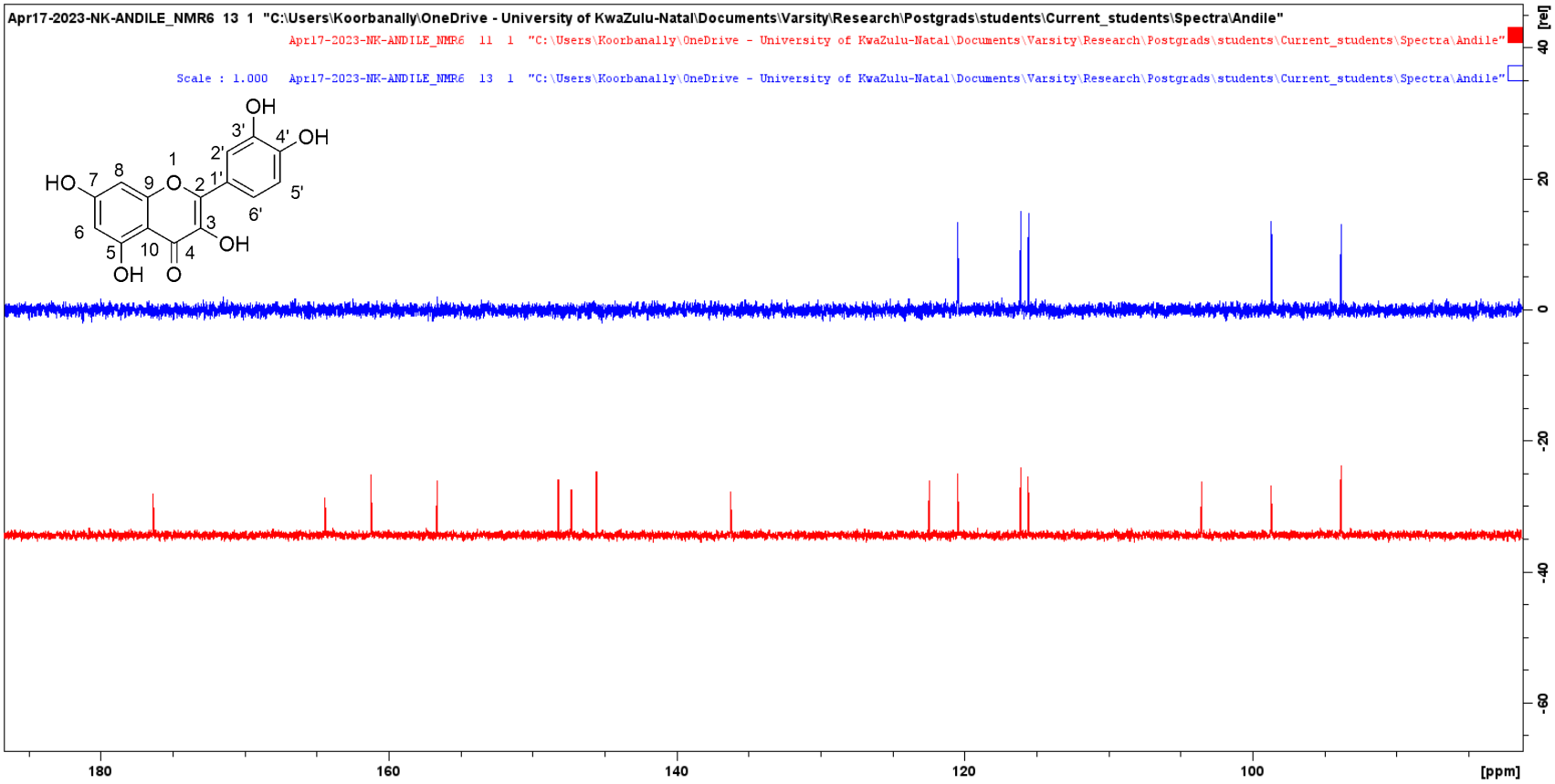

Figure S15: DEPT spectrum of quercetin (**S5**)

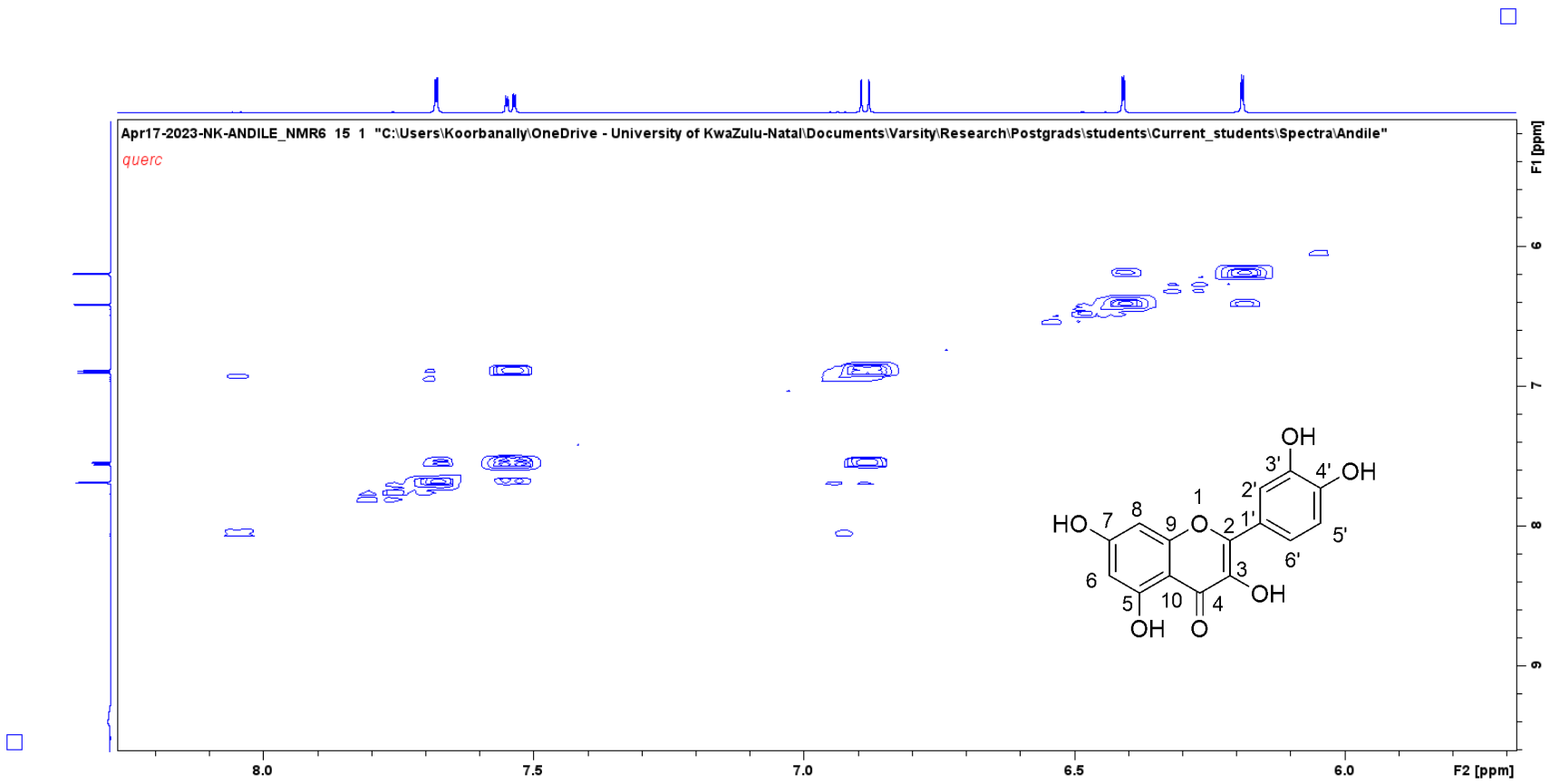

Figure S16: COSY spectrum of quercetin (**S5**)

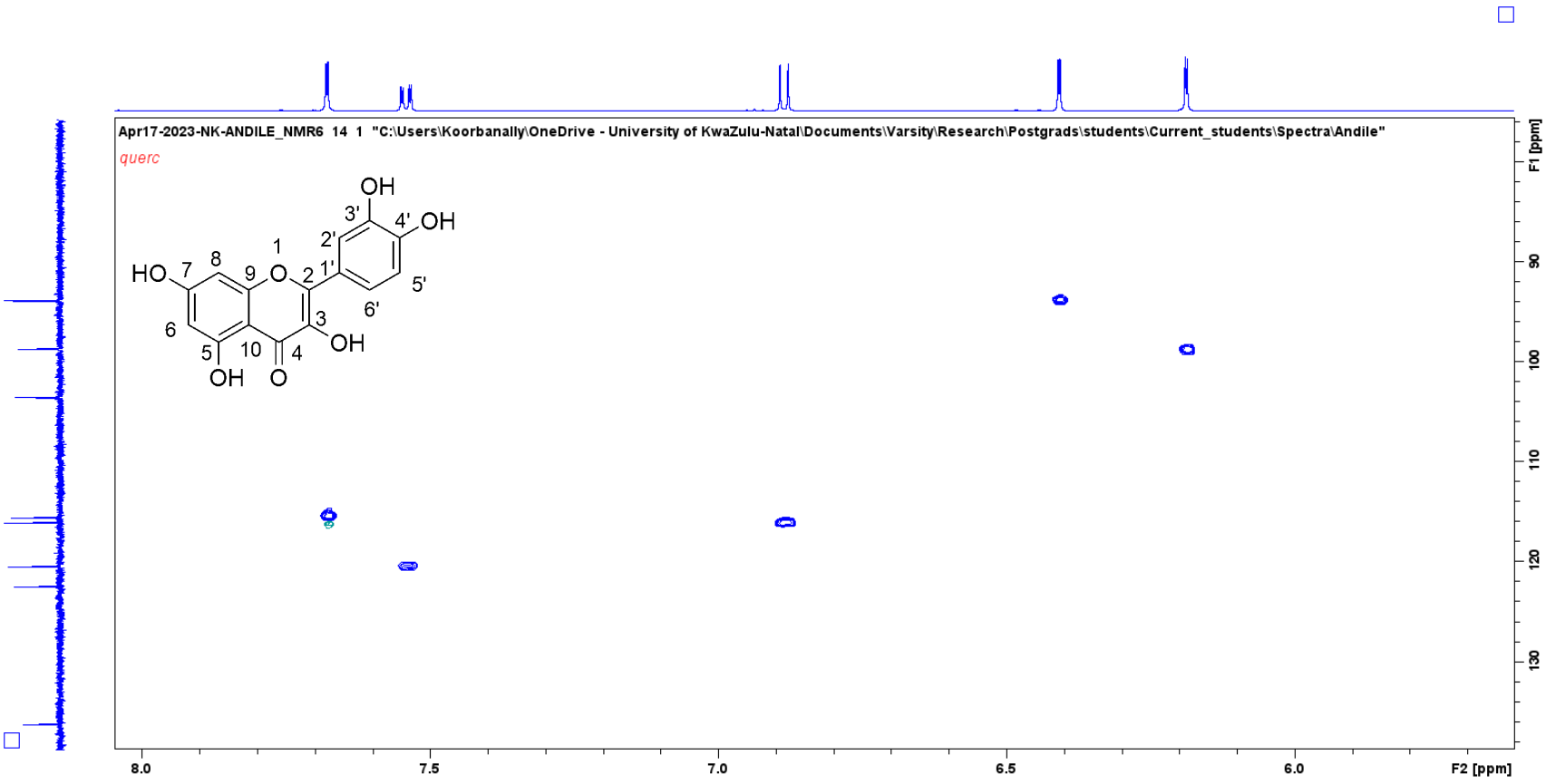

Figure S17: HSQC spectrum of quercetin (**S5**)

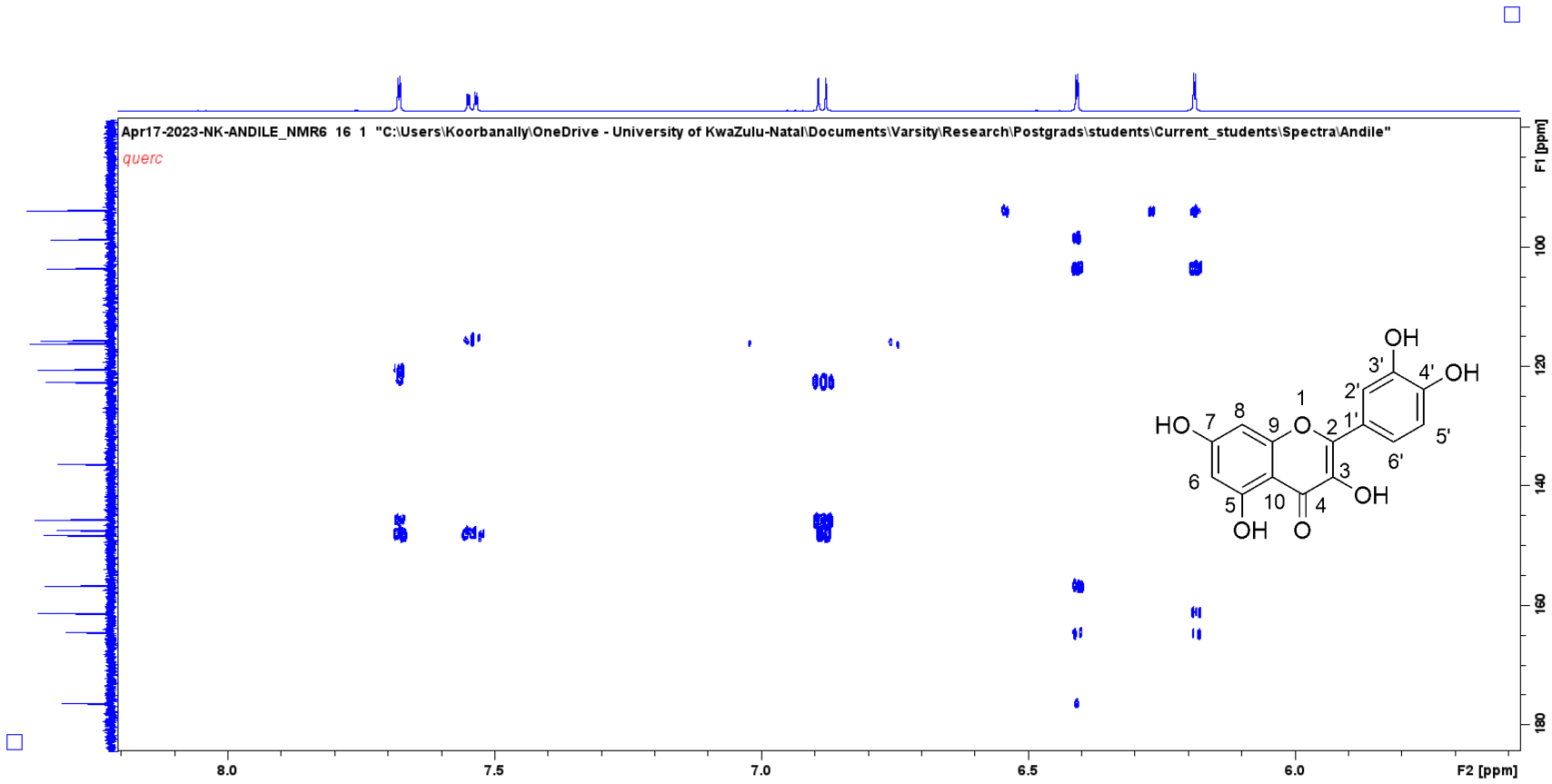

Figure S18: HMBC spectrum of quercetin (**S5**)

Elemental Composition Report **Page 1**

Single Mass Analysis

Tolerance = 5.0 PPM / DBE: min = -1.5, max = 50.0
Element prediction: Off
Number of isotope peaks used for i-FIT = 3

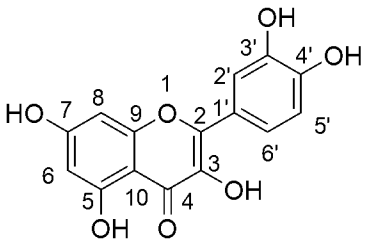

Monoisotopic Mass, Even Electron Ions
39 formula(e) evaluated with 1 results within limits (up to 50 closest results for each mass)
Elements Used:
C: 0-50 H: 0-100 O: 0-10

A QUE 102 (0.891) Cm (6:231)
TOF MS ES-

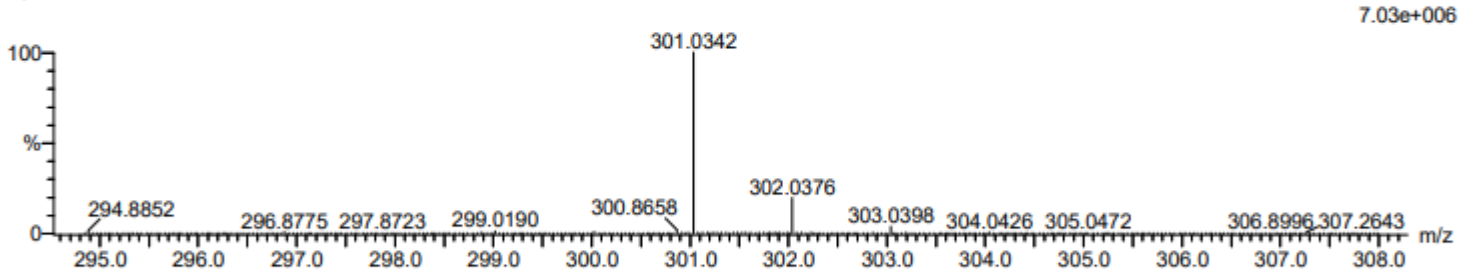

Minimum:				-1.5				
Maximum:		10.0	5.0	50.0				
Mass	Calc. Mass	mDa	PPM	DBE	i-FIT	Norm	Conf(%)	Formula
301.0342	301.0348	-0.6	-2.0	11.5	1119.7	n/a	n/a	C15 H9 O7

Figure S19: High Resolution Mass spectrum of quercetin (**S5**)

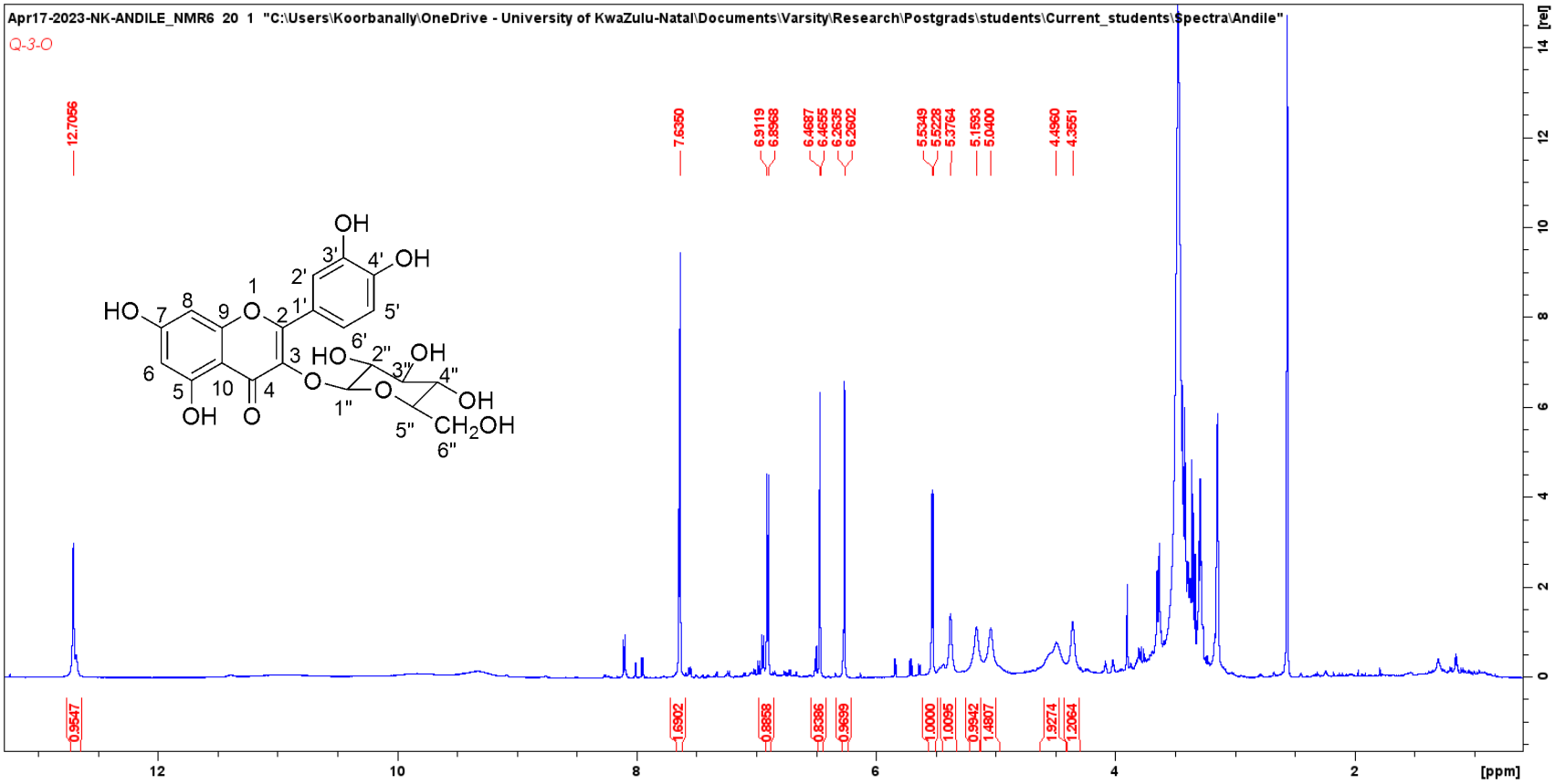

Figure S20: ^{1}H NMR spectrum of quercetin-3-*O*-glucoside (**S6**)

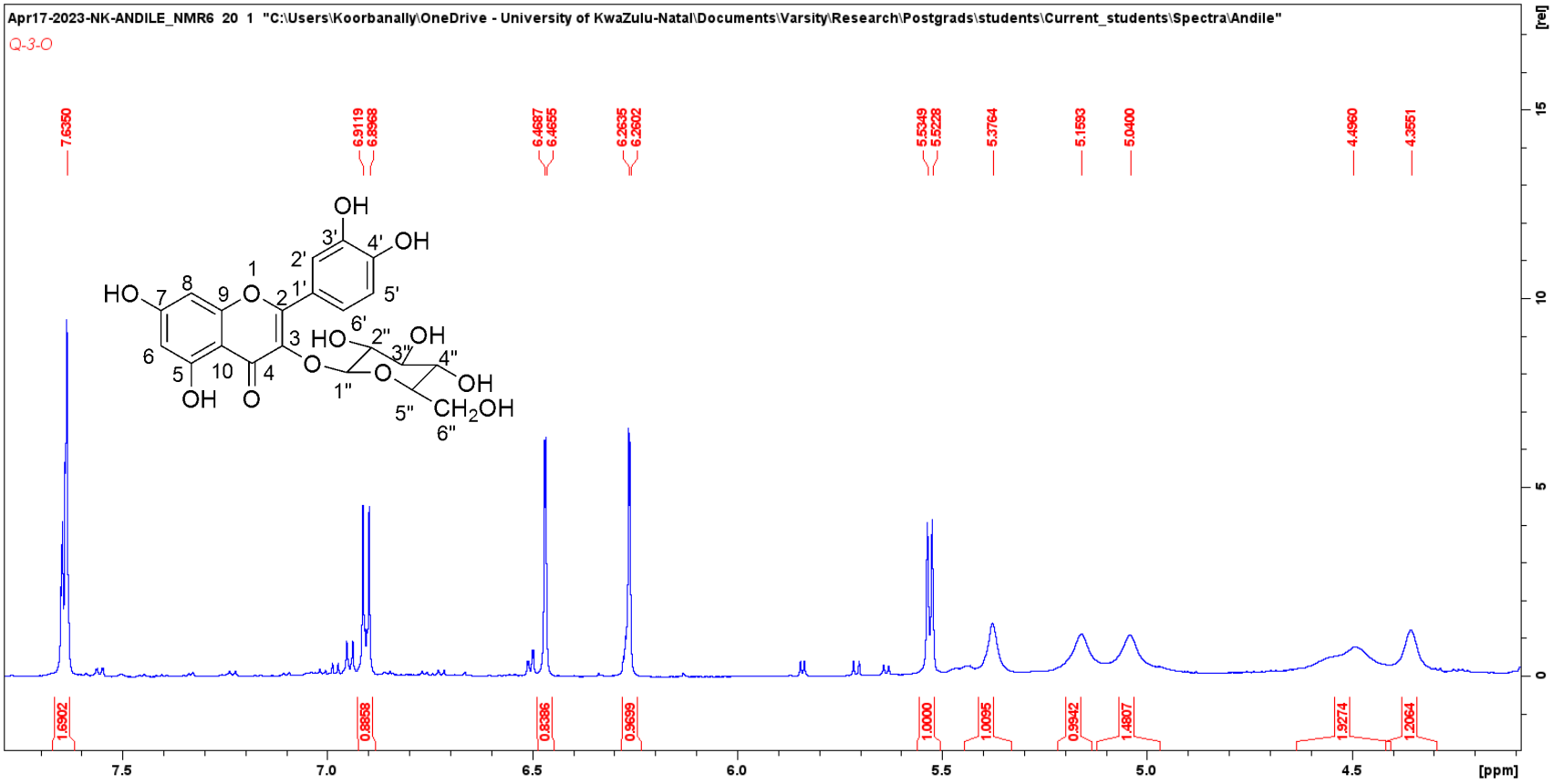

Figure S21: Expanded ^{1}H NMR spectrum of quercetin-3-*O*-glucoside (**S6**)

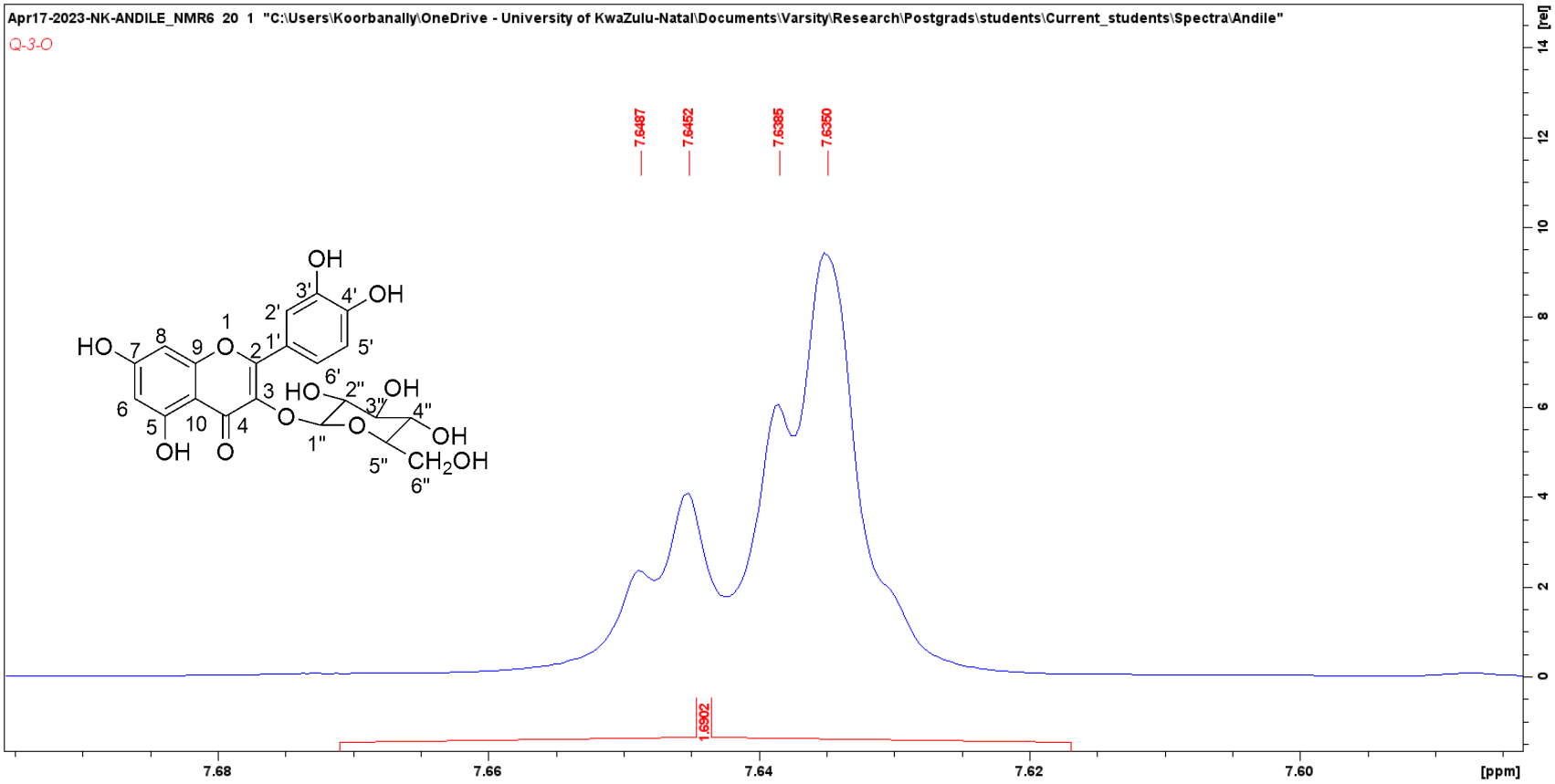

Figure S22: Expansion of the resonance at δ7.64 in quercetin-3-*O*-glucoside (**S6**)

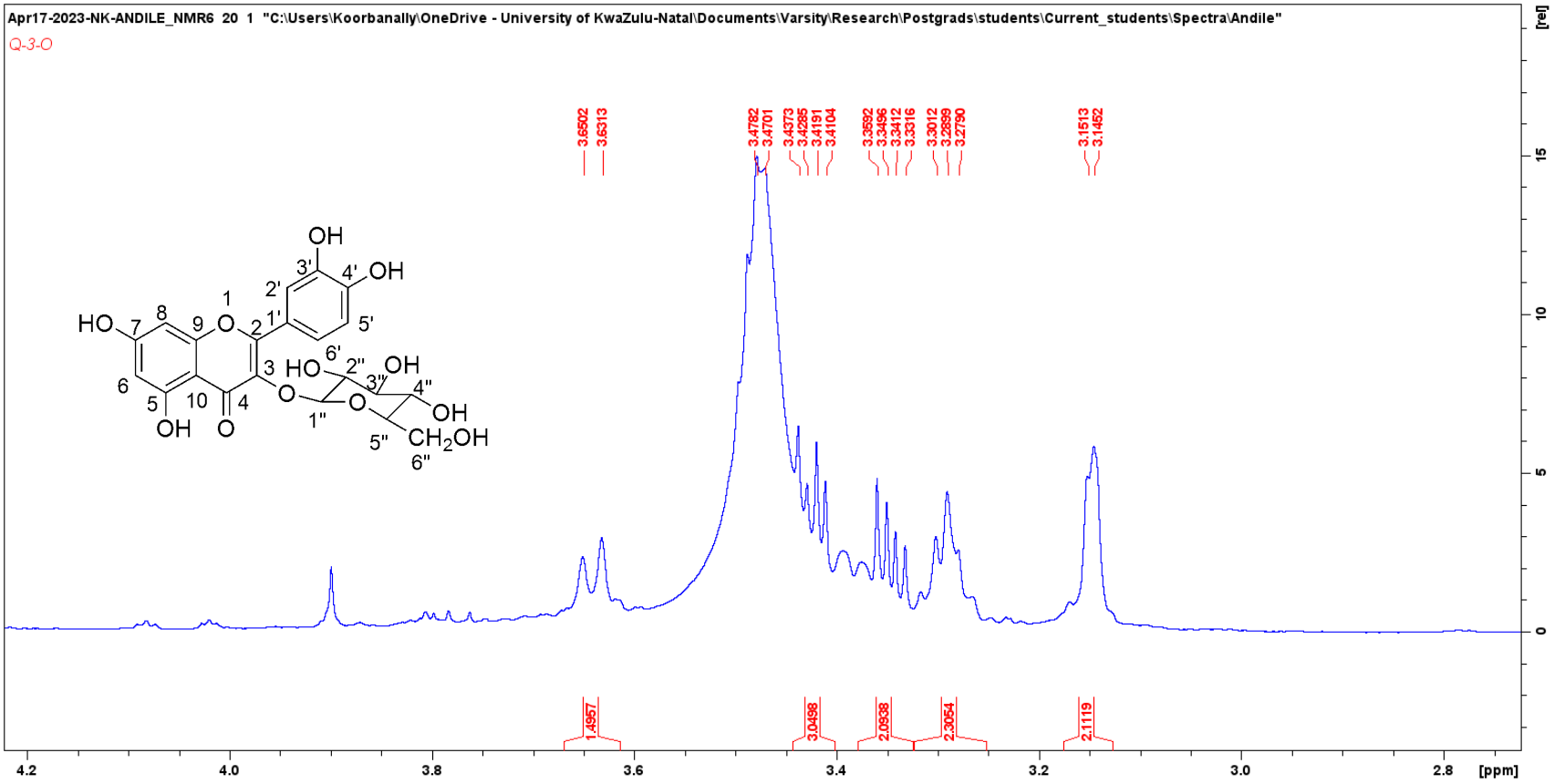

Figure S23: Expansion of the region between δ3.00 and 4.00 in quercetin-3-*O*-glucoside (**S6**)

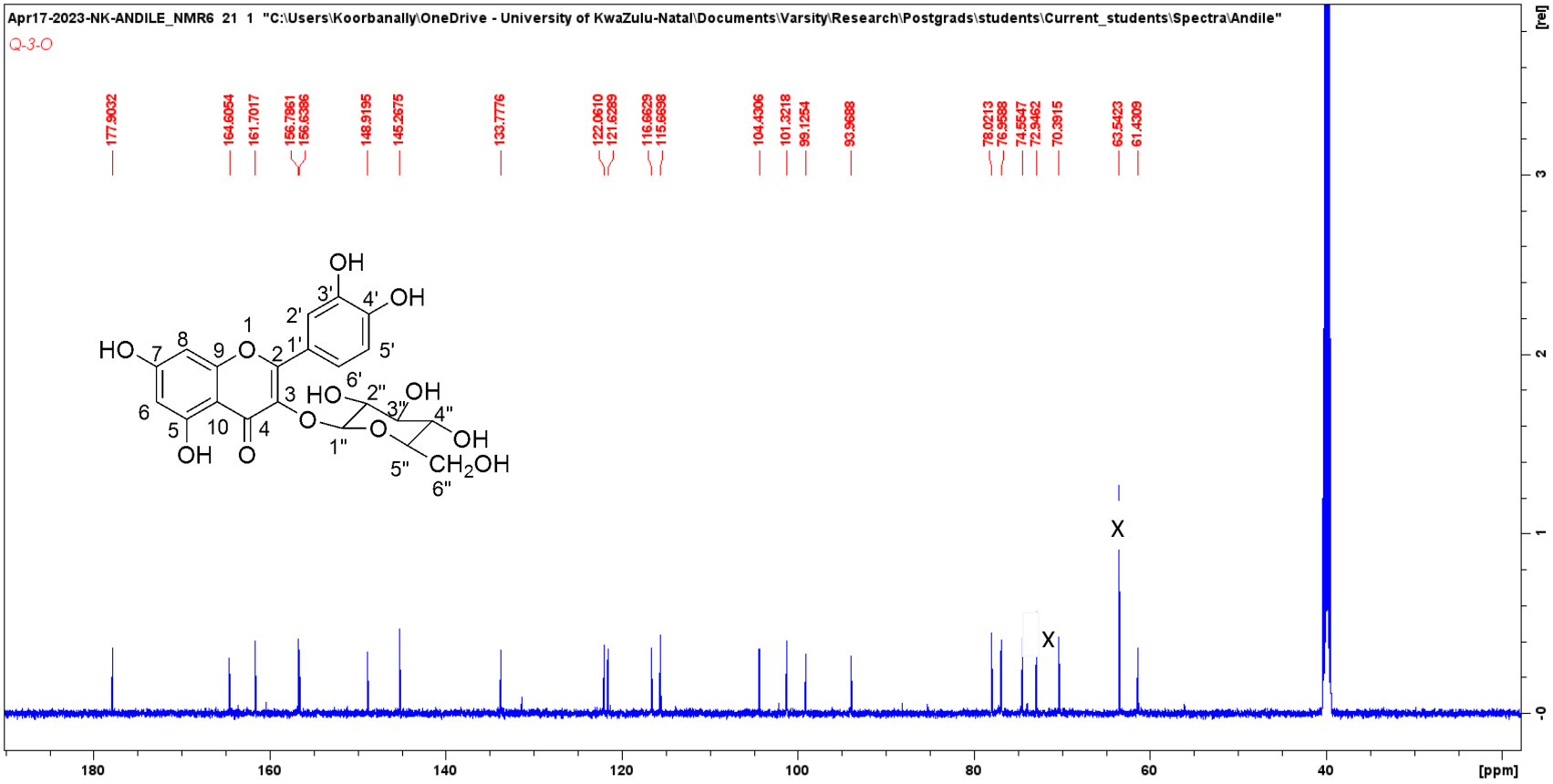

Figure S24: ^{13}C NMR spectrum of quercetin-3-*O*-glucoside (**S6**)

Elemental Composition Report **Page 1**

Single Mass Analysis

Tolerance = 5.0 PPM / DBE: min = -1.5, max = 50.0

Element prediction: Off

Number of isotope peaks used for i-FIT = 3

Monoisotopic Mass, Even Electron Ions

99 formula(e) evaluated with 1 results within limits (up to 50 closest results for each mass)

Elements Used:

C: 0-50 H: 0-100 O: 0-20

A QUE-3-O 98 (0.856) Cm (6:230)

TOF MS ES-

4.89e+006

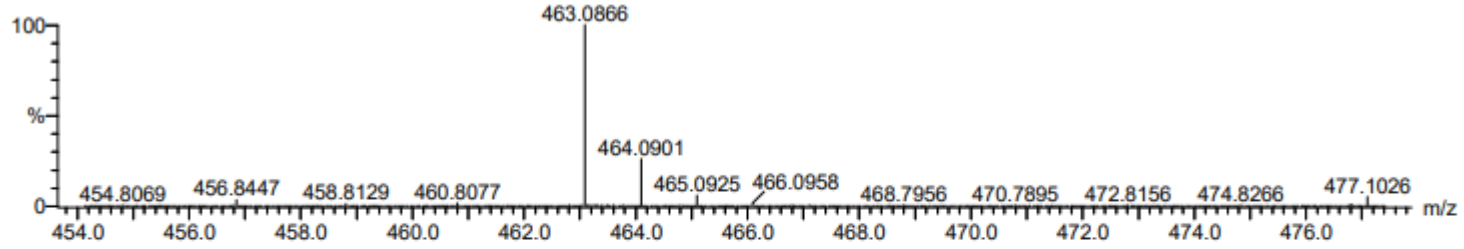

Minimum:				-1.5				
Maximum:		10.0	5.0	50.0				
Mass	Calc. Mass	mDa	PPM	DBE	i-FIT	Norm	Conf(%)	Formula
463.0866	463.0877	-1.1	-2.4	12.5	1049.5	n/a	n/a	C21 H19 O12

Figure S25: High Resolution Mass Spectrum of quercetin-3-*O*-glucoside (**S6**)

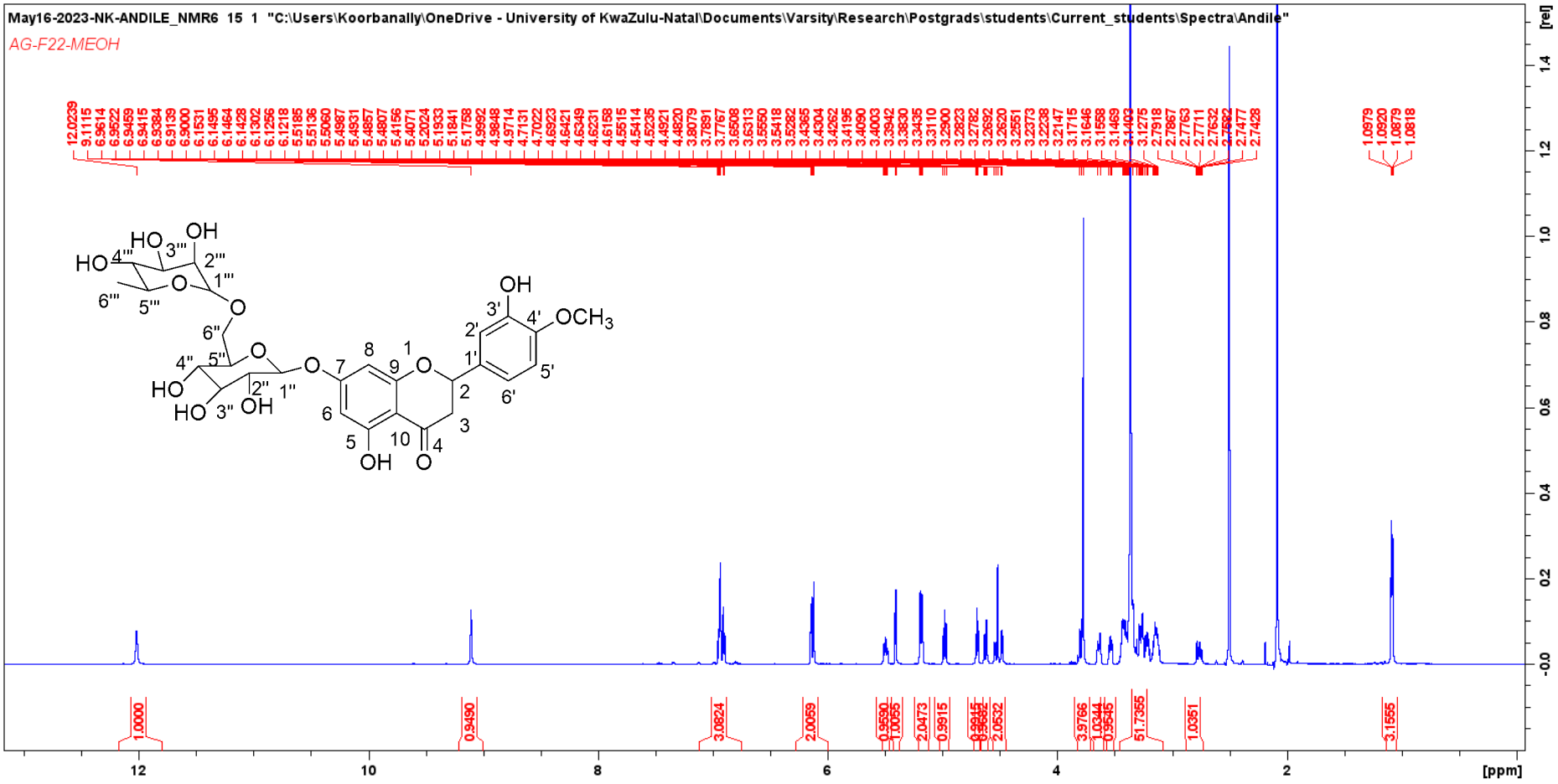

Figure S26: ^{1}H NMR spectrum of hesperidin (**S7**)

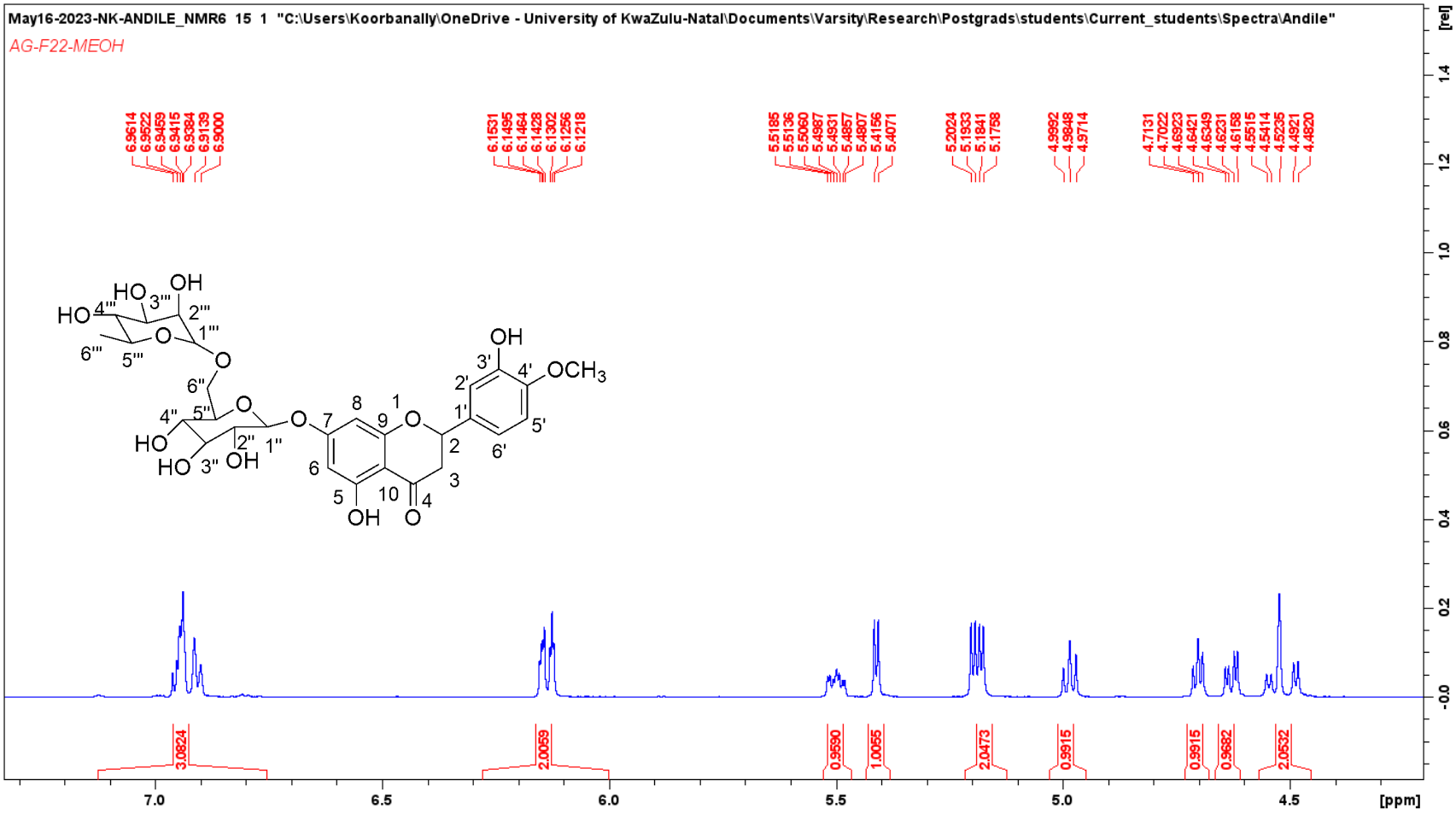

Figure S27: Expanded ^{1}H NMR spectrum of hesperidin (**S7**)

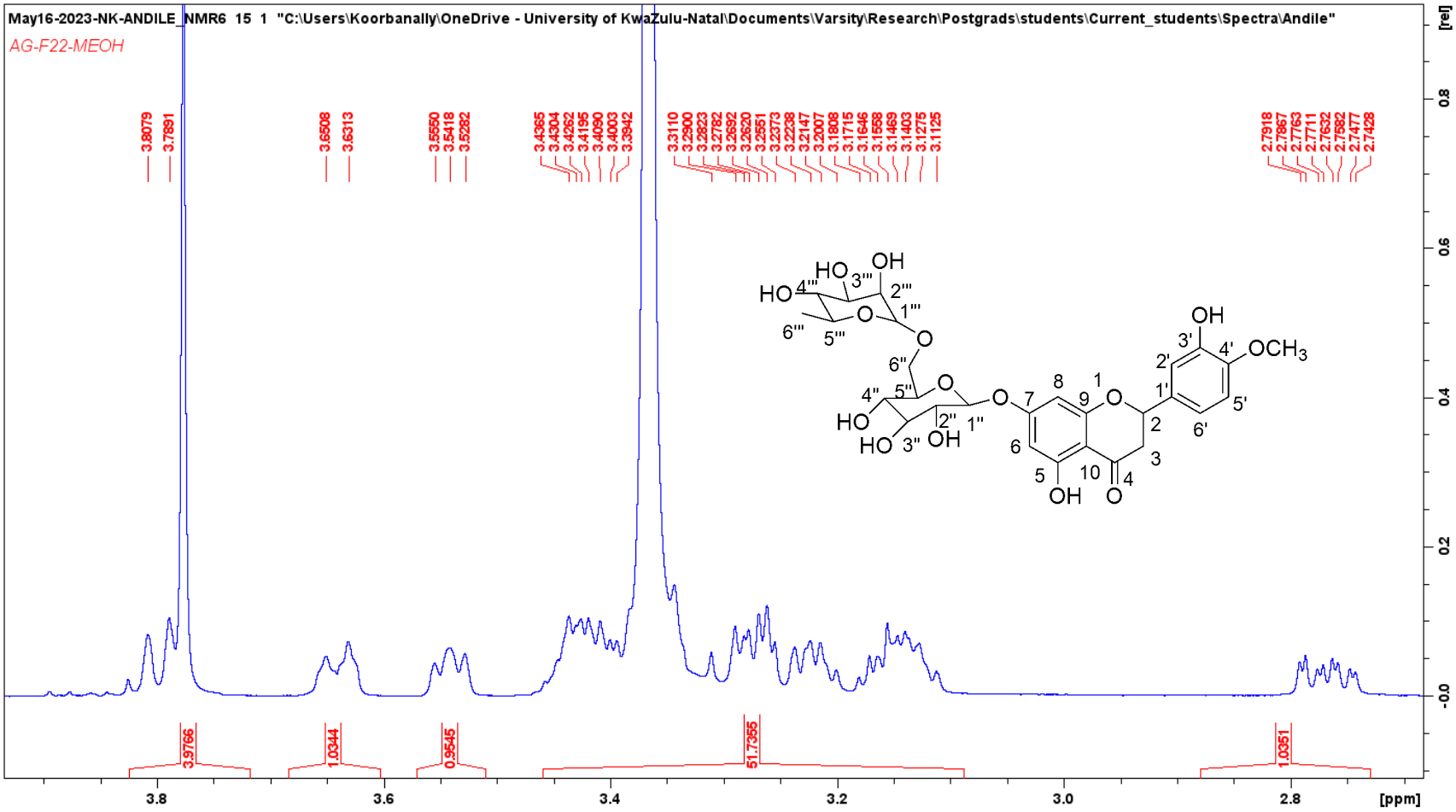

Figure S28: Expansion of the ^{1}H NMR spectrum of hesperidin (**S7**) between δ2.8 and 3.8

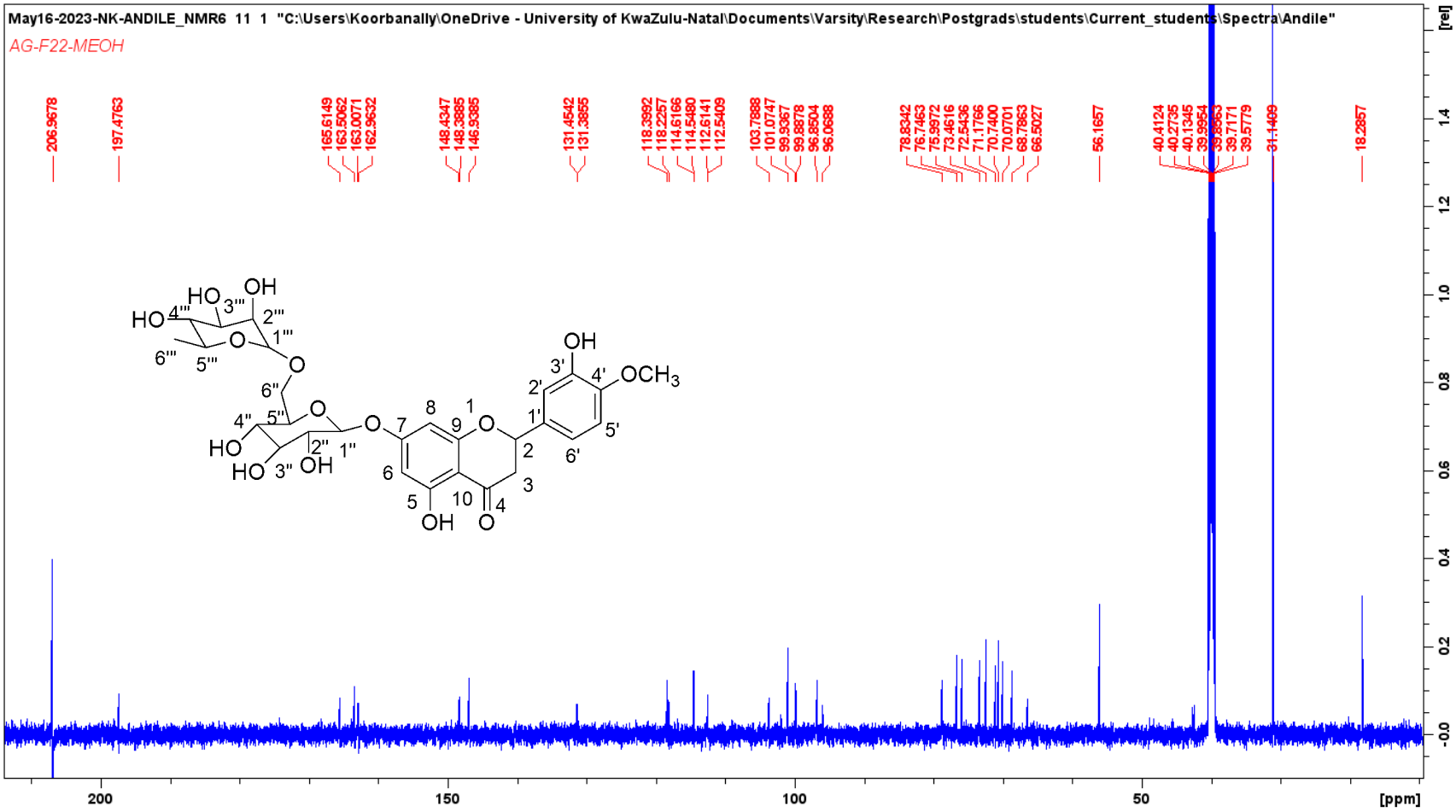

Figure S29: ^{13}C NMR spectrum of hesperidin (**S7**)

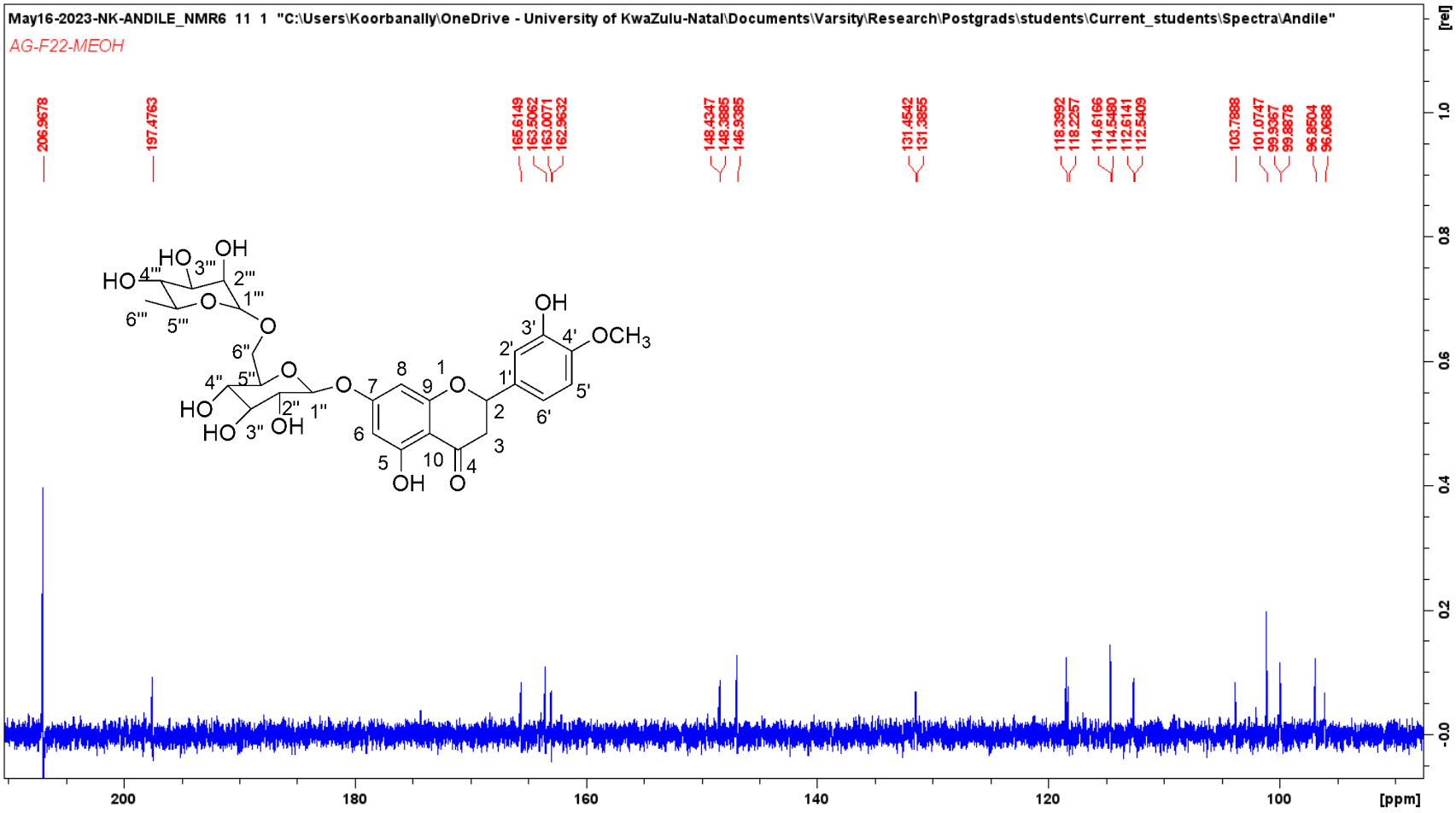

Figure S30: Expanded ^{13}C NMR spectrum of hesperidin (**S7**)

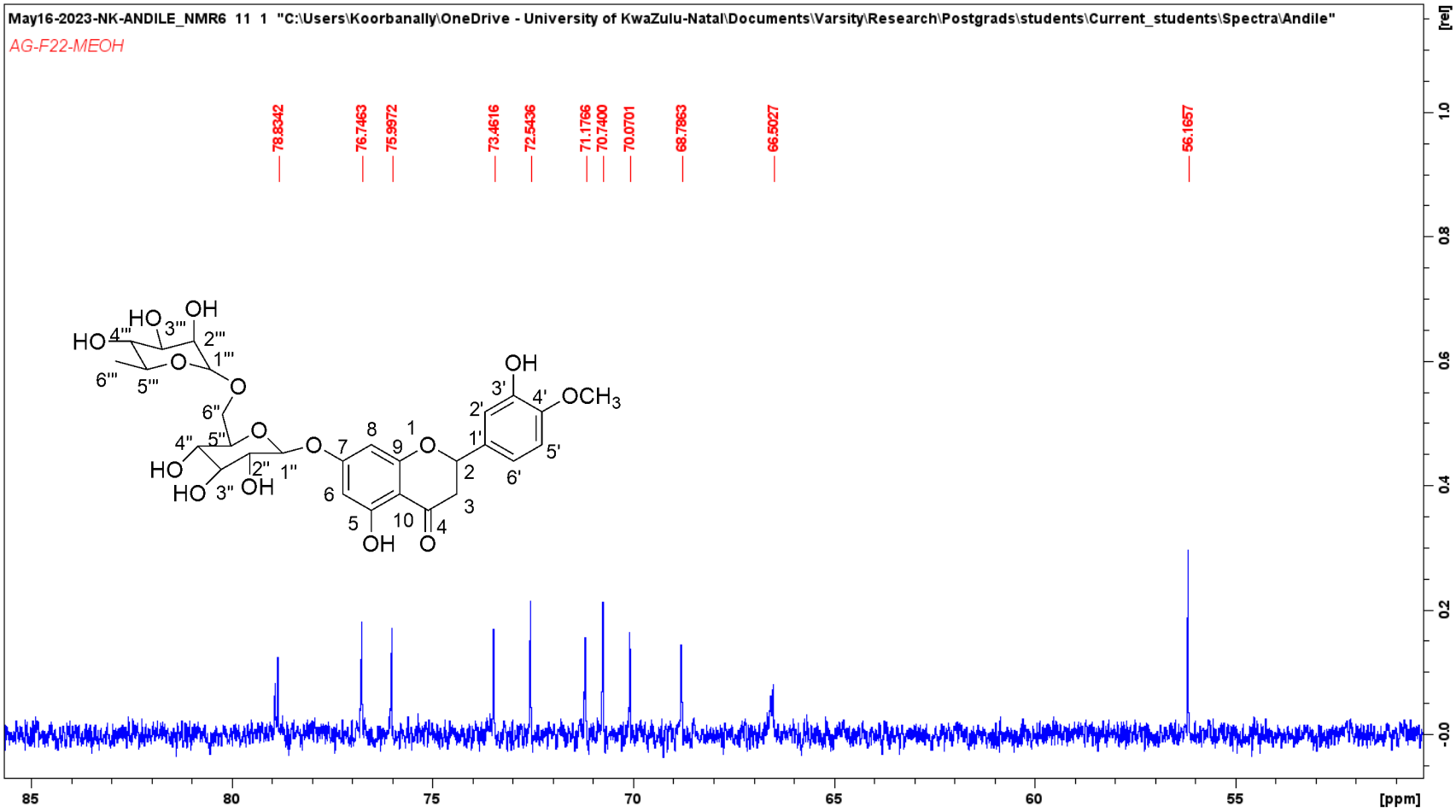

Figure S31: Expanded ^{13}C NMR spectrum of hesperidin (**S7**) in the region of δ 55-85

Elemental Composition Report **Page 1**

Single Mass Analysis
Tolerance = 5.0 PPM / DBE: min = -1.5, max = 50.0
Element prediction: Off
Number of isotope peaks used for i-FIT = 3

Monoisotopic Mass, Even Electron Ions
132 formula(e) evaluated with 1 results within limits (up to 50 closest results for each mass)
Elements Used:
C: 0-50 H: 0-100 O: 0-20
A HES 105 (0.917) Cm (6:230)
TOF MS ES-

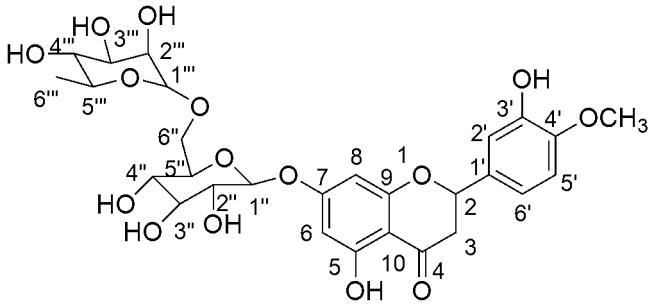

4.97e+006

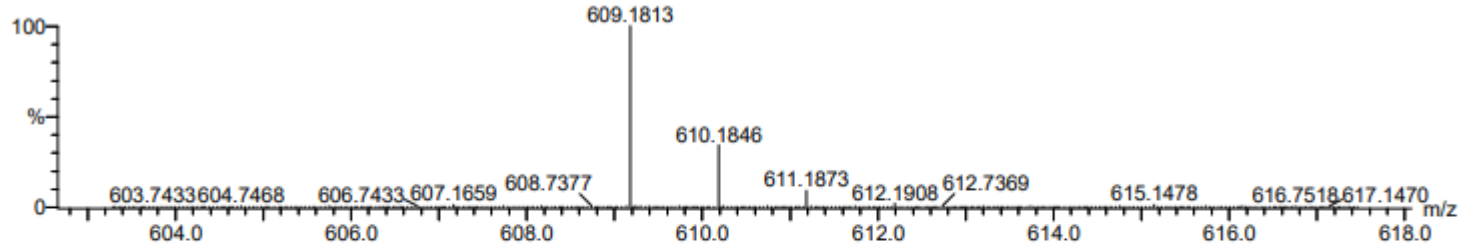

Minimum:				-1.5				
Maximum:		10.0	5.0	50.0				
Mass	Calc. Mass	mDa	PPM	DBE	i-FIT	Norm	Conf(%)	Formula
609.1813	609.1819	-0.6	-1.0	12.5	1083.4	n/a	n/a	C28 H33 O15

Figure S32: High Resolution Mass Spectrum of hesperidin (**S7**)

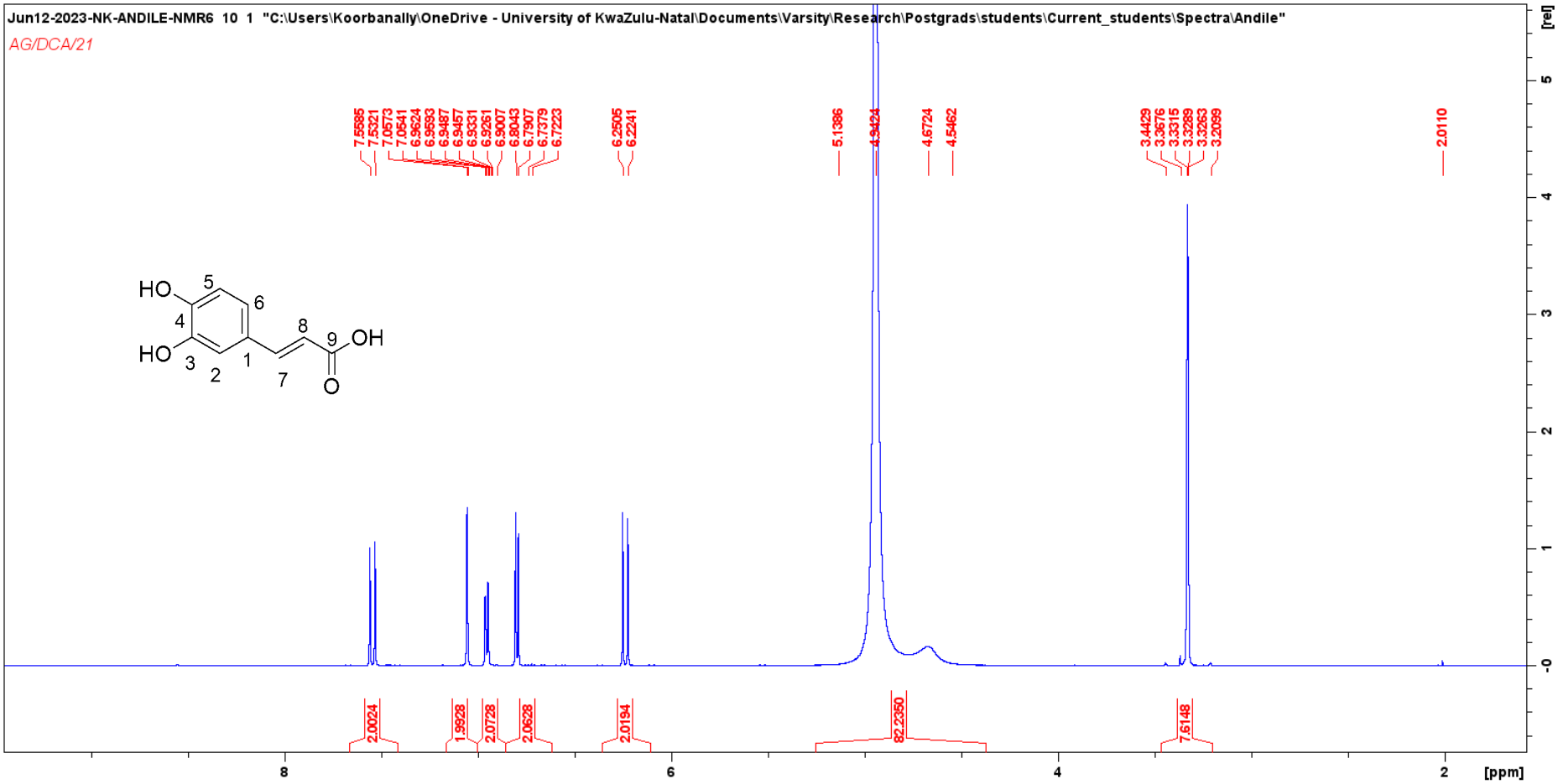

Figure S33: ^{1}H NMR spectrum of caffeic acid (**S8**)

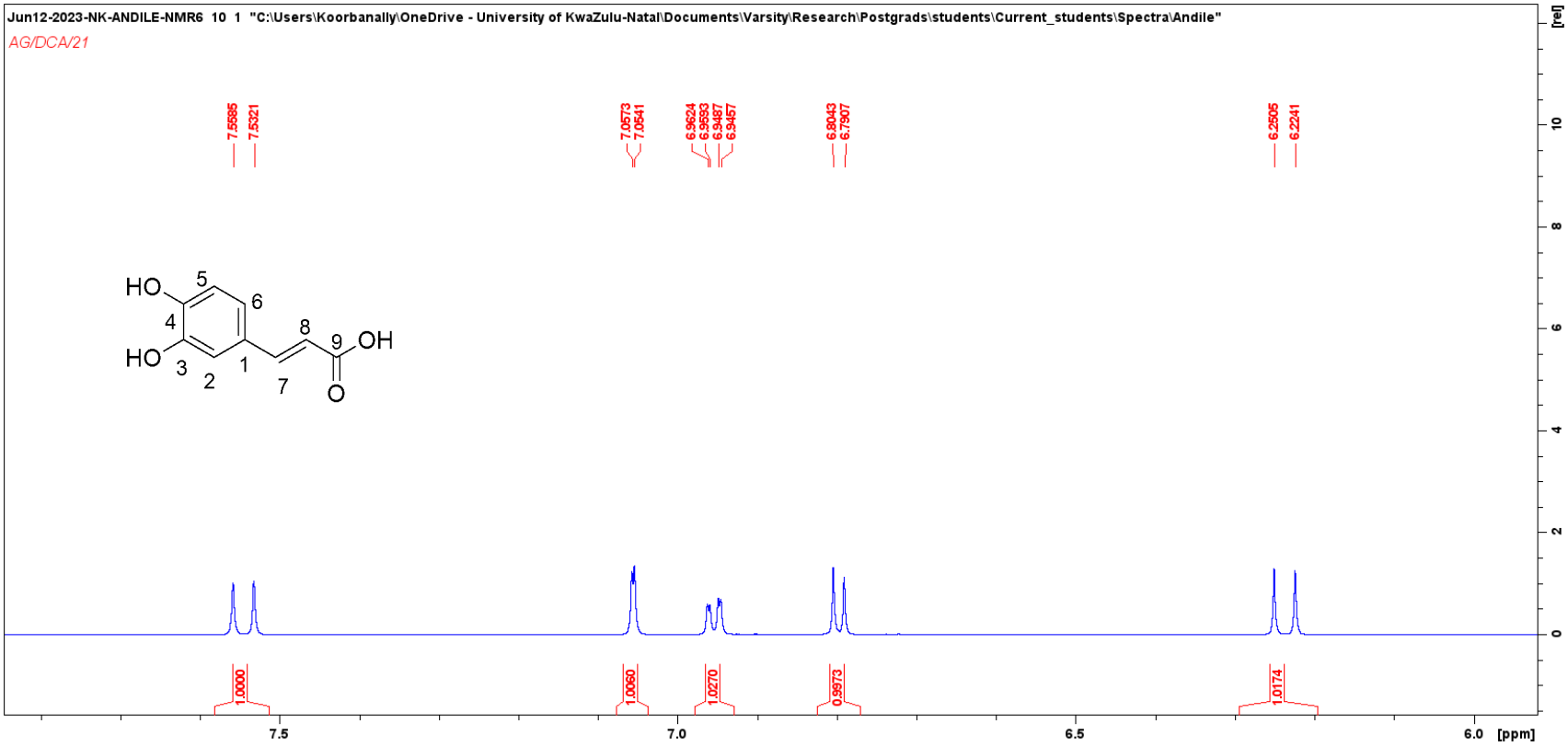

Figure S34: Expanded ^{1}H NMR spectrum of caffeic acid (**S8**)

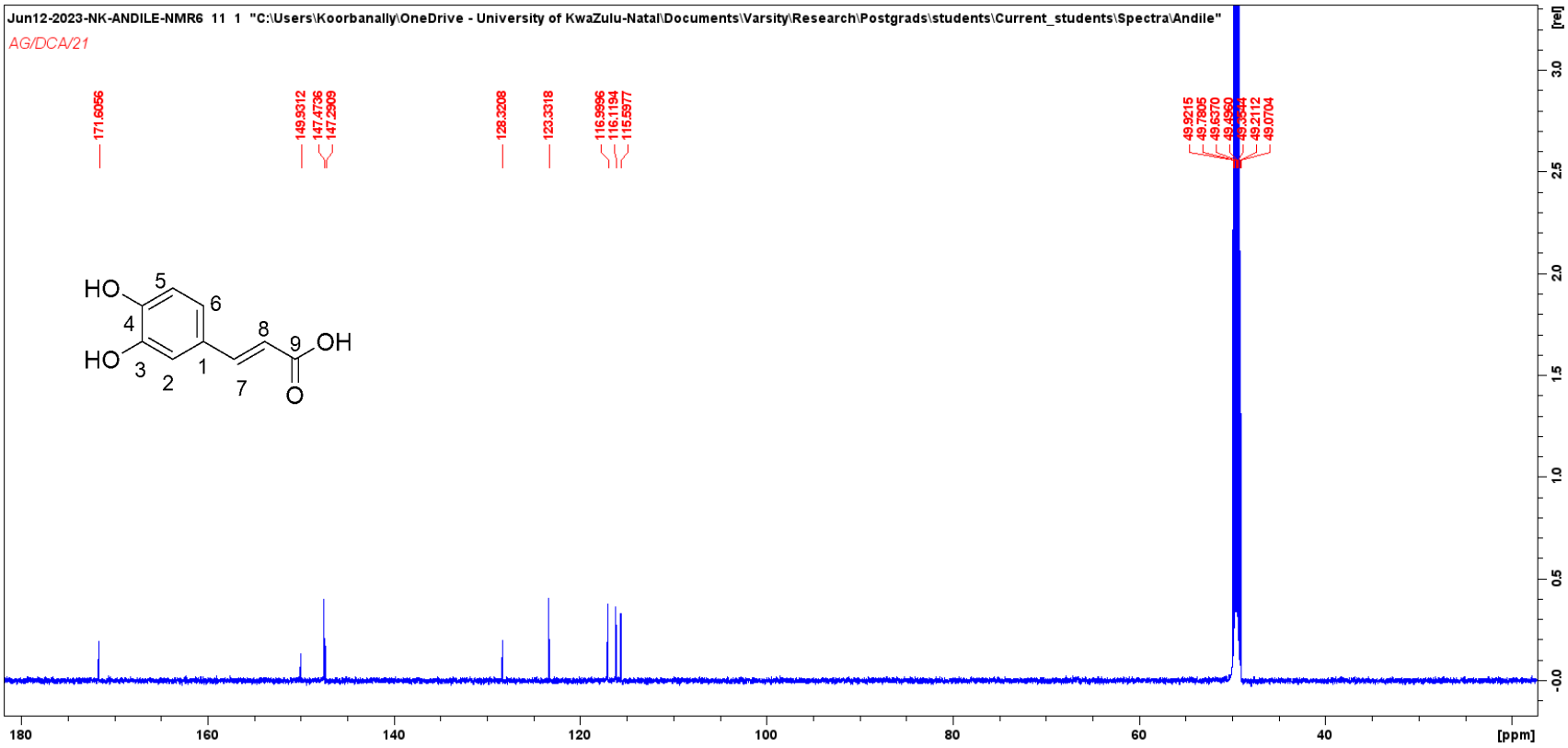

Figure S35: ^{13}C NMR spectrum of caffeic acid (**S8**)

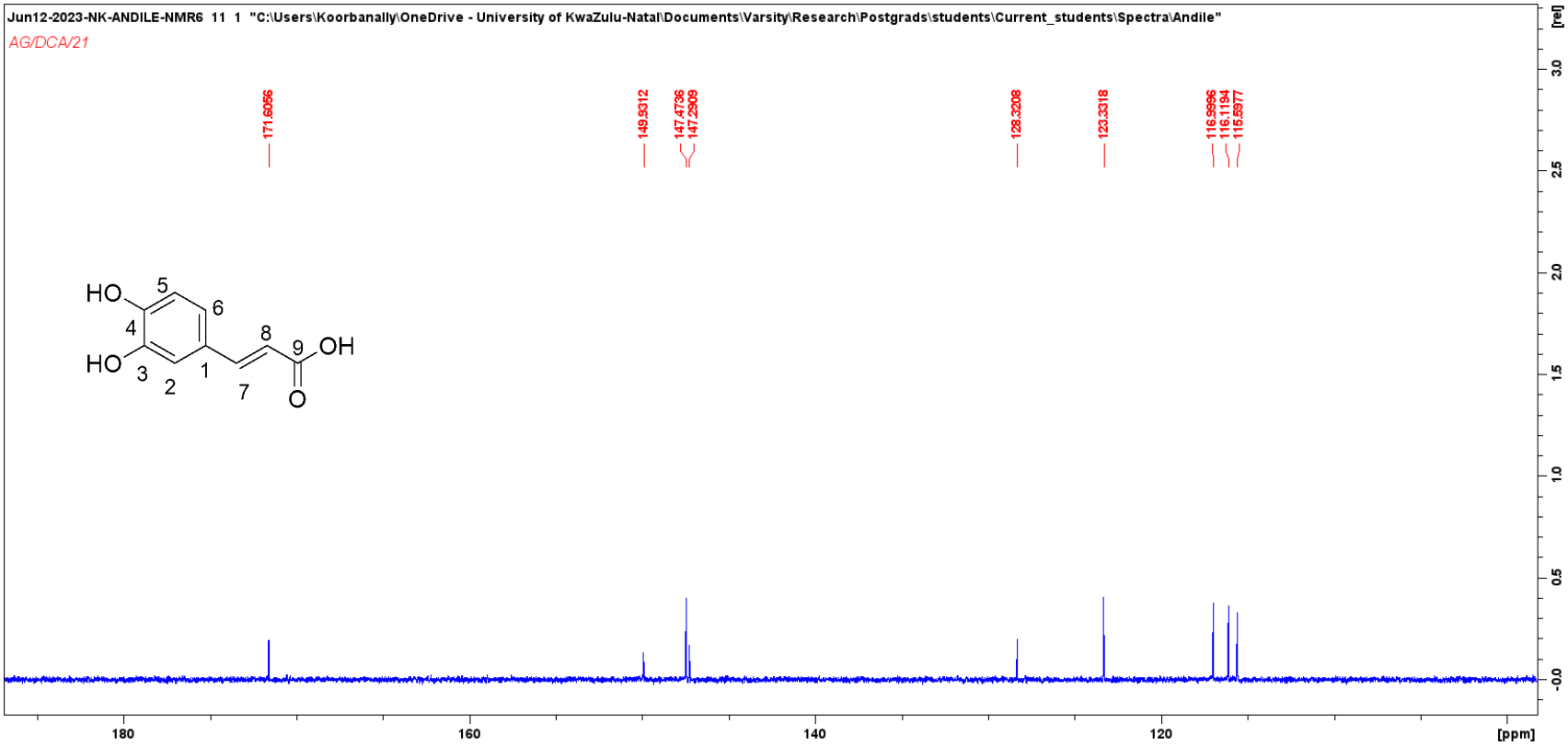

Figure S36: Expanded ^{13}C NMR spectrum of caffeic acid (**S8**)

Elemental Composition Report **Page 1**

Single Mass Analysis

Tolerance = 5.0 PPM / DBE: min = -1.5, max = 50.0

Element prediction: Off

Number of isotope peaks used for i-FIT = 3

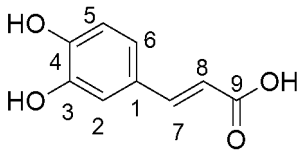

Monoisotopic Mass, Even Electron Ions

26 formula(e) evaluated with 1 results within limits (up to 50 closest results for each mass)

Elements Used:

C: 0-50 H: 0-100 O: 0-10

A CA 103 (0.899) Cm (6:230)

TOF MS ES-

9.56e+006

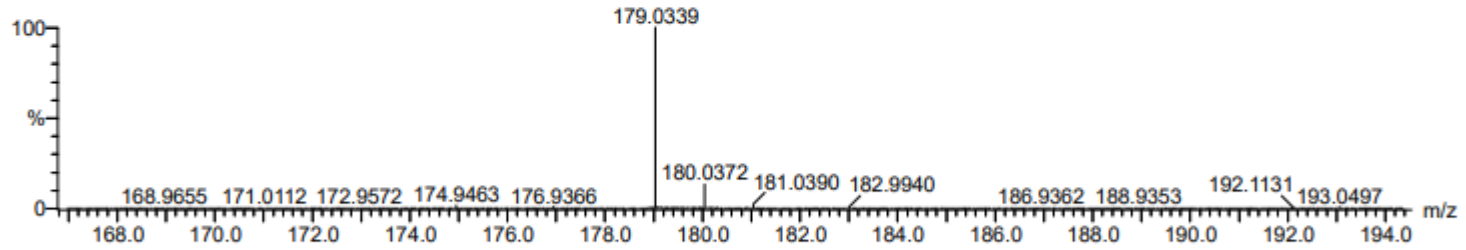

Minimum:				-1.5				
Maximum:		10.0	5.0	50.0				
Mass	Calc. Mass	mDa	PPM	DBE	i-FIT	Norm	Conf(%)	Formula
179.0339	179.0344	-0.5	-2.8	6.5	1208.2	n/a	n/a	C9 H7 O4

Figure S37: High Resolution Mass Spectrum of caffeic acid (**S8**)